Characterization of the Extreme Radiation Resistance Phenotype of *Deinococcus radiodurans* by Physiologic and Differential Expression Analyses

Thesis

Submitted in partial fulfilment of the requirements for the degree of

DOCTOR OF PHILOSOPHY

By

Amudhan Venkateswaran.

Under the supervision of

Dr. Michael J. Daly

BIRLA INSTITUTE OF TECHNOLOGY AND SCIENCE

PILANI (RAJASTHAN), INDIA

July 2003

The thesis entitled "Characterization of the Extreme Radiation Resistance Phenotype of *Deinococcus radiodurans* by Physiologic and Differential Expression Analyses" submitted by **Amudhan Venkateswaran**, is a result of his research work done under the supervision of **Dr. Michael J. Daly**, Associate Professor, Department of Pathology, Uniformed Services University of the Health Sciences (USUHS), Bethesda, Maryland, USA, at USUHS which is an off campus thesis station of Birla Institute of Technology and Science (BITS), Pilani – 333031 (Rajasthan) India.

Name of the Student **Amudhan Venkateswaran**

Name of the Supervisor **Dr. Michael J. Daly**
Associate Professor, Department of Pathology
Uniformed Services University of the Health Sciences (USUHS)
4301, Jones Bridge Road,
Bethesda, MD 20814, USA

ABSTRACT

Ever since the isolation of *Deinococcus radiodurans* from γ-radiation treated canned meat in 1956, this bacterium has been the subject of research aimed at understanding the extreme radiation resistance phenotype. The ability of *D. radiodurans* to survive extremely high doses of acute irradiation and grow vegetatively under chronic irradiation is now being developed by the U. S. Department of Energy (DOE) for microbiological treatment of radioactive waste sites generated by nuclear weapons production during the Cold War. Despite intensive computational analysis of the *D. radiodurans* genomic sequence, the molecular basis of its resistance phenotype remains unclear. This thesis develops new insight into resistance mechanisms using both physiological and differential expression approaches.

Previous reports have suggested that the resistance phenotype of *D. radiodurans* is a secondary characteristic that evolved to help the organism survive desiccation, where DNA repair genes play a dominant role in its recovery from DNA damage induced by free radicals produced following re-hydration. However, *D. radiodurans* mutants that are sensitive to desiccation, but resistant to radiation have recently been reported. A comprehensive understanding of this organism's resistance functions have been further confounded by its genomic annotation which revealed that *D. radiodurans* encodes fewer known DNA repair genes than the relatively radiation sensitive *Escherichia coli*. These findings suggest that the organism's extreme resistance phenotype may be attributable to still unknown genes and pathways.

Physiologic analyses for *D. radiodurans* reported in this thesis support a close relationship between its metabolic configuration, oxidative stress production, and DNA repair. Additionally, growth of *D. radiodurans* was found to be Fe-independent. Since

Fe-independent growth of obligate aerobic chemoorganotrophic bacteria is rare, it is possible that avoiding toxic free radicals typically generated by the Fenton reaction during metabolism or irradiation could facilitate the extreme resistance of *D. radiodurans*. In *D. radiodurans*, it appears that DNA repair systems operate with little interference from the genotoxic effects of free radicals typically generated by aerobic metabolism.

The possible contribution of metabolism to radiation resistance was further explored by studying the RNA expression dynamics of *D. radiodurans* recovering from an acute dose of radiation (15 kGy) using high throughput DNA microarrays and real-time polymerase chain reaction (RT-PCR). Genes induced in the early-phase of recovery included those involved in DNA replication, repair, recombination, cell wall metabolism, cellular transport, and many encoding uncharacterized proteins. In particular, differential expression of its tricarboxylic acid (TCA) cycle and glyoxylate bypass appeared to suppress production of oxygen free radicals, and many novel genes were implicated in cellular repair. Collectively, this thesis presents data supporting that the extreme radiation resistance phenotype is the product of both metabolic functions and DNA repair genes.

UNIFORMED SERVICES UNIVERSITY OF THE HEALTH SCIENCES
4301 JONES BRIDGE ROAD
BETHESDA, MARYLAND 20814-4799

CERTIFICATE

This is to certify that the thesis entitled "**Characterization of the Extreme Radiation Resistance Phenotype of *Deinococcus radiodurans* by Physiologic and Differential Expression Analyses**", and submitted by Amudhan Venkateswaran, Id. No. 1994PF29793 for the award of PhD degree of the institute, embodies original work done by him under my supervision.

Dr. Michael J. Daly
Associate Professor, Department of Pathology
Uniformed Services University of the Health Sciences (USUHS)
4301, Jones Bridge Road,
Bethesda, MD 20814, USA

Adjunct Professor
Birla Institute of Technology and Science (BITS), Pilani
Rajasthan – 333031, India

Date: 7/21/03

Dedication

To my mother and father,
Nagalakshmi and Subramanian Venkateswaran

Acknowledgements

I express my profound gratitude to my mentor and advisor **Dr. Michael J. Daly**, whose guidance and encouragement have been of immense value to me. He has been a great source of inspiration. His patience and intellectual curiosity will always guide me to work sincerely, laboriously and prudently in my future endeavors.

My sincere thanks to **Dr. S. Venkateswaran**, Director BITS, **Dr. Robert Friedman**, Chairman, Department of Pathology, USUHS, **Dr. Radha K. Maheshwari**, Coordinator, Indo-US activities, **Dr. L. K Maheshwari**, deputy director, BITS and **Dr. Ravi Prakash**, Dean, R&C division for giving me this unique opportunity to perform the research for this dissertation at USUHS, Bethesda, an off-campus station of BITS.

I particularly acknowledge **Dr. Debabrota Ghosal**, for being a constant source of support throughout my thesis work and teaching me microbial physiology.

I would like to thank **Dr. Hassan Brim, Dr. Kira Makarova, Dr. Alexander Vasilenko, Dr. Marina Omelchenko, Dr. Elena Gaidamakova** and **Dr. Vera Matrosova** for their valuable suggestions and advices during the course of my research. I am grateful to **Dr. Min Zhai** for her cooperation and technical help rendered at various stages of my investigations. My special thanks to **Mr. Matthias Hess**, my friend, for all his assistance.

I wish to extend a special acknowledgement to **Dr. Jizhong Zhou** and **Dr. Yongqing Liu**, for allowing me to use their laboratory facilities at ORNL, Tennessee, for all my microarray investigations.

I thank **Ms. Sofia del Castillo** at the Audio Visual Center, USUHS for her support with the pictures.

This thesis would have been impossible without the motivation of my parents who have instilled in me the desire to learn. Special thanks to my brothers for their constant support and encouragement throughout the course of my dissertation work.

While here at Maryland, I certainly enjoyed being in the company of **Anoop, Pankaj, Subhashree, Ranga, Praveena, Shirin, Karen, Peter, Katherine, Francis, Maria, Tina, Anuj, Sai, Mathangi, Brokee, Coop and Rajesh**.

I would like to record my thanks to the **U.S. Department of Energy** for funding all the work of this thesis.

Table of Contents

List of Figures

List of Tables

List of Abbreviations

Prefixes to the Names of Units	
Giga (G)	10^9
Mega (M)	10^6
Kilo (k)	10^3
Centi (c)	10^{-2}
Milli (m)	10^{-3}
Micro (μ)	10^{-6}
Units of Time	
Hour	h
Minute	min
Second	sec
Units of Volume	
Liter	l
Milliliter	ml
Microliter	μl
Units of Mass	
Gram	g
Microgram	μg
Dalton	Da
Units of Concentration	
Molar (mol/liter)	M
Millimolar	mM
Micromolar	μM
Units of Temperature	
Degree Celsius	°C
Units of Electricity	
Ampere	A
Volt	V

Units of Radioactivity	
Gray (1 Joule/Kg)	Gy
Kilo Gray	kGy
Physical and Chemical Quantities	
Optical Density	OD
Miscellaneous Units	
Revolutions per minute	rpm
Hydrogen ion concentration, negative log of	pH
Other Standard Abbreviations and Symbols	
About	~
Adenosine 5'-triphosphate	ATP
Adenosine 5'-diphosphate	ADP
Accurate Mass Tag	AMT
And	&
And Others	*et al.*
Base Pairs	bp
Colony Forming Unit	CFU
Complementary DNA	cDNA
Concentrated	conc.
Defined Minimal Medium	DMM
Deoxyribo Nucleic Acid	DNA
Deoxyribonuclease	DNase
United States Department of Energy	DOE
Double Strand Breaks	DSBs
Embden-Meyerhof-Parnas Pathway	EMP
Ethylenediaminetetraacetic Acid	EDTA
Gamma	γ
Genomic Informatic Based Expression	GIBE
Greater than	>
In the Original Position	*in situ*
Less than	<

Open Reading Frame	ORF
Pacific Northwestern National Laboratory, WA	PNNL
Percent	%
Polymerase Chain Reaction	PCR
Reactive Oxygen Species	ROS
Real – Time Polymerase Chain Reaction	RT-PCR
RiboNucleic Acid	RNA
Ribosomal RNA/DNA	rDNA/rRNA
Sodium Dodecyl Sulphate	SDS
Times	x
Tricarboxylic Acid	TCA
Two Dimensional	2-D
Ultraviolet	UV
Volume Per Volume	v/v
Videlicet – Namely	*viz.*
Weight Per Volume	w/v

Chapter 1: Introduction

1.1 Evolution of Extremely Radiation Resistant Bacteria

Gregor Mendel described the basic nature of the genetic unit of function (gene) in 1865 in his papers establishing the laws of inheritance, but the importance of his work was not realized until decades later. The rise to prominence of Mendel's work was at a time of growing evidence supporting the existence of atoms, occurrence of chemical bonds, and the interaction between chromosomes and radiation (Watson, 2000; Dewald, 1977). The study of the effects of radiation on living organisms subsequently gave rise to the field of radiation biology (Shapiro, 2002).

Ionizing radiation is the most lethal form of radiation because it causes DNA double-strand breaks (DSBs), which destroy the linear integrity of DNA and result in loss of genetic information if not repaired (Shapiro, 2002). Gamma (γ) and X-rays are uncharged, short wavelength, very high-energy electromagnetic waves released by certain atomic transformations (*e.g.*, ionization). They are emitted as packets of energetic photons and are frequently released together with beta (β)-particles (*e.g.*, ^{137}Cs $[\gamma, \beta^-]^E$; ^{60}Co $[\gamma, \beta^-]^E$), that also cause DNA damage (Shapiro, 2002). About 80% of DNA damage caused by ionizing radiation is believed to result from the indirect action of free radicals, the remaining 20% by direct interaction between γ-photons and DNA (Repine *et al.*, 1981). In the presence of water and oxygen, ionizing radiation is known to generate hydrogen peroxide (H_2O_2) by free radical chemistry arising from the radiolysis of water (Jakubovics, 2001). In the presence of Fe(II), the Fenton reaction rapidly decomposes H_2O_2 generating hydroxyl radicals ($^{\bullet}OH$) (Jakubovics, 2001), that damage DNA. Most organisms are extremely sensitive to the effects of ionizing radiation. An acute dose of just 5 Grays (Gy) (1 Gy = 100 rads) is lethal to the average human (Thronley, 1963). Typically because of their very large sizes, mammalian genomes (1-4 Giga [billion] base pairs [bp]) are more susceptible to radiation than organisms with relatively small genomes (0.5 – 10 Mbp for bacteria). However this simple correlation between genome size and radiation resistance breaks down when considering extremely radiation resistant bacteria that show even greater radiation resistance than some of the smallest known viruses (*e.g.*, coconut foliar decay virus, 1.2 kbp) (Rohde *et al.*, 1990). The genetic mechanisms underlying extreme radiation resistance in bacteria are unknown, but likely are a product of a complex set of genes and their interaction with the environment (Liu *et al.*, 2003).

The evolution of the extremely radiation resistant *D. radiodurans* (Anderson *et al.*, 1956) is remarkable given the apparent absence of highly radioactive habitats on Earth over geologic times. There are relatively few known environments on Earth that could have delivered acute doses, on the order of millions of Gy. Examples include environments that are frozen (*e.g.*, permafrost) (Friedmann, 1993) or desiccated (*e.g.*, salt deposits [Stan-Lotter *et al.*, 1999], amber [Lambert *et al.*, 1998], and desserts Lehner *et al.*, 2001). It is within these environments that immense doses of background radiation could have accumulated over millions of years.

Historically, the best-known radiation resistant bacterium is *D. radiodurans* (Anderson *et al.*, 1956). Questions addressed in this thesis revolve around the evolution of radiation resistance in *D. radiodurans* and the cellular and genetic mechanisms underlying this remarkable phenotype. After acute exposures to 15 kGy, *D. radiodurans* can reassemble its 3.285-Mbp genome, which consists of 4 haploid genomic copies per cell (Hansen, 1978), from hundreds of DNA DSB fragments without lethality or induced mutagenesis (Battista, 1997; Daly, 2000; Daly *et al.*, 1994a; Daly and Minton, 1996, 1997; Makarova *et al.*, 2001). In stationary phase, *D. radiodurans* does not show any lethality to irradiation up to about 10 kGy and 37% survival at about 15 kGy (Moseley and Evans, 1983). By comparison, *E. coli* shows 100% survival extending to 0.3 kGy and 37% survival at 0.5 kGy (Smith and Martignoni, 1976), a 30-fold difference in resistance (Sweet and Moseley, 1976). Furthermore, *D. radiodurans* can grow vigorously in the presence of chronic ionizing radiation (60 Gy/hour), whereas *E. coli* cannot and is rapidly killed (Lange *et al.*, 1998; Brim *et al*, 2000). Because most organisms, generally, can tolerate so few DSBs (Krasin and Hutchinson, 1977), radiation-induced DSBs and their repair have been difficult to study. In *D. radiodurans*, however, there are so many DSBs in fully viable irradiated cells following high-dose irradiation that the steps in DSB repair can be monitored directly in mass culture (Daly *et al.*, 1994a; Daly and Minton, 1996; Daly and Minton, 1997). These characteristics have been exploited and used to examine the timing of DNA recombination (Daly *et al.*, 1994a; Daly and Minton, 1996; Daly and Minton, 1997) following high-dose irradiation, and has revealed the sequential action of RecA-independent and RecA-dependent pathways during repair (Daly and Minton, 1996). These characteristics were also the impetus for sequencing the genome of *D. radiodurans* and the ongoing development of this organism for practical purposes such as bioremediation of radioactive waste sites (Brim *et al.*, 2000; Daly, 2000; Lange *et al.*, 1998).

1.2 Isolation of *D. radiodurans*

The bacterium *D. radiodurans* (formerly *Micrococcus radiodurans*) strain R1 was discovered as a contaminant in γ-radiation treated canned meat by Anderson and coworkers at the Oregon Agricultural Experiment Station in 1956 (Anderson *et al.*, 1956). Pure culture isolation yielded a red-pigmented, nonsporulating, nonpathogenic, obligate aerobic bacterium that was extremely resistant to γ-radiation (Anderson *et al.*, 1956). Further investigations revealed that *D. radiodurans* is also resistant to a range of other DNA damaging conditions such as desiccation, UV light (Tempest and Moseley, 1982), H_2O_2 (Wang and Schellhorn, 1995), and to certain mutagens like mitomycin C (Kitayama, 1982) and nitrous acid (Sweet and Moseley, 1976), but the molecular mechanisms underlying all of these capabilities remain unknown. Soon after the isolation of *D. radiodurans* R1, a second strain of *D. radiodurans* (SARK) was isolated as an air-contaminant in a hospital in Ontario, Canada (Murray and Robinow, 1958). Six other extremely radiation resistant deinococcal strains have been isolated since then: *Deinococcus radiopugnans* from haddock tissue (Davis *et al.*, 1963), *Deinococcus radiophilus* from Bombay duck (Lewis, 1971), *Deinococcus proteolyticus* from the feces of *Lama glama* (Kobatake *et al.*, 1973), the rod-shaped species *Deinococcus grandis* from elephant feces (Oyaizu, 1987), and two moderately thermophilic species *Deinococcus geothermalis* and *Deinococcus murrayi* from hot springs in Portugal and Italy, respectively (Ferreira *et al.*, 1997). These bacteria comprising the family *Deinococcaceae* were originally classified as belonging to the genus *Micrococcus* (Anderson *et al.*, 1956). However, a detailed biochemical and structural analysis of their cell wall distinguished them from true members of the genus *Micrococcus* (Brooks *et al.*, 1980). Later, 16S rRNA sequence analysis showed that the *Deinococcaceae* are very closely related to the genus *Thermus* (S_{AB} = 0.22 to 0.29) (Rainey *et al.*, 1997).

1.2.1 Natural Habitat of *Deinococci*

Usually described as soil bacteria, the natural habitat of *Deinococci* still remains undefined. Various ecological surveys have shown that these organisms can be isolated from a range of environments including nutritionally rich conditions such as meat (Davis *et al.*, 1963; Evans and Moseley, 1983), animal feces (Ito *et al.*, 1983), and damp surface soils (Masters *et al.*,

1991b), or from nutritionally restricted and desiccated conditions such as room dust (Christensen and Kristensen, 1981), medical instruments (Christensen and Kristensen, 1981), air purification systems, dried fruits (Maxcy and Rowley, 1978), textiles (Christensen and Kristensen, 1981), and the Antartic Dry Valleys (Counsell and Murray, 1986). The isolation of the *Deinococci* from such diverse environments does not explain the origin of the extreme radiation resistance phenotype. One possibility could be that this phenotype evolved as a defense mechanism against DNA damage resulting from cycles of desiccation and rehydration (Battista, 1997; Mattimore and Battista, 1996), where the desiccated state of *Deinococcus* represents a dormant stage of its life cycle.

1.2.2 Cell Structure of *D. radiodurans*

In nutrient rich medium, *D. radiodurans* grows as clusters of two and four cells (Figure 1.1) (Murray, 1986, 1992) known as diplococci and tetracocci, where each cell compartment contains 4-8 copies of its genome (Hansen, 1978). The cell envelope of *D. radiodurans* is very unusual (Murray, 1986, 1992). Although *D. radiodurans* stains Gram-positive, the structural and biochemical composition of its cell envelope also shares similarities with Gram-negative bacteria (Anderson et al., 1956, Murray, 1986, 1992). Electron microscopy reveals the presence of at least 6 different layers of the cell envelope: the innermost plasma membrane followed by the perforated peptidoglycan containing cell wall (Holey layer) (Murray, 1992; Makarova *et al.*, 2001). The third layer is the compartmentalized layer. The forth layer is the outer membrane followed by a fifth distinct electrolucent layer. The sixth layer is the S-layer, which contains regularly packed hexagonal protein subunits. Some of the deinococcal strains also exhibit an additional layer, a dense carbohydrate coat. The only layers involved in cell division are the cytoplasmic membrane and the peptidoglycan layers. Collectively, the others are regarded as a sheath, since they surround groups of cells and form on the surface of daughter cells as they separate (Murray *et al.*, 1983).

Figure 1.1. Analysis of *D. radiodurans* Cell Structure by Transmission Electron Microscopy (TEM). TEM of *D. radiodurans* grown in TGY medium showing wall structure and nucleoid morphology. *Panel A* shows an example of a D. radiodurans tetracoccus grown in rich medium (TGY). *Panel B* shows the cell wall structure of *D. radiodurans*. EM scale bars in A = 1 μm and B = 0.5 μm. **pg**, peptidoglycan layer; **cc**, carbohydrate coat.

Figure 1.1

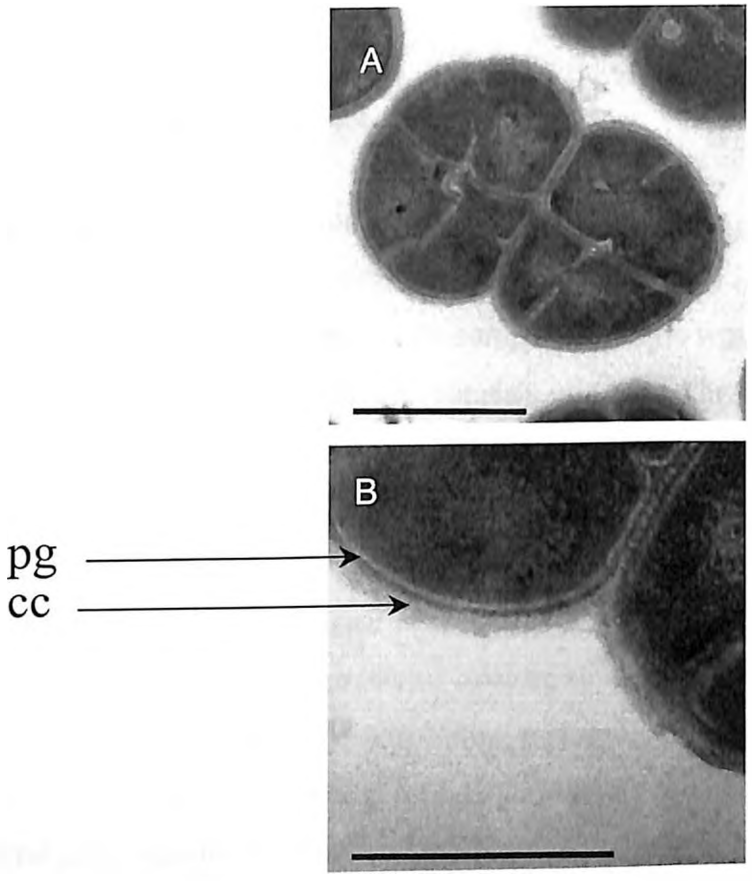

A. Vasilenko

Quintela and coworkers (1999) (Quintela *et al.*, 1999) have analyzed the biochemical structure of *D. radiodurans* SARK using mass spectrometry and compared its peptidoglycan fine structure to that of *Thermus thermophilis*, which is closely related to *D. radiodurans*. Their study indicated a similarly between their cell wall mureins, where both mureins originate from the same basic monomeric subunit. Furthermore, they found that *Deinococci* and *Thermus* species are the only two genus' yet identified which have the murein chemotype A3β (Quintela et al., 1999).

1.2.3 Genome of *D. radiodurans* R1

The construction of a whole genome shotgun optical map for *D. radiodurans* (strain R1 unless stated otherwise) was reported in September 1999 (Lin *et al.*, 1999), and this was immediately followed by the release of its complete genome sequence (White *et al.*, 1999). The 3,284,156 bp genome of *D. radiodurans* consists of a main chromosome (DR_Main: 2,648,638 bp), a smaller chromosome (DRA: 412, 348 bp), a megaplasmid (DRB: 177,466 bp) and a small plasmid (DRC: 45,704 bp) (Makarova *et al.*, 2001). While stationary phase cultures of *D. radiodurans* contain 4 copies of its genome per cell, exponentially growing cells have 8-10 copies of the genome per cell (Hansen 1978; Harsojo *et al.*, 1981). The GC rich (66.6%) genome of *D. radiodurans* encodes 3,195 predicted open reading frames (ORFs) (Makarova *et al.*, 2001) of which 90.9% were assigned as protein coding regions.

The *D. radiodurans* annotation reveals numerous genes that appear to have been acquired by horizontal gene transfer from several eukaryotes (Makarova *et al.*, 2001). Examples include the Vacuolar (V)-type proton ATP synthase that appears to have replaced the F_1F_0 form typically present in free-living bacteria; the presence of poxviruses topoisomerases IB (Krogh and Shuman, 2002); and phytochrome-like proteins that belong to a family of red/far-red light sensors typically found in photosynthetic organisms (Bhoo *et al.*, 2001). Horizontal gene transfer from archeae to *D. radiodurans* is also believed to have occurred. Fabrega and coworkers (2001) have described the presence of a unique cysteinyl-tRNA synthetase in *D. radiodurans* and *Methanococcus jannaschii* (Fabrega *et al.*, 2001). This cysteinyl-tRNA synthetase sequence lacks the characteristic sequence motifs classically associated with this synthetase in prokaryotes (Fabrega *et al.*, 2001).

Analysis of the *D. radiodurans* genome has identified a broad spectrum of DNA repair genes, which includes an intact *uvrABCD* system (nucleotide excision repair), the intact *recA* and *ruvABE* systems (recombinational repair system), and an intact mismatch repair system (Makarova *et al.*, 2001). Also identified are genes encoding the removal of oxygen free radicals (*sod* genes) via H_2O_2 (catalase, *katA*). How these encoded functions interact to protect and restore DNA in *D. radiodurans* is unknown, but it is clear that the presence of multiple genome copies per cell is important for homologous recombination (Daly *et al.*, 1994a; Daly and Minton, 1995a and 1997). This notwithstanding, genome multiplicity alone is insufficient to explain its radiation resistance (Harsojo *et al.*, 1981) since *Micrococcus luteus*, *Micrococcus sodonensis* and *Azotobacter vinelandii* all contain multiple genomic copy numbers, but are very sensitive to radiation (Majumdar and Chandra, 1985; Punita *et al.*, 1989; Sadoff *et al.*, 1979).

The number of DNA DSBs inflicted during an acute irradiation exposure depends on several factors including genome size, the dose of radiation, and the growth/physiologic state of the cells. An acute dose of 15 kGy has been reported to cause about 150 DSBs per haploid chromosome in *D. radiodurans* (Daly *et al.*, 1994a, 1994b), which it can repair within hours (Daly *et al.*, 1994a, 1994b; Kitayama and Matsuyama, 1971; Sweet and Moseley, 1974, 1976). By comparison, only 1-3 DSBs per chromosome is believed to be lethal to *E. coli* (Krasin and Hutchinson, 1977).

1.2.4 How Does *D. radiodurans* Survive Radiation?

Optical mapping of genomic DNA isolated from irradiated (17.5 kGy) *D. radiodurans* confirmed that it sustains ~ 200 DSBs per haploid genome, originally determined by pulsed field gel electrophoresis (Daly *et al.*, 1994b). Whether or not the same amount of DNA damage is inflicted at high irradiation doses in other organisms is unknown, but there is no doubt that the accumulation of DSBs ultimately leads to cell death irrespective of which organism is irradiated (Daly *et al.*, 1994a). Repairing DSBs without mutation or other rearrangements is very difficult since a DSB cannot be accurately repaired without a homologous DNA repair template. The observed persistent multiple genome copies in *D. radiodurans* meets the requirement for having homologous repair templates, and highly efficient interchromosomal and interplasmidic recombination following DNA damage has been reported (Daly *et al.*, 1994a; Daly and Minton,

1995a, 1996 and 1997). So, how does *D. radiodurans* achieve this feat of genomic restoration? One hypothesis proposes that the multiple genomic copies of *D. radiodurans* chromosomes are structurally aligned and where DSBs are never far removed from potential repair templates (Daly and Minton, 1995b; Minton and Daly, 1995). This could simplify the search for homology and could explain its efficient RecA-dependent and RecA-independent homologous DNA repair pathways (Daly and Minton, 1995b; Minton and Daly, 1995). However, little experimental data has been obtained to support this alignment hypothesis since it was originally proposed in 1995 (Daly and Minton, 1995b), and the most recent annotation of the *D. radiodurans* genome did not reveal an unusual assortment of DNA repair genes compared to other sequenced organisms (Makarova *et al.*, 2001; Karlin and Mrazek, 2001; Gerard *et al.*, 2001).

While the genetic and cellular systems responsible for extreme radiation resistance remain a mystery, the recovery of *D. radiodurans* following massive exposure to ionizing radiation does appear to result from an orderly process (Battista, 1997; Makarova *et al.*, 2001). Immediately following acute irradiation, DNA replication and cell division cease and DNA repair pathways are activated (Daly *et al.*, 1994; Daly *et al.*, 1997 Daly and Minton, 1995 and 1996). And, the time required for DNA restoration is dose dependent; *i.e.*, the larger the radiation dose, the longer the recovery time (lag phase) (Dean *et al.*, 1966; Lett *et al.*, 1967, Minton 1995, Daly *et al.*, 1994b).

Post–irradiation protein synthesis has been studied in *D. radiodurans* (Hansen, 1980). At least four uncharacterized proteins (α, β, γ, δ) are synthesized immediately after exposure to ionization radiation (Hansen, 1980). The induction of post-irradiation protein synthesis appears to be very important for cell survival. For example, RecA (Carroll *et al.*, 1996) is induced within one hour of exposure to γ-radiation, and *recA*$^-$ mutants are very sensitive to irradiation. Furthermore, exposure of *D. radiodurans* cell cultures recovering from irradiation to chloramphenicol results in cell death (Kitayama and Mastsuyama, 1971), underscoring the importance, in general, of protein expression during recovery. *D. radiodurans* can sense the completion of DNA repair and subsequently enters logarithmic growth after a lag-phase that can last up to 12 hours (Daly *et al.*, 1994a; Daly and Minton 1997; Daly and Minton, 1995a and 1996). The genetic systems responsible for recovery from acute doses of irradiation appear to be the same as those that allow growth of *D. radiodurans* under chronic radiation (60 Gy/hour)

(Lange *et al.*, 1998), since DNA repair mutants (*e.g.*, *recA*$^-$) cannot grow under chronic irradiation.

In *D. radiodurans*, the repair of DNA damage inflicted under acutely or chronically delivered irradiation is dependent on nutrient rich conditions (Minton, 1994). Following acute irradiation in rich medium, export of damaged DNA components from the cell has been reported (Varghese and Day, 1970; Vukovic-Nagy *et al.*, 1974). This form of cellular cleansing is believed to remove the damaged nucleotides from the cell and may prevent their incorporation into DNA during replication (Vukovic-Nagy *et al.*, 1974). The pyrophosphohydrolases of the Nudix superfamily ("nucleotide diphosphate linked to some other moiety x") are also considered to be involved in cellular cleansing (Bessman *et al.*, 1996). For example, the repair enzyme MutT, that is the founding member of the Nudix family, plays an important role in bacterial sanitization by its GTPase activity. Suggesting that metabolic regulation is also important to cellular recovery, a recent report (Fisher *et al.*, 2002) shows that the Nudix hydrolase enzyme encoded by DR2356 has 5-phosphoribosyl 1-pyrophosphate (PRPP) activity leading to the generation of ribose 1,5-biphosphate (Rib-1, 5-P_2), a physiological regulator of glycolysis and the fructose 6-phosphate/fructose 1,6-biphosphate cycle (Fisher *et al.*, 2002). Whether or not these responses to acute irradiation are also active in cells growing under chronic irradiation is unknown.

1.2.5 DNA Repair Pathways

Many conventional DNA repair pathways are present in *D. radiodurans* (Makarova *et al.*, 2001). These include the nucleotide excision repair (NER), base excision repair (BER), and recombinational repair systems. Bacterial NER systems identify bulky lesions such as UV-induced pyrimidine dimers and other damaged bases in DNA, and excise and repair such damage (Lewin, 2000). Of numerous excision repair systems identified in bacteria, the UVR repair system is the most characterized, and typically consists of three genes *uvrA*, *uvrB*, and *uvrC*, which work as a complex to repair UV-damaged nucleotides. The UvrAB combination recognizes and binds to damaged nucleotides. Then, UvrA dissociates and UvrC binds to UvrB. UvrBC, then makes a single-strand incision at flanking sides of the damaged nucleotide complex, which is followed by the release of single-stranded DNA between the two cuts by a

helicase (UvrD) (Figure 1.2). Two *uvrA* copies (*uvrA-1*, and *uvrA-2*) have been identified in *D. radiodurans* (Agostini *et al.*, 1996; Narumi *et al.*, 1997). The *uvrA-1* plays a dominant role in the NER and its product has 52% homology to *E. coli* and *Micrococcus luteus* UvrA. The annotation of *D. radiodurans* genome supports the presence of a functional UvrB (DR2275) and UvrC (DR2354). However, there is currently no experimental evidence to support direct interaction between UvrA, UvrB and UvrC in *D. radiodurans*.

In *D. radiodurans*, two independent excision repair pathways for UV light damage have been described (Mosseley and Evans, 1983). One excision pathway is activated by the protein endonuclease-α, which is the product of *uvrA-1* (Moseley *et al.*, 1983) and the other by endonuclease-β, a 36-kilo Dalton (kDa) manganese requiring protein, which is encoded by *uvs*. *uvrA-1*$^-$ strains of *D. radiodurans* show wild-type levels of resistance to UV light exposure (Agostini *et al.*, 1996) while mutational inactivation of *uvs* (*uvsC*, *uvsD*, or *uvsE*) results in only moderate sensitivity to UV damage (Gutman *et al.*, 1991). Induction of complete UV sensitivity in *D. radiodurans* requires inactivation of both genes: *uvrA-1* and *uvs* (Earl *et al.*, 2002b). There have been contradicting reports regarding the functional characterization of endonuclease–β; it was originally thought to have a pyrimidine-dimer DNA glycosylase function (Gutman *et al.*, 1991), but a recent report suggests that, it has UV damage endonuclease activity (Earl *et al.*, 2002b).

Generally, BER systems remove individual damaged/altered bases in DNA sequence. Damaged bases are first excised by DNA glycosylases and apurinic or apyrimidinic (AP)-specific endonucleases, which catalyze cleavage of sugar-base bonds in DNA, and exposed phosphodiester bonds, respectively. DNA polymerase and DNA ligase then restore the correct sequence using the undamaged strand as a template (Figure 1.3). The genomic annotation of *D. radiodurans* predicts the presence of three uracil-DNA glycosylases (DR0689, DR1751, and DR0022). Cloning and characterization of the products of these three loci have revealed the existence of a family class I (DR0689) and two family class IV (DR1751 and DR0022) uracil-DNA glycosylases (Sadigursky *et al.*, Unpublished data). Other DNA repair systems essential during replication such as thymine glycol glycosylase (Masters and Minton, 1992), and a decarboxyribophosphodiesterase, have been detected in cell extracts of *D. radiodurans* (Mun *et al.*, 1994).

Figure 1.2. Excision Repair of DNA by *E. coli* UvrABC Mechanism. Two molecules of UvrA and one from UvrB form a complex that moves randomly along DNA (steps 1 and 2). Once the complex encounters a lesion, conformational changes in DNA, powered by ATP hydrolysis, cause the helix to become locally denatured and kinked by 130° (step 3). After UvrA dimmer dissociates (step 4), the UvrC endonuclease binds and cuts the damaged strand at two sites separated by 12 or 13 bases (steps 5 and 6). UvrB and UvrC then dissociate, and helicase II unwinds the damaged region (step 7), releasing the single-stranded fragment with the lesion, which is degraded to mononucleotides. The gap is filled by DNA polymerase I, and the remaining nick is sealed by DNA ligase (step 8) [Adapted from Lodish *et al.*, Molecular Cell Biology, W. H. Freeman and Company, 4th edition; A. Sancar and J. Hearst, 1993, Science 259;1145].

Figure 1.2

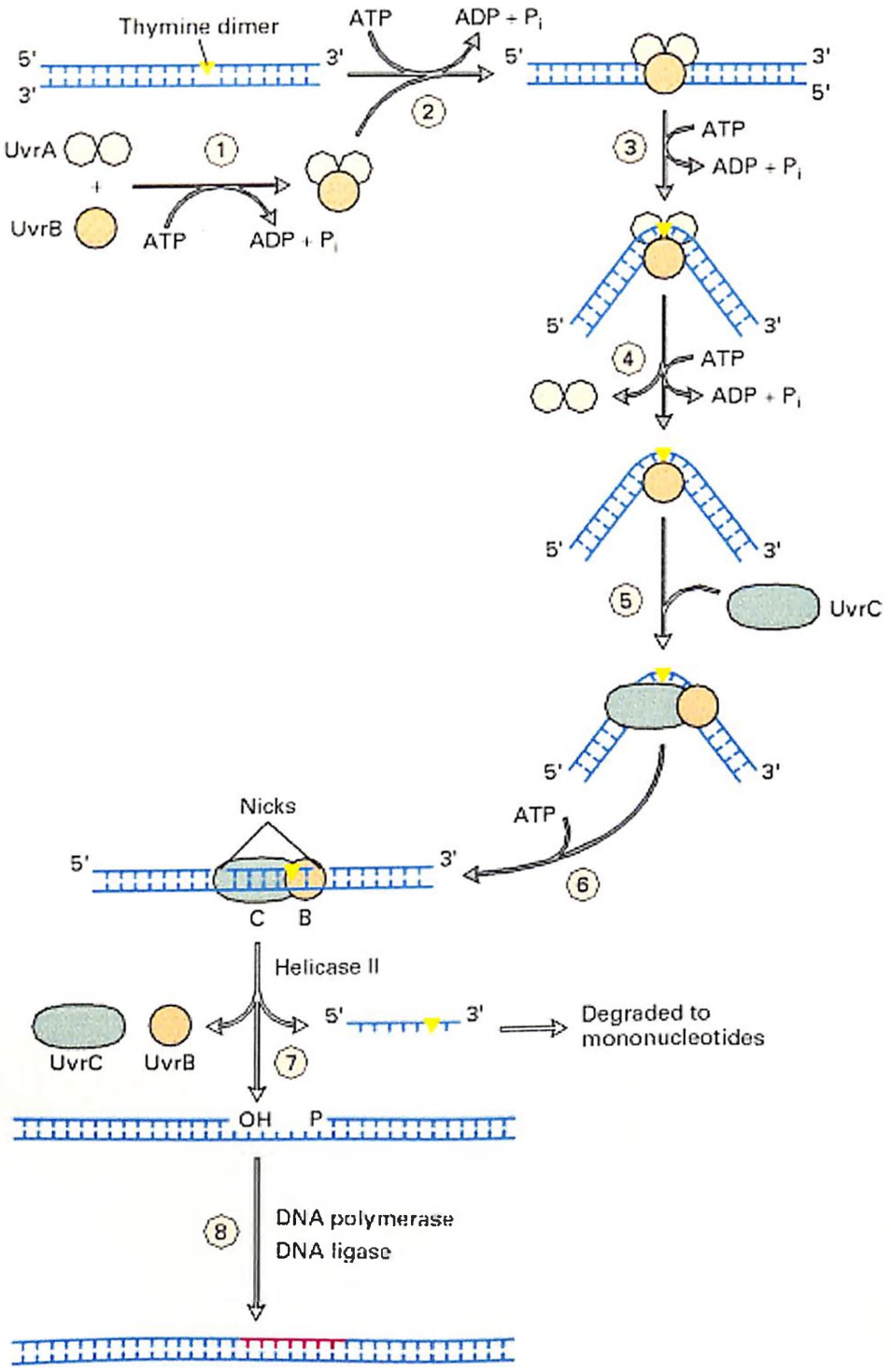

Lodish *et al.*

Figure 1.3. Base-Excision Repair. In this example, uracil (U) has been formed by deamination of cytosine (C) and is therefore opposite a guanine (G) in the complementary strand of DNA. The bond between uracil and the deoxyribise is cleaved by a DNA glycosylase, leaving a sugar with no base attached in the DNA (an AP site). This site is recognized by AP endonuclease, which cleaves the DNA chain. The remaining deoxyribose is removed by deoxyribosephosphodiesterase. The resulting gap is then filled by DNA polymerase and sealed by ligase, leading to incorporation of the correct base (C) opposite the G. [Adapted from The Cell, A Molecular Approach. 2nd Edition 2000].

Figure 1.3

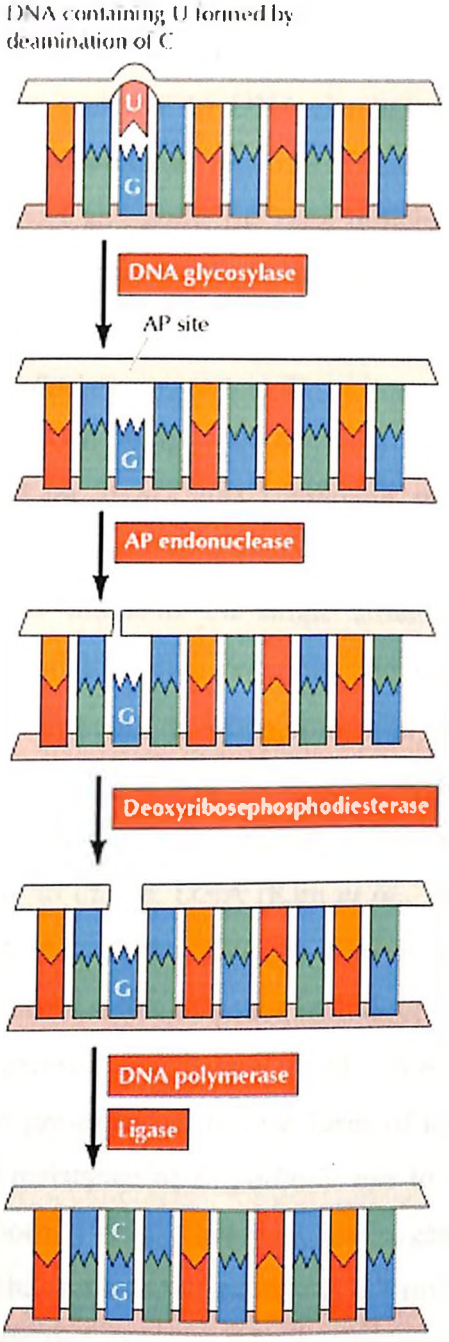

Geoffrey M. Cooper

Recombinational repair systems use an undamaged homologous sequence to restore the correct order of nucleotide sequences and play an important role in repair of DNA DSBs. RecA and PolA play a central role in recombinational repair. *D. radiodurans* synthesizes both, although *recA* is expressed at high levels only during DNA repair (Carroll *et al.*, 1996). *recA* mutants of *D. radiodurans* are sensitive to DNA damaging agents including mitomycin-C (Moseley and Copeland, 1978; Masters *et al.*, 1991a), ionization radiation, and UV light (Gutman *et al.*, 1993). Unlike *uvrA* and *polA*, the *recA* deficiency cannot be complemented by expression of *E. coli recA* in *D. radiodurans* even though *E. coli* RecA is 56% identical to *D. radiodurans* RecA (Gutman *et al.*, 1993).

The expression of *D. radiodurans recA* in *E. coli* was originally thought to be lethal (Dean *et al.*, 1970). However, Kim *et al.*, (2002) have recently re-cloned and expressed *Deinococcal* RecA in *E. coli* (Kim *et al.*, 2002) showing that *D. radiodurans* RecA could perform the typical functions associated with it (Kim *et al.*, 2002, Kim and Cox, 2002) which include the formation of striated filaments on single stranded and double stranded DNA, promotion of efficient DNA strand exchange reaction, and the presence of DNA dependent nucleoside triphosphate activity. Furthermore, when compared to *E. coli* RecA, *D. radiodurans* RecA was found to be unusual; *D. radiodurans* RecA promotes strand exchange best at pH 8.1 although it exhibits similar ATP hydrolysis rate in both higher and lower pH (Kim *et al.*, 2002) and shows more efficient binding to duplex DNA (Kim *et al.*, 2002). During DNA repair in *E. coli*, activation of RecA by LexA induces the SOS (error prone DNA repair) system (Friedberg, 1996), which involves expression of a series of genes including those that suppress cell division (*e.g.*, *sulA*), and prevent mutagenesis (*e.g.*, *umuD* and *umuC*). Characteristic of the SOS response, a few reports show that pre-exposure to low doses of ionization radiation, UV light or hydrogen peroxide increases the resistance of *D. radiodurans* to subsequent radiation (Tan and Maxcy, 1986; Wang and Schellhorn, 1995). However, investigation of RecA synthesis in *lexA* mutant strains of *D. radiodurans* has revealed that LexA is not involved in the induction of RecA (Narumi *et al.*, 2001) and supports that *D. radiodurans* does not display the classically defined SOS response system as observed in *E. coli*.

In an attempt to identify novel genes that contribute to recovery from DNA damage, Udupa and coworkers (1994) (Udupa *et al.*, 1994) generated 41 *D. radiodurans* mutants (by chemical mutagenesis) that are sensitive to ionization radiation (Udupa *et al.*, 1994). Further

investigation of one of these radiation sensitive strains, IRS24, which carries a mutation in an uncharacterized locus called *irrE*, revealed that it is a novel regulator of *recA* expression (Earl *et al.*, 2002a). The authors showed that mutation of this gene (DR0167) results in decreased *recA* expression following exposure to ionization radiation (Earl *et al.*, 2002a). Notwithstanding these reports, only few novel genes affecting radiation resistance in *D. radiodurans* have been identified. Over the last decade, this has confounded efforts to develop a clear understanding of the genetic systems underlying the extreme radiation resistance phenotype. Further complicating attempts to correlate *D. radiodurans*' ability to survive diverse forms of DNA damage, a recent report suggests that inactivation of two uncharacterized genes (DR1172 and DRB0118), that encode proteins similar to desiccation-induced proteins in plants, leads to desiccation sensitivity but not to sensitivity to ionizing radiation (Battista *et al.*, 2001). As such, these results (Battista *et al.*, 2001) weaken the hypothesis that the extreme radiation resistance phenotype is a secondary characteristic arising from the desiccation resistance phenotype, both of which are known to cause DNA DSBs (Daly *et al.*, 1994b; Mattimore and Battista, 1996). To date, the most unusual DNA repair system identified in *D. radiodurans* is the RecA-independent single-stranded DNA annealing pathway (Daly and Minton, 1996). This pathway, first reported in yeast (Fishman-Lobell *et al.*, 1992), was found to be active in *D. radiodurans* during and immediately after DNA damage and before the onset of RecA-dependent DNA repair, and accounted for repair of one third of all DSBs following exposure to acute irradiation (Daly and Minton, 1996). However, the genes encoding SSA in *D. radiodurans* repair remain unidentified.

1.3 New Technologies Developed For Analysis of Cellular Expression of RNA and Proteins.

The 50th anniversary of Watson and Crick's discovery of the structure of DNA highlights the beginning of a new where advances in molecular biology have made possible whole genome sequencing. And, unquestionably, one of mankind's greatest scientific triumphs has been the sequencing of the human genome (Venter *et al.*, 2000, Lander *et al.*, 2001). Rapid technological advances in DNA and protein analysis have followed this achievement and are transforming biology into a computationally driven science based on high-throughput technologies such as whole genome microarrays and high throughput proteomics.

1.3.1 DNA Sequencing

DNA sequencing is the process by which the accurate nucleotide order of a DNA strand is determined. DNA sequencing protocols developed by Sanger *et al.* (1977) (Sanger *et al.*, 1977) and Maxim and Gilbert (1977) (Maxim and Gilbert, 1977) have become the foundation of this extraordinary technique. The first complete genome sequence of a free-living organism (*Haemophilus influenzae*) was published in 1995 (Fleischmann *et al.*, 1995). Since then, 222 whole genome sequences have been deposited in Genbank and a further 134 genome projects are underway (http://www.ncbi.nlm.nih.gov/PMGifs/Genomes/bact.html). The first draft of the complete human genome was reported in June 2000 (Venter *et al.*, 2000; Lander *et al.*, 2001). The availability of the complete genome sequence of an organism plays an important role in understanding the unique characteristics associated with it. Biologists are now examining these genomes in an effort to decipher the many messages that Nature is presenting and rapid progress is being made in understanding life. The analysis of these genomes has already had a profound impact on human health, world agriculture, industrial bioproduction, and environmental biotechnology (*e.g.*, bioremediation with *D. radiodurans*).

The whole genome sequencing of free-living organisms from different taxonomic groups have further given rise to the field of 'functional genomics' that is dedicated to assigning (annotation) and experimentally confirming the function of open reading frames (ORFs). Programs such as Basic Local Alignment Search Tool (BLAST) (Altschul and Koonin, 1998; Altschul *et al.*, 1997) are used to compare newly sequenced genomes to those already annotated, thereby correlating the functional identity of predicted ORFs with other conserved genes and protein families. The current method of choice for DNA sequencing is the 'random shotgun method' which is a three-stage process: 1) Sequencing: Total DNA is purified from an organism and fragmented into short random segments (~2,000 bp). Segments are separately cloned, and individual clones analyzed by automated sequencing machines that read the linear DNA sequence of each biochemical "letter" (A, T, C, G) on a segment; 2) Assembly: Once the thousands of segments have been read, a super-computer arranges the information into contiguous sequences by finding overlaps on matching adjacent contiguous pieces (contigs); and 3) Annotation: Armed with the full sequence, bioinformaticists look for genes (*e.g.*, ftp://ncbi.nlm.nih.gov/pub/koonin/), and once genes are identified, researchers can begin to

confirm/determine the biochemical functions encoded by the genes (functional genomics) using high throughput approaches including DNA arrays that examine gene expression patterns.

1.3.2 DNA Microarrays

Whole genome DNA microarray chips now exist that allow expression analysis of entire genomes, where thousands of transcriptional profiles of unique messenger RNAs (mRNAs) can be examined simultaneously (Kurian et al., 1999). A typical DNA microarray chip consists of an orderly arrangement of either gene-specific PCR amplified sequences or oligonucleotides (Kurian *et al.*, 1999). Their potential applications span advances in identifying and treating human diseases (Toder, 2002), to understanding the responses in the simplest organisms adapting to changing environments (Tao *et al.*, 1999). DNA microarray technologies are based on three basic components: 1) a DNA array printer, 2) a spot fluorescence reader, and 3) computational and statistical analysis of data.

1. DNA array printer (http://www.gene-chips.com, Gershon, 2002): A highly sophisticated robotic printer equipped with special pins is used to spot cDNAs or oligonucleotides onto glass slides. The primary requirement for laying out a gene chip is the availability of a high quality whole or partial genome sequence. For example, the microarray construction of *D. radiodurans* was based on the entire genomic sequence data and annotation provided by The Institute for Genomic Research (TIGR, Rockville, MD) and the National Center for Biotechnology Information (NCBI), where a total of 3,195 putative open reading frames (ORFs) were assigned to its genome (Makarova *et al.*, 2001). For PCR, unique gene-specific primers were selected using, for example, the software PRIMEGENS (Xu *et al.*, 2002) (http://compbio.ornl.gov/structure/primegens/).
2. The florescence reader (http://www.gene-chips.com, Gershon, 2002): The hybridized array slides are scanned with a confocal laser scanner (*e.g.*, ScanArray™ 5000 microarray analysis system, GSI Lumonics, Watertown, MA), which detects the florescence emitted by the dyes used to label the cDNA (transcript probes) and generates hybridization images. Different florescent dyes are used to label the control and the experimental samples enabling differential expression display.

3. Computational analysis of data [http://www.gene-chips.com]: Specialized data quantification softwares such as Imagene5.2 convert the luminescence of hybridization images to numerical values. The images obtained from control and experimental samples are compared before quantification. Typically, the differences in labeling and detection efficiency of the two florescent tags are compensated using an internal control as a standard. Multiple replicate data points obtained from hybridization images are normalized and statistically analysed by software's such as GeneSpring (http://www.silicongenetics.com/cgi/SiG.cgi/Products/GeneSpring/index.smf), and ArrayStat (http://www.imagingresearch.com/products/AST.asp).

1.3.3 Proteomics

The differential expression of mRNA detected by microarray analysis cannot be directly correlated to protein levels in cells (Pandey and Mann, 2000; Shen and Smith, 2002) because of variability in the functional life span of mRNA and its protein products (Pandey and Mann, 2000). Therefore, a goal of high throughput genomic-based technologies has been to develop techniques that can determine the levels of distinct proteins within the environment of all cellular proteins. The cataloging of expression and structural analysis of every protein encoded within a sequenced genome is known as "Proteomics." The use of 2-D gel electrophoresis to resolve individual purified proteins from a mixture of thousands of proteins expressed by an organism (Pandey and Mann, 2000; Perkel, 2001) has until recently been the most common experimental approach in proteomics. However, 2-D proteomics is restricted by the large quantity of protein extract needed for analysis, lack of reproducibility, inability to resolve large proteins (*e.g.*, proteins with a size >100 kDa), extremely basic or acidic proteins, and membrane proteins. Many of these limitations have been overcome by recent advances in mass spectrometry (MS) (Perkel, 2001). Identification of proteins/peptides by MS involves their ionization into a gaseous phase (Figure 1.4) and separation using powerful magnetic fields, yielding mass (m) and charge (z) ratios that are specific to individual proteins/peptides (Pandey and Mann, 2000). For even higher resolution, tandem MS (see below) can be coupled with capillary separation techniques such as liquid chromatography and used to separate and analyze complex mixtures of proteins, based on extremely high resolution of peptides regardless of their size or polarity. When

correctly identified, these peptides have mass/charge ratios that are diagnostic of the proteins from which they are derived, and are referred to as 'acurate mass tags' (AMTs) (Lipton *et al.*, 2002). Furthermore, following purification of whole protein complexes (*e.g.*, epitope-tagging) (Mann *et al.*, 2001), protein-protein interactions also can be defined using the AMT-tandem MS approach. The mass spectrometric separation of proteins usually involves three components:

1. An ionizing source (Mann *et al.*, 2001): Ionizing sources such as matrix-assisted laser desorption ionization (MALDI) (Figure 1.4) or electrospray ionization (ESI) impart an electrical charge to peptide molecules. MALDI requires solid samples, which are mixed with an excess of matrix materials such as α-cyano-4-hydroxycinnamic acid or dihydrobenzoic acid and precipitated, and where subsequent exposure of this precipitated peptide matrix to laser light (337 nm) positively charges the molecules. In contrast, ESI is a liquid phase method where peptides are electrically charged by passage through a small capillary tip in the presence of an electric charge (Perkel, 2001).
2. An analyzer (Mann *et al.*, 2001): Once the peptide molecules are ionized, the MS instrument calculates its m/z ratio. The most commonly used mass analyzers are the time-of-flight (TOF), triple-quadrupole, quadrupole-TOF and ion trap instruments. TOF assumes that the ionized peptides have the same kinetic energy (mass x velocity) and hence can be separated by their masses (*i.e.*, the larger the masses are, the slower the peptides move, and the greater their flight-path is deviated). The quadrupole analyzers have four chambers with varying electric fields in them. So, ions with only certain mass/charge ratios are able to reach the detector. The TOF method is most commonly used in combination of MALDI while the quadrupole analyzers are used with ESI. Ion traps, on the other hand, capture the continuous beam of ions up to the limit of their space charge (maximum number of ions that can be introduced into the instruments without distorting the applied field) (Mann *et al.*, 2001). The ions are then subjected to additional electric fields, which eject one ion species after another from the trap, and are detected, to produce a mass spectrum (Pandey and Mann, 2000; Mann *et al.*, 2001; Perkel, 2001).

Figure 1.4. Schematic Diagram of MALDI Process and Instrument. (A) A sample cocrystallized with the matrix is irradiated by a lazer beam, leading to the sublimation and ionization of peptides. (B) About 100-500 ns after the laser pulse, a strong acceleration field is switched on (delayed extraction), which imparts a fixed kinetic energy to the ions produced by the MALDI process. These ions travel down a flight tube and are turned around in an ion mirror, or reflector, to correct for initial energy differences. The mass-to-charge ratio is related to the time it takes to reach the detector; the lighter ions arrive first. The ions are detected by a channeltron electron multiplier. [Adapted from Mann *et al.*, Annu Rev Biochem.70:443].

Figure 1.4

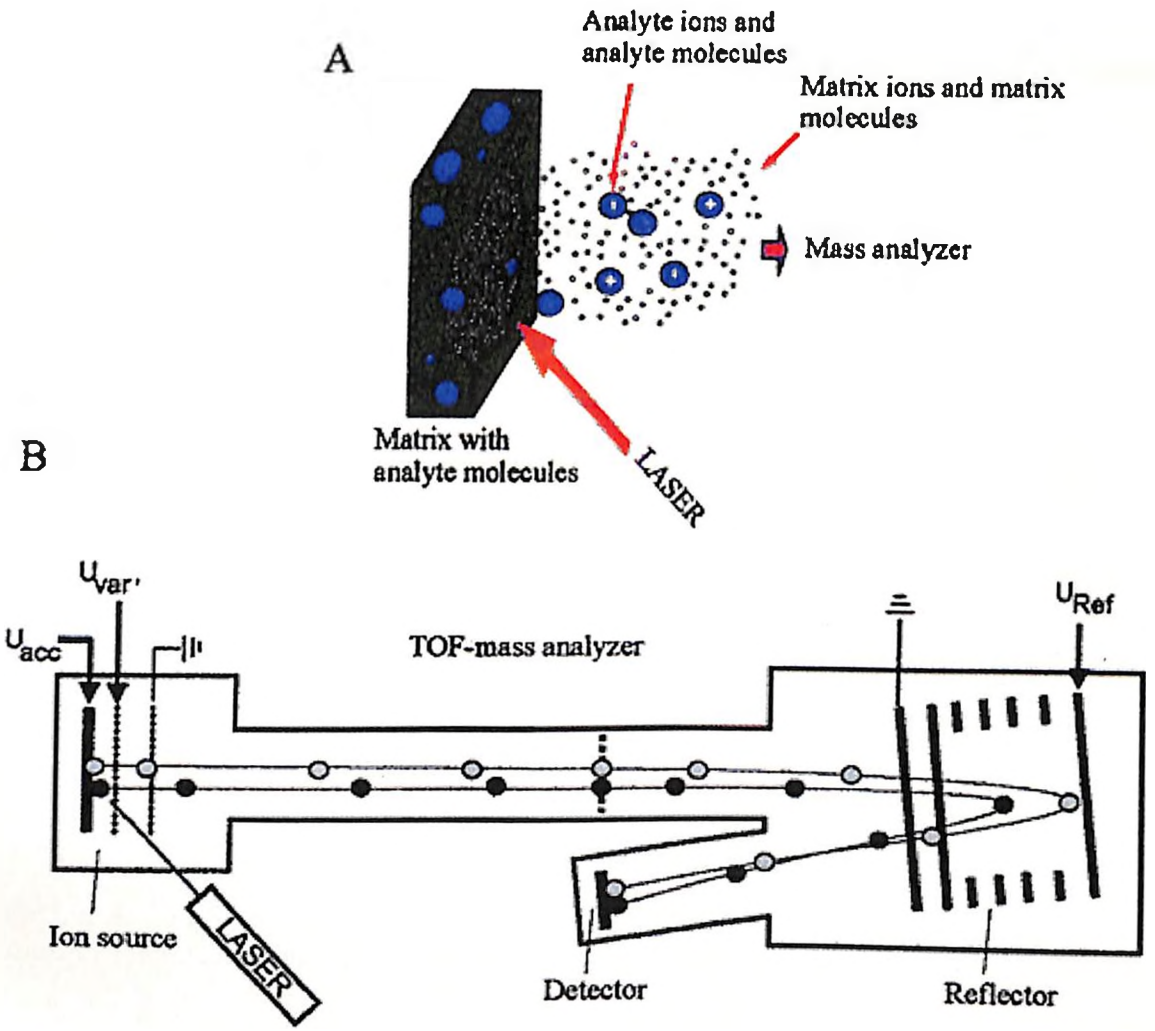

Mann *et al.*

3. The Detector (Mann *et al.*, 2001): The mass spectrum of a mixture of peptides is obtained by scanning the amplitude of the electric field and recording the ions at the detector. Based on their arrangement in relation to the analyzer, there are two types of mass spectrometers, the MS and MS/MS (tandem MS). Although the MS/MS configuration is a slower process when compared to MS, this method can be used to detect specific amino acids of certain peptides and sometimes even the sequence of these amino acids within peptides (Pandey and Mann, 2000; Perkel, 2001).

The applications of proteomics include identification of proteins, analysis of their post-translational modifications, and interactions. A new program, sponsored largely by the Department of Energy and the National Institutes of Health, is being conducted at a series of research centers dedicated to a branch of proteomics known as 'structural genomics'. The structural centers are detailing, over the next ten years, the shapes of 10,000 proteins most relevant to biology and medicine. Smaller groups, including the *Deinococcus* group at USUHS, are exploiting the early sequencing of their research organisms as a head-start in the development of high-throughput proteomic approaches (Lipton *et al.*, 2002; Smith *et al.*, 2002a, 2002b).

1.4 Specific Goals of Thesis

Research presented in this thesis aims to further define the multiple cellular components expressed by *D. radiodurans* that determine its resistance to ionizing irradiation. The work was conducted using experimental approaches that are based on a combination of physiologic, molecular, and computational biology, as well as recent developments in whole cell analysis by DNA arrays. These approaches were central to the conducted research on developing a better understanding of the global interactions between multiple cellular components and the functional networks within which they operate in *D. radiodurans*. The specific aims were as follows:

1. (Chapter 2): To examine the possibility that extreme radiation resistance could have evolved in permafrost-like conditions. Recent *D. radiodurans* mutant analyses suggest that genes encoding desiccation and radiation resistance may have evolved separately. This study examined the relationship between the age and radiation resistance amongst bacteria isolated from 3,000 – 15,000,000 year old permafrost with comparison to novel radiation resistant bacteria isolated from desiccated environments. Nutrient conditions were found to affect the radiation resistance phenotype.

2. (Chapter 3): To develop a defined minimal medium for growth of *D. radiodurans* as a tool to examine the relationship between metabolism and radiation resistance. This study identified key nutritional components that govern its radiation resistance phenotype, and how defects identified in its metabolic configuration may contribute to resistance functions. Dependence on amino acids, carbon sources, and metals was examined.

3. (Chapter 4): To examine the relationship between metabolism, oxidative stress, and radiation resistance in the family *Deinococcaceae*. This study demonstrates the global importance of metabolism in the family *Deinococcaceae* to their resistance phenotypes.

4. (Chapter 5): To study the expression dynamics of *D. radiodurans* recovering from exposure to acute ionization radiation. Using a whole genome DNA microarray for *D. radiodurans*, its transciptome dynamics were examined following high dose irradiation. This study supports the existence of novel DNA repair genes and that metabolic regulation in *D. radiodurans* plays an important role in its extreme resistance phenotype.

Chapter 2: Possible Evolutionary Mechanisms Contributing to the Appearance of the Extreme Radiation Resistance Phenotype

2.1 Introduction

The evolution of organisms that are able to grow continuously at 60 Gy per hour (Lange *el al.*, 1998) or survive acute irradiation doses of 15 kGy (Daly and Minton, 1995a, 1996, 1997) is remarkable given the apparent absence of highly radioactive habitats on Earth over geologic times. Notwithstanding a few natural fission reactors like those that gave rise to the Oklo uranium deposits (Gabon) 2 billion years ago (Naudet, 1976), the radiation levels in the Earth's surface environments, including its waters containing dissolved radionuclides, has provided only about 0.0005-0.20 Gy/year over the last 4 billion years (Sorenson, 1986). DNA damage is readily inflicted on organisms by a variety of other common physico-chemical agents (*e.g.*, ultraviolet light or oxidizing agents) or non-static environments (*e.g.*, cycles of desiccation/hydration, or high and low temperatures) and it seems more likely that radiation resistance evolved in response to chronic exposure to non-radioactive forms of DNA damage. Rapid advances in microbial genetics and molecular biology over the last half century have revealed that the major cause of lethality in organisms exposed to radiation is the generation and accumulation of genomic DSBs (Sweet and Moseley, 1974, 1976) (Minton, 1994) (Daly and Minton, 1996) (Mattimore and Battista, 1996). Radiation can be delivered as an acute dose, where metabolically inactive organisms (*e.g.*, dormant cells on ice; 0 °C) are exposed to high dose-rate irradiation, and which leads to the accumulation of genetic damage. Alternatively, metabolically active cells can be exposed to chronic radiation, where organisms may have the capacity to repair damage as it is growing (*e.g.*, irradiation of cells at growth temperatures and in the presence of a growth substrate). In the laboratory, an acute dose of irradiation is typically delivered by ^{60}Co (at ~10 kGy/h) at 0 °C, whereas resistance of cells to chronic radiation is tested in rich medium in the presence of a ^{137}Cs source (50 Gy/hour).

The number of irradiation-induced DSBs inflicted on an organism is believed to depend on a number of factors including genome size and irradiation dose (Minton, 1994) (Daly and Minton, 1996), but much is still not understood. For example, it is unknown how the metabolic

environment of a cell affects the amount of DNA damage deposited by radiation. Presumably the frequently cited 80:20 ratio of indirect versus direct damage caused by ionizing radiation under aerobic conditions (Repine *et al.*, 1981) could be affected by the known diversity of intracellular environments, but this has not yet been reported. In 1954, Rebecca Gershman and Daniel L. Gilbert (Gilbert, 1981) drew a parallel between the effects of O_2 and those of ionizing radiation and proposed that most of the toxic effects of O_2 to organisms could be attributed to the formation reactive oxygen radicals (ROS) such as superoxide ions ($O_2^{\bullet-}$), peroxides (RO_2) and hydroxyl radicals ($^{\bullet}OH$) (Gottschalk, 1985) (*e.g.*, Figure 2.10) (Halliwell and Gutteridge, 1999). The generation of energy in aerobic bacteria by the electron transport chain also leads to the production of ROS. Irrespective of the source of ROS, these free radicals are extremely damaging to biological macromolecules including DNA, proteins, and lipid components of the cell. (Schulte-Frohlinde, 1986; Zaider *et al.*, 1994).

Mattimore and Battista (1996) have shown that in *D. radiodurans*, genes that are necessary to survive irradiation are also necessary for desiccation resistance. However, a recent report by these authors (Battista *et al.*, 2001) has shown the existence of genes that affect desiccation resistance but not radiation resistance in *D. radiodurans*, indicating that resistance to these conditions may involve different mechanisms. Environments on earth that could have delivered high doses of acute irradiation, on the order of millions of Gy, include those, which have been frozen continuously for millennia (Friedmann, 1993). It is within such frozen environments, such as permafrost (Price *et al.*, 2002), that trapped organisms could be subjected to immense doses of background radiation. For example, a bacterium encased in ice for 2,000,000 years would accumulate about 1,000 Gy of background radiation. Unless DNA damage is prevented or is repaired, lethal doses of irradiation will be accumulated over long time spans. Environments subjected to periods of permafrost may have provided a selective environment within which radiation resistance evolved. Friedmann and coworkers (1997) (Shi *et al.*, 1997) isolated and partially characterized viable bacteria from permafrost core samples from Kolyama-Indigirka lowland of northeast Siberia. The organisms were isolated from different depths representing the age of the permafrost layer and hence the period of dormancy of the bacteria. An analysis of the radiation resistance profiles of these bacteria from permafrost, therefore, might identify a relationship between the time of their survival and radiation

resistance. Bacteria isolated from permafrost (Friedmann, 1993) could then be compared to those isolated from environments known to be enriched in radiation resistant microorganisms, *i.e.*, soil samples from arid environments (*e.g.*, dessert conditions).

In this study, radiation resistance profiles were constructed for bacteria isolated from diverse environments including Siberian permafrost, soil samples from Asia and North America, and from beneath radioactive DOE storage tanks. A novel Two-Dimensional (2-D) fingerprint technique was developed to distinguish the USUHS *D. radiodurans* strains from novel deinococcal isolates. Finally, based on the published *D. radiodurans* genomic sequence, a theoretical model of *D. radiodurans* metabolism was constructed and used to develop a hypothesis on how its metabolic configuration could facilitate its resistance to radiation. The specific aims of this chapter are as follows:

1. **To test the hypothesis that radiation resistant bacteria may be enriched in ancient permafrost and that such environments could promote the evolution of radiation resistant organisms.**

2. **To compare the radiation resistance characteristics of known and novel radiation resistant bacteria isolated from dry environments, and to identify any distinct or common traits shared with radiation resistant bacteria isolated from permafrost.**

3. **To confirm that two novel *D. radiodurans* isolates from beneath a highly radioactive tank at the DOE Hanford facility in south-central Washington state are distinct from the USUHS *D. radiodurans* strain R1. To achieve this goal, a novel method was developed to display a theoretical and experimentally derived genome fingerprint.**

4. **To reconstruct a theoretical metabolic pathway map for *D. radiodurans* and to examine if its configuration could facilitate its radiation resistance.**

2.2 Materials and Methods

2.2.1 Bacterial Strains and Their Growth

The bacterial strains used in this study are listed in Table 2.1, 2.2 and 2.3. The strains were grown at the indicated temperatures in either TGY (1% tryptone, 0.5% yeast extract and 0.1% glucose) or PTYG (1% glucose, 1% yeast extract, 0.5% peptone, 0.5% tryptone, 0.06% $MgSo_4.7H_20$, and 0.007% $CaCl_2.2H_2O$) broth. For solid medium, 1.5% w/v Bacto-agar (Difco) was added. All chemicals in this work were obtained from Sigma (St. Louis, MO) unless stated otherwise.

2.2.2 Viable Bacterial Strains from Northeast Siberia

A collection of 26 viable bacterial strains originally isolated by Friedmann and coworkers (1997) (Shi *et al.*, 1997) from permafrost core samples of Kolyama –Indigira of northeast Siberia were investigated (Table 2.1). Permafrost samples were originally obtained by means of drilling in northeast Siberia (Shi *et al.*, 1997). Samples representing three different horizons were identified; the upper Alas layer (youngest layer) is 3m deep and is 2000-5000 years old; Yedoma suite extends from 3-8m in depth and is about 40,000-50,000 years old; Olyor suite (oldest layer) extends from 8-50m in depth and is about 0.6-3 million years old (Shi *et al.*, 1997).

2.2.3 Isolation of Novel Radiation Resistant Soil Bacterium

Soil samples collected from different parts of North America and India were mixed with 25 ml TGY broth and allowed to grow at 32 °C for 48 hours. Cultures in the stationary phase were exposed to an acute dose of radiation (10 kGy) without change of broth on ice and allowed to recover for 48 hours at 32 °C on TGY plates. Distinct colony types on the plates were purified by sub-culturing on fresh TGY plates. Purified isolates were grown in TGY broth, concentrated by centrifugation, frozen, and stored at –80 °C in 50% sterile glycerol solution. The radiation resistant colonies thus obtained were further tested for their ability to grow under chronic

radiation (50 Gy/hour) (^{137}Cs Gammacell 40 irradiation unit [Atomic Energy of Canada Limited]) (Table 2.2).

2.2.4 Bacterial Strains from Beneath a Highly Radioactive Leaking Waste Tank

Fredrickson and coworkers (2000) (Fredrickson, unpublished data) (Fredrickson *et al.*, 2003) isolated more than 110 cultures of aerobic heterotrophic bacteria from core samples collected from the vadose zone (unsaturated zone above the water table) beneath the SX-108 waste tank of the 200W SX tank farm on the U.S. DOE's Hanford Site in south-central Washington. Four distinct bacterial strains (Table 2.4) were made available to our laboratory for this study. Details of core sample extraction and bacterial isolation are reported elsewhere (Fredrickson *et al.*, 2003). Figure 2.1 gives a schematic diagram describing the various zones and contaminants associated with a typical DOE contaminated plume.

The vadose zone layer consists of high concentrations of alkali, nitrate, aluminate, Cr(VI) and ^{137}Cs [(Jim Fredrickson, unpublished data)] and significant desiccation and heating of this region has been predicted due to the radioactive decay of short-lived isotopes and high concentrations of ^{137}Cs associated with high-level radioactive waste (HLW) (Fredrickson *et al.*, 2003).

Figure 2.1. The Vadose Zone. Sample contaminant plume consisting of mixed waste resulting from percolation from leaky tanks, land fills, basins, and trenches, as well as being formed through direct injection. Note the Vadose zone. Adopted from "Bioremediation of metals and radionuclides...what it is and how it works", Natural and Accelerated Bioremediation Research Program (NABIR), U.S. Department of Energy.

Figure 2.1

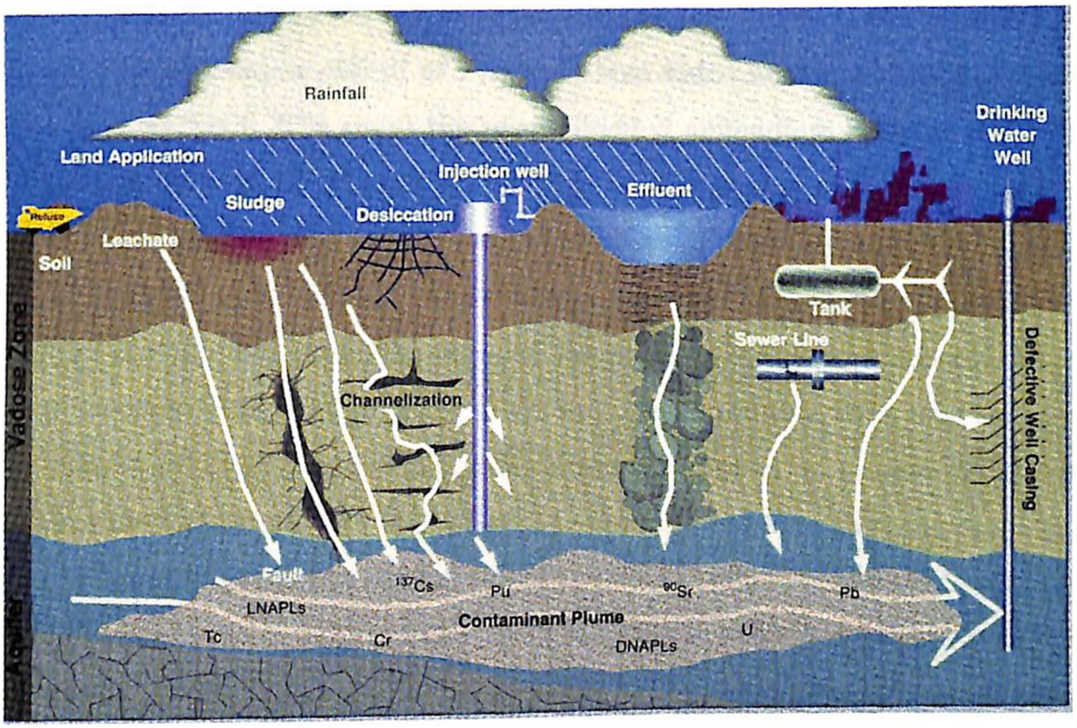

Mccullough *et al.*

2.2.5 Two-Dimensional (2-D) Genome Fingerprinting Analysis of Strains 7B-1 and 7C-1 and their Comparison to *D. radiodurans*

2.2.5.1 Genomic DNA Extraction

Strains were grown in 5 ml of TGY broth and incubated at 30 °C to late stationary phase. Aliquots (1.5 ml) of these cells were pelleted in a microcentrifuge. The pellets were then resuspended in 570 µl of TE buffer (10 mM Tris-HCl, pH 8; 1 mM EDTA) containing 20 µl of 20% sodium dodecyl sulphate (SDS) and 15 µl of 20 mg/ml proteinase K, and incubated at 37 °C for 45 minutes. To the solution, 100 µl of 5 M NaCl was added followed by 80 µl CTAB/NaCl solution [4.1% (w/v) NaCl, 10% (w/v) Hexadecytrimethyl ammonium bromide (CTAB)]. The samples were incubated at 65 °C for 10 minutes to disrupt the cell wall integrity. The chromosomal DNA was purified with an equal volume of 24:1 chloroform/isoamylalcohol solution. The solution was mixed by vortexing and centrifuged for 5 minutes in a microcentrifuge at room temperature to separate the aqueous and organic phases. The upper aqueous phase containing the total genomic DNA was transferred to a fresh tube and extracted with equal volume of 25:24:1 phenol/chloroform/isoamyl alcohol to remove all the protein membrane components. The solution was mixed by vortexing and spun in a microcentrifuge for 5 minutes. The upper aqueous phase was transferred to a fresh tube and nucleic acids were precipitated with 0.6 volume isopropanol. The precipitated nucleic acids were pelleted by microcentrifugation at 4 °C and resuspended in 50 µl TE buffer. The nucleic acids were then subjected to RNAse treatment. The concentration and purity of the DNA samples were determined by spectrophotometric ratio assay at 260 nm and 280 nm.

2.2.5.2 Two-Dimensional (2-D) Electrophoresis

Selection of Restriction Enzymes. Selection of enzymes for genome fingerprinting analysis was based on two criteria; 1) digestion of total genomic DNA of *D. radiodurans* R1 by the selected enzymes should yield DNA fragment sizes that can be clearly resolved by conventional agarose gel electrophoresis, and 2) Over digestion of DNA with the selected enzymes should not lead to 'star' activity of the enzyme. 'Star' activity of an enzyme refers to its

Figure 2.2. Two-Dimensional (2-D) Fingerprint Analysis. *Panel A.* Ethidium bromide stained agarose gel following 2-D electrophoresis. *D. radiodurans* genomic DNA was digested with *ApaL*I and electrophosed in a 0.5% agarose gel (not shown). A thin vertical gel lane containing the cleaved DNA was cut from the gel and digested with *Nsp*I. The gel lane with the double-digested DNA was placed horizontally in a new gel and electrophoesed yielding a 2-D spread of genomic DNA fragments. *Panel B.* Computer predicted spread of *D. radiodurans* genomic DNA similarly treated. Arrows show position of *D. radioaurans recA* (DR2340), which is central to genomic restoration following irradiation (Minton, 1994). λ/H, lambda phage DNA cut with *Hind*III.

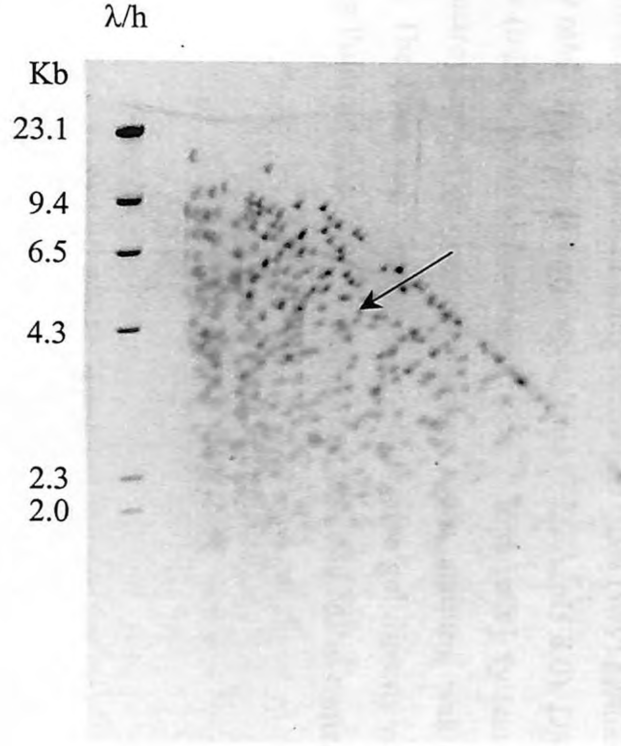

A

Figure 2.2

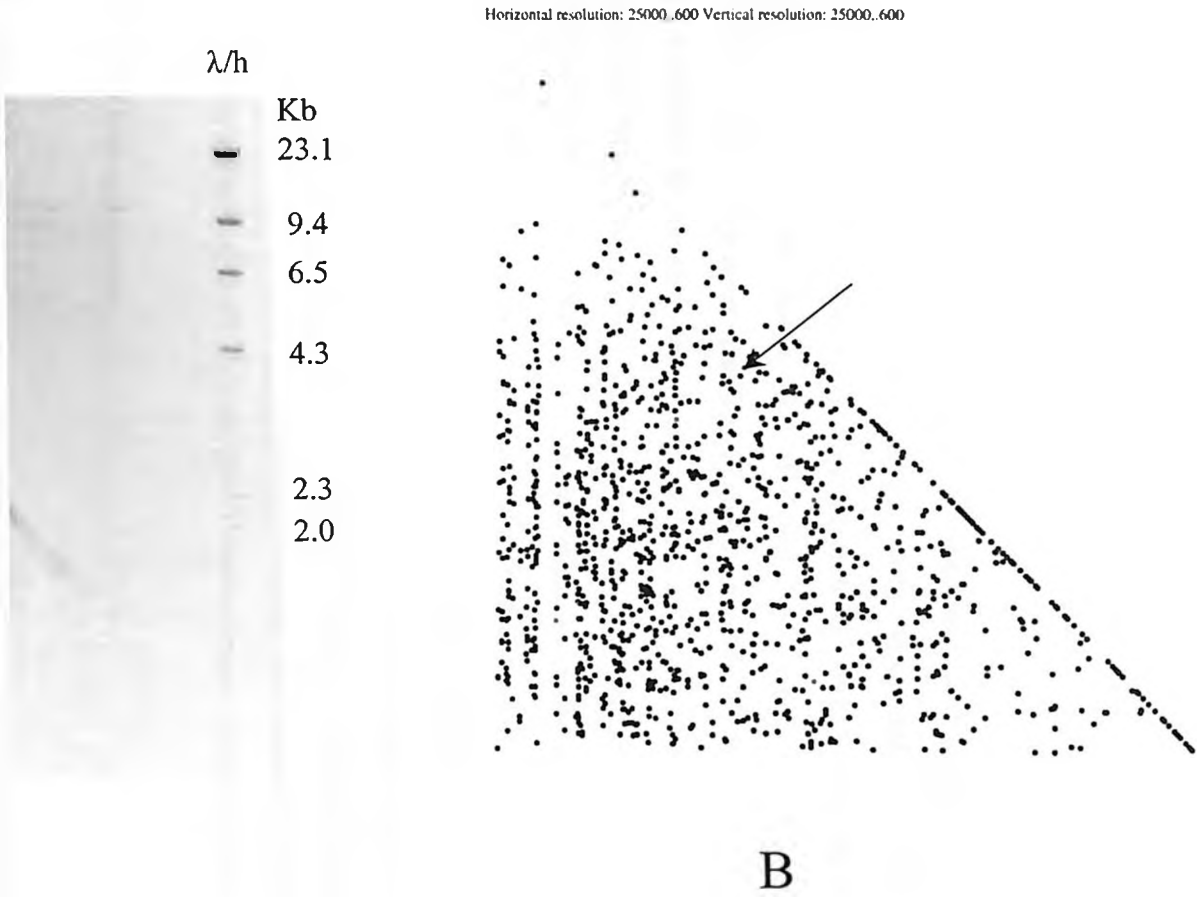
Horizontal resolution: 25000 .600 Vertical resolution: 25000..600
λ/h
Kb
23.1
9.4
6.5
4.3
2.3
2.0
B

ability to cleave sequences, which are similar but not identical to their defined recognition sequence. Star activity may occur under extreme non-standard conditions or due to over-digestion. Based on these criteria, *D. radiodurans* genomic DNA was digested by enzyme *ApaI* followed by *in situ* digestion with enzyme *Nsp*I.

DNA Digestion and 2-D Gel Electrophoresis. Enzymes and buffers used in this study were purchased from New England biolabs, Inc. (Beverly, MA) and were used according to manufacturers' instructions. About 80 μg of total genomic DNA (concentration ~ 1 μg/μl) previously extracted from *D. radiodurans* R1, 7B-1 and 7C-1, were digested with 80 units of enzyme *Apa*LI in a 200 μl digestion reaction by incubation at 37 °C for 1.5-3 hours. The fragments were separated by agarose gel electrophoresis (0.5% w/v agarose) in two separate lanes. One half of gel containing one of the two lanes with the digested DNA was stained with ethidium bromide to visualize the DNA. Using the ethidium bromide stained gel as a reference for migration of DNA fragments, a thin vertical gel lane containing DNA was removed from the unstained gel and subjected to *in situ* cleavage with an excess of enzyme *Nsp*I at 37 °C for 15 hours. Once the digestion of embedded DNA was complete, the gel strip was set horizontally in a new gel, and electrophoresed again yielding a 2-D spread (Figure 2.2A) of fragments that were transferred to a hybridization membrane by Southern blotting. The membrane was hybridized with 24 probes randomly generated by PCR from the *D. radiodurans'* genomic DNA.

2.2.5.3. Agarose Gel Electrophoresis

DNA fragments were separated using horizontal 0.5% (w/v) agarose slab gels in 1X TBE running buffer (89 mM Tris, 89mM boric acid, 2 mM EDTA, pH 8.0). DNA samples containing 1X loading buffer (0.25% [w/v] bromophenol blue, 0.25% [w/v] xylene cynol FF, 30% [w/v] glycerol) were electrophoresed at constant voltage. DNA staining was done with 0.5 μg/ml ethidium bromide. The DNA was visualized by placing the gel directly on a UV light box and photographed using Polaroid type 55 or 57 film with a Polaroid MP-4 camera.

2.2.5.4 Southern Transfer

DNA in the gel was depurinated by incubating the gel in 0.25 N HCl for 15 minutes with gentle shaking, followed by denaturation with 0.4 N NaOH-0.6 M NaCl solution for 30 minutes and neutralization in 1.5 M NaCl-0.5 M Tris pH8.0. The denatured DNA fragments were then transferred onto a nylon-based membrane (Gene Screen Plus, NEN Life Science Products) by capillary transfer method. After Southern transfer, the DNA was fixed on the nylon membrane by exposure to UV light for 2 minutes.

2.2.5.5 Preparation of ^{32}P DNA Probe

Twenty-four PCR fragments representing each of the 4 *D. radiodurans*' genome components were used as templates to generate the radiolabelled probe mixture. The PCR sequences were originally generated at TIGR (Table 2.4). Random priming method was used for radiolabeling. Random sequences of hexanucleotides were hybridized to the previously denatured double-stranded fragments. The 3' OH ends of the hexanucleotides were used as the polymerizing starting point by the Klenow fragment. In the process of polymerization, a mixture of the dNTPs (A, T and G plus ^{32}P labelled dCTP) was used to generate the radiolabelled probes.

2.2.5.6 Pre-hybridization

The membrane was prehybridized before incubation in hybridization solution to block any non-specific binding of the single stranded probe onto the membrane. Calf thymus DNA (10 mg/ml) was used with the prhybridization buffer as the blocking agent. The prehybridizaion mixture had the following composition: 4 ml 20xSSPE (17.53% [w/v] NaCl, 0.276% [w/v] NaH2Po4, 0.00074% EDTA, pH 7.4; Biofluids Inc., Rockville, MD), 2 ml 20% SDS, 2 ml BLOTTO (10% w/v skim milk) and 31 ml sterile water. Prehybridization was carried out for 3 hours at 65 °C.

2.2.5.7 Hybridization

After the completion of prehybridization, the prehybridization solution was replaced with the hybridization solution containing the denatured radiolabelled probes. The hybridization buffer had the following composition: 3 ml 20X SSPE, 1.5 ml 20% SDS, 1.5 ml BLOTTO (10% w/v skim milk), 4 ml Dextran Sulfate 25% and 20 ml sterile water. Hybridization was carried out for 18-20 hours at 65 °C.

2.2.5.8 Computer Program

A computer program to predict the migration positions of DNA fragments generated by the 2-D electrophoresis analysis of *D. radiodurans*' genomic DNA (Figure 2.2B) digested with enzyme *ApaLI* and *Nsp*I was developed by Drs. Yuri Wolf and Kira Makarova at the National Center for Biotechnology Information (NCBI), National Institute of Health (NIH), Bethesda, MD. The comparison of an ethidium bromide stained agarose gel showing the migration the 2-D digested *D. radiodurans* genomic DNA fragments with the computer predicted spread of the genomic DNA similarly treated is shown in Figure 2.2.

2.2.6 Generation of Radiation Survival Curves

All bacterial strains were grown to their stationary-phase (OD_{600} = 0.9-1.2) in the indicated growth medium and temperatures. Cells were irradiated without change of broth on ice with ^{60}Co at 10 kGy/h (^{60}Co Gammacell irradiation unit [J. L. Shepard and Associates, Model 109]). At the indicated doses, viable cell counts were determined by plating appropriate cell dilutions for colony formation units (CFU) on either TGY agar or PTGY agar at their respective optimal growth temperature. Viability data was used to construct survival curves.

2.2.7 Exposure to Chronic Radiation

All strains were grown in the presence of continuous γ-radiation (50-60) Gy/hour in a ^{137}Cs Gammacell 40 irradiation unit (Atomic Energy of Canada Limited [Ottawa]) at 24 °C. *E. coli* (wild-type strain AB1157) was used as a negative control. Survival rates were determined by plating appropriate dilutions of irradiated cells and counting the colony forming units (CFU) on plates.

2.2.8 Preparation of *D. radiodurans* Competent Cells and Transformation

Competent *D. radiodurans* cells were prepared by using the procedure originally developed by Tirgari and Moselay (1980) (Tirgari and Moselay, 1980). *D. radiodurans* cultures previously grown in TGY broth for 18 hours were diluted in 1:10 ratio into fresh TGY broth and were incubated at 32 °C in a baffled 250 ml flask until an OD_{600} of 0.5 was obtained. The cells were pelleted and resuspended in freshly prepared TGY containing 100 mM $CaCl_2$ and 10% glycerol. To *D. radiodurans* competent cells thus obtained (100 µl), 1-5 µg of DNA was added in a sterile 50 ml tube. The solution was mixed gently and placed on ice for 10 minutes followed by incubation at 32 °C for 30 minutes with gentle shaking. To the transformation mixture, 900 µl sterile TGY was added followed by incubation at 32 °C with vigorous shaking. After 18 hours of incubation, 100 µl of the transformation mixture was spread on appropriate selective agar.

2.2.9 Fatty Acid Profiles and their Library Matches

Selected novel radiation resistant strains were sent to Microbial ID inc., DE, for their identification. An organism was identified by comparing its fatty acid similarity index to the mean fatty acid composition of the strains used to create a library. An exact match of the fatty make-up of an unknown sample to the mean of a library entry results in a similarity index of 1.000. The similarity index will decrease as each fatty acid varies from the mean percentage; a similarities of 0.600 or higher are good matches, where a similarity index of 0.400-0.600 is a

species match, while values lower than 0.400 suggest that the species is not in the database [http://www.microbialid.com/NewFiles/DatabasePage.html].

2.2.10 Transmission Electron Microscopy (TEM)

TEM was a collaborative effort with Dr. Alexandar Vasilenko at USUHS, Bethesda, MD. Briefly, bacterial suspensions were rinsed in 0.1 M cacodylate buffer (pH 7.4), fixed in 2.5% gluteraldehyde in the same buffer, and postfixed in osmium tetraoxide. Fixed samples were embedded in Epon-araldite resin, and 50-70 nm sections were cut from these and stained with uranyl acetate followed by lead citrate (Reynolds, 1963). Samples were examined with a Philips CM 100 electron microscope, yielding 16,000-41,000 x magnification. Images were captured by a Kodak Megaplus camera (model 1.4) using ATM Camera software.

2.3 Results

Experimental Rationale

The goal of this study was to identify if there is a common basis for radiation resistance in organisms isolated from diverse environments (*e.g.*, between radiation resistant bacteria isolated from permafrost and dessert conditions). This approach was supplemented by a computational analysis of the *D. radiodurans* genome that considered how its metabolic configuration might be contributing to its resistance phenotype.

2.3.1 Radiation Resistance of Novel Bacterial Strains

2.3.1.1 Defining Radiation Resistance

The term 'radiation resistant' is a comparative description that relates the resistance of two or more organisms. *D. radiodurans* is typically referred to as 'extremely radiation resistant' because cultures can survive doses of irradiation greater than 10 kGy. The D_{37} for a *D.*

radiodurans tetracoccus is ~15 kGy; pure diplococcus culture, ~8 kGy. By comparison, a culture of single-celled *E. coli* is referred to as 'radiation sensitive' because it cannot survive exposures greater than 1 kGy. However, *E. coli* is considered radiation resistant compared to mammalian cells. Thus, for the purposes of this thesis bacterial radiation resistance has been broadly divided into 3 categories: 1) extreme resistance: cells with a D_{37} >4 kGy (*e.g.*, *Deinococcal* species); 2) moderate resistance: cells with a D_{37} of 1-4 kGy (*e.g.*, *Bacillus* species); and 3) radiation sensitive: cells (*e.g.*, *E. coli*) with a D_{37} of <1 kGy.

2.3.1.2 Viable Strains from Siberian Permafrost

Previously, permafrost samples were collected by Freidmann and coworkers (1989-1990) (Shi *et al.*, 1997) from northeastern Siberia (Kolyma Indigirka lowland) (Shi *et al.*, 1997), and a collection of twenty-six distinct bacteria isolated from those environmental samples were made available to our laboratory for study in 2001. The twenty bacterial strains examined for resistance to irradiation are listed in Table 2.1 and have been divided into 2 groups based on their age. The first group (group I) includes bacteria isolated from the oldest (deepest layer) permafrost (from the Olyor suite, 0.6–3 million years old) and the second group (group II) includes bacteria isolated from the youngest permafrost (Alas and Yedoma zones, 3,000-8,000 years old) (Table 2.1). In Figures 2.3 and 2.4, the ionizing irradiation resistance profiles of group I and group II bacteria are presented.

Radiation Resistance of Group I and II Bacteria. Three (MD832, MD836 and MD840) of the twelve group I strains displayed moderate resistance to acute irradiation (Figure 2.3). The remaining group I strains were radiation sensitive. Strains MD832 and MD836 could grow under chronic irradiation (50 Gy/hour), but strain MD840 and the other group I strains could not (Table 2.1).

None of the 8 bacteria of group II displayed moderate resistance to acute irradiation (Figure 2.4). Only strain MD846 was able to grow under chronic irradiation (Table 2.1). Therefore, it appears that the ability to survive acute doses of irradiation is distinct from a strain's ability to grow under chronic radiation, and vice versa.

Table 2.1. Phenotypic Characteristics of Bacteria from Siberian Permafrost

*Strain number	#Genebank accession number	#Age of original sample (Years)	#Cell Shape	#Gram stain	#Optimal Growth Temp. (°C)	#Affiliation[a]	#Spore	[1]Growth medium	[2]Growth under chronic irrradiation (50 Gy/Hour)	[3]Resistance to acute irradiation $^{4}D_{37} \sim 1\text{-}4$ kGy
Group I										
MD830	U31495	$1.8x10^6$	Coccus	-ve	32°C	β-pr	-	TGY	No	No
MD831	U31484	$1.8x10^6$	Short rod	-ve	32°C	HGC	-	PTGY	No	No
MD832	U31491	$1.8\text{-}3.0x10^6$	Rod	+ve	32°C	LGC	+	TGY	Yes	Yes
MD833	U31490	$1.8\text{-}3.0x10^6$	Coccus	-ve	32°C	γ-pr	-	TGY	No	No
MD834	U31493	$1.8\text{-}3.0x10^6$	Rod	+ve	32°C	HGC	-	PTGY	No	No
MD835	U31494	$1.8\text{-}3.0x10^6$	Shot rod	-ve	32°C	β-pr	-	PTGY	No	No
MD836	U31483	$3.0x10^6$	Short rod	+ve	32°C	HGC	-	TGY	Yes	Yes
MD837	U31497	$3.0x10^6$	Short rod	-ve	32°C	γ-pr	-	TGY	No	No
MD838	U31498	$3.0x10^6$	Short rod	-ve	32°C	γ-pr	-	TGY	No	No
MD839	U31477	$1.8\text{-}3.0x10^6$	Short rod	+ve	32°C	HGC	-	PTGY	No	No
MD840	U31478	$1.8\text{-}3.0x10^6$	Filamentous	-ve	32°C	β-pr	-	TGY	No	Yes
MD841	U31487	$1.8\text{-}3.0x10^6$	Rod/ Coccus	+ve	20°C	HGC	-	PTGY	No	No
Group II										
MD842	U31488	$5\text{-}8x10^3$	Rod	-ve	32°C	LGC	+	TGY	No	No
MD843	U31472	$5\text{-}8x10^3$	Rod	-ve	32°C	LGC	-	TGY	No	No
MD844	U31473	$5\text{-}8x10^3$	Rod	-ve	32°C	LGC	+	TGY	No	No
MD845	U31474	$5\text{-}8x10^3$	Coccus	-ve	32°C	β-pr	-	TGY	No	No
MD846	U31476	$5\text{-}8x10^3$	Rod	-ve	32°C	LGC	+	TGY	Yes	No
MD848	U31481	$5\text{-}8x10^3$	Rod	+ve	32°C	LGC	+	TGY	No	No
MD849	U31482	$5\text{-}8x10^3$	Rod	+ve	32°C	LGC	+	PTGY	No	No
MD850	U31485	$3\text{-}4x10^4$	Rod	-ve	20°C	HGC	-	TGY	No	No

Footnote Table 2.1

#Columns were adopted from Table 2, Shi *et al.*, 1996

[a]GC, high-GC Gram-positive; LGC, low GC-Gram-positive; β-pr, β-proteobacteria; γ-pr, γ- proteobacteria

*MD, Michael Daly strain collection number,

[1]Growth media, TGY, (1% tryptone, 0.5% yeast extract and 0.1% glucose), [2]PTGY, (1% glucose, 1% yeast extract, 0.5% peptone, 0.5% tryptone, 0.06% $MgSo_4.7H_20$, and 0.007% $CaCl_2.2H_2O$)

[2]Resistance of cells to chronic radiation was tested on TGY agar in the presence of a ^{137}Cs source (50 Gy/hour)

[3]An acute dose of irradiation was delivered by ^{60}Co source (at ~10 kGy/h) at 0 °C. Acute irradiation profile of all the strains is shown in Figure 2.3 and Figure 2.4.

[4]D_{37}, Dose that yields 37% survival

Figure 2.3. Resistance of Group I (0.6–3 million years old) Strains from Siberian Permafrost to Acute Irradiation. The indicated strains (Table 2.1) were inoculated into TGY[a]/PTGY[b] medium at 10^6 colony forming units (CFU)/ml and grown at 32 °C to the early stationary phase (10^8 cells/ml). Cells were then irradiated without change of broth on ice with ^{60}Co at 10 kGy/h. At the indicated doses, viable cell counts were determined by plating appropriate cell dilutions for CFU on TGY/PTGY agar at 32 °C. Values are from a single plating experiment. The strain names are color coded as follows: Red, high resistance to acute irradiation; Blue, moderate resistance to acute irradiation; Black, sensitive to acute radiation.

[a]TGY, 1% tryptone, 0.5% yeast extract and 0.1% glucose; [b]PTGY, (1% glucose, 1% yeast extract, 0.5% peptone, 0.5% tryptone, 0.06% $MgSo_4.7H_20$, and 0.007% $CaCl_2.2H_2O$).

Figure 2.3

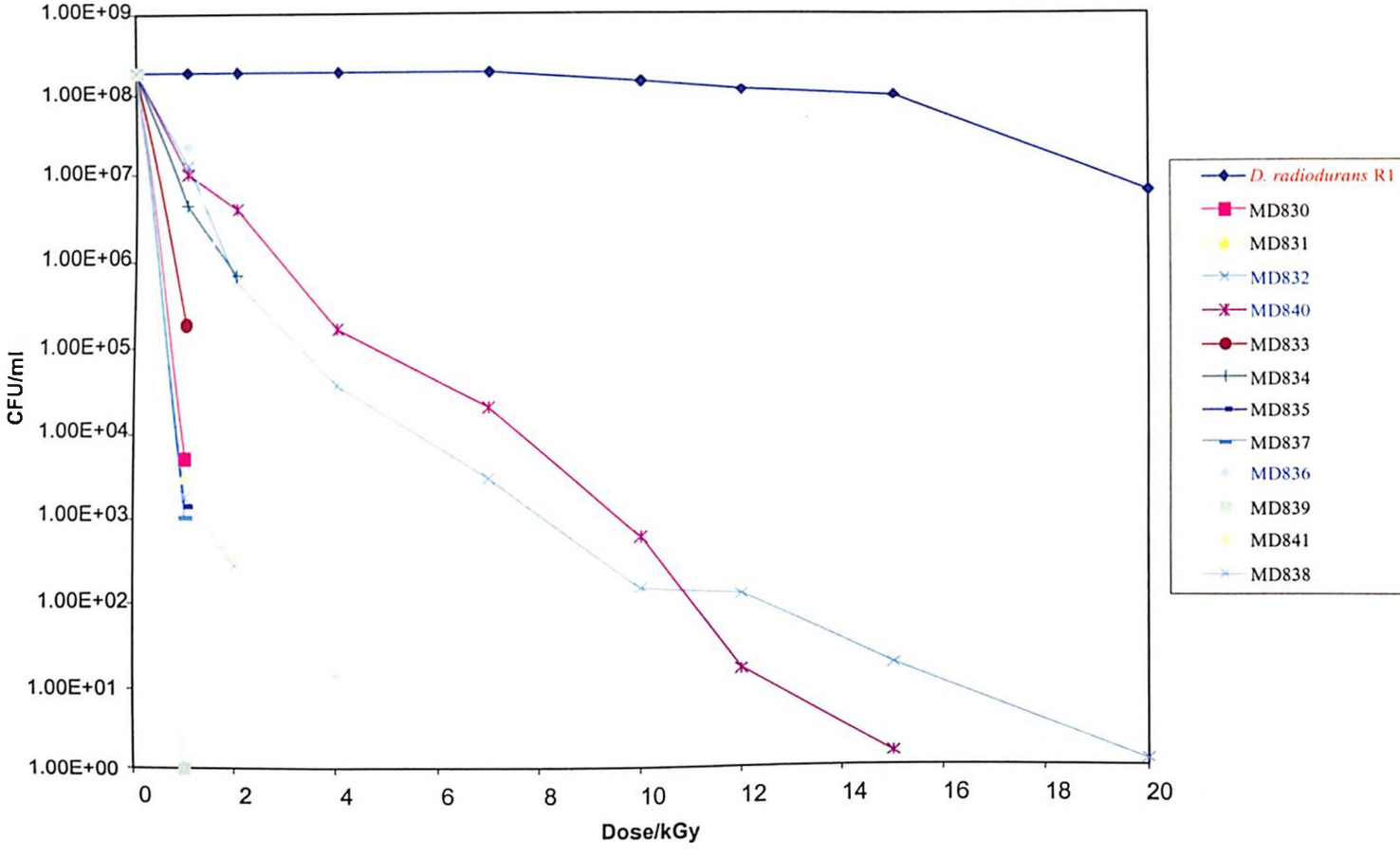
1.00E+09
1.00E+08
1.00E+07
1.00E+06
1.00E+05
1.00E+04
1.00E+03
1.00E+02
1.00E+01
1.00E+00
CFU/ml
0
2
4
6
8
10
12
14
16
18
20
Dose/kGy
D. radiodurans R1
MD830
MD831
MD832
MD840
MD833
MD834
MD835
MD837
MD836
MD839
MD841
MD838

Figure 2.4. Resistance of Group II (3,000-8,000 years old) Strains from Siberian Permafrost to Acute Irradiation. The indicated strains (Table 2.1) were inoculated into TGY[a]/PTGY[b] medium at 10^6 CFU/ml and grown at 32 °C to the early stationary phase (10^8 cells/ml). Cells were then irradiated without change of broth on ice with ^{60}Co at 10 kGy/h. At the indicated doses, viable cell counts were determined by plating appropriate cell dilutions for CFU on TGY[a]/PTGY[b] agar at 32 °C. Values are from a single plating experiment. The strain names are color coded as follows: Red, high resistance to acute irradiation; Blue, moderate resistance to acute irradiation; Black, sensitive to acute radiation.

[a]TGY, 1% tryptone, 0.5% yeast extract and 0.1% glucose; [b]PTGY, (1% glucose, 1% yeast extract, 0.5% peptone, 0.5% tryptone, 0.06% $MgSo_4.7H_20$, and 0.007% $CaCl_2.2H_2O$.

Figure 2.4

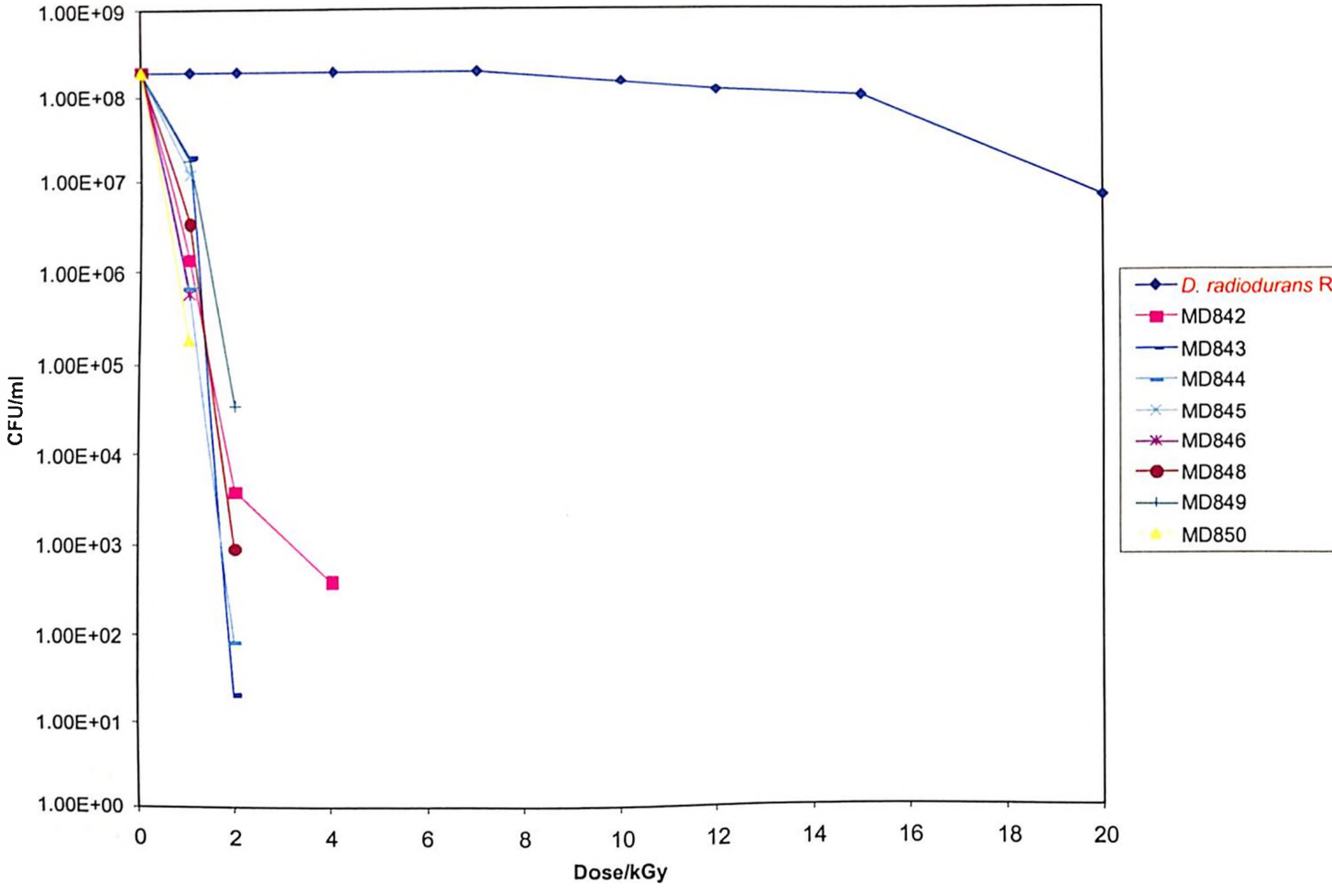
1.00E+09
1.00E+08
1.00E+07
1.00E+06
1.00E+05
1.00E+04
1.00E+03
1.00E+02
1.00E+01
1.00E+00
CFU/ml
0
2
4
6
8
10
12
14
16
18
20
Dose/kGy
D. radiodurans R
MD842
MD843
MD844
MD845
MD846
MD848
MD849
MD850

This suggests that there may be different cellular mechanisms underlying the chronic- and acute-radiation resistance phenotypes.

2.3.1.3 Novel Radiation Resistant Bacteria Isolated from Soil

Soil samples were collected from regions of northern and southwestern India. Additional soil samples were obtained from North America (Washington and New Mexico). Soil samples were inoculated into rich medium, and radiation resistant bacteria were selected by exposing the cultures to a high dose of acute radiation (10 kGy). Ten distinct strains (Table 2.2) were purified and tested for their resistance to irradiation either delivered as an acute dose or chronic dose.

Whereas 7 of the10 isolates were resistant to acute radiation, all ten soil isolates were resistant to chronic radiation (Figure 2.5 and Table 2.2). Specifically, 6 strains (MD869, MD870, MD871, MD872, MD873, and MD874) showed extreme resistance (up to 10 kGy), 1 strain (MD868) showed moderate resistance, and 3 strains (MD866, MD867 and MD877) were sensitive to acute radiation (Figure 2.5 and Table 2.2). A summary of these strains Gram stain and fatty acid similarities are given in Table 2.2. Based on fatty acid similarities to known bacteria, several of the isolates revealed good matches to the following genera: *Bacillus*, *Staphylococcus*, *Deinococcus*, *Brevibacillus*, and *Eneterococcus* (Table 2.2).

2.3.1.4 Novel Radiation Resistant Bacteria Isolated from Beneath a Highly Radioactive Leaking Waste Tank

Fredrickson and coworkers (2000) (Fredrickson *et al.*, 2003) collected radioactive sediments from a nuclear waste plume in the vadose zone (region of unsaturated sediment above the water table) beneath the leaking tank SX-108 at DOE's Hanford Site in Richland, WA. These contaminated environmental samples were analyzed for the distribution of aerobic heterotrophic bacteria. Of the approximately 110 isolates, 4 distinct radiation resistant bacteria were made available to our laboratory for study (Table 2.3).

Table 2.2. Viable Strains from Vadose Zone Underneath the Radioactive Tanks in Hanford, WA.

*Strain number	Strain name	Cell shape	Gram stain	Growth temperature range	Growth medium#	Cell transformabilty	[1] Fatty acid analysis Similarity to bacterium/ *simalirity index value*	[2]Resistance to chronic radiation (50 Gy/hour)	[3]Resistance to acute irradiation up to 10 kGy
MD878	SX-108 7B-1 (Pink)	Coccus	+ve	25-32°C	TGY	Yes	*D. radiodurans* R1/*0.448*	Yes	Yes
MD880	SX-108 7L-1 (Yellowish white)	Coccus	+ve	25-32°C	TGY	N/A	*Micrococcus lylae*-GC subgroup C/*0.425*	Yes	No
MD879	SX108 7C-1 (Pink)	Coccus	+ve	25-32°C	TGY	Yes	*D. radiodurans* R1/*0.317*	Yes	Yes
MD877	RG1-1MR-1C (Yellow)	Coccus	+ve	25-32°C	TGY	N/A	*Micrococcus lylae*-GC subgroup B/*0.364*	Yes	No

Footnote Table 2.2

*MD, Michael Daly strain collection number
#TGY, 1% tryptone, 0.5% yeast extract and 0.1% glucose
[1]Fatty acid similarity comparison was done by Micribial Id., Inc., Delaware
[2]Resistance of cells to chronic radiation was tested on TGY agar in the presence of a ^{137}Cs source (50 Gy/hour)
[3]An acute dose of irradiation was delivered by ^{60}Co source (at ~10 kGy/h) at 0 °C. Acute irradiation profile of all the strains is shown in Figure. 2.6.

Table 2.3. Radiation Resistant Soil Bacteria Isolated from Different Parts of the World

Strain number*	Soil samples from City/Country	Optimal growth temperature	Gram stain	Growth medium#	[1]Fatty acid similarity to strain/ *similarity index value*	[2]Resistance to chronic radiation (50 Gy/hour)	[3]Resistance to acute irradiation up to 10 kGy
MD866	Hanford/USA	32 °C	+ve	TGY	*Bacillus cereus*-GC subgroup A/*0.976*	Yes	No
MD867	Hanford/USA	32 °C	+ve	TGY	*Bacillus cereus*-GC subgroup A/*0.870*	Yes	No
MD868	Hyderabad/ India	32 °C	+ve	TGY	*Staphylococcus epidermidis/0.605*	Yes	No
MD869	Hyderabad/ India	32 °C	+ve	TGY	*Deinococcus proteolyticus/0.013*	Yes	Yes
MD870	Hyderabad/ India	32 °C	+ve	TGY	*Deinococcus proteolyticus/0.033*	Yes	Yes
MD871	Hyderabad/ India	32 °C	+ve	TGY	*Brevibacillus* brevis/*0.431*	Yes	Yes
MD872	Madras/India	32 °C	+ve	TGY	*Brevibacillus brevis/0.430*	Yes	Yes
MD873	Madras/India	32 °C	+ve	TGY	*Deinococcus proteolyticus/0.018*	Yes	Yes
MD874	New Delhi/ India	32 °C	+ve	TGY	*Bacillus megaterium*-GC subgroup A/*0.950*	Yes	Yes
MD875	New Mexico/USA	32 °C	+ve	TGY	*Enterococcus casseliflavus/0.872*	Yes	No Data
MD876	New Mexico/USA	32 °C	+ve	TGY	*Bascillus cereus*-GC subgroup A/*0.919*	Yes	No

Footnote Table 2.3

*MD, Michael Daly strain collection number, #TGY, (1% tryptone, 0.5% yeast extract and 0.1% glucose

[1]Fatty acid similarity comparison was done by Micribial Id., Inc., Delaware

[2]Resistance of cells to chronic radiation was tested on TGY agar in the presence of a ^{137}Cs source (50 Gy/hour)

[3]An acute dose of irradiation was delivered by ^{60}Co source (at ~10 kGy/h) at 0 °C. Acute irradiation profile of all the strains is shown in Figure. 2.5.

Figure 2.5. Resistance of Novel Soil Strains to Acute Irradiation. The indicated strains (Table 2.2) were inoculated into TGY medium at 10^6 CFU/ml and grown at 32 °C to the early stationary phase (10^8 cells/ml). Cells were then irradiated without change of broth on ice with ^{60}Co at 10 kGy/h. At the indicated doses, viable cell counts were determined by plating appropriate cell dilutions for CFU on TGY agar at 32 °C. Values are from a single plating experiment. The strain names are color coded as follows: Red, high resistance to acute irradiation; Blue, moderate resistance to acute irradiation; Black, sensitive to acute radiation.

Figure 2.5

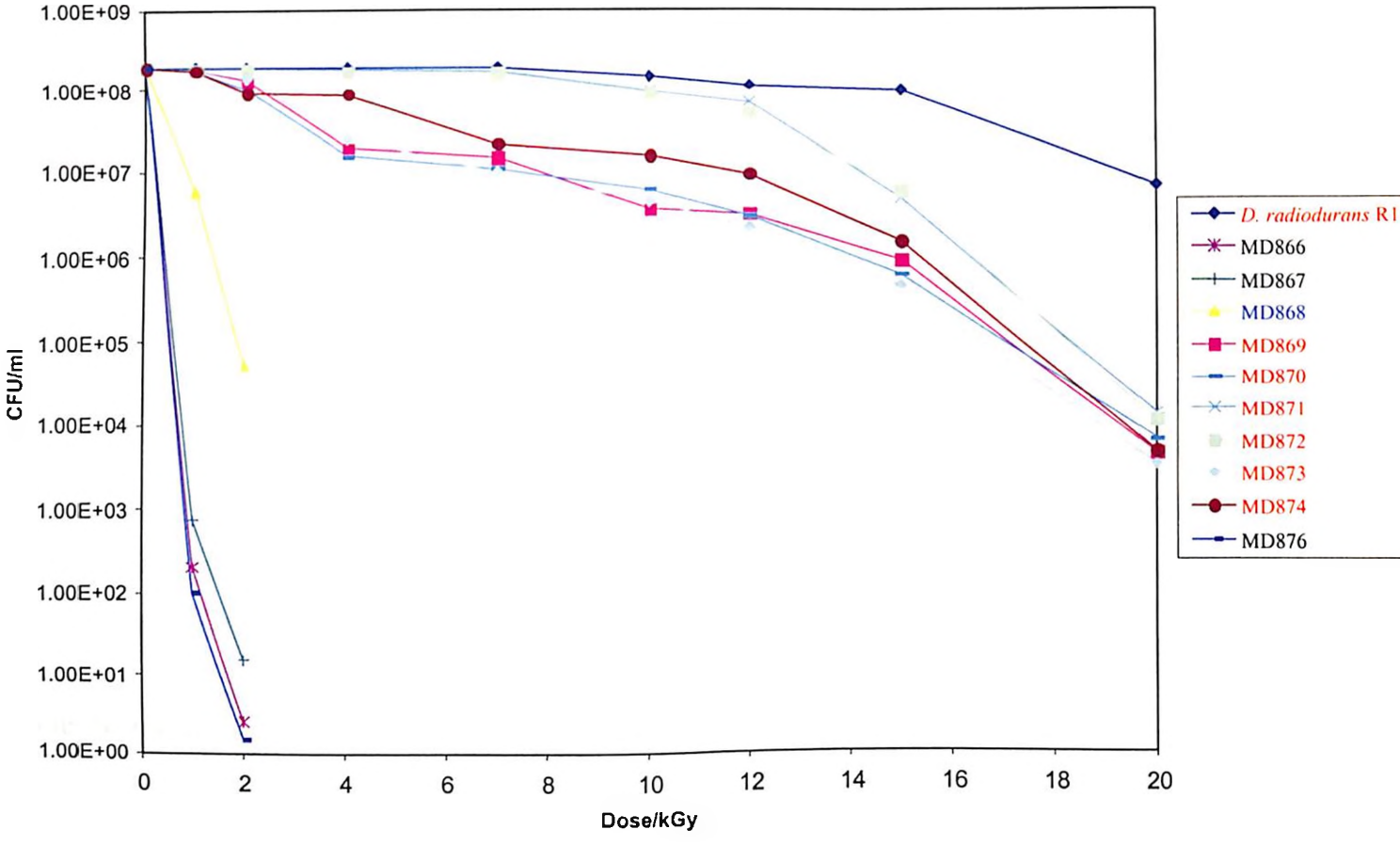
1.00E+09
1.00E+08
1.00E+07
1.00E+06
1.00E+05
1.00E+04
1.00E+03
1.00E+02
1.00E+01
1.00E+00
CFU/ml
0
2
4
6
8
10
12
14
16
18
20
Dose/kGy
D. radiodurans R1
MD866
MD867
MD868
MD869
MD870
MD871
MD872
MD873
MD874
MD876

Acute radiation resistance profiles for the 4 novel isolates were constructed by exposing early stationary phase cultures (OD_{600} ~ 1.00) to increasing doses of irradiation. Their ability to grow under high chronic (50 Gy/hour) irradiation was also tested by plating them on TGY agar and incubating the plates in a ^{137}Cs irradiator. All 4 strains were resistant to chronic radiation (Table 2.3). Strains 7B-1 and 7C-1 showed extreme resistance to acute irradiation while strains 7L-1 and RG1-1MR-1C showed moderate resistance to acute irradiation (Figure 2.6).

Based on 16S rRNA comparisons (Fredrickson *el al.*, 2003), strains 7B-1 and 7C-1 were identified as *D. radiodurans* strain R1. Given the importance of this finding and to rule out the possibility of contamination of samples with laboratory-maintained strains of *D. radiodurans*, further investigations were conducted. Comparisons of strains 7B-1 and 7C-1 with the USUHS laboratory strain R1 (also used at PNNL) included their transformability, growth temperature range, cell structure, and genome fingerprints.

Transformability of Strains 7B-1 and 7C-1. Most deinococcal environmental isolates have been reported to be non-transformable (Daly, 2000). However, *D. radiodurans* strain R1 is highly transformable with either chromosomal DNA or autonomously replicating plasmids (Smith *et al.*, 1988; Daly *et al.*, 1994a; Daly and Minton, 1995a; Daly and Minton, 1996). This ability of *D. radiodurans* has been exploited by our group to express metal-detoxifying (Brim *et al.*, 2000) and organic compound-degrading (Lange *et al.*, 1998) genes in radioactive laboratory environments. Given the prospect of engineering naturally occurring radiation resistant bacteria for environmental biotechnology, it was important to determine the transformability of the most radiation resistant bacteria yet isolated from a radioactive environmental sample (7B-1 and 7C-1) (Fredrickson *et al.*, 2003).

The novel *D. radiodurans* strains 7B-1 and 7C-1 were tested for their ability to be transformed with *D. radiodurans* R1 plasmid-encoded resistance markers for Kanamycin (Km), chloramphenicol (Cm), and Tetracycline (Tet). Exponentially growing cultures were transformed with pMD68 (Km^R, Tc^R) (Daly *et al.*, 1994a) and pMD308 (Cm^R) (Daly and Minton, 1996) using the conventional $CaCl_2$-based deinococcal transformation protocol (Tirgari and Moselay, 1980). Strains 7B-1 and 7C-1 were transformable with similar efficiency to *D. radiodurans* R1.

Figure 2.6. Resistance of Strains Isolated from Beneath a Highly Radioactive Leaking Waste Tank to Acute Irradiation. The 4 strains were inoculated into TGY medium at 10^6 CFU/ml, and grown at 32 °C to the early stationary phase (~10^8 cells/ml). Cells were then irradiated without change of broth on ice with ^{60}Co at 10 kGy/h. At the indicated doses, viable cell counts were determined by plating appropriate cell dilutions for CFU on TGY agar at 32 °C. Values are from a single plating experiment. The strain names are color coded as follows: Red, high resistance to acute irradiation; Blue, moderate resistance to acute irradiation; Black, sensitive to acute radiation.

Figure 2.6

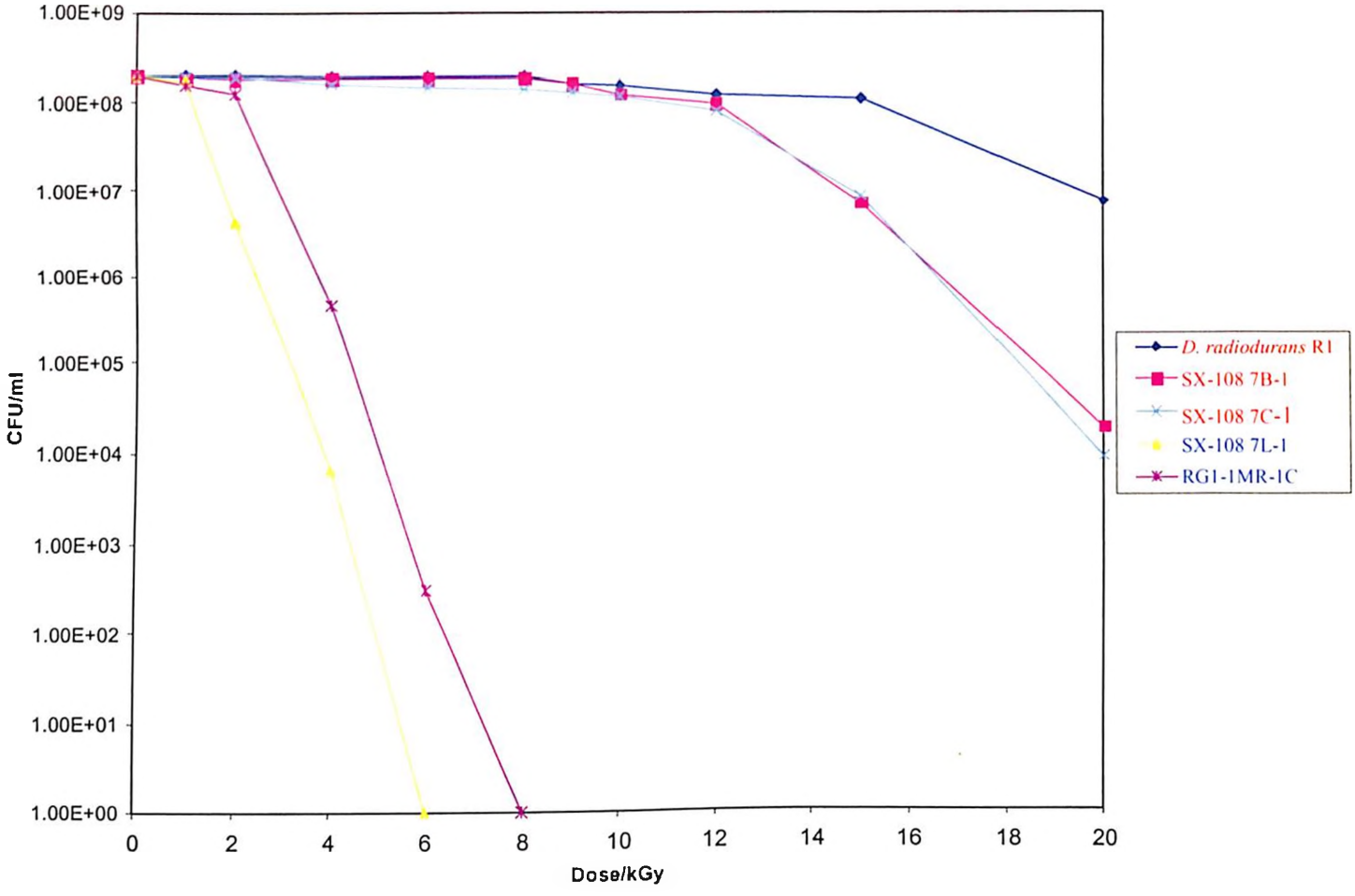
1.00E+09
1.00E+08
1.00E+07
1.00E+06
1.00E+05
1.00E+04
1.00E+03
1.00E+02
1.00E+01
1.00E+00
CFU/ml
0
2
4
6
8
10
12
14
16
18
20
Dose/kGy
D. radiodurans R1
SX-108 7B-1
SX-108 7C-1
SX-108 7L-1
RG1-1MR-1C

Growth Temperature Range of Novel Isolates. Due to the decay of short-lived radionuclides, the temperature of soil sediments beneath tank SX-108 likely reached 100°C during early operation. Currently, the sediment temperature from which strains 7B-1, 7C-1, 7L-1 and RG1-1MR-1C were isolated is about 65 °C (Fredrickson *et al.*, 2003). *D. radiodurans* R1 is a non-sporulating mesophilic bacterium (growth temperature 20-39 °C), and it is known to be killed at temperatures above 40 °C (Daly, 2000). Yet, 2 closely related *D. radiodurans* R1 strains appear to have been isolated from a chronically hot environment. The growth temperature ranges of the 4 isolates were examined and were shown not to exceed 37 °C. Specifically, their growth was tested at 25 °C, 32 °C, 37 °C, 45 °C and 50 °C. *D. radiodurans*, *E. coli* and *D. geothermalis* were used as controls having optimum growth temperatures of 32 °C, 37 °C, and 50 °C, respectively. The 4 novel strains showed luxuriant growth on rich medium between 25-37 °C; growth of strains below 25 °C was not tested. While it is unknown how these mesophilic organisms survived long exposure to 65-100 °C, it is known that desiccation stabilizes protein structures, making them particularly resistant to heat denaturation (Black and Pritchard, 2003), and it is significant that *D. radiodurans* R1 is highly resistant to desiccation (Mattimore and Battista, 1996).

Analysis of Cell Structure by Transmission Electron Microscopy (TEM). TEM of the four novel isolates (7B-1, 7C-1, 7L-1 and RG1-1MR-1C) was a collaborative effort with Dr. Alexander Vasilenko at USUHS, MD. Electron micrographs for the strains are shown in Figure 2.7.

Strains 7B-1, 7C-1 and *D. radiodurans* R1 showed essentially identical morphologies that included: similar sized (~1.8 μM diameter) cells with tetracocci, diffuse nucleoid, and cell wall. 7B-1 and 7C-1 exhibited the presence of the typical *D. radiodurans* multi-layered cell wall structure with a prominently visible thick peptidoglycan layer (holey layer) and an outer dense carbohydrate coat (Figure 2.7A and Figure 2.7C).

Strains 7L-1 and RG1-1MR-1C were morphologically distinct from *D. radiodurans* displaying smaller sized diplococci/monococci (0.9 μM diameter and 0.5 μM diameter, respectively) and no ringlike nucleoids (Figure 2.7B and Figure 2.7D).

Comparison of 2-Dimensional (2-D) Whole Genome Fingerprint of Novel *D. radiodurans* Isolates (7B-1 and 7C-1) and USUHS Laboratory Strain *D. radiodurans* R1. The sediments beneath tank SX-108 are contaminated with high concentrations of alkali, nitrate, aluminate, Cr(VI), and ^{137}Cs, and significant desiccation and heating (up to 70 °C) of this region has also been reported (Fredrickson *et al.*, 2003). It is, therefore, surprising that novel strains of *D. radiodurans* R1, which is a known mesophile, were isolated from such hot environments. If the isolation is true ecological representation, then this finding is highly significant because it underscores the priority the DOE has assigned *D. radiodurans* for development for bioremediation of radioactive wastes. To conclusively rule out the possibility of laboratory contamination, the novel deinococcal strains were subjected to detailed genomic fingerprinting based on a newly developed approach. The novel 2-D fingerprint analysis technique is somewhat analogous to microarrays in that it can be used to examine genomic expression based on hybridization with mRNA-derived probes. Whereas microarrays use glass slides with DNA printed on their surfaces, this technique uses agarose gels to separate digested genomic DNA. For the purpose of genomic finger printing, the approach used is to electrophoretically separate an entire genome in 2 dimensions, followed by gel-blotting and diagnostic probing, that generates a strain specific 2-D constellation of hybridizing spots. This procedure is made possible by having a whole genome sequence, which allows selection of suitable restriction enzymes that yield DNA fragment sizes that can be clearly resolved be conventional agarose gel electrophoresis.

2-D fingerprint analysis is dependent on 1) having a very high quality genomic sequence like the one obtained for *D. radiodurans* (White *et al.*, 1999); 2) restriction enzymes; 3) southern blotting capabilities; and 4) a computer program to predict the migration positions of DNA fragments following DNA cleavage and two-dimensional (2-D) electrophoresis. Briefly, genomic DNA is first cut with one enzyme and the fragments are separated by agarose gel electrophoresis. A thin vertical gel lane containing DNA is removed and subjected to *in situ* cleavage with a second restriction enzyme. Once the embedded DNA is digested, the gel strip is set horizontally in a new gel, and electrophoresed again yielding a 2-D spread of fragments that can be transferred to a hybridization membrane by blotting. These blots can be analyzed by

Figure 2.7. Analysis of Cell Structure by Transmission Electron Microscopy (TEM). TEM of Hanford strains grown in TGY medium showing wall structure and nucleoid morphology. Note that the strains 7B-1 (*Panel A*) and 7C-1 (*Panel C*) tertacocci have a similar cell wall and nucleoid structure when compared to the electron micrograph of *D. radiodurans* R1 (Figure 1.1). Strain 7L-1 (*Panel B*) and RG1-1MR-1C (*Panel D*) are structurally distinct from that of *D. radiodurans* R1 with smaller sized monococci and diplococci structures. EM scale bars in A, B, C and D = 0.5 μm. **pg**, peptidoglycan layer; **cc**, carbohydrate coat.

Figure 2.7

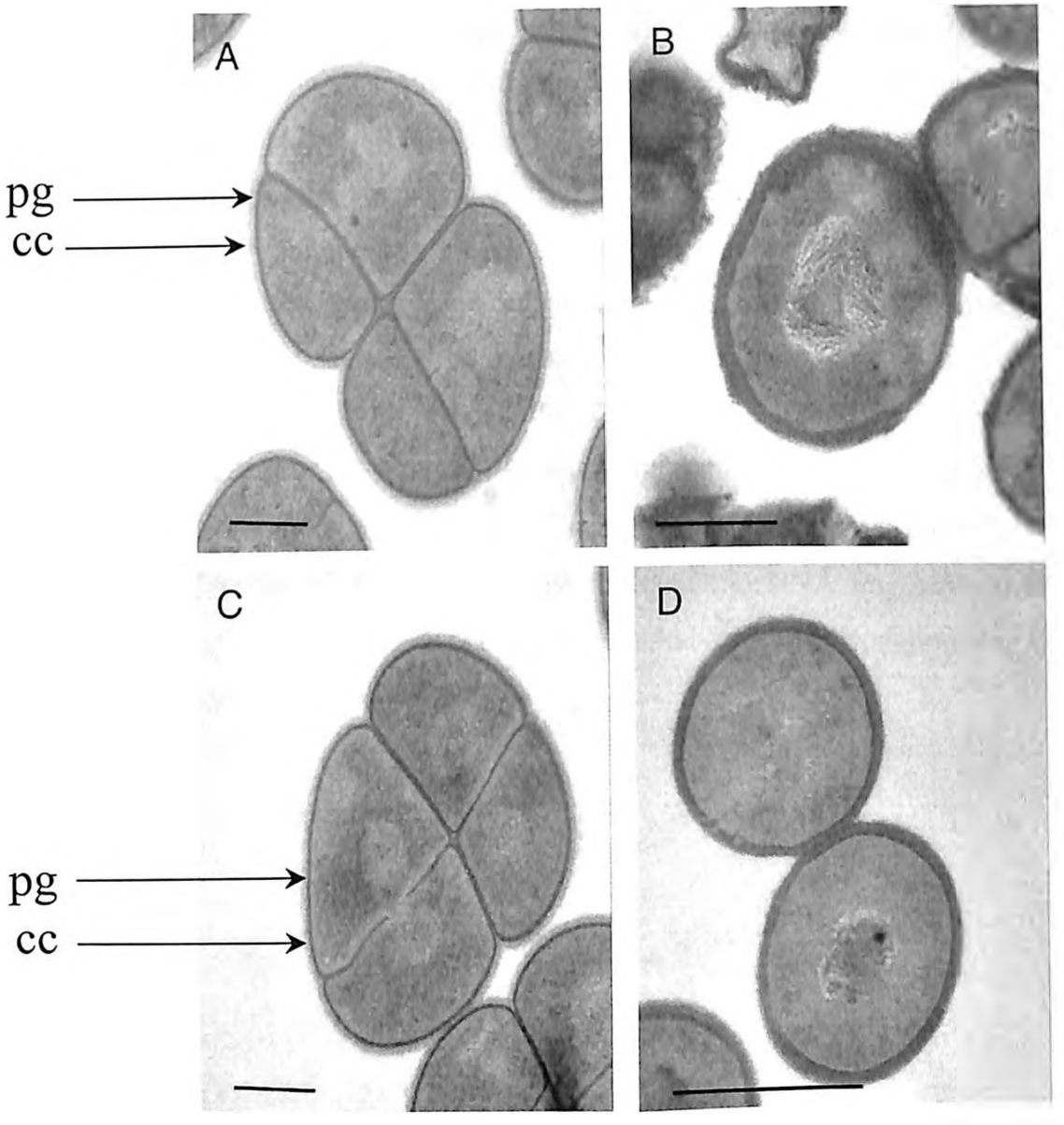

either labeled cDNA probes generated from total RNA preparations or used for genomic fingerprinting using labeled single or multiple gene-specific probes. Hybridizing spots can be identified by comparison with a computer-generated template of fragments or used directly to compare closely related strains.

Total genomic DNA extracted from strains *D. radiodurans*, 7B-1 and 7C-1 was first subjected to restriction digestion with the enzyme *ApaI*. DNA fragments were separated by agarose gel electrophoresis and then subjected to *in situ* cleavage with the enzyme *NspI*. A second round of electrophoresis of the horizontally placed gel strip yielded a diagnostic 2-D spread of the DNA fragments for each strain (Figure 2.8). The 2-D spreads of DNA fragments were transferred to and immobilized on nylon membranes followed by hybridization with 24 ^{32}P-labeled probes. These probes were markers for different regions of each of the four genomic partitions of *D. radiodurans* R1 (Table 2.4). The 2-D hybridizing constellation of spots (fingerprint) of strains 7B-1 and 7C-1 were the same, but distinct from *D. radiodurans* R1 (Figure 2.9). Thus, the novel deinococcal isolates are distinct from the laboratory strain. Based on the overall spread of *ApaI –NspI* digested genomic DNA fragments revealed by ethidium bromide staining, all three genomes share a remarkable similarity, supporting the conclusion that 7B-1 and 7C-1 are *D. radiodurans*.

Table 2.4. List of PCR Amplified Probes Used for Genome Fingerprinting.

Serial Number	Probe Name	Probe Coordinates (Kilo base)	Associated with genome component
1	BC35	20	plasmid
2	JK91	80	megaplasmid
3	HZ52	140	megaplasmid
4	SQ29	10	Small chromosome
5	AD64	70	Small chromosome
6	SP87	300	Small chromosome
7	SU93	10	Main chromosome
8	JO64	100	Main chromosome
9	OV19	200	Main chromosome
10	IB62	400	Main chromosome
11	GQ15	600	Main chromosome
12	DQ03	800	Main chromosome
13	EJ74	900	Main chromosome
14	NU62	1000	Main chromosome
15	IJ95	1200	Main chromosome
16	JW20	1400	Main chromosome
17	JJ87	1500	Main chromosome
18	MI39	1600	Main chromosome
19	HX43	1700	Main chromosome
20	FL36	1800	Main chromosome
21	AA67	2000	Main chromosome
22	EC08	2100	Main chromosome
23	IZ66	2300	Main chromosome
24	EG62	2500	Main chromosome

Figure 2.8. Comparison of 2-D Whole Genome Spread of Strains 7B-1 and 7C-1 with *D. radiodurans* R1. Ethidium bromide stained agarose gel following 2-D electrophoresis. Genomic DNA was digested with *ApaL*I and electrophosed in a 0.5% agarose gel (not shown). A thin vertical gel lane containing the cleaved DNA was cut from the gel and digested with *Nsp*I. The gel lane with the double-digested DNA was placed horizontally in a new gel and electrophoesed yielding a 2-D spread of genomic DNA fragments. *Panel A. D. radiodurans* R1. *Panel B.* Strain 7B-1 and *Panel C.* 7C-1. Note that diagnostic 2-D spread of the DNA fragments of both novel isolates (7B-1 and 7C-1) looks very similar that of *D. radiodurans* R1. Arrows show position of *D. radioaurans recA* (DR2340), which is central to genomic restoration following irradiation (Minton, 1994). λ/H, lambda phage DNA cut with *Hind*III.

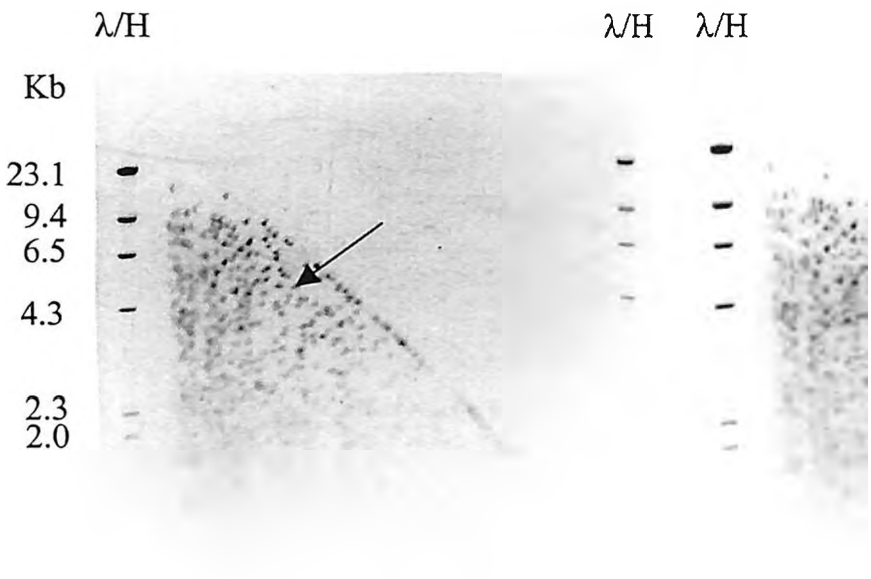
λ/H
λ/H
λ/H
Kb
23.1
9.4
6.5
4.3
2.3
2.0

Figure 2.8

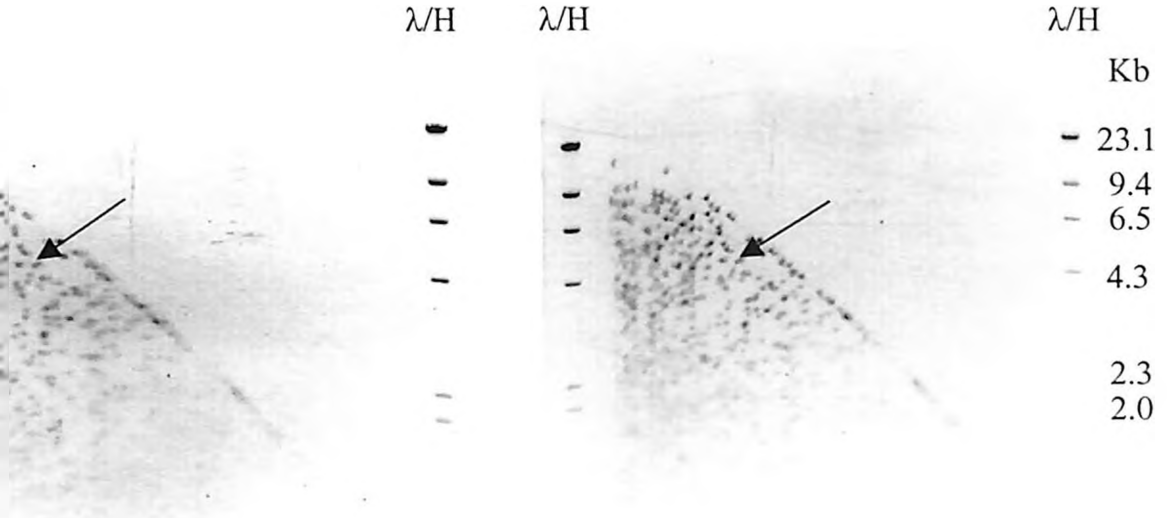

B C

Figure 2.9. Comparison of 2-D Genome Fingerprint of Strains 7B-1 and 7C-1 with *D. radiodurans* R1. Blots of gels shown in Figure 2.8 A, B and C representing the 2-D whole genome spread of strains *D. radiodurans* R1, 7B-1 and 7C-1, respectively, were hybridized with 24 probes ^{32}P-labeled probes generated by PCR from the 4 *D. radiodurans*' genome compartments (Table 2.1). Note that the 2-D hybridizing constellation of spots (fingerprint) of strains 7B-1 and 7C-1 were the same, but distinct from *D. radiodurans* R1.Arrows point all the spots unique to *D. radiodurans* R1 genome. λ/H, lambda phage DNA cut with *Hind*III.

Figure 2.9

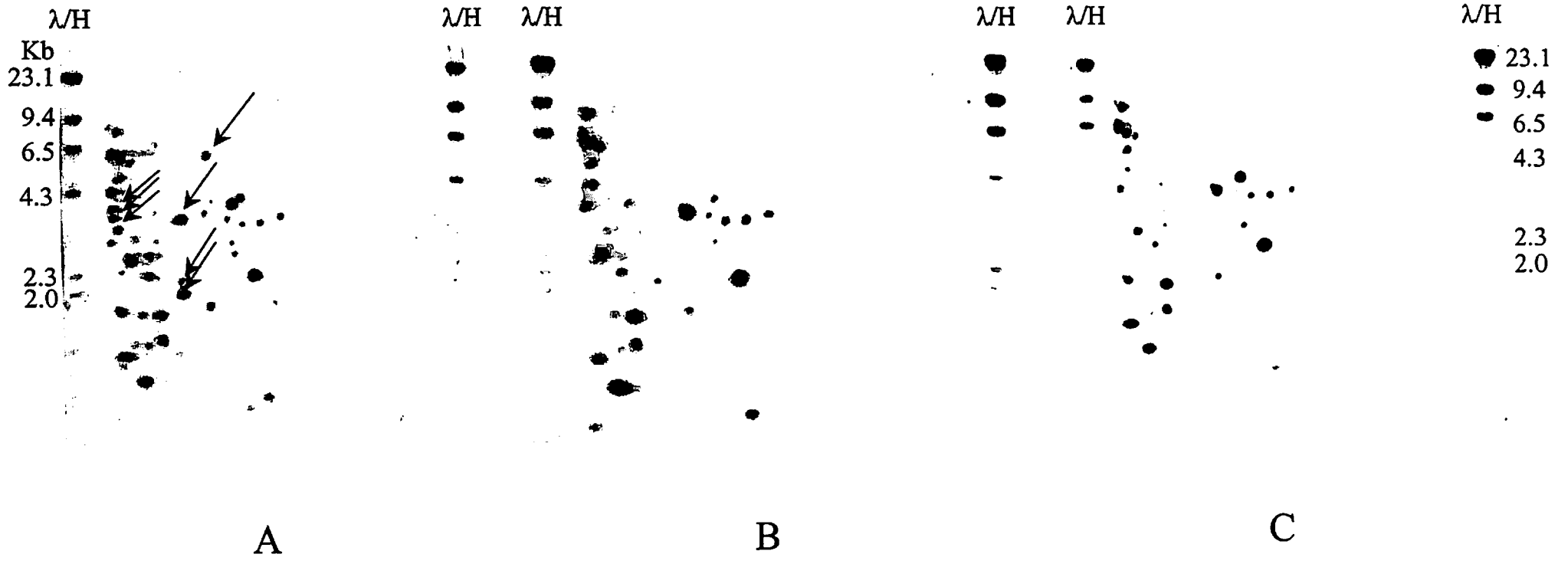

2.4 Discussion

Extreme radiation resistance in bacteria has historically been attributed mostly to efficient DNA repair systems. Yet the molecular mechanisms involved in extreme resistance are unknown (Minton, 1994) (Battista, 1997) ((Makarova *et al.*, 2001). Annotation of the complete genome sequence of *D. radiodurans* has failed to identify DNA repair pathways that are unique to this organism (Makarova *et al.*, 2001) (White *et al.*, 1999). And, much emphasis has been placed on identifying novel repair genes currently hidden within the group of hypothetical genes predicted by genomic annotation (Udupa *et al.*, 1994) (Makarova *et al.*, 2001) (Earl *et al.*, 2002b). However, very few novel repair genes have been identified experimentally (Earl *et al.*, 2002a, Liu *et al.*, 2003) in spite of intense 'gene-hunting' research in several laboratories over the last five years.

Radiation resistant organisms that were isolated from permafrost, arid soils, and radioactive sediments could be categorized into three distinct groups: 1) resistant to chronic and acute γ-radiation; 2) resistant to chronic, but sensitive to acute γ-radiation; and 3) sensitive to chronic, but resistant to acute γ-radiation. This spectrum of resistance characteristics suggests that an organism's ability to survive radiation may be attributable to a combination of protection and repair mechanisms. For example, an organism with a high degree of DNA protection, but inefficient DNA repair mechanisms may be able to grow under chronic irradiation, but is sensitive to acute radiation doses. Alternatively, an organism with a high degree of DNA protection and efficient DNA repair processes may be extremely radiation resistant. The nature of DNA protection systems are not well characterized, but likely are significantly affected by the metabolic repertoire of the cell (Black and Pritchard, 2003). The key findings for bacteria isolated from permafrost, arid soils, and radioactive sediments follow:

Resistance Characteristics of Bacteria Isolated from Siberian Permafrost (Table 2.2, Figure 2.3, Figure 2.4). Viable bacteria in permafrost need to be able to resist freezing temperatures (Shi *et al.*, 1997) (Price *et al.*, 2002), low nutrient conditions (shi *et al.*, 1997), and high levels of background radiation accumulated over time spans extending up to 3,000,000 years. Assuming that background radiation accumulates at 0.005 Gy/year, the total accumulated dose in the oldest

permafrost (~3 million years old) may be as high as 15,000 Gy (Makarova et al., 2001). Such a high dose would be expected to select for very radiation resistant organisms. Yet most of the bacteria (Group 1: 1.5-3 Myears) from 3,000,000 year old permafrost are radiation sensitive, with only a few moderately resistant bacteria identified. Of the bacteria investigated belonging to Group 2 (5-8 kyears) (Table 2.2), most of those were also radiation sensitive. However, one isolate (MD846) was able to grow in the presence of chronic radiation. Collectively, these results suggest that permafrost is unlikely to be an environment that promotes the evolution of radiation resistant bacteria. While the survival strategies of radiation sensitive bacteria in ancient permafrost are unknown, it is likely that being frozen contributed to their survival. Freezing contributes to radiation resistance in two distinct ways: 1) water in a solid state suppresses the formation of DNA damaging free radicals generated by radiation (VanGerwen *et al.*, 1999); and 2) freezing of water external to cells can cause a water potential gradient and result in desiccation (Black and Pritchard, 2003). In a frozen/desiccated state, free radical formation is limited by the amount of "free" water due to the absence of cellular metabolism and prevention of water radiolysis (Gottschalk, 1985). Thus, it is conceivable that viable isolates from permafrost may have efficient cellular protection systems that minimize damage from free radicals generated during cellular revival.

Resistance Characteristics of Bacteria Isolated from Arid Soils (Table 2.3, Figure 2.5). Unlike permafrost conditions that are static, many arid environments are subjected to periodic exposures to water (*i.e.*, rain and humidity). Bacteria from environmental soils prone to drought need to develop defense mechanisms not only to resist exposure to desiccation, but also to free radicals that arise following rehydration (Sanders and Maxcy, 1979). Since 80% of DNA damage caused by radiation is believed to arise by the indirect effects of free radicals, extreme conditions in arid soil are expected to select organisms that are resistant to radiation. This hypothesis is consistent with published reports on the isolation of radiation-resistant bacteria from desiccated environments without exposure to irradiation (Sanders and Maxcy, 1979). This is further supported by results presented here that many bacteria isolated from arid soils are extremely resistant to both chronic and acute irradiation (Table 2.3, Figure 2.5). However, as for bacteria isolated from permafrost, a few bacteria isolated from dry soils showed resistance to chronic

irradiation, but were sensitive to acute irradiation (Table 2.3, Figure 2.5). Thus, the resistance spectrum of bacteria isolated from arid soils, generally, is greater than observed for the permafrost isolates, and suggests that cellular protection and repair mechanisms are important to the survival of bacteria indigenous to arid surface soils.

Based on fatty acid similarities to known bacteria, several of the most radiation resistant isolates showed high similarity to *Bacillus*, *Staphylococcus*, *Deinococcus*, *Brevibacillus*, and *Eneterococcus* species (Table 2.3). These bacterial groups are known for their high radiation resistance (Van Gerwen *et al.*, 1999; Thronley, 1963).

Resistance Characteristics of Bacteria Isolated from Radioactive Sediments (Table 2.4, Figure 2.6- Figure 2.9). The extreme conditions beneath leaking radioactive tank SX-108 (Fredrickson *et al.*, 2003) include temperatures as high as 70 °C, low O_2 concentrations, desiccation, low nutrient conditions, and high-levels of background radiation. Under such conditions, the microbial population would be expected to have been reduced to groups of bacteria that are thermophilic, anaerobic, and radiation resistant. However, the majority of isolated bacteria were aerobic, heterotrophic, desiccation sensitive, and radiation sensitive. Only two of the hundreds of bacterial isolates from beneath the radioactive Hanford Site tank were extremely radiation resistant, and notably, both were provisionally identified (Fredrickson *et al.*, 2003) and confirmed in this thesis as *D. radiodurans*.

Permafrost and the radioactive dry sediments share physico-chemical characteristics. Both have limited "free" water, are nutritionally restricted, and contain dormant bacteria that have been exposed to high doses of accumulated background irradiation. As such, these environments would be expected to select for bacteria that are radiation resistant. However, most bacterial isolates from these two environments were sensitive to radiation (Figure 2.3, 2.4 and 2.6). In contrast, radiation resistant organisms were readily isolated from non-radioactive surface soil samples collected from arid regions of India and North America (Figure 2.5). Unlike permafrost and dry radioactive sediments that are static, arid surface soil environments are non-static. Surface soils are subjected to periodic exposures to high levels of oxidative stress during cycles of drying and hydration. Over geologic times, the non-static soil environments would be expected to drive the evolution of organisms that are resistant to DNA-damage caused by ROS.

In static dry/frozen environments cells are dormant, unable to replicate, and not evolving, and were exposed to one cycle of selection, *i.e.*, during their original recovery from DOE sediment or permafrost. Notably, high levels of ROS are also produced by aerobic metabolism (Georgiou, 2002), where oxidative stress occurs when the rate of generation of ROS exceeds the detoxification capacity of the organism/cell (Georgiou, 2002). In general, aerobic organisms have evolved powerful mechanisms to detoxify or prevent the production of ROS. Given that *D. radiodurans* is an obligate aerobe, it is possible that the evolution of both desiccation and radiation resistance is related to systems that protect the organism from the toxic byproducts of the aerobic metabolism.

Correlating Oxidative Stress and Radiation Resistance. An organism's ability to withstand high levels of oxidative stress may be attributable to a wide range of protection and detoxification mechanisms. Desiccation by itself does not cause much cellular damage, rather it stabilizes protein structures making them particularly resistant to aging (Black and Pritchard, 2003) (Franks *et al.*, 1991; Constantino *et al.*, 1998) and heat denaturation (Black and Pritchard, 2003). Damage from desiccation arises upon rehydration and the resumption of normal cellular activity (Black and Pritchard, 2003) during revival. In facultative and obligate aerobes, cellular protection systems against metabolism-induced free radicals include efficient catalytic scavenging systems such as superoxide dismutase (Sod) and catalase. Other free radical scavengers include carotenoid pigments (Carbonneau *et al.*, 1989) (*e.g.*, deionoxanthin in *D. radiodurans* [Lemme *et al.*, 1997]) that are present in the cell walls of certain bacteria, and biological anti-oxidants such as vitamin A and E (Slater *et al.*, 1987).

To further explore the relationship between metabolism and radiation resistance, a detailed computational analysis of the whole genome sequence of *D. radiodurans* was undertaken with particular emphasis on its metabolic repertoire and systems that generate and defend it from free radicals (Figure 2.10). Interestingly, some of the primary biosynthetic pathways were found to be defective in *D. radiodurans*. The nicotinamide adenine dinucleotide (NAD) pathway was disrupted and predicted to be non-functional with 4 of its genes (*nadB*, *nadA*, *nadC* and *nadD*) missing. Biosynthetic pathways for the amino acid cysteine was also predicted to be non-functional. While it is not known how the disruption of cysteine or NAD

biosynthesis could contribute to the radiation resistance phenotype, cysteine is known to facilitate the formation of 2Fe-2S and 4Fe-4S centers that are critical to respiratory enzymes (Gottschalk, 1985). Free radicals formed during exposure to ionizing radiation are known to attack Fe-S centers releasing the transition metal. And, free Fe^{2+} efficiently catalyzes the reduction of H_2O_2 to the highly reactive $^{\cdot}OH$ by the Fenton reaction. These observations are consistent with the theoretical predictions by Karlin and Mrazek (Karlin and Mrazek, 2001), which suggest that the capability of *D. radiodurans* to resist extreme doses of ionizing and UV radiation is attributed to an unusually high number of predicted highly expressed (PHX) chaperone/degradation, protease, and detoxification genes (Karlin and Mrazek, 2001). The authors report that when compared with all the current complete prokaryotic genomes, *D. radiodurans* contains the greatest number of PHX detoxification and protease proteins (Karlin and Mrazek, 2001). The relationship between metabolic defects *in D. radiodurans* and radiation resistance is considered in the next chapter.

2.5 Conclusions

1. **Static Environments such as Siberian permafrost do not appear to promote the evolution of radiation resistant bacteria even though bacteria encased in ancient permafrost may have accumulated large doses of background radiation.**

2. **In contrast to bacteria isolated from Siberian permafrost and dry radioactive Hanford sediments, many bacteria isolated from arid surface soils were found to be extremely radiation resistant. This is consistent with previous reports and suggests that surface soil environments exposed to cycles of desiccation and rehydration may facilitate the evolution of radiation resistant bacteria.**

3. **The identity of two novel *D. radiodurans* isolates (7B-1 and 7C-1) from radioactive sediments at Hanford, WA were confirmed using a novel 2-D genome fingerprint technique. This identification underscores the DOE's investment in *D. radiodurans* as a candidate for bioremediation of genotoxic environments.**

4. **A reconstruction of the metabolic configuration of *D. radiodurans* based on genomic annotation has identified several defects in its primary biosynthetic pathways that may contribute to its resistance characteristics.**

Figure 2.10. Overview of the Basic Metabolic Pathways of *D. radiodurans* and Systems that Generate and Defend Against Free Radicals. The pathways are color coded as follows: Black, catabolism of fructose, lactate and acetate; pyruvate oxidative decarboxylation; TCA cycle. Brown, reactions of the glyoxylate bypass. Blue, methionine, serine biosynthesis, and electron transfer coupled to ATP synthesis. Purple, cysteine biosynthesis and sulfate reduction. Green, basic ammonia metabolism. For each reaction, the gene name and/or *D. radiodurans* gene number is shown. Red crosses show the location of predicted disruptions (missing genes) of biosynthetic pathways. Red arrows and boxes show the dominant reactions leading to the generation of free radicals. Typically during irradiation, ~80% of DNA damage is caused indirectly by irradiation-induced short-lived free radicals, the remaining ~20% by direct interaction between γ-photons and DNA (Schulte-Frohlinde, 1986; Zaider *et al.*, 1994). Black boxes include defense systems against free radical damage. Blue boxes outside the cell show proteases and substrates: Blue substrates in these boxes have predicted specified transporters, orange substrates do not have predicted specified transporters. Long dashed blue lines show conventional pathways leading to degradation of amino acids. Abbreviations: APS, adenylylsulfate; PAPS, phosphoadenylylsulfate; NAD, nicotinamide adenine dinucleotide (oxidized form); NADH, nicotinamide adenine dinucleotide (reduced form); NADP, nicotinamide adenine dinucleotide phosphate (oxidized form); NMN, nicotinamide mononucleotide; FMN, flavin mononucleotide; FAD, flavin adenine dinucleotide (oxidized form); FADH, flavin adenine dinucleotide (reduced form); ATP, adenosine triphosphate; ADP, adenosine diphosphate; PEP, phosphoenolpyruvate; nicotinate-AD, nicotinic acid adenine dinucleotide; nicotinate-NM, nicotinic acid mononucleotide; E1, subunit of phosphotransferase system; Pi, orthophosphate; PPi, pyrophosphate; Q, ubiquinone; SOD, superoxide dismutase; $O_2^{\cdot}$, superoxide radical; O_2^{-}, peroxide ion; $OH^{\cdot}$, hydroxyl radical; e^{-}_{aq}, hydrated electrons.

Figure 2.10

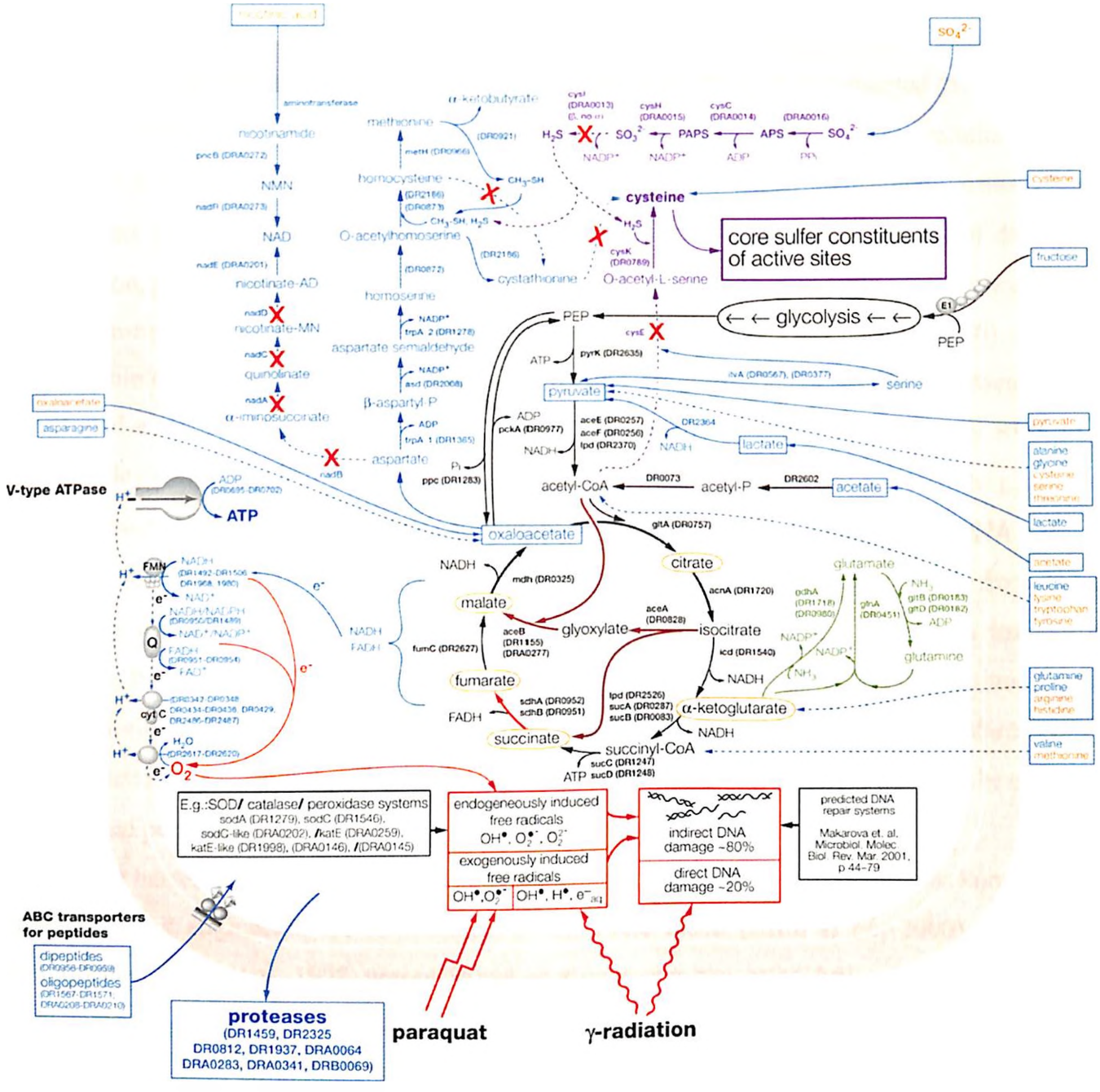
cysteine
core sulfer constituents of active sites
glycolysis
PEP
pyruvate
acetyl-CoA
acetate
lactate
oxaloacetate
citrate
isocitrate
α-ketoglutarate
succinyl-CoA
succinate
fumarate
malate
glyoxylate
glutamate
glutamine
NADH
ATP
V-type ATPase
ABC transporters for peptides
dipeptides
oligopeptides
proteases
(DR1459, DR2325 DR0812, DR1937, DRA0064 DRA0283, DRA0341, DRB0069)
paraquat
γ-radiation
E.g.:SOD/ catalase/ peroxidase systems
sodA (DR1279), sodC (DR1546), sodC-like (DRA0202), /katE (DRA0259), katE-like (DR1998), (DRA0146), /(DRA0145)
endogeneously induced free radicals
exogenously induced free radicals
indirect DNA damage ~80%
direct DNA damage ~20%
predicted DNA repair systems
Makarova et. al. Microbiol. Molec. Biol. Rev. Mar. 2001, p.44-79

Chapter 3: Physiologic Determinants of Radiation Resistance in *Deinococcus radiodurans*

3.1. Introduction

While the lethal consequences of ionizing radiation are well documented (Shapiro, 2002), relatively little is known about how organisms protect themselves against radiation damage. Comparison of radiation resistance profiles of bacteria isolated from different environments (Chapter 2) suggests that aerobic soil environments, where bacteria are exposed to cycles of drying and rehydration, promote the evolution of radiation resistant bacteria. An inevitable consequence of life in an oxygen-rich environment is the formation of metabolically induced ROS (Figure 2.10), which are toxic to biological macromolecules such as DNA and proteins (Geiorgiou, 2002). Bacteria have developed a variety of systems to protect themselves against the damage caused by ROS (*e.g.*, superoxide dismutases [SOD] and catalase, Chapter 2). Oxidative stress occurs when the generation of ROS exceeds their elimination by antioxidant defense mechanisms resulting in DNA damage. Extreme conditions such as high-dose irradiation generate H_20_2 and release Fe^{2+} from heme-containing proteins (Touati, 2000). In its reduced form, Fe contributes to oxygen toxicity by converting hydrogen peroxide to reactive hydroxyl radicals ($^{\bullet}OH$) via the Fenton reaction (Touati, 2000; Geiorgiou, 2002). A detailed analysis of the metabolic components of *D. radiodurans* could lead to a better understanding of its survival mechanisms and how this phenotype could be exploited for practical purposes.

The bacterium *D. radiodurans* is one of the most radiation resistant organisms known, and is currently being engineered for remediation of the toxic metal (Brim *et al.*, 2000) and organic components (Lange *et al.*, 1998) present in radioactive wastes generated during the Cold War (Daly, 2000, Lange *et al.*, 1998, Brim *et al.*, 2000, Riley *et al.*, 1992). Understanding *D. radiodurans*' biotic potential and global physiologic integrity in nutritionally restricted radioactive environments are important in elucidating not only its extreme radiation resistance phenotype, but also its development for *in situ* bioremediation. The molecular mechanisms underlying the extreme radiation resistance phenotype have been the subject of several investigations (Daly *et al.*, 1994a, 1995, 1996; Dardalhon-Samsonoff and Averbeck, 1980; Mattimore *et al.*, 1995; Minton, 1996). However, the role of the

organism's metabolic repertoire and physiologic state at the time of irradiation is far less characterized. Little is known about this relationship other than that exponentially growing *D. radiodurans* cells are more sensitive to radiation than stationary-phase cells (Minton, 1994; Thornley, 1963), and freezing or desiccating *D. radiodurans* substantially increases its resistance phenotype (Daly *et al.*, 1994; Mattimore and Battista, 1996; Richmond *et al.*, 1999).

In radioactive environments that do not destroy an organism, but rather limit or prevent metabolism, genetic damage is accumulated and survival is dependent on repairing and preventing the accumulation of irreversible (lethal) genetic damage (Daly *et al.*, 1994a, 1994b, 1995). Genetic recovery of *D. radiodurans* following such accumulated DNA damage is heavily dependent on energy metabolism and protein synthesis (Minton, 1994). The ability of *D. radiodurans* to grow in the presence of 60 Gy/hour in nutrient-rich conditions, with no effect on either its viability, growth rate, or ability to express cloned genes has also been demonstrated (Lange *et al.*, 1998). By comparison, *E. coli* is killed at 60 Gy/hour irrespective of nutrient conditions (Lange *et al.*, 1998).

Notably, the identities of two novel isolates (7B-1 and 7C-1) from radioactive sediments at Hanford, WA were confirmed as *D. radiodurans* (Chapter 2, Section 2.3.1.4). Nutrient conditions at DOE radioactive waste environments are poor and the effect of such conditions on the growth and survival of *D. radiodurans* is unknown. In this study, the effect of nutrient conditions on *D. radiodurans*' ability to survive acute or chronic irradiating exposures was examined using a defined minimal medium (DMM) developed here. Nutrient conditions had a profound effect on the survival and growth of *D. radiodurans* during chronic irradiation exposure, but not following acute irradiation. In nutrient-limiting conditions during chronic irradiation, DNA repair was found to be limited by this organism's metabolic capabilities and not by any nutritionally induced defect in genetic repair. Specific aims of this chapter are as follows:

1. **To develop a chemically defined minimal medium for *D. radiodurans* and to characterize its dependence on defined carbon sources and amino acids.**

2. **To identify nutritional components that govern radiation resistance in *D. radiodurans*.**

3. **To correlate experimentally determined growth characteristics of *D. radiodurans* with those predicted by genome annotation.**

4. **To examine the amino acid starvation response in *D. radiodurans* and the response of the global metabolic regulators *RelA* and *SpoT*.**

3.2 Materials and Methods

3.2.1 Growth of Cells

D. radiodurans (strain R1) was grown on nutrient rich medium (TGY; 1% bactotryptone, 0.5% yeast extract; and 0.1% glucose) or defined minimal medium (DMM) (Table 3.1), in the absence or presence of chronic irradiation, 60 Gy/hour (^{137}Cs Gammacell 40 irradiation unit [Atomic Energy of Canada Limited]) (22 °C), as described previously (Lange *et al.*, 1998). To facilitate growth, liquid DMM was inoculated with cells (10^4-10^5 cells/ml) pre-grown on solid DMM. All chemicals in this work were obtained from Sigma Chemical Company; Bacto-agar and Noble agar were obtained from Difco. In liquid culture, cell density was determined at 600 nm in a Beckman spectrophotometer. For acute high-level radiation exposures, stationary phase cultures were irradiated without change of broth on ice at 10 kGy/h (^{60}Co Gammacell irradiation unit [J. L. Shepard and Associates, Model 109]). Following irradiation, cell viability was determined by plate assay, as described previously (Daly *et al.*, 1994).

3.2.2 *rel* Gene Functional Assay

rel function was assayed according to the procedures described by M. Cashel (Cashel, 1994). All eubacteria so far tested are capable of forming guanine nucleotide analogs of GDP and GTP, bearing a pyrophosphate group esterified to the 3'-hydroxyl of the ribose moiety; these are abbreviated as ppGpp and pppGpp, respectively. The RNA control locus *relA* encodes (p)ppGpp synthetase and sometimes forms a hybrid locus containing *spoT*, that encodes 3'-pyrophosphohydrolase (*e.g.*, in

Bacillus subtilis [Wendrich and Marahiel, 1977]). RelA is synthesized in bacteria in response to amino acid starvation and indirectly reduces protein synthesis by repression of stable RNA synthesis when concentrations of amino acids cannot keep up with the demands in protein biosynthesis. RelA-induced RNA suppression has pleitropic effects including a reduction in DNA replication, transcription, translation, and growth. Together with SpoT, RelA participates in integrating carbon and nitrogen metabolism (Cashel and Rudd, 1996). RelA activity in *D. radiodurans* cells was determined as follows: cells were grown on TGY solid medium for 60 hours or on solid DMM (Table 3.1A) for 170 hours. ~10^8 cells were suspended in Phosphate-Free Labeling Medium (PFLM: 0.1 M MOPS, 0.2% dextrose, and 100 μCi/ml carrier-free ^{32}P-orthophosphoric acid) with or without 1 mg/ml serine hydroxamate, that blocks translation and is used to induce *relA/spoT* activity. Authenticity of (p)ppGpp and pppGpp spots were established by using *E. coli* wildtype (CF1648) and a mutant *E. coli* strain (CF1652) lacking *relA* (Mechold *et al.*, 1996), as controls. A cell suspension (25 μl) was mixed with an equal volume of 13 M formic acid, placed on dry ice and freeze-thawed twice. The mixture (4 μl) was then spotted onto a cellulose polyethyleneimine (PEI)-thin layer chromatography (TLC) (Fisher Scientific) plate and the TLC plate was developed with 1.5 M KH_2PO_4 (pH 3.4). When the solvent front reached 15 cm, the plate was air-dried and exposed overnight to X-ray film.

3.2.3 Transmission Electron Microscopy (TEM) and Confocal Laser Scanning Microscopy (CSLM)

TEM and CSLM was a collaborative effort with Dr. Alexandar Vasilenko at USUHS, Bethesda, MD.

TEM. As described in section 2.2.9

CSLM. Bacterial cells were harvested and washed with 0.1 M Tris-HCl, 0.01 M EDTA buffer (pH 8.0), fixed in 77% ethanol (0 °C), and stained with acridine orange. The stained preparations were visualized with a Bio-Rad MRC-600 confocal laser scanning microscope interfaced with a Zeiss Axiovert microscope as well as a Merdian ULTIMA ACAS 570 CSL Microscope, using 100 x immersion objectives. Images were reproduced by using a New Codonics NP1600 Postscript printer. Acridine orange-double stranded nucleic acid results in a complex that has an absorption maximum

between 450-490 nm that gives rise to green fluorescence and was used to localize DNA, with a 520 nm barrier filter. Acridine orange-single stranded nucleic acid complex has an absorption maximum between 510-560 nm that gives rise to red fluorescence and was used to localize RNA, with a 590 nm barrier filter (Darzynkiewicz, 1994).

3.2.4 Nucleic Acid Isolation and Manipulation

~3 x 10^8 *D. radiodurans* cells pregrown in either rich or DMM were harvested at the indicated time points and resuspended in 570µl of TE buffer (10 mM Tris-HCl, pH 8; 0.1 mM EDTA). The cells were lysed by the addition of 15 µl 20% (w/v) sodium dodecyl sulfate (SDS) and 300 µg of proteinase K, and incubation at 37°C for 60 minutes. Cell lysates were phenol/chloroform-extracted and nucleic acids were precipitated with a 0.6 volume of isopropanol, and dissolved in TE buffer. The concentration and purity of both DNA and RNA samples were determined by spectrophotometric ratio assay at 260 nm and 280 nm.

3.2.5 Agarose Gel Electrophoresis

As described in section section 2.2.5.3.

3.3 Results

3.3.1 Development of a Defined Minimal Medium (DMM) Suitable for Analysis of *D. radiodurans* Growth

A previous report of a *D. radiodurans* minimal medium preparation that was used to assess growth, described a synthetic medium that contained excessively high concentrations (30 - 600 µg/ml each) of 17 amino acids, yielding a medium containing greater than 5 mg/ml amino acids (Shapiro *et al.*, 1977). In addition, this reported minimal medium included a large variety of minerals and vitamins that were also shown to be unnecessary for *D. radiodurans* growth. The excessive use of

non-essential nutrients rendered this medium neither minimal nor useful for deinococcal growth studies. In fact, *D. radiodurans* could grow in this medium in the absence of typical Embden-Meyerhof-Parnas (EMP) pathway substrates (*e.g.*, fructose, glucose, and maltose). Therefore, the development of a synthetic medium that is truly minimal, highly characterized and suitable to testing this organism's metabolic capabilities as guided by analysis of the genomic sequence, was needed.

In developing a synthetic minimal medium, many combinations of varying amounts of carbohydrates, amino acids, salts and vitamins in both liquid and solid medium (using Noble agar) were systematically tested. By a process of elimination, minimal nutrient constituents, and their concentrations, necessary for luxuriant growth were identified (Table 3.1A). This synthetic medium preparation for *D. radiodurans* is distinct from those published by others (Raj *et al.*, 1960; Shapiro *et al.*, 1977) in that it is much simpler, and growth of *D. radiodurans* in such medium is completely dependent on a carbon/energy source (*e.g.*, fructose; Figure 3.1). In addition to a metabolizable carbon source, growth of *D. radiodurans* was found to be dependent on exogenous amino acids and a vitamin; addition of sulfur-rich amino acids, together with nicotinic acid were particularly effective at supporting growth. However, the specificity of amino acids was shown not to be stringent since many different combinations of amino acids supported growth (Chapter 4 further defines the amino acid requirements of *D. radiodurans* and related species). A factor that strongly influenced the extent of growth was the total amino acid concentration in the growth medium (Figure 3.2), not the composition of the amino acid pool. Among the carbon sources tested, the following supported luxuriant to slow growth in the following order: fructose > pyruvate > lactate > glucose > oxaloacetate > acetate > glycerol (Figure 3.1). There are numerous examples of free-living bacteria with absolute specificity to sugar metabolism (*e.g.*, *Arthrobacter* can utilize fructose, but not glucose [Sobel and Kruwlwich, 1973]). Surprisingly, the tricarboxylic acid (TCA) cycle intermediates fumarate, citrate, malate, and succinate were ineffective at supporting growth (Figure 3.1).

Table 3.1. Minimal Nutrient Requirements for Growth of *D. radiodurans* in the Absence (A) and Presence (B) of γ-Radiation (60 Gy/hour)

	Components	Concentrations	
		A (Without irradiation)	B (With irradiation)
BSM[a]	Potassium Phosphate Buffer (pH7.5-8.0)	20 mM	20 mM
Salts	Magnesium Chloride, Tetrahydrate	0.2 mM	0.2 mM
	Calcium Chloride, Dihydrate	0.1 mM	0.1 mM
	Manganese (II) Acetate, Tetrahydrate	5.0 μM	5.0 μM
	Ammonium Molybdate, Tetrahydrate	5.0 μM	5.0 μM
	Ferrous Sulfate, Heptahydrate	5.0 μM	5.0 μM
Amino Acids	L-Histidine	25 μg/ml	**200 μg/ml**
	L-Cysteine	30 μg/ml	**30 μg/ml**
	L-Methionine	50 μg/ml	**50 μg/ml**
	L-Alanine	----------	**500 μg/ml**
	L-Arginine	----------	**800 μg/ml**
	L-Asparagine	----------	**800 μg/ml**
	Glycine	----------	**300 μg/ml**
	L-Leucine	----------	**500 μg/ml**
	L-Lysine	----------	**300 μg/ml**
	L-Glutamine	----------	**500 μg/ml**
	L-Proline	----------	**370 μg/ml**
	L-Serine	----------	**300 μg/ml**
	L-Threonine	----------	**200 μg/ml**
	L-Tryptophan	----------	**200 μg/ml**
	L-Tyrosine	----------	**200 μg/ml**
	L-Valine	----------	**200 μg/ml**
Vitamin[b]	Nicotinic Acid	1.0 μg/ml	1.0 μg/ml
Carbon	Carbon Source	2 mg/ml	2 mg/ml

Footnote Table 3.1 [a]Basal Salt Medium (BSM) was autoclaved and then supplemented with sterile preparations of salts, amino acids, and nicotinic acid at the indicated concentrations. For solid medium, Noble Bacto Agar was added before autoclaving BSM, to 1.5% (w/v). [b]Substitution of nicotinic acid with Basal Medium Eagle Vitamin Solution (GibcoBRL) improved growth slightly. For growth in liquid DMM, cells used for inoculation were pre-grown on solid DMM.

Figure 3.1. Growth of *D. radiodurans* in Defined Minimal Medium (DMM) (Table 3.1A). containing 2 mg/ml of the indicated carbon sources. An OD_{600} of 1.0 = ~1 x 10^8 CFU /ml. CFU, colony-forming units. Cells were pre-grown on solid DMM before inoculation into liquid DMM.

Figure 3.1

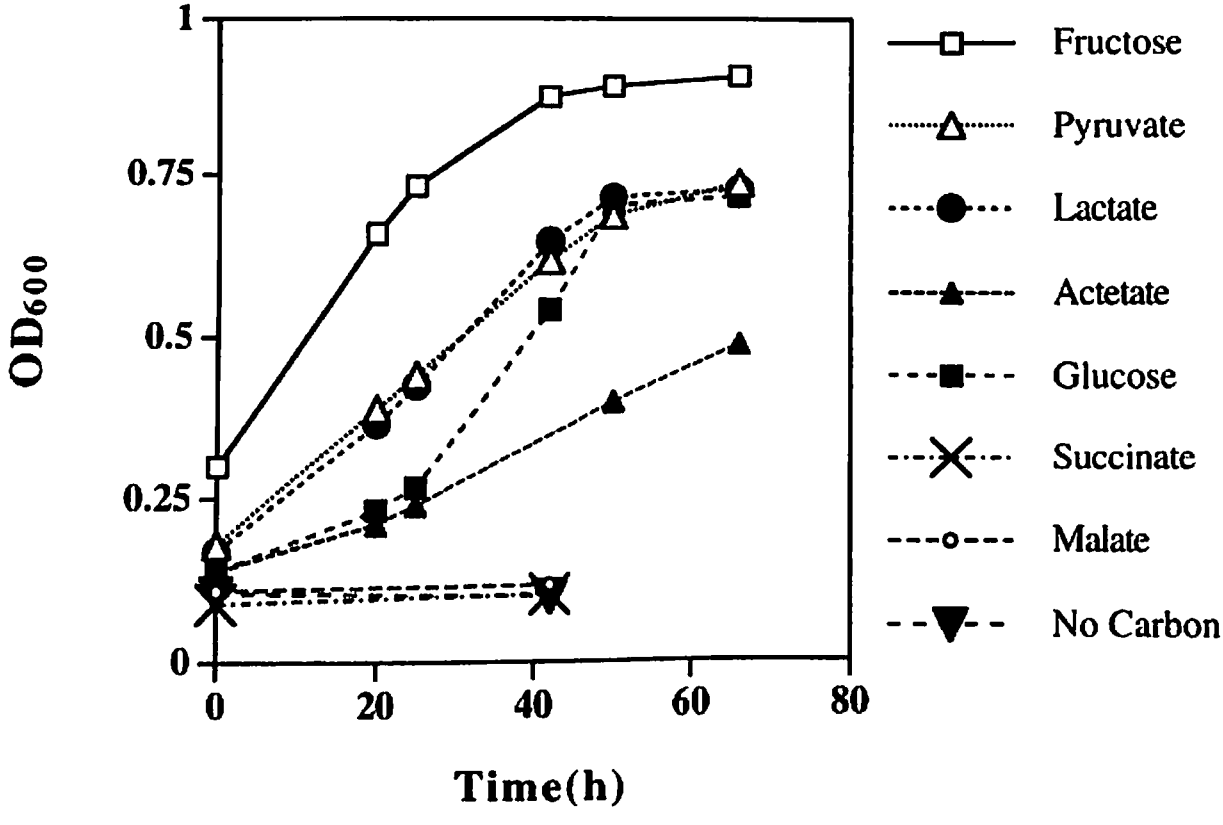
1
0.75
0.5
0.25
0
0
20
40
60
80
OD600
Time(h)
Fructose
Pyruvate
Lactate
Actetate
Glucose
Succinate
Malate
No Carbon

Figure 3.2. Relationship Between Amino Acid Concentration and Growth of *D. radiodurans* in Liquid DMM. The nutrient conditions were as described in Table 3.1A with the exception of amino acid composition. Fructose was the carbon source. Amino acid composition: 25% glutamine; 18% cysteine; and 10% (tyrosine, tryptophan and phenylalanine, buffered with 5% glycine). Cultures were inoculated at 5 x 10^6 CFU/ml using cells pre-grown on solid DMM (Table 3.1A). OD_{600} measurements were made at 96 hours following inoculation.

Figure 3.2

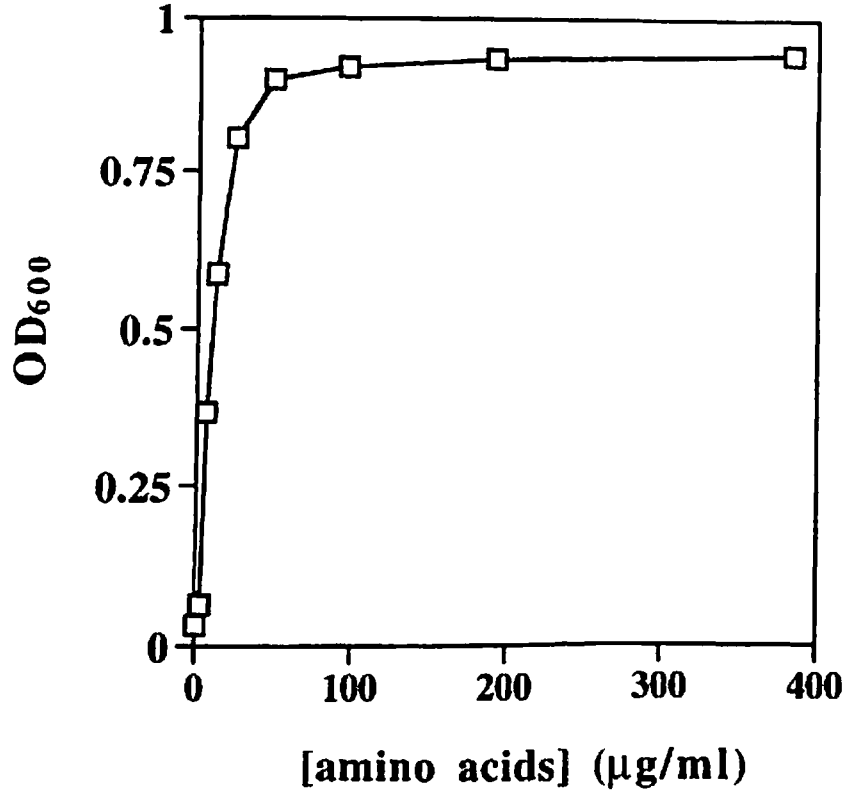

D. radiodurans cells grown in DMM were examined by electron microscopy (Figure 3.3). Unexpectedly, almost all DMM-cultured cells grew as diplococci; cells grown in TGY grow as tetracocci in the late stages of growth (Figure 3.3A/B). There were also morphological differences in cell wall structures observed between cells grown in DMM and TGY (Figure 3.3 C/D). In rich medium, the cell wall consists of multiple layers and is about 150 nm thick (2, 31); the order of layers from the inside to outside are: cytoplasmic membrane (not visible in Figure 3.3), peptidoglycan layer (pg), holey layer (hl; darkest layer) that has an hexagonally packed structure, and the carbohydrate coat (cc) (Figure 3.3 B/D). *D. radiodurans* cells grown in DMM (Table 1A) displayed a holey layer which appears to be more electron transparent than the holey layer of cells in TGY (Figure 3.3C).

3.3.2 Sensitivity of *D. radiodurans* Grown in Synthetic Medium to Chronic and Acute Irradiation

To investigate the effect of *D. radiodurans*' nutritional state on its radiation resistance phenotype, cells were exposed to continuous γ-radiation in a ^{137}Cs irradiator (60 Gy/hour) in different growth conditions. Control cultures were incubated in the absence of radiation at the same temperature. For cells grown on rich medium (TGY), growth was not affected by continuous exposure to 60 Gy/hour compared to growth on TGY in the absence of radiation. In contrast, growth in DMM (Table 3.1A) was eliminated by chronic exposure to 60 Gy/hour. To determine if chronic radiation under minimal conditions was bactericidal or bacteriostatic, a series of inoculated DMM plates were exposed to 1, 2, 3, 4, or 5 kGy in the irradiator. Following exposure, the plates were incubated in the absence of radiation to monitor survival. A chronic dose of 3 kGy was lethal to cells; this contrasts dormant (on ice) *D. radiodurans*' ability to survive 17 kGy of acute radiation with high survival if cells are allowed to recover and grow in rich medium (Daly *et al.*, 1994a, 1994b, 1995, 1996). Cell viability and the DNA repair capabilities of chronically irradiated *D. radiodurans* cells incubated in either liquid TGY or DMM (Figure 3.4) were further examined. Following incubation in the ^{137}Cs irradiator, cells were collected at intervals extending to 96 hours. A portion of the cells was plated for survival (Figure 3.4A) and the remainder frozen until total DNA was prepared and examined for degradation (Figure 3.4B).

Figure 3.3. Transmission Electron Microscopy (TEM) of *D. radiodurans* Grown in DMM (Table 3.1). (**A** and **C**) and TGY (**B** and **D**) showing wall structure and nucleoid morphology. Note that cells grown in TGY medium exist as tetracocci (B). By comparison, in DMM, cells exist as diplococci (A). The nucleoids in TGY-grown cells are distinct and ring-shaped (B) and are not visible in cells grown in minimal medium. EM scale bars in A & B = 1 μm; in C & D = 100 nm. **pg**, peptidoglycan layer; **hl**, holey layer; **cc**, carbohydrate coat.

Figure 3.3

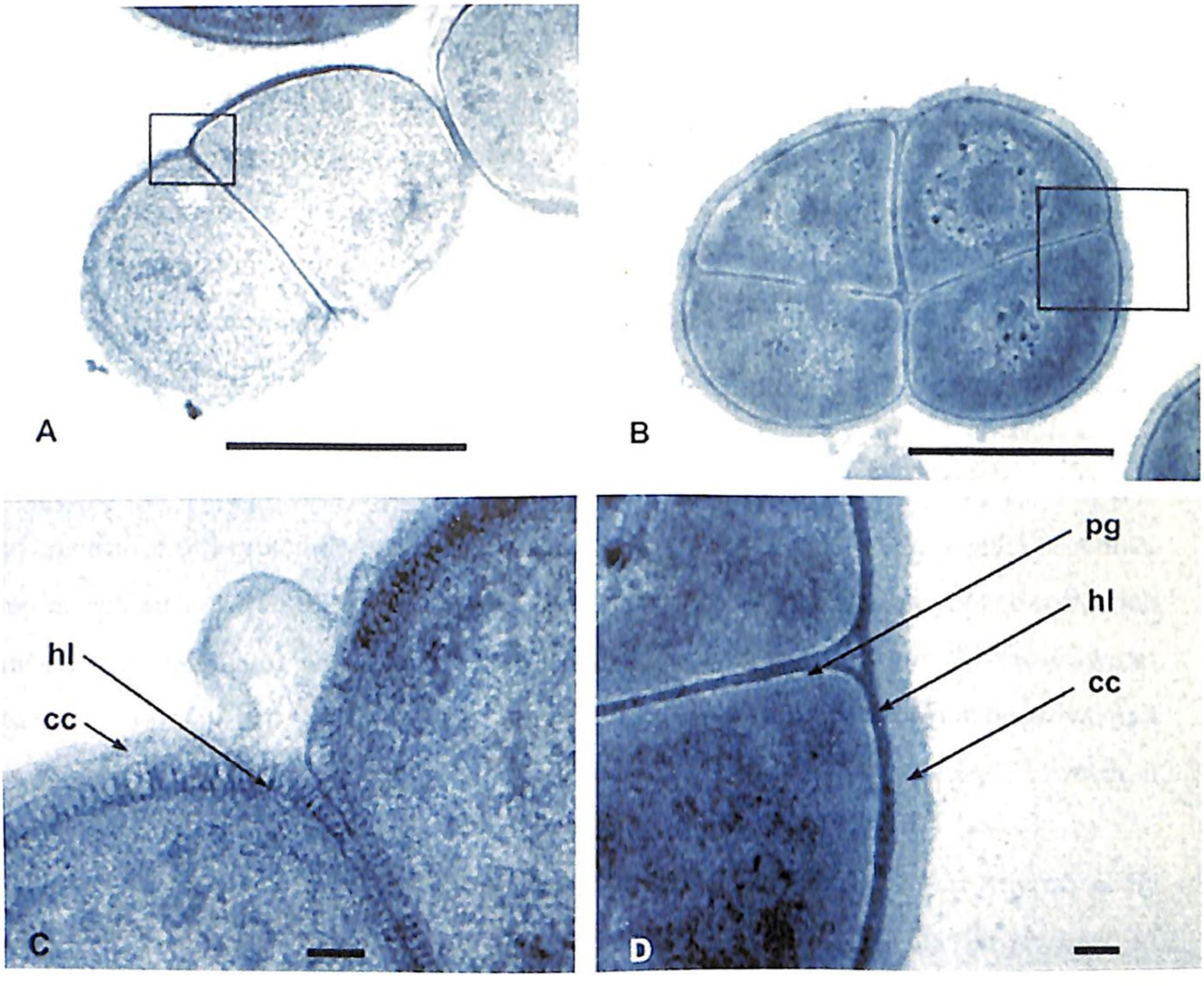

Rapid degradation of DNA occurred in cells incubated in DMM, whereas there was little evidence for DNA degradation in TGY-incubated cells. Some DNA degradation, and a loss in viability, in TGY-incubated cells was observed at the 48 and 96 hour time points, presumably due to the depletion of metabolizable nutrients and the inevitable accumulation of DNA damage in slowly- or non-replicating cells. By comparison, cells incubated in DMM plus irradiation showed a very large decrease in viability almost immediately. After 24 hours of irradiation (1.44 kGy; Fig 3.4B) the DNA was highly degraded, and all cells were killed by 96 hours (5.76 kGy; Figure 3.4).

To rule out the possibility that cells grown in DMM (Table 3.1A) were inherently sensitive to radiation, or that certain nutritional-dependent repair factors were lacking in the synthetic medium, TGY- and minimally-grown *D. radiodurans* cells were tested for their ability to survive extremely high doses of acute gamma radiation. Figure 3.5 shows that irrespective of the pre-irradiation growth medium or post-irradiation recovery substrate, the resistance of *D. radiodurans* was similar. As expected, the D_{37} of the diplococcus culture (grown in DMM) was ~6 kGy, one half the D_{37} of the tetracoccus *D. radiodurans* culture (~12 kGy) (Figure 3.3B). The very long shoulder of resistance of *D. radiodurans* grown in rich medium (Figure 3.5) results from its morphology, where each of four independent cells of a tetracoccus needs to be killed to eliminate a colony forming unit (CFU). Failure to correct for cell-grouping can lead to exaggerated resistance values based on CFU counts. For example, very high resistance has been reported for *Kineococcus radiotolerans*, but no correction was made for cell-grouping (Phillips *et al.*, 2002). In liquid medium, *K. radiotolerans* grows as organized clumps of >100 cells (Phillips *et al.*, 2002). Because *D. radiodurans* cannot be grown as a monococcus, the D_{37} for a single-celled population cannot be determined experimentally. However, it is estimated to be about one half the D_{37} of the diplococcus culture (Figure 3.3A).

The minimal nutrient conditions required to support growth at 60 Gy/hour were determined by variably increasing the concentrations of the nutrients shown in Table 3.1A. In the presence of continuous radiation, growth was restored only when high concentrations of amino acids were provided together with an EMP or Entner-Doudoroff (ED) carbon substrate (Table 3.1B, Figure 3.1).

Figure 3.4. Effect of Growth- and Recovery-Substrate on Survival of *D. radiodurans* Following Acute γ-Radiation. Cells were grown to early stationary phase and irradiated on ice at 10 kGy/h. **Open square**: Cells pre-grown in liquid TGY, irradiated, and plated on solid TGY; **Solid triangle**: Cells pre-grown in liquid TGY, irradiated, and plated on solid DMM [Table 3.1A]; **Open circle**: Cells pre-grown in liquid DMM, irradiated, and plated on solid TGY; **Solid diamond**: Cells pre-grown in DMM, irradiated, and plated on DMM.

Figure 3.4

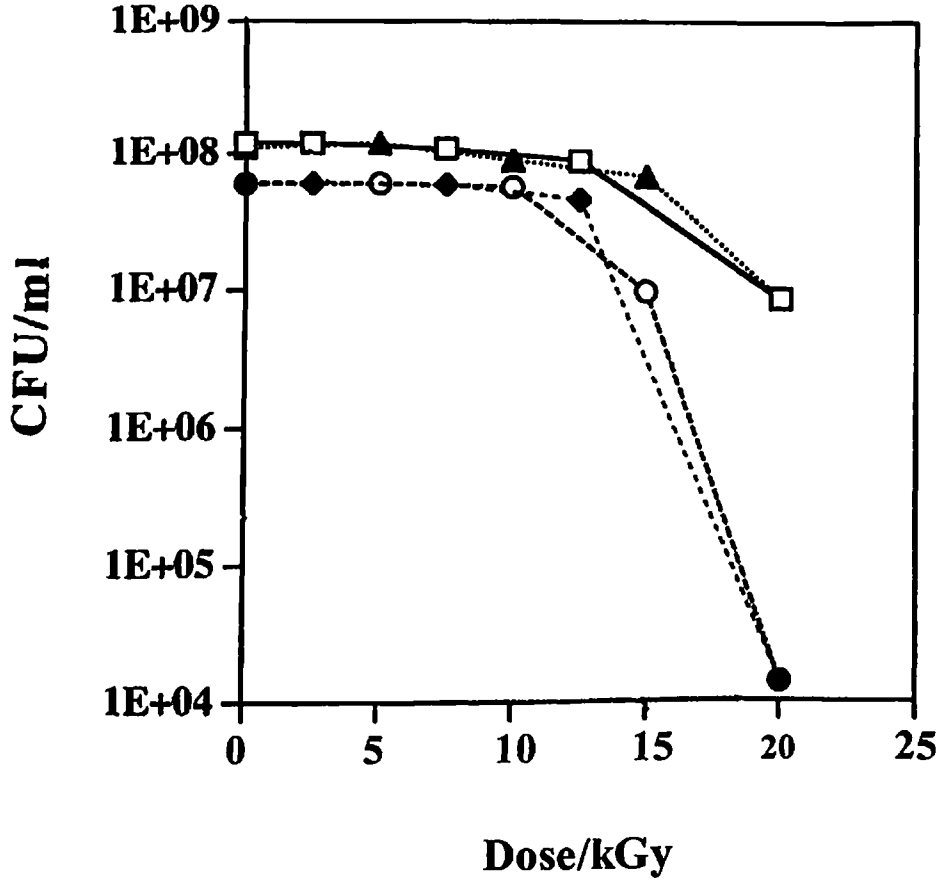

Figure 3.5. Effect of Nutrient Conditions on the Viability and DNA Content of *D. radiodurans* Exposed to Chronic γ-Radiation, in Liquid Culture. Cells were irradiated at 60 Gy/hour (23 °C). For both irradiated and control cultures, cells were diluted to 5 x 10^6 CFU/ml at the start of the experiment. **A)** Survival curves. **Solid square**: control, TGY, no radiation. **Open square**: TGY plus γ-radiation. **Solid circle**: control, DMM [Table 3.1A], no radiation. **Open circle**: DMM [Table 3.1A], plus γ-radiation. **B)** Total DNA was prepared from cells corresponding to each of the time points shown in panel A. Each lane contains DNA from ~3 x 10^6 cells, as determined by hemocytometer count (Daly *et al.*, 1994a). TGY+ γ, cells grown in TGY plus γ-radiation; Min + γ, cells grown in DMM (Table 3.1A) plus γ-radiation; TGY and Min lanes, shown on the right, are from the controls incubated in the absence of irradiation. λ/H, lambda phage DNA cut with HindIII. DNA size in kilo bases (kb) is shown on the left. The gel migration positions of DNA and rRNA are indicated on the right. Gel electrophoresis was in a 0.66% agarose gel for 17 hours at 45 V.

Figure 3.5

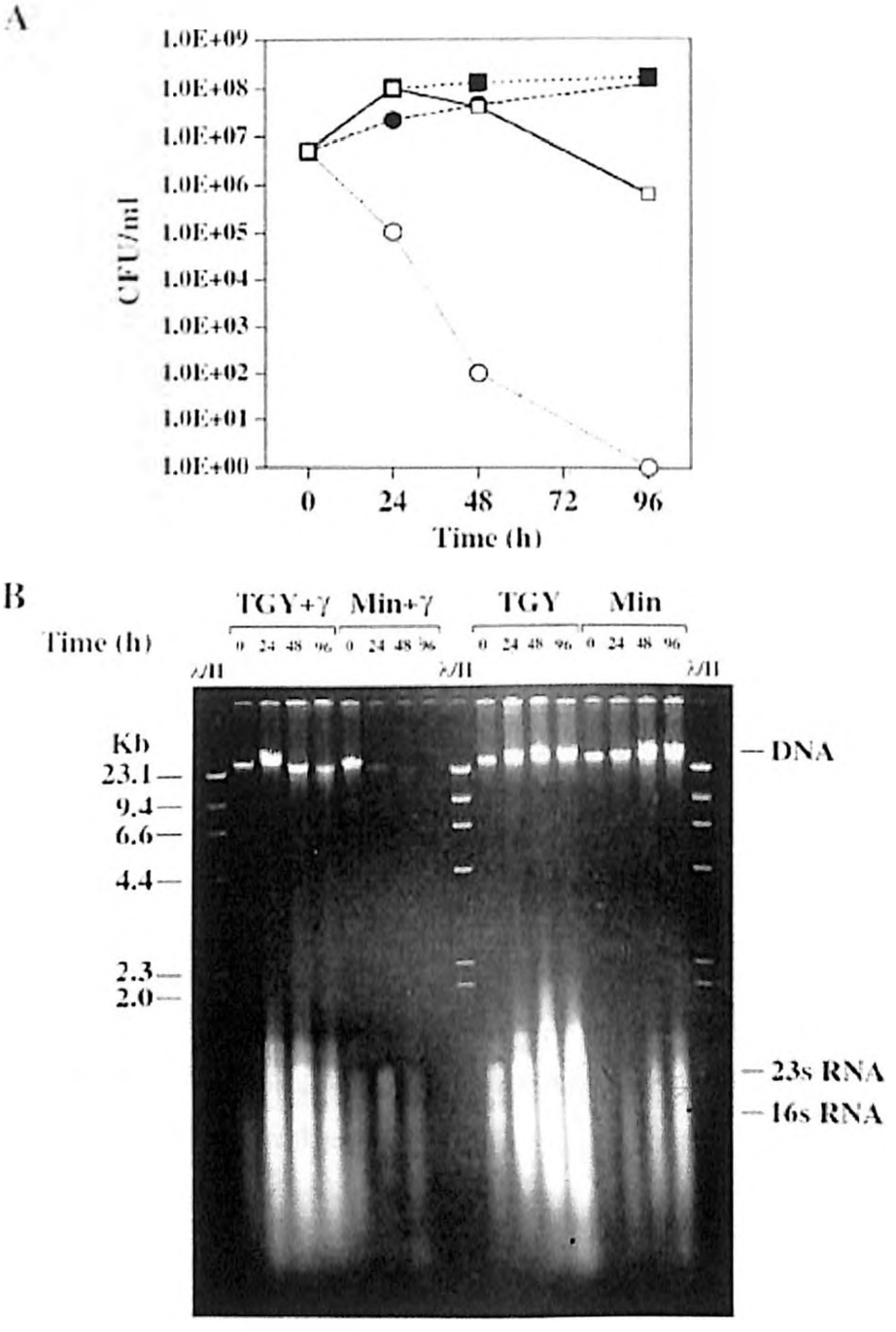
A
1.0E+09
1.0E+08
1.0E+07
1.0E+06
1.0E+05
1.0E+04
1.0E+03
1.0E+02
1.0E+01
1.0E+00
CFU/ml
0
24
48
72
96
Time (h)
B
TGY+γ
Min+γ
TGY
Min
Time (h)
0 24 48 96 0 24 48 96 0 24 48 96 0 24 48 96
λ/H
λ/H
λ/H
Kb
23.1
9.4
6.6
4.4
2.3
2.0
DNA
23s RNA
16s RNA

Increasing the concentration of the carbon source or non-amino acid supplements beyond the concentrations described in Table 3.1A had no effect on resistance. Similarly, in the absence of a carbon source, high concentrations of amino acids alone did not support growth in the irradiator. Table 3.1B shows the minimum nutrients, and their concentrations, that supported luxuriant *D. radiodurans* growth at 60 Gy/hour.

3.3.3 Physiologic Genomic Analysis of *D. radiodurans*

In the course of annotation of the *D. radiodurans* genome (White *et al.*, 1999) most metabolic pathway genes key to this analysis were present. For example, the EMP and ED pathways were found to be intact, and *D. radiodurans* could grow on fructose, glucose, maltose and mannose, as expected. However, there were three examples where the primary biosynthetic pathways of amino acids were incomplete (Table 3.2). Further, *D. radiodurans* could not utilize ammonia as a nitrogen source and its growth was entirely dependent on exogenous amino acids. Therefore, the genomic sequence was carefully examined for defects that could effect nitrogen assimilation. Generally, the key step in assimilating inorganic nitrogen into amino acids is the synthesis of glutamine and glutamate from ammonia by the action of glutamine synthetase (*gln*A). In *D. radiodurans* strain R1 there are two copies of *glnA*, *glnA*-1 (chromosomal position [cp]: 2049790) is disrupted by a frameshift mutation while *glnA*-2 (cp: 447280) appears to be intact. The glutamate synthase subunit genes (*gltB* and *gltD*) also appeared to be functional (cp of operon: 181526); GltB/D integrated carbon and nitrogen metabolism by the synthesis of glutamine from glutamate. Yet, this bacterium could not use 2-oxoglutarate as a growth substrate in DMM supplemented with a variety of inorganic nitrogen sources (*e.g.*, ammonium sulfate), suggesting there may be a defect in the assimilation of ammonia by the glutamine synthetase/glutamate synthase cycle.

Table 3.2. [a]Effectiveness of Carbon Sources as Precursors for *D. radiodurans* Growth

Carbon/Energy Source	Growth	[b]Biosynthetic Pathway	[c]Existence (genome data)	Defect
Pyruvate	+ ++	Alanine	complete	-
		Valine	complete	-
		Leucine	complete	-
Oxaloactate	++	Isoleucine	complete	-
		Threonine	complete	-
		Lysine	**incomplete**	*dapABDF* absent
		Methionine	complete	-
		Aspartic acid	complete	-
Phosphoglycerate	+	Serine	**incomplete**	*serCB* absent
		Glycine	complete	-
	-	Cysteine	**incomplete**	*cysEJDN* absent

Footnote Table 3.2: [a]Acetate and lactate are effective growth substrates while the TCA cycle intermediates malate, succinate, fumarate and citrate, are ineffective. [b]Pathways indicated correspond to entry points to biosynthesis for the indicated amino acids from the compounds listed in the first column. [c]For genomic comparison, we used metabolic pathways present in *E. coli*. All genes necessary for histidine biosynthesis are present. +++, excellent; ++, good; +, poor; -, no growth.

3.3.4 Correlation Between Amino Acid Limited Growth and *relA* Activity

RelA and SpoT are responsible for integrating carbon and nitrogen metabolism (Cashel and Rudd, 1996), and when their regulation is defective these genes have pleiotropic effects on cells, that include a dependence on exogenous amino acids for growth and suppression of cellular RNA levels (Cashel and Rudd, 1996). Therefore, *rel* function in *D. radiodurans* was examined at both genomic informatic and experimental levels.

D. radiodurans was found to encode a predicted protein that is most similar (58% identity) (Altschul *et al.*, 1997) to the RelA/SpoT protein [(p)ppGpp synthetase/3'-pyrophosphohydrolase] of *Bacillus subtilis* (Wendrich and Marahiel, 1977). The functional integrity of the putative *rel* locus in *D. radiodurans* was tested by monitoring the diagnostic synthesis of ppGpp and pppGpp under amino acid deprivation (Figure 3.6A). Cells were shifted from TGY or DMM to labeled phosphate medium (PFLM) containing a single carbon/energy source plus or minus serine hydroxamate (Figure 3.6B, 3.6C). In these conditions, ppGpp and pppGpp were rapidly synthesized and expressed at levels comparable to those seen in *E. coli* (Figure 3.6). These data support normal *rel* function in *D. radiodurans* and its induction in amino acid-limiting conditions.

Consistent with the induction of *rel* functions, cells grown in DMM conditions (Table 3.1A) had substantially reduced cellular RNA levels, as seen by gel electrophoresis of total nucleic acid (Figure 3.3B). Suppression of cellular RNA content was verified directly by microscopy of cells using Confocal Laser Scanning Microscopy (CSLM) and acridine orange cell staining (Figure 3.7). Differential staining of DNA and RNA showed that cells grown in DMM (Table 3.1A) had highly reduced levels of RNA compared to cells growing in nutrient rich medium (TGY).

Figure 3.6. Panel A. Production of pp(p)Gpp in *D. radiodurans* and *E. coli.* ^{32}P-labeled ppGpp and pppGpp were detected by PEI cellulose chromatography (Materials and Methods). Stationary-phase cells grown in either TGY or DMM (Table 3.1A/B) were suspended in PFLM (Materials and Methods) with or without the amino acid analogue serine hydroxamate. Lanes: 1 & 2) *D. radiodurans* cells from DMM (Table 3.1A) incubated in PFLM plus serine hydroxamate (these lanes are equivalent to Panel B, lanes 4 & 5); 3 & 4) *D. radiodurans* cells from DMM (Table 3.1A) incubated in PFLM plus 16 amino acids listed in Table 3.1B (final amino acid concentration: 50 μg /ml); 5) *D. radiodurans* cells from TGY medium incubated in PFLM plus serine hydroxamate; 6) *E. coli* (*relA* deleted) incubated in PFLM plus serine hydroxamate, control; 7) *E. coli* (wildtype) incubated in PFLM plus serine hydroxamate, control.

Panel B. Formation of ppGpp and pppGpp in *D. radiodurans*. Cells were treated as described in Panel A in the presence of serine hydroxamate. Lanes: 1) control, no cells; 2 & 3) cells grown in TGY medium (duplicate lanes); 4 & 5) cells grown in DMM (Table 3.1A) (duplicate lanes).

Panel C. Formation of ppGpp and pppGpp in *D. radiodurans* grown in DMM. Cells were treated as described in Panel A. Lanes: 1) cells treated in the absence of serine hydroxamate; 2) cells treated in the presence of serine hydroxamate.

Figure 3.6

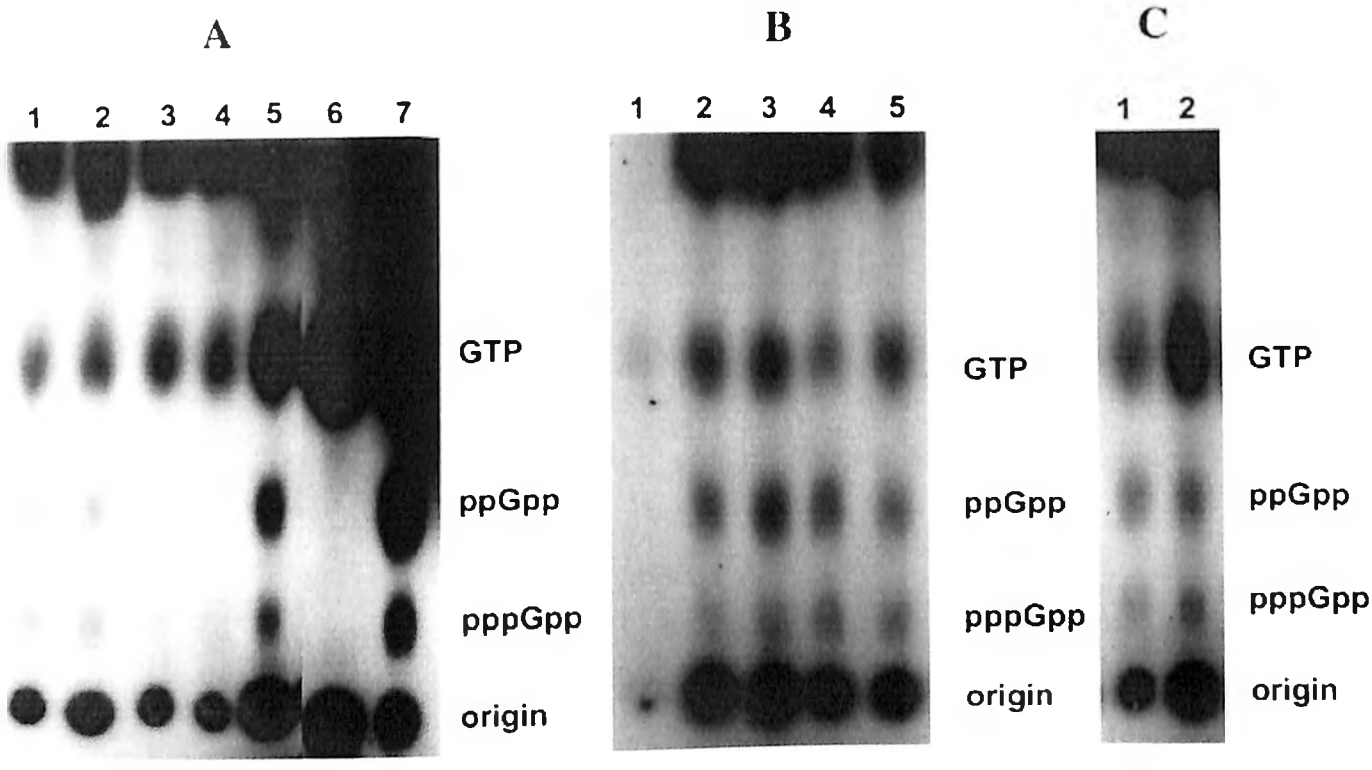
A
1 2 3 4 5 6 7
GTP
ppGpp
pppGpp
origin
B
1 2 3 4 5
GTP
ppGpp
pppGpp
origin
C
1 2
GTP
ppGpp
pppGpp
origin

Figure 3.7. Confocal Laser Scanning Microscopy (CSLM). Bacterial cells were stained with acridine orange. Acridine orange-single stranded nucleic acid results in a complex that gives rise to red fluorescence and was used to localize RNA. Acridine orange-double stranded nucleic acid complex gives rise to green fluorescence and was used to localize DNA. Note that when DNA and RNA are both present the cells appear yellow. a) DMM (Table 3.1A); b) TGY medium. Scale bars: 5 μm.

Figure 3.7

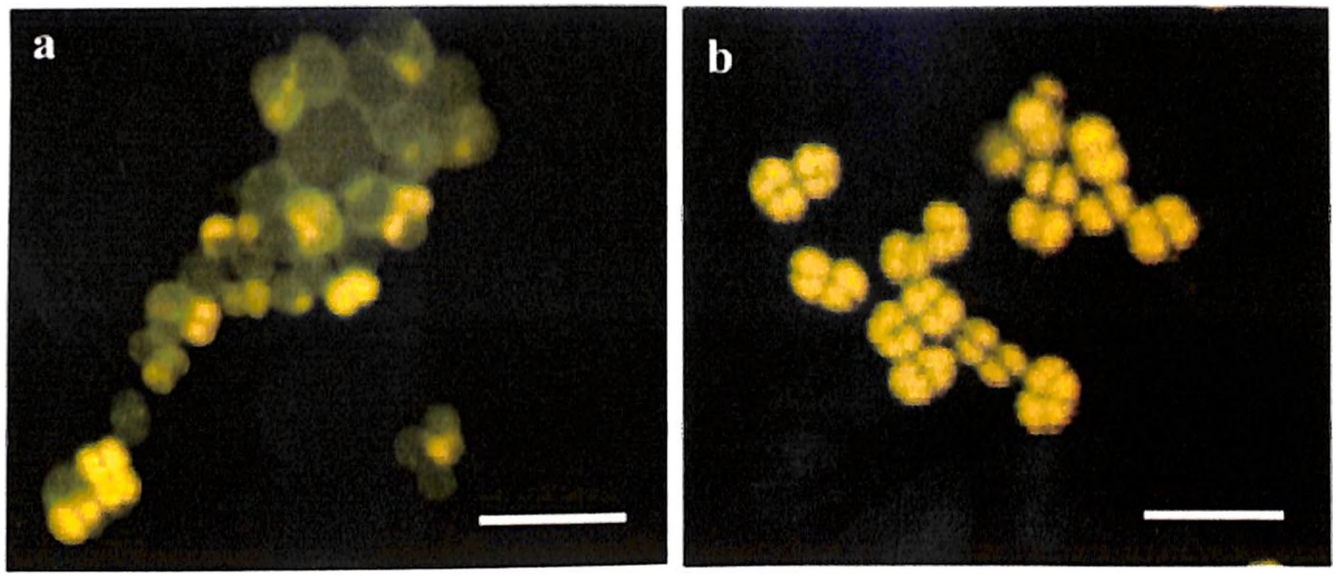

3.4 Discussion

The development of a synthetic medium for *D. radiodurans* played an important role in testing the relationship between its metabolic capabilities, ambient nutrient conditions, and radiation resistance. *D. radiodurans*' growth was unaffected by chronic exposure to 60 kGy/hour in nutrient rich conditions (Lange *et al.*, 1998). However, cells are unable to grow and are killed in radioactive nutritionally restricted environments that support luxuriant growth in the absence of radiation. This phenotypic reversal from radiation resistance to sensitivity is of great interest and concern since it reveals the importance of metabolism in radiation resistance, but questions the suitability of *D. radiodurans* as a bioremediation host in radioactive waste sites. The data show that cells grown in DMM are similarly resistant to acute gamma radiation (0-12 kGy) as those grown in nutrient rich conditions (TGY) (Figure 3.5), and that the principle factor limiting survival and growth in chronically irradiated conditions (Figure 3.4) is the cells' ability to utilize certain nutrients. This study identified key nutritional constituents that restore growth of *D. radiodurans* in radioactive nutrient-limiting environments (Table 3.1B).

These results reinforce the previous assertion that DNA repair requires nutrient-rich conditions (Minton, 1994). In earlier studies of *D. radiodurans* exposed to acute radiation (5-20 kGy), DNA repair required fresh TGY medium (Daly *et al.*, 1994). In the absence of such conditions, it has been reported that DSB-induced DNA degradation is relentless, leading to cellular death (Daly *et al.*, 1994; Minton, 1994). Considering DNA degradation and repair within the context of *D. radiodurans* also burdened with *de novo* synthesis of cell components on DMM, the added metabolic demands of repairing 4-10 copies (Hansen, 1978) of its genome (3.28 Mbp) during chronic radiation are likely to be profound. Indeed, degradation of DNA within chronically irradiated cells incubated in DMM is rapid and progressive (Figure 3.4B). Therefore, during its growth in DMM (Table 3.1A) under radioactive conditions, the rate of DNA repair and synthesis is overwhelmed by the rate of DNA degradation.

For growth under chronic irradiation, phenotypic reversion from radiation sensitivity (in DMM; Table 3.1A), to resistance could be induced by enriching the growth substrate. Specifically, restoration of radiation resistance during growth was highly dependent on an exogenous abundant

amino acid source (Table 3.1B). Genomic analysis showed that *D. radiodurans* contains most amino acid biosynthetic pathways (Table 3.2). However, the primary biosynthetic pathways for cysteine, lysine and serine are incomplete (Table 3.2). Yet, *D. radiodurans* could grow in the absence of these pathways, supporting the hypothesis that secondary biosynthetic pathways for these three amino acids exist in *D. radiodurans*. In particular, the annotation of *D. radiodurans* genome (Makarova *et al.*, 2001) reveals the presence of gene orthologs for an alternate α-animoadipate pathway of lysine biosynthesis (in contrast to the diaminopimelate pathway, which is typical of most other bacteria) that was originally discovered in *Thermus thermophilus* (Kobashi *et al.*, 1999). Furthermore, transamination reactions facilitate the interconversion of many amino acids as well as *de novo* synthesis from TCA cycle intermediates. Given *D. radiodurans*' inability to assimilate inorganic nitrogen, the existence of such transamination capabilities are consistent with the finding that *D. radiodurans*' growth in DMM, while not dependent on any specific amino acids, is absolutely dependent on a non-specific exogenous amino acid source.

In eubacteria, global regulation of various metabolic processes, including transcription and protein synthesis, is known to be under stringent control of the loci *relA* and *spoT* (Mechold and Malke, 1997); in amino acid-limiting conditions *relA* is induced. *relA* activity in eubacteria is well known for its global suppression of RNA synthesis and induction of amino acid synthesis (Mechold *et al.*, 1996). In *D. radiodurans*, with its disruption of three major biosynthetic pathways, *relA* function may be easily triggered. Therefore, testing RNA suppression in *D. radiodurans* would be important since it not only would support *relA* function, but also could help explain the inhibition of *D. radiodurans*' growth in nutrient-limiting conditions during chronic radiation. Growth of *D. radiodurans* in amino acid-limiting conditions resulted in *rel*-associated functions; pp(p)Gpp- was induced (Figure 3.5) and the cellular RNA content was highly reduced (Fig 3.4B, 3.7). In the majority of cell-types, about 80% of total cellular RNA is rRNA (Darzynkiewicz, 1994). The rRNA content is, thus, a good indicator of total cellular RNA and the translational potential of the cell. Global suppression of RNA in *D. radiodurans* would likely suppress its metabolism, and this could explain the inability of cells exposed to radiation in DMM to survive and grow. If true, these cells are unable to generate the levels of precursors required for cell division as well as DNA repair and, consequently, cells became overwhelmed by accumulated genetic damage. However, direct evidence correlating *relA*

function and radiation sensitivity in *D. radiodurans* grown in DMM is lacking.

Collectively, the growth studies and analysis of the *D. radiodurans* genomic sequence support the existence of several defects in *D. radiodurans*' global metabolic regulation that limit carbon, nitrogen and DNA metabolism. Several of its amino acid biosynthetic pathways including that of the sulfur containing amino-acid cysteine are disrupted (Table 3.2). The ability of *D. radiodurans* to use acetate as the sole carbon source indicates the presence of an active glyoxylate bypass of its TCA cycle. Whether these observed metabolic defects are common to all deinococcal members and how these defects affect the extreme radiation resistance phenotype in family *Deinococcaceae* is examined in the next chapter.

3.5 Conclusions

1. **A defined minimal medium (DMM) was developed for *D. radiodurans* to test its growth characteristics predicted by genomic annotation. In the absence of radiation, *D. radiodurans* growth required an EMP carbon source (2 mg/ml), nicotinamide (1 μg/ml), transition metals (0.315 mM), and a mixture of amino acid (50 μg/ml).**

2. **DMM was used to analyze *D. radiodurans*' growth in the presence of continuous radiation (60 Gy/hour). Whereas cell growth in DMM was unaffected in the absence of radiation, cells did not grow and were killed under continuous radiation. The key nutritional constituents needed to restore growth of *D. radiodurans* in radioactive environments were high concentrations of amino acids.**

3. **The growth studies and analysis of the complete *D. radiodurans* genomic sequence support the existence of several defects in *D. radiodurans*' global metabolic regulation that limit carbon, nitrogen and DNA metabolism.**

4. **The amino acid starvation response in *D. radiodurans* was studied by examining the functional integrity of its putative *rel* locus by monitoring the diagnostic synthesis of**

ppGpp and pppGpp under amino acid deprivation. These data support normal *rel* function in *D. radiodurans* and its induction in amino acid-limiting conditions. Consistent with the induction of *rel* functions, cells grown in minimal medium conditions had substantially reduced cellular RNA levels.

Chapter 4: Relationship between Metabolism, Oxidative Stress and Radiation Resistance in the Family *Deinococcaceae*

4.1 Introduction

In the previous chapter a defined minimal medium (DMM) was developed for *D. radiodurans* to test its growth characteristics as predicted by genome annotation and to identify specific nutrients that govern its growth under chronic radiation. The data obtained from a combination of growth studies and analysis of the *D. radiodurans* genomic sequence support the existence of several defects in *D. radiodurans*' global metabolic regulation that limit its carbon, nitrogen and DNA metabolism (Chapter 3). The ability of *D. radiodurans* to use acetate as the sole carbon source indicated the presence of a functional glyoxylate bypass of its TCA cycle.

D. radiodurans is the most characterized member of the radiation resistant bacterial family *Deinococcaceae*, comprised of seven distinct obligate aerobic species that form a distinct eubacterial phylogenetic lineage most closely related to the genus *Thermus* (Makarova *et al.*, 2001) (Chapter 1). Although it is believed that its multiple resistance phenotypes stem from efficient DNA repair processes (Battista, 1997), the mechanisms underlying its extraordinary survival remain poorly understood (Makarova *et al.*, 2001). To determine how metabolic processes may be contributing to *D. radiodurans*' resistance functions and if such processes operate similarly throughout *Deinococcaceae*, deinococcal species (Anderson *et al.*, 1956; Davis *et al.*, 1963; Ferreira *et al.*, 1997; Kobatake, *et al.*, 1973; Lewis, 1971; Oyaizu *et al.*, 1987) were examined for their amino acid utilization, protease secretion, expression of superoxide dismutase (SOD), tricarboxylic acid (TCA) cycle function, and resistance to ionizing radiation.

During growth in DMM, *D. radiodurans* is exposed to metabolically induced oxidative stress due to the added burden of *de novo* synthesis of cell components. As stated in earlier chapters, oxidative stress is generated in aerobic organisms when molecular oxygen oxidizes redox enzymes, forming superoxide ($O_2^{\bullet-}$) that subsequently can yield more toxic hydroxyl radicals ($^{\bullet}OH$) via Fe^{2+}-catalyzed reduction of hydrogen peroxide (Chevion, 1988; Messner and Imlay, 2002).

The development of a DMM for cultivation of *D. radiodurans* (Venkateswaran *et al.*, 2000) has allowed comparisons to be made between members of *Deinococcaceae* with emphasis on their metabolism and how it relates to their radiation resistance and oxidative stress. The results presented here support that *Deinococcaceae* may use similar metabolic strategies, not generally associated with DNA protection, to enhance resistance functions. For *D. radiodurans*, quantitative real-time PCR (RT-PCR) expression analysis of its TCA cycle was done for cells growing in DMM versus rich medium. Unexpectedly, the expression of *D. radiodurans*' TCA cycle was found to be repressed in cells growing in DMM, which could restrict the production of oxidative stress.

The goal of this study was to correlate *D. radiodurans*' physiological growth characteristics with its predicted metabolic functions and to examine the possibility that its metabolic configuration contributes to its resistance phenotype. Metabolic convergence between *D. radiodurans* and other species of *Deinococcaceae* was investigated to identify shared metabolic traits that could enhance DNA protection and repair systems. The specific aims of this chapter are as follows:

1. **To examine different deinococcal species for their metabolic diversity, amino acid and NAD utilization, and secretion of proteases.**

2. **To examine the relative resistance to γ-radiation in the family *Deinococcaceae*.**

3. **Evaluating TCA cycle expression in *D. radiodurans* growing in DMM versus rich medium (TGY) by quantitative real-time PCR (RT-PCR).**

4. **To study the expression of superoxide dismutase (SOD) in *D. radiodurans*. To achieve this goal, *sodA* mutants of *D. radiodurans* were constructed and evaluated for Sod expression together with other *Deinococcal* species. Resistance of wild-type and mutant strains to paraquat (inducer of the oxidative stress) and chronic radiation was also examined.**

4.2 Materials and Methods

4.2.1 Growth of Cells and Irradiation

The deinococcal strains used in this study are listed in Table 4.1. *Deinococci* were grown on nutrient rich medium (TGY; 1% bactotryptone, 0.5% yeast extract, and 0.1% glucose) or deinococcal minimal medium (DMM) (Chapter 3, Table 3.1). For solid medium, Bacto-agar (Difco) or Noble agar (Difco) were added to TGY or minimal medium, respectively, to 1.5% w/v. *Escherichia coli* was grown on Luria-Bertani medium or *E. coli*-minimal medium (M9) (Sambrook *et al.*, 1989). Unless otherwise stated, deinococcal DMM contained fructose, nicotinic acid, methionine (50 μg/ml), phosphate buffer and salts, as summarized in Table 4.2. Growth of cells in the absence or presence of chronic irradiation, 50 Gy/hour (^{137}Cs Gammacell 40 irradiation unit [Atomic Energy of Canada Limited]) (at 22 °C), was as described in chapter 2. All chemicals in this work were obtained from Sigma (St. Louis, MO) unless stated otherwise. In liquid culture, cell density was determined at 600 nm in a Beckman spectrophotometer; OD_{600} 1.0 = ~1 x 10^8 colony forming units (CFU)/ml for all *Deinococcus* strains examined. For high-level acute radiation exposures, early stationary phase cultures (OD_{600} = 1.0) were irradiated without change of broth on ice at 10 kGy/hour (^{60}Co Gammacell irradiation unit [J. L. Shepard and Associates, Model 109]). For the deinococcal species under investigation, three independent cell cultures and irradiation treatments of the same kind were performed. Following exposure to the indicated doses, cell suspensions were appropriately diluted and assayed for viability by plate assay on rich (TGY) or DMM (Daly *et al.*, 1994; 1995; Chapter3). Viability data was used to construct survival curves according to conventional formats (Ferreira *et al.*, 1997; Gutman *et al.*, 1993; Mattimore and Battista, 1996; Oyaizu *et al.*, 1997).

4.2.2 Protease Secretion

Tests for secretory proteases were carried out on indicator plates containing skimmed milk (10 mg/ml) (Difco) or gelatin (10 mg/ml) (Kelly and Post, 1991). For skimmed milk plates, protease secretion by strains was indicated by the formation of halo-shaped zones of clearing around colonies. For gelatin plates, hydrolysis was visualized by flooding the plates

with acidic mercuric chloride after incubation of the inoculated plate (Kelly and Post, 1991).

4.2.3 Construction of MD885

MD885 is a *sodA*⁻ derivative of *D. radiodurans* strain R1 (wild-type *D. radiodurans* lacks *sodB*) (Makarova *et al.*, 2001). To ensure isogenicity with the *D. radiodurans* strain sequenced by The Institute for Genomic Research (White *et al.*, 1999), and used exclusively by our laboratory since 1988, we transferred the *sodA*⁻ disruption of the previously constructed *sodA*⁻ *D. radiodurans* strain KK7004 (Markillie *et al.*, 1999) to our *D. radiodurans* by conventional transformation with KK7004 genomic DNA and kanamycin selection (Daly and Minton, 1995), yielding strain MD885. The *D. radiodurans recA*⁻ strain rec30 (Daly and Minton, 1995) was similarly transformed to generate the *sodA*⁻*recA*⁻ double mutant MD886.

4.2.4 *In Situ* Assays of Superoxide Dismutase (SOD) Activity

The SOD assay was a collaborative effort with Dr. Alexander Vasilenko and Dr. Debabrota Ghosal. The relative abundance of SOD in total protein extracted from cultures was determined by subjecting total cell extracts to non-denaturing polyacrylamide gel electrophoresis (PAGE), followed by staining gels according to SOD detection protocols developed by Beauchamp and Fridovich (1971) (Beauchamp and Fridovich, 1971). Briefly, cells were harvested and suspended in 0.1 M sodium phosphate buffer (pH 7.0) containing 0.1 mM $MgSO_4$, 150 μg/ml chloramphenicol, and lysed by French press treatment (20,000 psi). Lysed samples were centrifuged at 12,000 *g* for 10 min at 4 °C. The concentration of protein in lysates was determined by sample dilution as described by Lowry *et al* (1951) (Lowry *et al.*, 1951). Equal amounts of total soluble protein (~ 30 μg) from the indicated lysates were subjected to PAGE in 10% non-denaturing gels. *In situ* SOD activity was localized in gels by photoreduction of nitro blue tetrazolium to blue formazan (Tauati *et al.*, 1995).

4.2.5 Immunnoblots

This result was a collaborative effort involving researches from other laboratories. Whole cell extracts were prepared as for SOD activity assays. Proteins were separated by sodium

dodecyl sulfate (SDS)-PAGE (Sambrook *et al.*, 1989) and then blotted onto a polyvinylidene difluoride membrane. Purified *E. coli* Mn SOD and bovine Cu/Zn SOD were included on gels as controls. Proteins with immunoaffinity to purified rabbit anti-Mn SOD or rabbit anti-Cu/Zn SOD polyclonal antibodies (StressGen Biotechnologies Corp., BC, Canada) were detected using secondary antibodies conjugated with horseradish peroxidase (Amersham Biosciences Corp., NJ). Chemiluminescence was recorded by Kodak Bioscience Image film "Biomax ML."

4.2.6 Induction of Oxidative Stress

Paraquat (1,1-Dimethyl-4,4-bipyridinium dichloride, methyl viologen) was used to generate oxidative stress. Strains were examined for their growth characteristics in liquid DMM containing different concentrations of paraquat, and supplemented with cysteine (50 μg/ml), Methionine (25 μg/ml), and Histidine (25 μg/ml). Three independent cell cultures and paraquat treatments of the same kind were performed for each strain under investigation.

4.2.7 RT-PCR

Total cellular RNA was extracted from 1 x 10^9 *D. radiodurans* cells harvested from three separate cultures growing exponentially in DMM (Chapter 3, Table 3.1). For RT-PCR comparisons, total cellular RNA was similarly isolated from 1 x 10^9 *D. radiodurans* cells growing exponentially in rich medium (TGY). RNA was prepared using TRIzol reagent (Invitrogen) and treated with Rnase-free DNaseI (Qiagen) at 37 °C for 30 minutes. Upon inactivation of DNaseI by treatment at 65 °C for 10 minutes, the total RNA was purified using RNeasy Minikit columns (Qiagen). The quality and quantity of RNA was determined spectrophotometrically at 260/280 nm and by agarose gel electrophoresis.

Fifteen gene-specific oligonucleotide primer-sets were designed for each of the TCA cycle genes (including the glyoxylate bypass genes), and 3 control primer sets were used for amplifying 23S, 16S, and 5S rRNA gene products (Table 4.1). The first-strand cDNA was synthesized in 100 μl of reaction buffer containing 5 μg of total cellular RNA, 30 μg of random hexamers (Invitrogen), 10 mM dithiothreitol, 500 μM dNTPs, and 2,000 U of Supescript™ II RNase H$^-$ reverse transcriptase (Invitrogen) at 42°C for 60 min. Before adding the reverse transcriptase, 10 μl of each reaction was saved to serve as a negative control. The cDNAs and the

Table 4.1 Sequences of the Primers Used in the Quantitative Real-Time PCR Assays

Gene ID		Annotation	Primer sequences	Product Size/bp
DR0083	*sucB*	Dihydrolipoamide succinyltransferase	GCCTCAAGGAAGTGCAGAAC CTTCACGAACTGGTCCTGGT	107
DR0287	*sucA*	2-oxoglutarate dehydrogenase	GGTCATGGAGACGCTGAACT GGGTCGGAGATGGTAAAGC	102
DR0325	*mdh*	Malate dehydrogenase	CACCCAGTACCCTGACCTGT GGTGGGGATGTAGTCGTTCT	97
DR0757	*gltA*	Citrate synthase II	GACCTGGGCATCAAGAAGG CGGTTGTCCTGGCTGTACTC	98
DR0828	*aceA*	Isocitrate lyase	CCTTCGTGGAACTTCAGGAG GCGAGACGAGGTCGAAGTAG	104
DR0951	*sdhB*	Fumarate/succinate dehydrogenase type Fe-S protein	CCAGATCCAGACTCCCGTTA CGCAGGACCTTGACTTTCAG	105
DR0952	*sdhA*	Succinate dehydrogenase flavoprotein	GGCCACATGATCCTTCAGAC GCCCGTCTTCGATAATCAGG	109
DR1155	*aceB*	Malate synthase	GCACCTGGACTTTGATGGAC CAGCTTGGGCACGTAGATGT	103
DR1247	*sucC*	Succinyl-CoA synthetase, beta chain	GTGAACAAGGTGCTGGTGAC CCATCAGGGTGTAGCTCTGG	103
DR1248	*sucD*	Succinyl CoA synthetase, alpha chain	CGTGGTCGTGATTGGTGA CCGAGATAAAGGCCACGAC	98
DR1540	*icd*	Isocitrate dehydrogenase	CTGATCCTCAAGGGTCTGGA ACTCGCTGGTCTTGACTTCG	100
DR1720	*acnA*	Aconitase	CAACGGTCAGGACGTGTTC GCCGTCGTAGACCTTCTTGA	109
DR2526	*lpd*	Lipoamide dehydrogenase, component E3	CAAGGTGGACCAGCACTACC CTTCTTCCTCGGCCTTGTG	98
DR2627	*fumC*	Fumarase	CACATCGGCTACGACAAGG ATTCGTCCTCGGTCACGTAG	106
DRA0277	*aceB*	Malate synthase	CGTTCGAGATGGACGAGATT TGCGCAGCTTCTTGATGTAG	102
DRA5S		Ribosomal 5S RNA	ATAGCACTGTGGAACCA TGACCGACTTTTCCGGGA	100
DRA16S		Ribosomal 16S RNA	CGACTCCGTGAAGTTGGAAT TCTACTCCCATGGTGTGACG	102
DRA23S		Ribosomal 23S RNA	GCTATGTCCGGAACGGATAA GGTCTTCCGGGAGTCTTACC	99

negative controls were subsequently used as templates for RT-PCR. The PCR amplifications were done on microtiter plates as 50 μl reactions containing the appropriate primers at a final concentration of 0.4 μM, 0.5 μl of the synthesized cDNAs, and 20,000 X diluted SYBR Green I fluorescent dye (Eugene, OR). Amplification was carried out by incubating the PCR mixture at 96 °C for 15 s, 55 °C for 30 s, and 72 °C for 30 s for 45 cycles. Melting curve generation followed the amplification, starting at 55°C, with 0.5°C increments at 10-second intervals.

All assays were performed with the icycler iQ Real-Time Detection System (Bio-Rad, Herculus, CA). The fluorescent intensity of SYBR green I, a double-stranded DNA specific dye, was monitored at the end of each extension step, and copy numbers of the target cDNAs were estimated by the threshold cycles according to the standard curve (Witter *et al.*, 1997). Standard curves were constructed with cDNA fragments of known size and copy number. For each gene, 3 cDNA templates derived from different independent DMM cell cultures were amplified, and each cDNA template was repeated 3 times in the same plate. Three independent PCR amplifications of the same design were performed in different plates for each gene, so a total of 27 data-points for each gene were obtained. T-distribution (TDIST) test was used to estimate statistically significant differences between the levels of expression-analyzed genes (Table 4.3).

4.3 Results

4.3.1 TCA Cycle and NAD Dependence, and Protease Secretion

All TCA cycle genes in *D. radiodurans* (including genes for its glyoxylate bypass) are present based on its genome annotation (Makarova *et al.*, 2001) (Chapter 2, Figure 2.1) and functionally expressed based on whole proteome analysis (Lipton *et al.*, 2002). However, *D. radiodurans* is unable to use succinate, fumarate, malate, or α-ketoglutarate as sole carbon/energy sources for growth in DMM (Chapter 2, Figure 2.1; Chapter 3; Table 4.2A). Four genes (*nadABCD*) required for nicotinamide adenine dinucleotide (NAD) biosynthesis are absent (Chapter 2, Figure 2.1) (Makarova *et al.*, 2001), and consistent with this prediction, *D. radiodurans* is dependent on exogenous nicotinic acid (Table 4.2A). Results for substrate utilization for the deinococcal strains are shown in Table 4.2A.

A striking informatic (Chapter 2, Figure 2.1) (Makarova *et al.*, 2001) and experimentally

Table 4.2A. Utilization of Carbon Substrates by *Deinococci* Grown in [a]Defined Minimal Medium (DMM). See Footnotes on the Bottom of the Table 4.1B.

Species / [b,c]Substrate	*D. radiodurans* (1)	MD885 Sod⁻ / MD886 Sod⁻*recA*⁻	*D. geo thermalis* (13)	*D. grandis* (43)	*D. murrayi* (13)	*D. radio philus* (28)	*D. radio pugnans* (12)	*D.proteo lyticus* (26)
Fructose + C,H,L,A,M,P	+++	+++ / ++	+++	+++	++	+	+++	+++
Fructose +Met	+++	+++ / +	+++	++	+	[d]+	++	+
Fructose -aa	–	-/-	+++	–	–	–	–	–
Fructose - NAD + Met	–	-/-	+++	+	–	[d]–	–	–
Pyruvate +Met	+++	+++ / +	+++	+++	–	–	–	+
Acetate +Met	++	++ / +	++	++	++	–	–	+
α-Ketoglutarate +Met	–	-/-	++	–	–	–	–	–
Succinate +Met	–	-/-	++	–	–	–	–	–
Fumarate +Met	–	-/-	++	–	–	–	–	–
Malate +Met	–	-/-	+	–	–	–	–	–
Oxaloacetate +Met	+	± / -	++	+	–	–	–	+

Table 4.2B. Other Characteristics of Designated Strains

Species / Characteristic	*D. radiodurans*	MD885 Sod⁻ / MD886 Sod⁻*recA*⁻	*D. geo thermalis*	*D. grandis*	*D. murrayi*	*D. radio philus*	*D. radio pugnans*	*D.proteo lyticus*
Growth in TGY (rich medium)	+++	+++ / ++	+++	+++	++	++	+++	+++
Growth in TGY + 50 Gy/h	+++	++ / -	+++	+++	++	++	+++	+++
Growth on [c]DMM + 50 Gy/h	++	++ / -	++	++	++	++	++	++
[f]Protease secretion	yes	yes / yes	no	yes	yes	yes	yes	yes
SOD Activity in cells grown in TGY and MFM	yes	no / no	yes	yes	yes	yes	yes	yes
$NH_4^{2+}SO_4^{2-}$ utilization	no	no / no	yes	no	no	no	no	no

Footnotes for Table 4.2:

[a]Deinococcal defined DMM (Venkateswaran *et al.*, 2000) consisted of the indicated EMP carbon source (Substrate) at 2 mg/ml and basal salt medium supplemented with sterile preparations of salts ($CaCl_2$ (0.18 mM), $MgSO_4$ (0.8 mM), $MnSO_4$ (5.4 μM)), nicotinic acid (1 μg/ml), and Met (50 μg/ml), unless stated otherwise.

[b]Growth on substrate: +++, good; ++, moderate; +, poor; -, absent.

[c]Abbreviations: Fructose + C,H,L,A,T,P (L-forms), fructose plus [Cysteine (Cys), Histidine (His), Lysine (Lys), Aspartate (Asp), Methionine (Met), and Proline (Pro), each @ 50 μg/ml]; +Met, only Methionine added; -aa, no amino acids added. -NAD, no nicotinic acid added; TGY, tryptone/glucose/yeast extract (rich) medium. MFM, minimal fructose medium.

[d]Cells were tested in the presence of Met, His and Lys, each at 50 μg/ml. Met alone did not support growth for *D. radiophilus*.

[e]For growth under chronic radiation, cells were tested in the presence of Cys, His, Lys, Asp, Met, and Pro, each at 50 μg/ml on solid medium. Met alone did not support growth.

[f]Protease secretion tests were carried out on indicator plates containing skimmed milk or gelatin.

determined feature of wild-type *D. radiodurans* is its inability to use inorganic sulfate (Table 4.2B) in the biosynthesis of amino acids, that results in its dependence on an exogenous source of amino acids for growth (Chapter 3). Table 4.2 further defines the amino acid requirements of deinococcal strains. During growth under chronic irradiation (50 Gy/hour) an EMP/NAD source plus a mixture of at least six amino acids (*e.g.*, Methionine + [Cysteine + Histidine, Lysine, Asparagine, and Tryptophan], each at 50 μg/ml) was necessary for growth (Table 4.2B). While growth under chronic irradiation in DMM is dependent on sulfur containing amino acid (methionine), the other amino acids were interchangeable without any noticeable effect on the resistance phenotype. Other *Deinococci* were similarly tested for their amino acid utilization (Table 4.2A) showing that *D. geothermalis* is the only known deinococcal species that can grow without exogenously provided amino acids, or precursors of NAD, and can utilize inorganic sulfate (ammonium sulfate).

At least ten complete open reading frames with considerable sequence similarity to secreted subtilisin-like proteases of *B. subtilis* have been identified in the *D. radiodurans* genome (Makarova *et al.*, 2001). *D. radiodurans* growth was tested on protease-indicator plates containing skimmed milk or gelatin. On both substrates, *D. radiodurans* showed luxuriant growth and generated large halo-shaped areas of clearing around colonies engaged in protein hydrolysis (Table 4.2B, Figure 4.2). Other strains were similarly tested for protease secretion (Table 4.2B, Figure 4.2). The only strain tested that did not secrete detectable levels of proteases was *D. geothermalis.*

4.3.2 *Deinococcaceae*: Relative Resistance to γ-Radiation

D. radiodurans, *D. radiopugnans*, *D. radiophilus*, *D. proteolyticus*, *D. grandis*, *D. geothermalis* and *D. murrayi* previously have been tested for their ability to grow in the presence of chronic radiation (Daly, 2000). Under chronic radiation, no differences in growth were detected compared to unirradiated controls when cells were grown on rich medium. For growth on DMM under chronic irradiation, at least five other amino acids are required (Table 4.2B). Since a single comparative analysis of these strains' resistance to acute irradiation under standardized conditions has not been reported, their relative resistance to γ-radiation extending to 20 kGy was examined.

Figure 4.1. Protease Secretion. Representative protease secretion assay on a protease-indicator plate containing skimmed milk. 1) *D. geothermalis*; 2) *D. radiodurans*; 3) *D. radiopugnans*; 4) *D. grandis*. Note the halo-shaped areas of clearing around protease secreting colonies. Complete results for protease secretion are given in Table 4.2B.

Figure 4.1

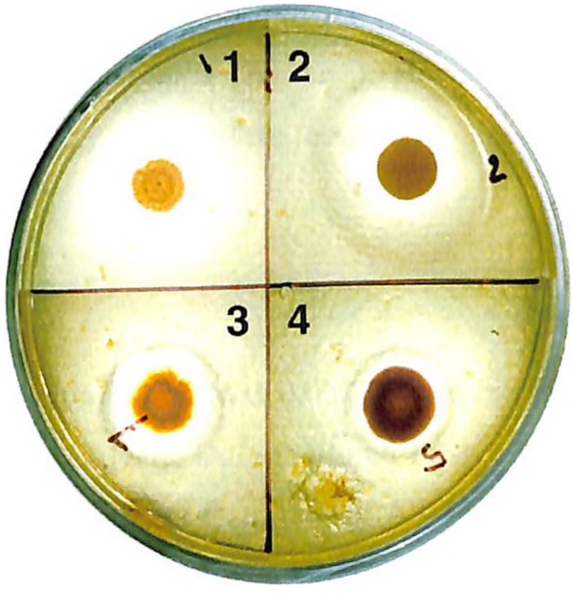

Stationary-phase (OD_{600} 1.2) cells were evaluated. For each of the strains under investigation, three independent replicate irradiations were performed. Figure 4.2 shows that among the deinococcal strains tested, *D. geothermalis* is the least resistant to acute doses of γ-radiation. The higher sensitivity of *D. geothermalis* to acute doses when compared to *D. radiodurans* or *D. murrayi* is consistent with a previously published report (Ferreira *et al.*, 1997). *D. radiophilus* (Figure 4.2) is less resistant than previously reported (Lewis, 1971). Also significant, but not reflected in the survival curves, was the observation that most of the *D. geothermalis* post-irradiation colonies arising on recovery plates (rich medium, 5 days) were very small (< 0.5 mm diameter) compared to its unirradiated control (> 2 mm) and the other six strains, suggesting a diminished repair capacity for *D. geothermalis*. Recovery of colonies on minimal fructose medium compared to rich (TGY) medium following acute irradiation was slower (7 days), and substantially slower for *D. geothermalis* (21 days). However, the ultimate number of post-irradiation colonies on recovery plates were essentially the same irrespective of recovery medium.

4.3.3 RT-PCR

D. radiodurans pre-cultured in DMM or TGY was inoculated at 5 x 10^6 CFU/ml into minimal or TGY medium, respectively, and monitored for growth. For both growth conditions, mid-exponential cells were harvested at OD_{600} ~0.6. All 15 TCA cycle gene expression levels were examined by RT-PCR (Table 4.3). In DMM, only one gene (*aceA*) was statistically significantly up-regulated (3.36-fold), where AceA is the key enzyme of the glyoxylate bypass; 6 genes displayed no significant changes (*gltA*, *sucB*, *lpd*, *sucD*, *fumC*, and *aceB* (DR1155); and 8 genes were down-regulated (*acnA*, *icd*, *sucA*, *sucC*, *sdhB*, *sdhA*, *aceB* (DRA0277), and *mdh*) (Table 4.3). For rRNA control amplifications, no significant changes in expression were observed (data not shown).

4.3.4 Superoxide Dismutase (SOD) of *D. radiodurans*

Along with the advantages of aerobic respiration comes toxicity caused by oxygen intermediates such as $O_2^{\bullet-}$, H_2O_2, and $^{\bullet}OH$ (Imlay and Linn, 1995) (*e.g.*, Chapter 2, Figure 2.1).

Figure 4.2. Resistance to Acute Irradiation. The indicated *Deinococci* were inoculated into TGY medium at 10^6 CFU[a]/ml and grown at 32 °C to the early stationary phase (10^8 cells/ml). *E. coli* was similarly pre-grown in LB medium at 37 °C. Cells were then irradiated without change of broth on ice with ^{60}Co at 10 kGy/h. At the indicated doses, viable cell counts were determined by plating appropriate cell dilutions for CFU on TGY agar at 32 °C. *E. coli* was allowed to recover on LB medium at 37 °C. Values are from three independent trials, with standard deviations shown. [a]CFU, colony forming unit.

Figure 4.2

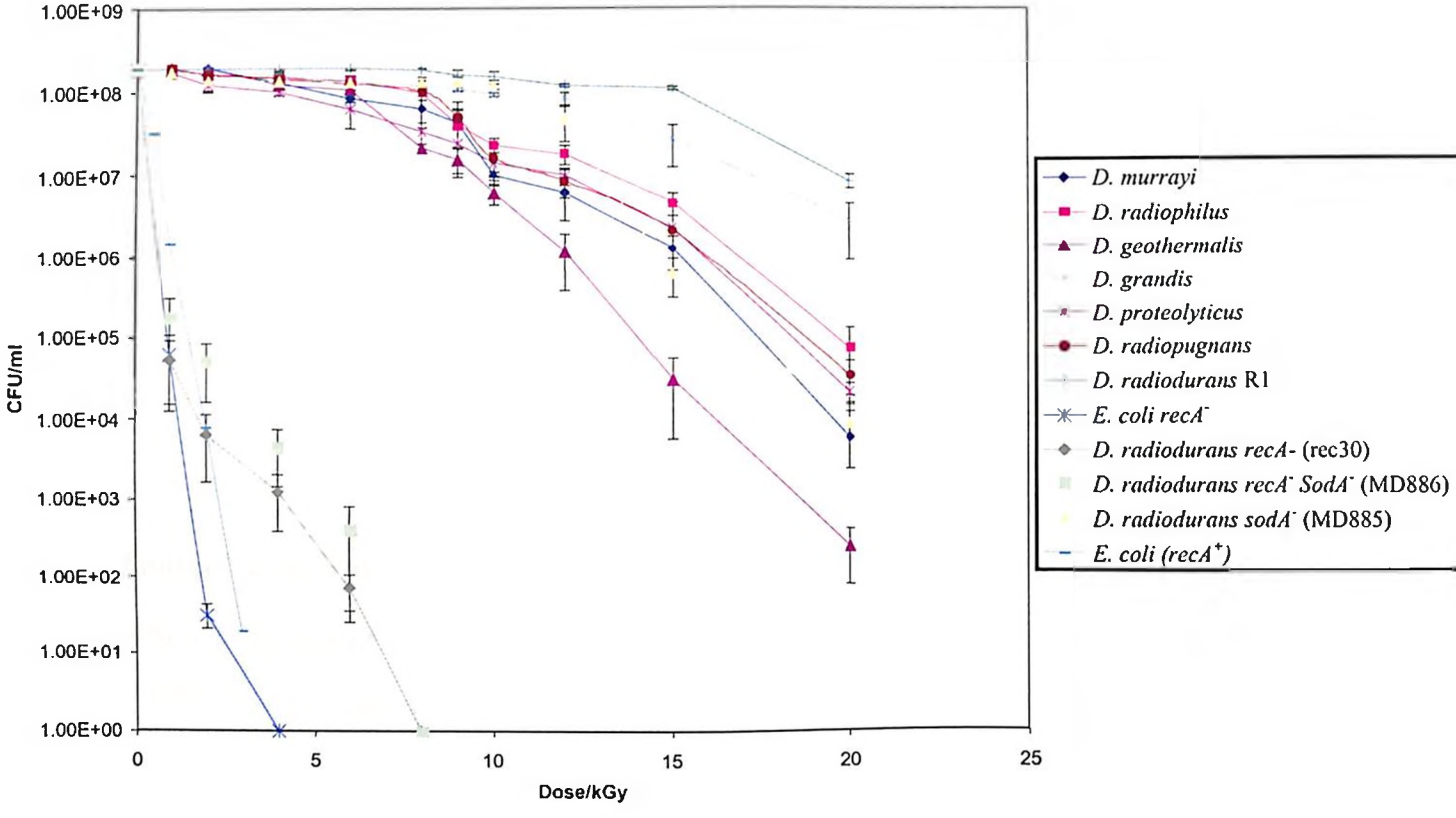
1.00E+09
1.00E+08
1.00E+07
1.00E+06
1.00E+05
1.00E+04
1.00E+03
1.00E+02
1.00E+01
1.00E+00
CFU/ml
0
5
10
15
20
25
Dose/kGy
D. murrayi
D. radiophilus
D. geothermalis
D. grandis
D. proteolyticus
D. radiopugnans
D. radiodurans R1
E. coli recA-
D. radiodurans recA- (rec30)
D. radiodurans recA- SodA- (MD886)
D. radiodurans sodA- (MD885)
E. coli (recA+)

Table 4.3. Relative Expression Levels for TCA Cycle and Glyoxylate Bypass Genes of *D. radiodurans* Growing in DMM Versus that in Rich (TGY) Medium

Gene ID		Annotation	[a]CV	[b]Min vs. TGY	[c]T DIST
DR0083	*sucB*	Dihydrolipoamide succinyltransferase	0.23	1.04	no
DR0287	*sucA*	2-oxoglutarate dehydrogenase	0.18	0.62	yes
DR0325	*mdh*	Malate dehydrogenase	0.31	0.42	yes
DR0757	*gltA*	Citrate synthase II	0.34	0.66	no
DR0828	*aceA*	Isocitrate lyase	0.22	3.36	yes
DR0951	*sdhB*	Fumarate/succinate dehydrogenase type Fe-S protein	0.19	0.38	yes
DR0952	*sdhA*	Succinate dehydrogenase flavoprotein	0.08	0.55	yes
DR1155	*aceB*	Malate synthase	0.25	0.87	no
DR1247	*sucC*	Succinyl-CoA synthetase, beta chain	0.28	0.25	yes
DR1248	*sucD*	Succinyl CoA synthetase, alpha chain	0.27	0.92	no
DR1540	*icd*	Isocitrate dehydrogenase	0.52	0.22	yes
DR1720	*acnA*	Aconitase	0.20	0.64	yes
DR2526	*lpd*	Lipoamide dehydrogenase, component E3	0.10	0.92	no
DR2627	*fumC*	Fumarase	0.22	0.71	no
DRA0277	*aceB*	Malate synthase	0.07	0.37	yes

Footnotes for Table 4.3:

[a]CV, coefficient of variation.

[b]DMM vs. TGY, gene expression ratio of cells in DMM versus in rich (TGY) medium.

[c]TDIST, the results of statistical method (t-distribution test) implemented for estimating differences in the levels of expression. Yes, statistically significant change. No, no significant change.

The growth and physiological adaptation to oxidative stress of *D. radiodurans* was compared to *E. coli* using wild-type and Sod$^-$ strains. In *E. coli* there is a constitutively expressed Fe-dependent SOD (SodB) and a Mn-dependent SOD (SodA) which is under stringent control of the global regulatory genes *soxR* and *soxS* and expressed predominantly under conditions of oxidative stress (Fredovich, 1995; Liochev and Fridovich, 1992); its SodC (Cu-Zn-dependent) is periplasmic, also under control of the *soxRS* regulon, and may be involved in removing superoxide from the periplasm (Gort *et al.*, 1999). The annotated *D. radiodurans* genome predicts the presence of three SOD proteins: DR1279 (SodA), DR1546 (Cu-Zn-dependent, SodC) and SodC-like DRA0202 (Makarova *et al.*, 2001); *D. radiodurans* lacks *sodB*. For wild-type, the cumulative data support that SodA (DR1279) dominates SOD function in *D. radiodurans* and that it is constitutively expressed (Figures 4.3, 4.4) (Lipton *et al.*, 2002). No SOD activity was detected in strain *sodA*$^-$ MD885 (Figure 4.3). Immuno-blotting of *D. radiodurans* cell extracts using polyclonal anti-SodB or anti-SodC antibodies showed the absence of SodB and SodC (Figure 4.4). Furthermore, *D. radiodurans* Sod-activity bands (Figure 4.3) were insensitive to the inhibitory effects of KCN (specific for Cu-Zn SOD (Beauchamp and Fridovich, 1971), data not shown), supporting that SodC (DR1546) is not functional under the nutrient conditions reported here.

The inability to demonstrate any SOD activity in strain MD885 (*sodA*$^-$) supports that it is equivalent to *sodA*$^-$*sodB*$^-$ (*sodC*$^+$) *E. coli* (Strain JI132) (Carlioz and Touati, 1986). Yet, whereas *sodA*$^-$*sodB*$^-$ *E. coli* (JI132) cannot grow on minimal medium because of increased oxidative stress levels (Fridovich, 1995; Keyser *et al.*, 1995), growth of strain MD885 in DMM in the absence or presence of chronic radiation (Table 4.2) was only marginally less than wild-type, and displayed an identical substrate utilization pattern as wild-type (Table 4.2A). Furthermore, growth of the *D. radiodurans* double mutant *sodA*$^-$(*B*$^-$)*recA*$^-$ (MD886, DNA damage sensitive, Figure 4.2) (Table 4.2A) on DMM or rich medium was present, albeit at reduced levels compared to wild-type or MD885. In contrast, *sodA*$^-$*B*$^-$*recA*$^-$ *E. coli* is nonviable under any aerobic nutrient condition (Tauti *et al.*, 1995). *sodA*$^-$ *D. radiodurans* (strains MD885, KK7004 [Markillie *et al.*, 1999]) shows little difference in resistance to acute irradiation compared to wild-type (Figure 4.2). This is consistent with a previous report (Markillie *et al.*, 1999) and was expected under acute irradiation conditions at 0 °C, where *de novo* expression of defense mechanisms in dormant cells is limited and irradiation-induced free radical damage is progressively accumulated.

Figure 4.3. In-Gel Activity Staining for SOD. (A) Non-denaturing activity gels. Lanes, 1) Purified Mn SOD (*E. coli* SodA), Fe SOD (*E. coli* SodB), and Cu/Zn SOD (bovine SodC); 2) *E. coli*/LB (grown in rich medium); 3) *E. coli*/DMM (defined minimal medium); 4) *D. radiodurans*/TGY (rich medium); 5) *D. radiodurans*/DMM; 6) *D. geothermalis*/TGY; 7) *D. geothermalis*/DMM; 8) *D. grandis*/TGY; 9) *D. grandis*/DMM; 10) as for lane 1; 11) MD886 (*sodA*$^-$*recA*$^-$)/DMM; 12) rec30 (*recA*$^-$)/DMM; 13) *D. radiopugnans*/TGY; 14) *D. radiopugnans*/DMM; 15) *D. proteolyticus*/TGY; 16) *D. proteolyticus*/DMM; 17) *D. radiophilus*/TGY; and 18) *D. murrayi*/TGY. Lanes 1 and 10 contain 0.23 μg of Mn SOD, 2.4 μg of Fe SOD, and 0.07 μg of Cu/Zn SOD. Lanes 2-9 and 11-18 contain ~30 μg of total protein. (**B**) SDS-PAGE of *Deinococcus* crude protein extracts. Lane numbers as in panel A. Lanes labeled C, 10-160 kD size standards (Amersham, CA). (**C**) Activity gel. Lanes, 1) as for Panel A lane 1; 2-5) *D. radiodurans*/TGY: 20 μg, 15 μg, 10 μg, and 5 μg of total protein, respectively; 6) *D. radiodurans*/TGY + 50 Gy/h; 7) *D. radiodurans* /DMMA (DMM suplemented with amino acids, see Table 1B) + 50 Gy/h; 8) MD885/TGY + 50 Gy/h; 9) MD885/DMMA + 50 Gy/h. Lanes 6-9 contain ~25 μg of total protein. (**D**) SDS-PAGE of *Deinococcus* crude protein extracts. Lanes as in Panel C. Lane labelled 'C' as in Panel B.

Figure 4.3

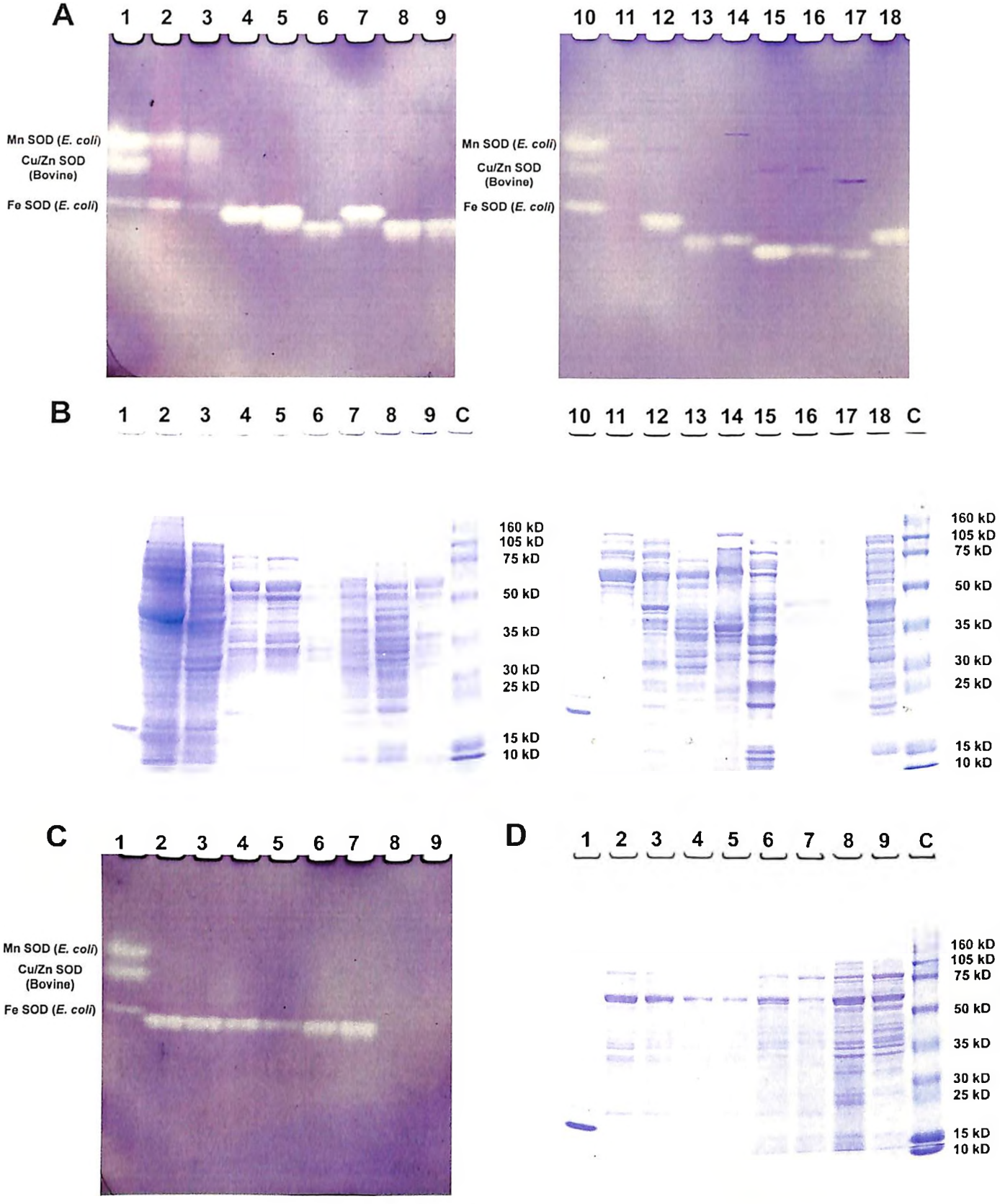

Figure 4.4 Immuno-Blotting for SOD. (A) Probing with anti-Mn SOD (SodA) following

Figure 4.4 Immuno-Blotting for SOD. (A) Probing with anti-Mn SOD (SodA) following SDS-PAGE. (B) Probing with anti-Cu/Zn SOD (SodC). Lanes, 1-3) *D. radiodurans* /MM, 2.5, 5, and 10 μg total soluble proteins, respectively; 4-6) *D. radiodurans* /TGY, 2.5, 5 and 10 μg total soluble proteins, respectively; 7-9) purified SodA (*E. coli*) and SodC (bovine), 3, 6 and 12 ng each for purified protein, respectively. Immunoblots were stained with HRP conjugated secondary antibodies for luminol-based detection. Abbreviations as in Figure 4.3.

Figure 4.4

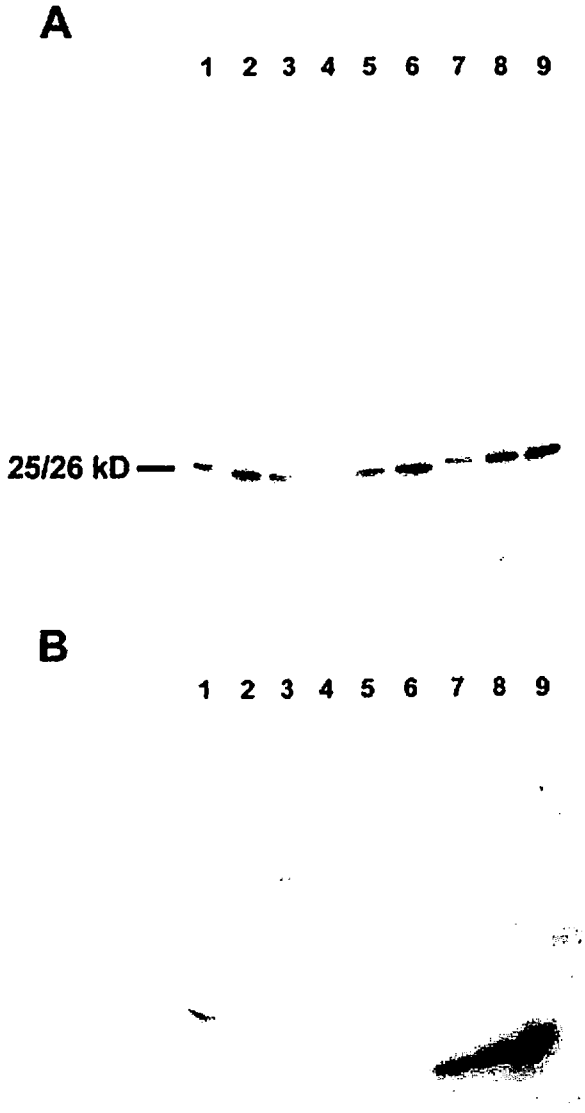

4.3.5 Resistance to Paraquat

Paraquat is known to be a powerful cellular inducer of oxidative stress (Chevion, 1988). Its biological action appears to be mediated by the production of paraquat radical cations produced when paraquat accepts electrons, for example from FADH with the subsequent transfer of electrons to O_2, yielding $O_2^{\bullet-}$ that subsequently can give rise to $^{\bullet}OH$ via H_2O_2 (Chapter 2, Figure 2.1). Like free radicals produced during metabolism or irradiation (Halliwell and Gutteridge, 1999; Tao *et al.*, 1999; Zaider *et al.*, 1994), paraquat-induced free radicals also damage DNA (Chevion, 1988).

In rich medium, wild-type *E. coli* is marginally affected at paraquat concentrations of 100 μM or less (Carlioz and Touati, 1986), but is much more sensitive (<30 μM) in minimal medium when its oxidative burden is increased by a TCA cycle actively generating metabolic precursors and reducing equivalents (Gottschalk, 1985; Keyser *et al.*, 1995). As expected, an *E. coli sodA*$^-$ *sodB*$^-$ double mutant (JI132) (Carlioz and Touati, 1986) was unable to grow on minimal medium with or without paraquat because of overwhelming oxidative stress. For cells growing in minimal medium, paraquat sensitivity (Figure 4.5) was examined in strains CF1648 (Markillie *et al.*, 1999) (*E. coli*, wild-type), MD885 (Sod$^-$), rec30 (*recA*$^-$), and *D. geothermalis*. Three independent replicate paraquat treatments for each strain showed that the mutants and *D. geothermalis* are substantially more sensitive to paraquat than wild-type *D. radiodurans* (Figure 4.5).

Figure 4.5 Resistance to Paraquat-Induced Oxidative Stress. Deinococcal strains were inoculated into DMM supplemented with cysteine, methionine, and histidine, and adjusted to the indicated concentrations of paraquat. Growth of *E. coli* was in M9 medium supplemented with cysteine, methionine, and histidine (as for deinococcal DMM). OD_{600} measurements were taken 72 hours after inoculation and incubation at 32 °C and 37 °C for deinococcal and *E. coli* cells, respectively. Values are from three independent trials, with standard deviations shown. Note, MD866 (*sodA*⁻(*B*)*recA*⁻ was not tested because of poor growth in liquid DMM (Table 4.2A).

Figure 4.5

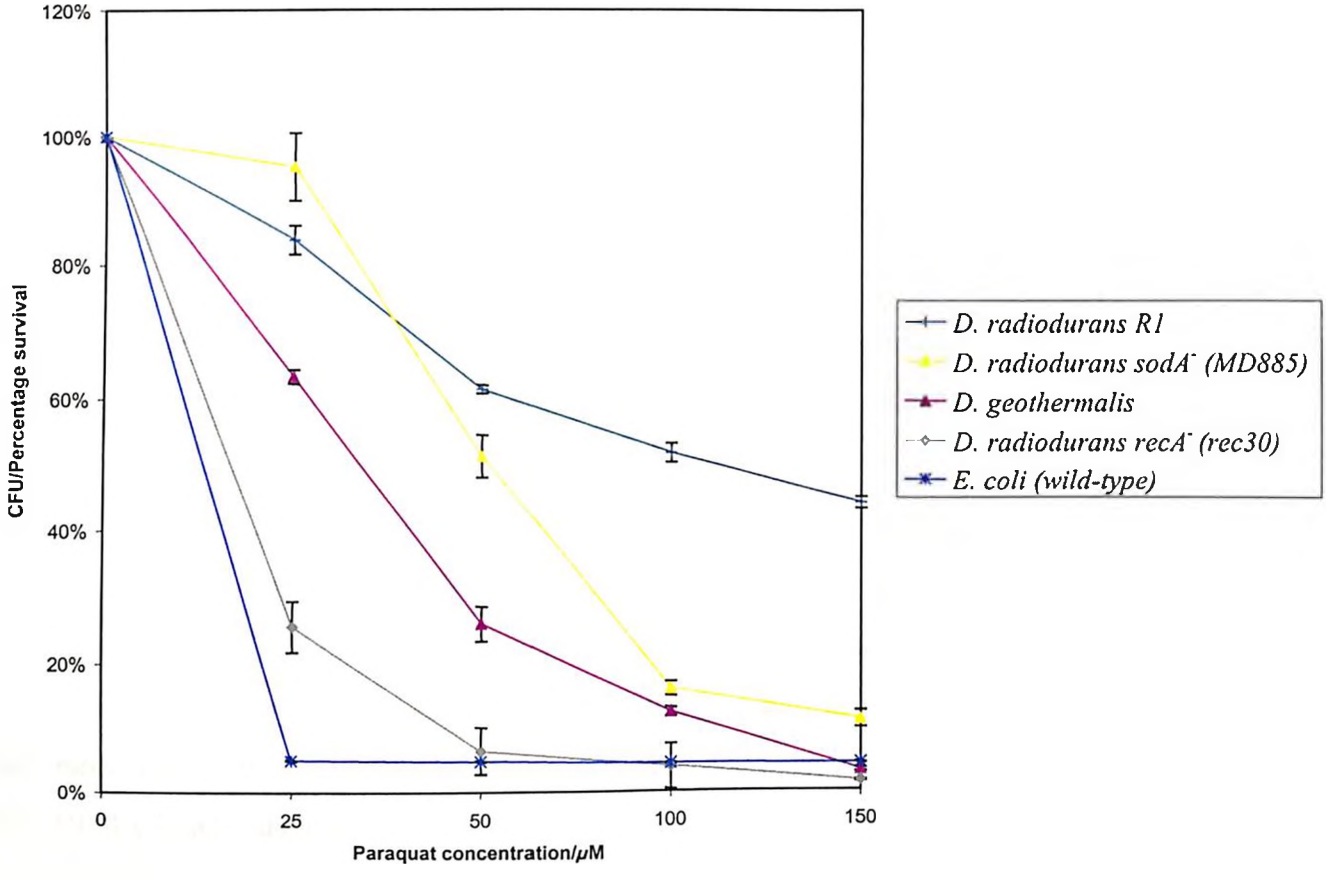
120%
100%
80%
60%
40%
20%
0%
CFU/Percentage survival
0
25
50
100
150
Paraquat concentration/μM
D. radiodurans R1
D. radiodurans sodA⁻ (MD885)
D. geothermalis
D. radiodurans recA⁻ (rec30)
E. coli (wild-type)

4.4 Discussion

Remarkably, the number of genes identified in *D. radiodurans* that are known to be involved in DNA repair is less than that reported for *E. coli* (Makarova *et al.*, 2001), and most of the DNA repair genes identified in *D. radiodurans* have functional homologs in other prokaryotic species (Makarova *et al.*, 2001). These findings together with results reported in chapter 2 (Section 2.3) support that the determinants of the extreme radiation resistance phenotype might also include functions not conventionally associated with DNA repair. A variety of *D. radiodurans* genes have been predicted highly expressed (PHX) and implicated by Karlin and Mrazek (Karlin and Mrazek, 2001) as contributing to its resistance phenotype. Among 28 complete prokaryotic genomes, *D. radiodurans* contains the greatest number of PHX proteases, and consistently, several of its ABC transporter genes for peptides and branched chain amino acids were PHX. One of the top PHX genes in *D. radiodurans* is *aceA* of the glyoxylate bypass (Figure 2.1), and *sodA*, key to removing free oxygen radicals, has one of the highest PHX ratings for enzymes involved in detoxification. This work examined how global processes dependent on these genes might be contributing to its resistance phenotype (Daly *et al.*, 1994; 1995; Makarova *et al.*, 2001).

Several genetic defects were observed in *D. radiodurans* that limit amino acid metabolism and energy production (Chapter 2, Figure 2.1). While the significance of these defects is unclear, it is possible that loss of part of its metabolic repertoire was a consequence of its maintenance in laboratory culture on non-selective nutrient rich medium since its isolation in 1956 (Anderson *et al.*, 1956). Specifically, *D. radiodurans* and a second strain of *D. radiodurans* isolated in 1958 (SARK, data not shown) are completely dependant on exogenous methionine and nicotinic acid for growth and cannot utilize certain TCA cycle intermediates provided as sole carbon sources in defined minimal medium (DMM) (Table 4.2A). To determine the distribution of these metabolic deficiencies within the family, other more recently isolated species of *Deinococcus* were examined for their dependence on these substrates (Table 4.2A). *D. radiopugnans* (isolated 1963) (Davis *et al.*, 1963), *D. radiophilus* (1971) (Lewis, 1971), *D. proteolyticus* (1973) (Kobatake *et al.*, 1973), *D. grandis* (1987) (Oyaizu *et al.*, 1987), and *D. murrayi* (1997) (Ferreira *et al.*, 1997) all showed a similar dependence on amino acids and nicotinic acid (Table 4.2A), supporting that this metabolic configuration is prevalent in the

family and is unlikely to have arisen from extended laboratory culture. This trend is reinforced by recent environmental isolates of *D. radiodurans* (2001) from radionuclide-contaminated sediments at Hanford, WA that have almost identical nutritional requirements as *D. radiodurans* (Chapter 2, Section 2.3.1.4; Fredrickson *et al.*, 2003). The only species of *Deinococcus* shown to have complete metabolic capabilities is *D. geothermalis* (1997) (Ferreira *et al.*, 1997) (Table 4.2A), and significantly it is also the least radiation resistant of the family *Deinococcaceae* (Figure 4.2, Table 4.2B).

A family of subtilisin-like proteases is expanded in *D. radiodurans* (Makarova *et al.*, 2000) and high expression has been predicted for their genes (Karlin and Mrazek, 2001). Consistently, *D. radiodurans* was found to secrete proteases and with the exception of *D. geothermalis*, the other deinococcal strains also showed high levels of secretion on proteases indicator plates (Table 4.2B, Figure 4.1). Secretion of proteases by *D. radiodurans* is likely to help overcome a severe defect in its amino acid biosynthetic capabilities (Makarova *et al.*, 2001, Chapter 3).

Since growth of the NAD-dependent *Deinococci* (Table 4.2A) was inhibited in all but the most nutritionally favorable environmental conditions, these species would be dormant in most nutritionally restricted environments. Since DNA repair in *Deinococcus* is dependent on growth conditions (Daly *et al.*, 1994; Minton, 1994; Chapter 3), DNA damage likely is accumulated during periods of dormancy. For example, DNA damage is accumulated during environmental cycles of desiccation and rehydration (*e.g.*, arid soil environment [Chapter 2, Section 2.4], Mattimore and Battista, 1996), and/or by background radiation (~0.0005 Gy/year) over very long time spans (Richmond *et al.*, 1999). To avoid additional DNA damage caused by metabolism-induced free radicals (*e.g.* Figure 2.1) (Keyser *et al.*, 1995), dormant deinococcal cells may restore growth only under conditions that generate very low levels of endogenous oxidative stress. Free radicals formed either during exposure to high-energy radiation or as a result of oxidative stress are known to react with Fe-S centers releasing Fe^{2+}, which catalyzes the reduction of H_2O_2 to $^{\bullet}OH$. It has recently been reported that high levels of intracellular cysteine in *E. coli* can promote the reduction of Fe^{3+} to Fe^{2+} and the ensuing oxidative DNA arising from the Fenton (Park and Imlay, 2003). Consistently, analysis of *D. radiodurans*' genome sequence reveals multiple defects in cysteine biosynthesis pathway suggesting possibly low intracellular cysteine concentration in *D. radiodurans*.

The observed physiological growth characteristics of *D. geothermalis* were distinct from those of the other *Deinococcaceae* (Table 4.2A). Based on its pattern of substrate utilization, *D. geothermalis* is apparently the only strain of the seven tested that has an unrestricted TCA cycle, was not dependent on exogenous amino acids for growth, and could utilize inorganic sulfate (Table 4.2B). Also, *D. geothermalis* secreted no proteases compared to the other deinococcal species (Figure 4.1, Table 4.2B), and it was the least resistant to acute irradiation among the known *Deinococci* (Figure 4.2, Table 4.2B). If TCA cycle-based metabolism were more dominant in *D. geothermalis* than other *Deinococci*, this species would be expected to be burdened by higher oxidative stress levels arising from TCA cycle activity (Gottschalk, 1985). Consistently, *D. geothermalis* displayed post-irradiation colonies on rich and DMM that were substantially slower to recover than the other strains, possibly due to higher oxidative stress levels experienced by this species.

Microarray data for *E. coli* grown in minimal versus rich medium show that its TCA cycle genes are significantly upregulated during growth in minimal medium (Cronan and LaPorte, 1996; Tao *et al.*, 1999). Genomic informatic (Makarova *et al.*, 2001), and proteomic analyses (Lipton *et al.*, 2002) for *D. radiodurans* support that it has a functional TCA cycle. However, unlike *E. coli* (Tao *et al.*, 1999), expression of the TCA cycle genes in *D. radiodurans* grown in DMM were down-regulated or unchanged (Table 4.3). Only one gene, *aceA*, showed significant induction, and it is possible that this response reflects upregulation of its glyoxylate bypass.

The chronic production of $^{\bullet}OH$ and $O_2^{\bullet-}$ radicals is typically associated with the aerobic lifestyle (*e.g.*, Chapter 2, Figure 2.1), and are extremely toxic to cells (Schulte_Frohlinde, 1986; Zaider *et al.*, 1994). Facultative and obligate aerobes have developed efficient catalytic scavenging systems to eliminate these DNA damaging ions. Generally, SodA and SodB are a major defense against superoxide radicals (Fridovich, 1999). Using high throughput proteomics, the presence of SodA was detected in high abundance in *D. radiodurans* cells grown in a variety of conditions including minimal and rich medium (Lipton *et al.*, 2002). SodB is not encoded in *D. radiodurans* (Makarova *et al.*, 2001), and DR1546 (Cu-Zn-dependent, SodC) and SodC-like DRA0202 were detected in only relatively low abundance under rich or minimal growth conditions (Lipton *et al.*, 2002). Those data suggest that SodA dominates SOD function in *D. radiodurans* and that SodA is constitutively expressed. Consistently, data presented in Figure 4.3

shows that SodA expression in *D. radiodurans* was essentially unaffected in DMM compared to rich medium (Table 4.2B) (Lipton *et al.*, 2002), and neither SodC (Figure 4.4) nor its activity (Figure 4.3) could be detected in cells grown in rich or DMM.

E. coli sodA⁻B⁻ mutants readily grow in nutrient rich media where very little oxidative stress arises, but cannot grow in minimal medium (Keyser *et al.*, 1995) where demand for TCA cycle dependent ATP and metabolic intermediates is dramatically increased and high levels of toxic free radicals are generated (Carlioz and Touati, 1986; Imlay, 1988; Keyser *et al.*, 1995). In contrast, a *sodA⁻*(*sodB⁻*) *D. radiodurans* (MD885) showed essentially no difference in growth on minimal or rich medium (Table 4.1A). Additionally, the radiation sensitive double mutant MD886 (*sodA⁻*(*B⁻*)*recA⁻*) (Figure 4.2) also grew in either medium (Table 4.2A). By comparison, *E. coli sodA⁻B⁻recA⁻* is non-viable in aerobic conditions irrespective of nutrient conditions because of the lethal effects of oxidative stress (Touati *et al.*, 1995). It appears, therefore, that stringent metabolic regulation in *D. radiodurans* suppresses the production of high levels of endogenous free radicals, and this may equally apply to the other deinococcal species given their similar patterns of substrate utilization (Table 4.2A) and expression of SOD activities (Figure 4.4).

If oxidative stress levels in *D. radiodurans* are naturally low because of its TCA cycle expression pattern (Table 4.3), then increasing its endogenous free radical levels by the addition of a chemical inducer of oxidative stress could mimic the lethal effects experienced by *sodA⁻B⁻ E. coli* in minimal medium. The effect of the oxidative stress inducer paraquat was examined on growth in DMM for *D. radiodurans* wild-type, *recA⁻* (rec30), and *sodA⁻*(*B⁻*) (MD885) (Figure 4.5). Compared to wild-type, increasing concentrations of paraquat had a substantial inhibitory effect on the growth of the *D. radiodurans* mutants compared to their growth in DMM without paraquat. This indicates that SOD plays a dominant role in removing free radicals in *D. radiodurans*, but that its primary function likely is not protecting cells from reactive byproducts of aerobic metabolism. Rather, these observations suggest that constitutively expressed deinococcal SodA (Figure 4.4) (Lipton *et al.*, 2002) acts to protect the cells from exogenously induced free radicals. In view of the findings on expression of *D. radiodurans* SodA and its TCA cycle (Table 4.3), it makes sense that its SodA is constitutively expressed. *D. radiodurans* SodA likely is one of the first defenses against sudden, sporadic free radicals encountered in its natural environment [*e.g.*, cycles of desiccation and rehydration associated with arid soils (Chapter 2,

section 2.4) (Mattimore and Battista, 1996).

Auto-oxidizing enzymes that contain flavins are believed to be the primary site of electron transfer to oxygen in the production of $O_2^{\bullet-}$ (Messner and Imlay, 1999), and it is noteworthy that *D. radiodurans* lacks three flavin-containing enzymes prominently associated with free radical production: fumarate reductase (FrdA), aspartate oxidase (NadB) and the α-subunit of sulfite reductase (CysI) (Makarova *et al.*, 2001). It has been proposed that a low titer of flavoproteins in cells may lower the degree of oxidative stress (Messner and Imlay, 2002). Furthermore, three TCA cycle genes known to use FAD or NAD as cofactors (succinate dehydrogenase, isocitrate dehydrogenase, and malate dehydrogenase) were down-regulated in DMM (Table 4.3). Avoiding the production of metabolically-induced oxidative stress likely is only one of several contributing determinants of the extreme radiation resistance phenotype of *D. radiodurans*. In the next chapter, DNA microarray technology and proteomics were used to further study *D. radiodurans*' gene and protein expression patterns induced by environmental stress, including growth in DMM and exposure to ionizing radiation.

4.5 Conclusions

1. **With the exception of *D. geothermalis*, all *Deinococcus* strains showed dependence on sulfur containing amino acids and nicotinic acid for growth, and secrete proteases.**

2. ***D. geothermalis* is able to synthesize all amino acids and is significantly less resistant to ionizing radiation than the other deinococcal species.**

3. **Quantitative real-time PCR (RT-PCR) expression analysis of TCA cycle genes of *D. raiodurans* grown in DMM showed significant induction of *aceA*, a constituent of its glyoxylate bypass enzyme, but repression of the other TCA cycle genes (*e.g.*, *sdhA* & *sdhB*, fumarate/succinate dehydrogenase). This unexpected result suggests that regulation of its TCA cycle is distinct from most other reported aerobic bacteria, and which could limit the production of oxidative stress in nutrient restricted environments.**

4. **Physiologic studies, bioinformatic analyses, RT-PCR expression analyses, and the dispensability of SodA in *D. radiodurans* generally support the hypothesis that production of oxidative stress levels in *D. radiodurans* is very low.**

Chapter 5: Transcriptome Dynamics of *Deinococcus radiodurans* Recovering from Ionizing Radiation

5.1 Introduction

Following growth in rich medium, the irradiation dose yielding 37% survival (D_{37}) of *D. radiodurans* tetracocci (OD_{600}, 1.2) is ~15 kGy (Chapter 4, Figure 4.2). By comparison, the D_{37} dose of *E. coli*, that grows as single cells in rich medium, is ~0.5 kGy (Chapter 4, Figure 4.2), a 30-fold difference in survival (Sweet and Moseley, 1976). Irradiation-induced DSBs will lead to cell death if they are not repaired, and to deletions and other genetic rearrangements if rejoined by non-homologous end-joining (NHEJ) (Haber, 2000; Sweet and Moseley, 1976). *D. radiodurans* maintains 4-8 haploid copies of its genome per cell (Hansen, 1978), and the repair of DSBs is known to be mediated by *recA*-independent (single-stranded annealing) (Daly and Minton, 1996) and *recA*-dependent (Daly and Minton, 1995) homologous recombination, but NHEJ does not occur. Yet, the identity of the genetic systems underlying those repair processes in *D. radiodurans* remains unknown in spite of experimental DNA repair studies (Daly *et al.*, 1994a, 1994b; Daly and Minton 1995a, 1996, 1997) genome sequencing (White *et al.*, 1999) and annotation (Makarova *et al.*, 2001), and whole proteome analysis of cells recovering from high-dose irradiation (Lipton *et al.*, 2002).

Comparative-genomic and proteomic analyses support the view that *D. radiodurans'* extreme radiation resistance phenotype is complex, likely determined collectively by an assortment of protection and DNA repair systems, as well as by more subtle structural peculiarities of proteins and DNA that are not readily inferred from the sequences (Makarova *et al.*, 2001). The number of DNA repair enzymes identified in *D. radiodurans* during annotation is less than reported for *E. coli* (Makarova *et al.*, 2001) and the predicted expression levels of its repair proteins compared to other prokaryotes are similarly low (Karlin and Mrazek, 2001). These findings justify systematic analysis of the dynamic changes in the global gene and protein expression profiles of *D. radiodurans* induced by environmental stress, including growth in defined minimal medium (DMM) and exposure to ionizing radiation.

The lack of a clearly identifiable unique DNA repair system in *D. radiodurans* (Makarova *et al.*, 2001) has given rise to at least three competing views of its extraordinary survival; (a) there are novel repair genes hidden within the group of hypothetical proteins predicted by genomic annotation; or (b) *D. radiodurans* uses conventional DNA repair pathways, but with much greater efficiency than other bacteria; and/or (c) the metabolic configuration of *D. radiodurans* is a key determinant of its resistance phenotype (Chapters 2 and 3). As a step towards investigating these possibilities, a whole genome microarray was constructed for *D. radiodurans* at Oak Ridge National Laboratory, Oak Ridge, TN in collaboration with Dr. Jizhong Zhou, and used as part of this thesis work. The goals of this chapter are:

1. **To participate in the DOE-sponsored effort to validate the *D. radiodurans* annotation published by Makarova *et al.* (2001), and thereby facilitate the design, fabrication, and use of a whole genome microarray constructed for *D. radiodurans*.**

2. **To study the dynamic changes in *D. radiodurans*' global gene expression profiles in cells recovering from a high dose of γ-radiation.**

3. **To test the robustness of the microarray expression data using RT-PCR of selected mRNAs.**

4. **To analyze expression data with emphasis on the possible role of metabolism in the extreme radiation phenotype.**

5.2 Materials and Methods

5.2.1 Accurate Mass Tag (AMT) Directed Proteomics

The AMT approach for *D. radiodurans* proteome analysis was developed by Lipton and coworkers (2002) (Lipton *et al.*, 2002) at PNNL, Richland, WA. This

approach utilizes instrumentation that combines high pressure reversed phase capillary liquid chromatography (LC) with high magnetic field Fourier transform ion cyclotron resonance (FTICR) mass spectrometry and tandem mass spectrometry (MS/MS) (Lipton *et al.*, 2002). This approach for defining AMTs provides extremely high confidence for protein identification due to AMT identification using MS/MS with standard database searching/identification combined with validation using high accuracy mass measurements. The AMT-based protein identification allows subsequent high throughput proteome measurements, including the use of ^{15}N labeling strategies, where the distinctive peptide AMTs (<1 ppm by FTICR) and LC elution times are used to identify proteins. This strategy was used to determine expression levels of TCA cycle and glyoxylate bypass enzymes in ^{15}N-labeled DMM versus ^{14}N-labeled rich (TGY) medium. The cells were quantitatively combined to ensure that all subsequent processing was equal for the two cultures. The resulting peptides were analyzed with an 11.5 tesla FTICR mass spectrometer, and the peptides were identified utilizing the existing AMT database (Lipton *et al.*, 2002). Once identification was confirmed, the abundance ratio for each peptide was calculated by comparison of the abundance of the ^{15}N peak with the ^{14}N peak.

5.2.2 Microarray Analysis

5.2.2.1 Cell Growth and Irradiation

D. radiodurans was grown at 32 °C in liquid nutrient rich medium TGY (1% bactotryptone, 0.1% glucose, and 0.5% yeast extract) or on TGY medium solidified with 1.5% BactoAgar. In liquid culture, cell density was determined at 600 nm by a Beckman spectrophotometer. For high-dose irradiation exposure, 150 ml of an ESP *D. radiodurans* culture (OD_{600} = 1.0, ~$1x10^8$ colony forming units [CFU]/ml) (Daly *et al.*, 1994a) were divided in half. 75 ml were irradiated without change of broth on ice at 2.7 Gy/second to a total dose of 15 kGy (^{60}Co gammacell irradiation unit, J. L. Shepard and Associates, Model 109). Cells from the unirradiated 75 ml *D. radiodurans* culture (non-irradiated control) were harvested by a brief centrifugation, washed and then frozen in RNAlater

solution (Ambion, Austin, TX), and stored at –80 °C. Following exposure to 15 kGy, the irradiated cell culture (75 ml) was diluted 20-fold into fresh TGY medium and incubated at 32 °C in an orbital shaker. At the indicated recovery time-points, ~1 x 10^9 cells were harvested, washed and frozen in RNAlater solution as for the non-irradiated control. Cell viability and cell numbers were determined by plate assay and hemocytometer count. Three independent cell cultures and irradiation treatments of the same kind were performed and served as biological replicates for gene expression experiments as well as for determining irradiation resistance profiles.

5.2.2.2 Genomic DNA and Total Cellular RNA Extraction

Sub-samples containing about 3 × 10^8 cells were thawed to room temperature and pelleted in 1.5 ml eppendorf tubes. The pellets were subjected to three consecutive freeze/thaw cycles using liquid nitrogen and then suspended in 500 µl of TE buffer (10 mM Tris-HCl, pH 8; 0.1 mM EDTA) containing 500 µg of lysozyme and 2.5 µg of lysostaphin, and incubated at 37°C for 10 min. Lysozyme/Lysostaphin-treated cells were lysed by the addition of 50 µl 20% (w/v) sodium dodecyl sulfate (SDS) and 300 µg of proteinase K, and incubation at 40°C. Cell lysates were phenol/chloroform-extracted and nucleic acids were precipitated with an equal volume of 80% (v/v) isopropanol, and dissolved in TE buffer. Total cellular RNA was isolated using TRIzol™ Reagent (Gibco BRL, Life Technologies, Gaithersburg, MD), treated with RNase-free DNase I (Ambion, Austin, TX), and purified using Mini RNeasy kit (Qiagen, Chatsworth, CA). DNA components were treated with DNase-free RNase A (Ambion, Austin, TX) and purified using a genomic DNA cleanup kit (Promega Corporation, Madson, WI). The concentration and purity of both DNA and RNA samples were determined by spectrophotometric ratio assay at 260 nm and 280 nm.

5.2.2.3 Microarray Fabrication

The microarray fabrication was done as a collaborative effort at the Oak Ridge National Laboratory (ORNL), Tennessee. Briefly, PCR products of 2,976 distinct open

reading frames (ORFs) of *D. radiodurans* genome were spotted in duplicates onto SuperAmine glass slides (TeleChem International, Inc.) using a PixSys 5500 robotic printer (Cartesian Technologies, Inc., Irvine, CA) equipped with 16 ChipMaker III pins (TeleChem International, Inc.). Also spotted were the appropriate positive and negative controls that included internal standards derived from 10 human genes subcloned into the pCR or pBluescript SK+ vectors. The printed DNA fragments were cross-linked to the glass slides using 65 mJ of UV (254 nm) light, and denatured by submersion into boiling water for 3 min. The processed slides were subsequently air-dried and stored at RT until further use.

5.2.2.4 cDNA Labeling and Microarray Hybridization

For probe synthesis and labeling, 20 μg of the total cellular RNA was incubated together with 5 ng of a spike mRNA at 70 °C for 10 min in the presence of 9 μg of random hexamers (Gibco BRL). The labeling reaction was catalyzed by 200 U of Supescript™ II RNase H⁻ reverse transcriptase (Gibco BRL) in the presence of 500 μM dATP, dGTP, and dTTP; 50 μM dCTP; and 50 μM of the fluorophor Cy3-dCTP or Cy5-dCTP (Perkin Elmer/NEN Life Science Products, Boston, MA). The reverse transcription reaction was incubated at 42 °C for 2 h, followed by RNA hydrolysis in 1 N NaOH at 37°C for 10 min. The labeled cDNA probe was purified using a Qiagen PCR purification column and concentrated in a Savant speedvac centrifuge (Savant Instruments Inc., Holbrock, NY). For each biological replicate, dye-switch was adopted, *i.e.* the non-irradiated control and irradiated samples were labeled either with Cy5 and Cy3, respectively, or with Cy3 and Cy5, respectively, to avoid possible bias dye incorporation. In addition to the duplicates of arrays on the same slide, three biological cell samples were included with two dye-switch combinations, yielding a total of 12 replicates of hybridization for the majority of genes subjected to each microarray analysis.

For microarray hybridization, the concentrated probes derived from both 'irradiated' and 'unirradiated' cDNAs were mixed and resuspended in a 30-μl total volume of hybridization solution that contained 3X saline-sodium citrate (SSC), 0.33% (w/v) SDS, 40% (v/v) formamide, and 24 μg of unlabeled herring sperm DNA (Gibco

BRL). After a rapid denaturation by exposure to 100 °C for 3 min, the hybridization solution was immediately applied onto the microarray slide. Hybridization was carried out in a waterproof CMT-slide chamber (Corning, Corning, NY) submerged in a 50 °C water bath in the dark for 16 h. Following hybridization, arrays were washed with 1 × SSC/0.2% (w/v) SDS and 0.1 × SSC/0.2% (w/v) SDS for 5 min each and with 0.1 × SSC for 30 sec, and air-dried at RT before scanning.

5.2.2.5 Array Quantification and Data Process

Hybridized microarray slides were double channel-scanned to record intensities for both Cy3- and Cy5-fluorophor signals using a confocal laser fluorescent microscope (ScanArray® 5000 Microarray Analysis System, GSI Lumonics, Watertown, MA). Laser power and PMT gain were calibrated and adjusted for each fluorophor, so that overall intensities for most array spots were neither saturated nor too weak, and more comparable in both fluorescent channels. Image analysis to quantify spot signal and background fluorescent intensity, and to identify empty spots and spots of poor quality (high pixel intensity variation) was performed using ImaGene version 4.2 (Biodiscovery Inc., Los Angeles, CA). After removal of all empty and poor spots from data spreads, the quantified data were subject to normalization and statistical analyses. The ratios of the irradiated samples to the non-irradiated control were normalized with the Pooled-Common-Error model (similar to the most commonly used geometric mean normalization method) using the statistical analysis software ArrayStat version 2.0 (Imaging Research Inc. Ontario, Canada). The outliers, or those data points that were not consistently reproducible and had a disproportionately large effect on the statistical result, were removed. A student T-test was performed for each arrayed spot so that a two-tailed probability of a mean deviating from 1.0 could be calculated and used to assign the significance for each data point. The statistically analyzed data were then loaded into the robust software GeneSpring version 4.1 (Silicon Genetics, Redwood City, CA) for detailed gene expression plotting analyses of the annotated functional groups or metabolic pathways, and for exploiting possibly related functions for the genes encoding conserved hypothetical and hypothetical proteins based on their expression patterns data

was used for blotting and hierarchical clustering analysis. Hierarchical clusters were constructed using the software Cluster (http://rana.stanford.edu/). For all clustering analyses, the average-linkage clustering model was applied. The resulting clusters were visualized with the software TreeView (http://rana.stanford.edu/).

5.2.3 Real-Time Quantitative PCR

RT-PCR was carried out as described in chapter 4 section 4.2.7.

5.3 Results

5.3.1 Proteome Analyses

Quantitative proteomics for *D. radiodurans* was conducted as described elsewhere (Lipton *et al.*, 2002). *D. radiodurans* R1 cells grown in rich (TGY) or defined minimal medium (DMM) were compared to reference cells grown in ^{15}N-labeled DMM. Unlabeled cells from the TGY and stressed cultures were mixed in equal numbers with the ^{15}N-labeled cells and analyzed. The relative abundances of peptide AMTs (Lipton *et al.*, 2002) for TCA cycle and glyoxylate bypass enzymes yielded relative (minimal/rich) abundance ratios shown in Table 5.1. The ratios support that part of the TCA cycle is suppressed in DMM compared to rich medium; the glyoxylate bypass is more active in DMM than in rich medium.

The complete data set for all expressed protein detected under different growth and stress conditions evaluated is published as supporting information of the Proceedings of the National Acedemy of Sciences (PNAS), USA, website (http://www.pnas.org/content/vol0/issue2002/images/data/172170199/DC1/1701Table4.xls). The collaborative proteomics work (Lipton *et al.*, 2002) provided physical validation that ~ 61% of predicted *D. radiodurans* ORFs (Makarova *et al.*, 2001) are expressed as proteins. This justified the construction of a whole genome microarray for *D. radiodurans* based on two very similar annotations of the *D. radioduans* genome (White *et al.*, 1999; Makarova *et al.*, 2001).

was used for blotting and hierarchical clustering analysis. Hierarchical clusters were constructed using the software Cluster (http://rana.stanford.edu/). For all clustering analyses, the average-linkage clustering model was applied. The resulting clusters were visualized with the software TreeView (http://rana.stanford.edu/).

5.2.3 Real-Time Quantitative PCR

RT-PCR was carried out as described in chapter 4 section 4.2.7.

5.3 Results

5.3.1 Proteome Analyses

Quantitative proteomics for *D. radiodurans* was conducted as described elsewhere (Lipton *et al.*, 2002). *D. radiodurans* R1 cells grown in rich (TGY) or defined minimal medium (DMM) were compared to reference cells grown in ^{15}N-labeled DMM. Unlabeled cells from the TGY and stressed cultures were mixed in equal numbers with the ^{15}N-labeled cells and analyzed. The relative abundances of peptide AMTs (Lipton *et al.*, 2002) for TCA cycle and glyoxylate bypass enzymes yielded relative (minimal/rich) abundance ratios shown in Table 5.1. The ratios support that part of the TCA cycle is suppressed in DMM compared to rich medium; the glyoxylate bypass is more active in DMM than in rich medium.

The complete data set for all expressed protein detected under different growth and stress conditions evaluated is published as supporting information of the Proceedings of the National Acedemy of Sciences (PNAS), USA, website (http://www.pnas.org/content/vol0/issue2002/images/data/172170199/DC1/1701Table4.xls). The collaborative proteomics work (Lipton *et al.*, 2002) provided physical validation that ~ 61% of predicted *D. radiodurans* ORFs (Makarova *et al.*, 2001) are expressed as proteins. This justified the construction of a whole genome microarray for *D. radiodurans* based on two very similar annotations of the *D. radioduans* genome (White *et al.*, 1999; Makarova *et al.*, 2001).

Table 5.1. [a]Abundance Ratios of Indicated Proteins Observed in *D. radiodurans* R1 Cells Grown in DMM Versus Rich Medium.

ORF Designation	ORF NAME	Abundance ratio min medium/TGY(Rich)
DR0757	Citrate synthase	0.66
DR1540	Isocitrate dehydrogenase	0.44
DR0287	2-oxoglutarate dehydrogenase	0.91
DR2526	Lipoamide dehydrogenase	0.65
DR1247	Succinyl CoA synthetase β-chain	0.47
DR1248	Succinyl CoA synthetase α-chain	0.48
DR2627	Fumarase	0.83
DR0828	Isocitrate lyase	1.43

Footnote for Table 5.1

[a]*D. radiodurans* R1 cells were harvested for proteomic expression analysis at an absorbance of 600 nm (A_{600}) of 0.5. Data was derived from cells compared to the ^{15}N-labeled reference proteome [R1 cells grown in DMM containing Cys (chapter 3, Table 3.1)]. Relative abundances were used to calculate expression ratios, revealing changes in expression for the indicated ORFs (open reading frames).

5.3.2 Microarray Analysis

5.3.2.1 Response of Cells to Irradiation

The exposure of *D. radiodurans* grown to the early stationary phase (ESP) (OD_{600} ~1.0) to 15 kGy (60Co) induced ~150 DNA DSBs/haploid chromosome (Daly *et al.*, 1994a; Daly and Minton, 1995a; Daly and Minton, 1996; Daly *et al.*, 1994b) (data not shown). As expected, its recovery in fresh medium resulted in a 9-hour growth during which DNA was repaired. After the 9-hour growth-lag, cells grew exponentially and reached stationary phase 15 hours later, yielding a typical *D. radiodurans* growth curve between 12-24 hours (Figure. 5.1). Previous studies showed that when a single irradiation dose of ~17 kGy is applied to an ESP *D. radiodurans* culture, cellular recovery is dependent on nutrient-rich conditions; without change of broth, cells die with no evidence for DNA repair (Daly and Minton, 1995a; Daly and Minton, 1996; Daly *et al.*, 1994b; Minton, 1996). The following gene expression experiments were designed to optimize recovery and ensure that the genes involved in post-irradiation repair and stress response were optimally induced.

D. radiodurans recA is central to genomic restoration following irradiation; the *recA* gene is substantially upregulated upon DNA damage and then down-regulated before the onset of exponential growth (Carroll *et al.*,1996). Following a dose of 15 kGy, *D. radiodurans* recovery typically progresses through three phases (Carroll *et al.*, 1996; Daly *et al.*, 1994a; Daly and Minton, 1995a; Daly *et al.*, 1994b): 1) early-phase (0-3 hours): *recA* is induced, but there is little evidence for DNA repair; 2) mid-phase (3-9 hours): ongoing growth arrest and DNA repair; and 3) late-phase (9-24 hours): repression of *recA* and restoration of growth.

5.3.2.2 Quality of Microarray Hybridization Data

Because microarray hybridization exhibits inherent high variability, experimental replications are essential for obtaining reliable results (Lee, *et al.*, 2000). In this study, samples were taken at 9 time intervals over a period of 24 hours. At each time point, three replicated samples were obtained. Each microarray slide contained two duplicate

Figure. 5.1

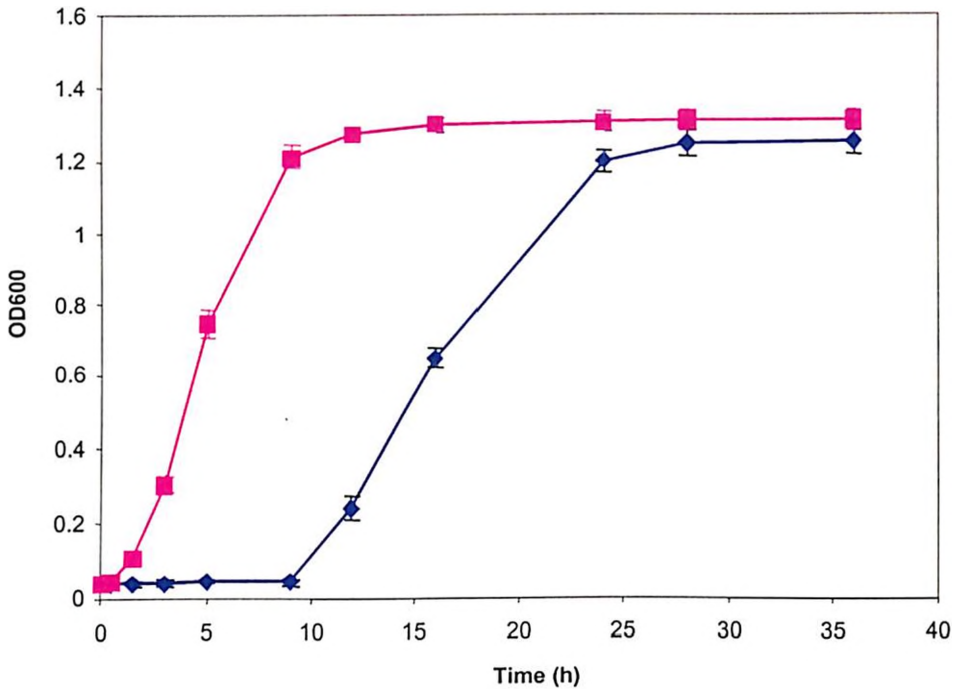

Figure 5.1. Effect of High-Dose Acute Irradiation on *D. radiodurans* Growth.

Squares, early stationary phase (ESP) cells (~1 x 10^8 cells /ml) were irradiated with 15 kGy on ice and then diluted 1/20 in fresh TGY medium. Cell growth was monitored by periodic OD_{600} measurements. At 0, 0.5, 1.5, 3, 5, 9, 12, 16, and 24 hours into recovery, about 1 x 10^9 cells were harvested for microarray analysis. Circles, non-irradiated ESP control *D. radiodurans* cells inoculated and monitored as for irradiated cells. Values are the means ± standard deviations of the triplicate experiments (n = 9).

sets of gene fragments, and the RNA obtained from each sample was hybridized with two microarrays using fluorescent-dye reversal. Thus, 12 data points were available for each time point and enabled the use of statistical tests to determine significant changes in gene expression. Only those genes with statistically significant differences were further analyzed. The following three additional methods were used to test the robustness of the microarray hybridization data:

1. Correlation between Gene Expression Patterns within the Same Operon. Operons are the principal form of gene co-regulation in prokaryotes, so the expression patterns of genes within an operon are expected to be strongly correlated. Consistently, analysis of 435 genes within 141 predicted operons showed highly significant correlation of their expression patterns compared to genes in "random operons."
2. Independent Verification by RT-PCR. Seven genes were randomly selected and their expression was independently verified by RT-PCR analysis (Table. 5.2A and 5.2B). The expression data of six of these genes were similar to that obtained from their microarray expression. This further validated the microarray data.
3. Disruption Analysis of DR0070. The ORF disruption experiments were carried out by Dr. Elena K. Gaidamakova at USUHS, MD. The uncharacterized gene DR0070 encodes a hypothetical protein (199 amino acids in length) that is unique to *D. radiodurans* and that is highly expressed after radiation. To confirm that this gene is involved in radiation resistance, DR0070 was disrupted. The radiation resistance of a mutant (MD891) with a confirmed homozygous disruption for DR0070 was compared to wild-type *D. radiodurans*. While MD891 shows no metabolic or growth deficiencies in the presence or absence of chronic γ-radiation (60 Gy/hour), it is substantially more sensitive to acute irradiation than wild-type *D. radiodurans* (Liu *et al.*, 2003).

Taken together, these observations suggest that the expression array data presented here are of sufficiently high quality to be used to investigate patterns of expression-induction and -repression that occur in *D. radiodurans* cells in response to high-dose irradiation.

Table 5.2A Comparison of Expression Levels Produced in Microarray and Real-Time (RT) – PCR Experiments for a Set of 7 *D. radiodurans* Genes

Gene ID	Annotation	Method	Time (h) post irradiation Responds to radiation (folds)								
			0	0.5	1.5	3	5	9	12	16	24
DR0007	Unknown	Microarray	1.02	3.93	2.99	1.39	1.73	1.53	1.88	1.17	1.78
		RT PCR	0.21	0.37	1.77	0.69	0.95	1.31	1.38	1.89	1.49
DR2340	RecA	Microarray	1.13	6.62	7.98	5.02	5.27	4.06	3.70	2.15	1.44
		RT PCR	0.65	1.67	9.96	11.23	2.06	0.63	0.91	0.30	0.10
DRB0100	DNA ligase	Microarray	1.63	1.47	9.24	14.43	9.42	6.24	4.42	4.16	2.28
		RT PCR	2.38	7.98	17.82	12.18	8.64	4.14	3.97	3.93	1.68
DR2339	LigT-RNA ligase	Microarray	1.68	6.00	14.06	13.44	13.85	9.50	5.01	1.22	1.03
		RT PCR	3.51	6.52	14.24	2.88	1.51	2.48	2.94	0.52	1.42
DR0422	SAM-dependent melyltransferase	Microarray	1.28	13.99	18.85	10.95	8.18	4.39	2.69	1.79	1.14
		RT PCR	3.00	16.86	18.32	5.27	4.92	4.48	1.77	3.28	3.36
DR0053	DinB family	Microarray	1.67	4.49	10.16	10.25	6.10	3.67	2.30	1.35	1.30
		RT PCR	0.68	3.61	10.70	11.31	9.83	2.42	3.63	3.13	0.15
DR0207	ComA	Microarray	2.14	2.83	10.89	15.47	12.40	3.86	3.87	1.87	1.35
		RT PCR	1.37	5.41	18.68	19.96	33.22	21.12	16.95	3.30	4.34

Table 5.2B Sequences of the Primers Used in Real-Time Quantitative PCR

DR #	Gene product	Primer sequence	PCR product size (bp)
DR0007	Unknown	CAGTGGTGCTGATCGTGAGT ATAGACGAGTTCGCGCAGTT	116
DR2340	RecA protein	CCCCTTCAAGGAAGTCGAAC CGCCGTAGGAGTAGAAGCTG	125
DRB0100	DNA ligase	GCGAGTCAAATACCCTTCCA GGTAGAGGCTGGTGTTTTCG	146
DR2339	2'-5' RNA ligase	AACACCAACCGTCCACCTAC AGGTACGAGAGGGTGACGTG	145
DR0422	SAM-dependent melyltransferase	GCTTCGACCTGCTGTACTCC GTCGTGATTTGCTGGAACCT	128
DR0053	DinB/YfiT family	CCGCAGGTAAGCACTGAGAT TGGACCTCGTTGTCAATCAA	101
DR0207	ComA protein	CCCGGTAAACGTCAACACTG GCCTTTGACCTTTTTGACCA	133

5.3.2.3 Overview of General Genomic Expression Response to Radiation in *D. radiodurans*

The complete microarray data set for the recovery time-course is listed in supplementary material (SM)_Table A located at the website http://www.esd.ornl.gov/facilities/genomics/functional_genomics.html, which also contains supplementary results (SM_Results), figures (SM_Figs), and tables (SM_Tables). A two fold change in the expression levels of genes from their basal level was considered to be significant. At least at one recovery time point, 832 genes were induced while 451 genes were repressed, with many genes showing substantially greater induction than the threshold level (Figure. 5.2A). There was active gene expression at the initial recovery period (0-3 hours), even though the DNA was still fragmented (Figure 5.2A). The genes induced during this stage included those involved in DNA repair. In general, most of the DNA repair genes were induced between the 0-9 hour recovery time, when no replication/cell division was observed.

A more systematic approach to analysis of the gene expression profiling involved functional categorization of the genes according to the Clusters of the Orthologous Groups (COGs) of proteins database (http://www.ncbi.nlm.nih.gov/cgi-bin/COG/palox). The 'Stress' category was additionally introduced on the basis of previous functional assignments for *D. radiodurans* (Makárova *et al.*, 2001). For most functional groups, the maximum response occurred concurrently around the 3-hour post-irradiation time-point (Figure 5.3). Expression of genes within the 'translation', 'replication and repair' and 'cell wall metabolism' categories showed the greatest changes (primarily up-regulation) compared to the other functional categories (Figure 5.3) in the early-phase of recovery. Significantly, expression dynamics for most genes implicated in DNA repair resembles the expression pattern of *recA* (Figure 5.4), which is considered a dominant marker for the onset of homologous recombination (Carroll *et al.*, 1996). The observation that genes within diverse functional groups are differentially regulated in the early-mid-phase time intervals indicates that recovery from irradiation is a complex process that involves numerous cellular systems (Figure 5.3). Significant changes in metabolic expression profiles were observed in the late-phase of recovery (restoration of growth).

Figure 5.2. Gene Expression in *D. radiodurans*. A. Activation and repression of *D. radiodurans* genes as a function of time post- irradiation. The data are for two-fold activation or repression; Up, activation; Down, repression. **B.** Activation of gene expression in response to irradiation in the four genomic partitions of *D. radiodurans*.

Figure 5.2A

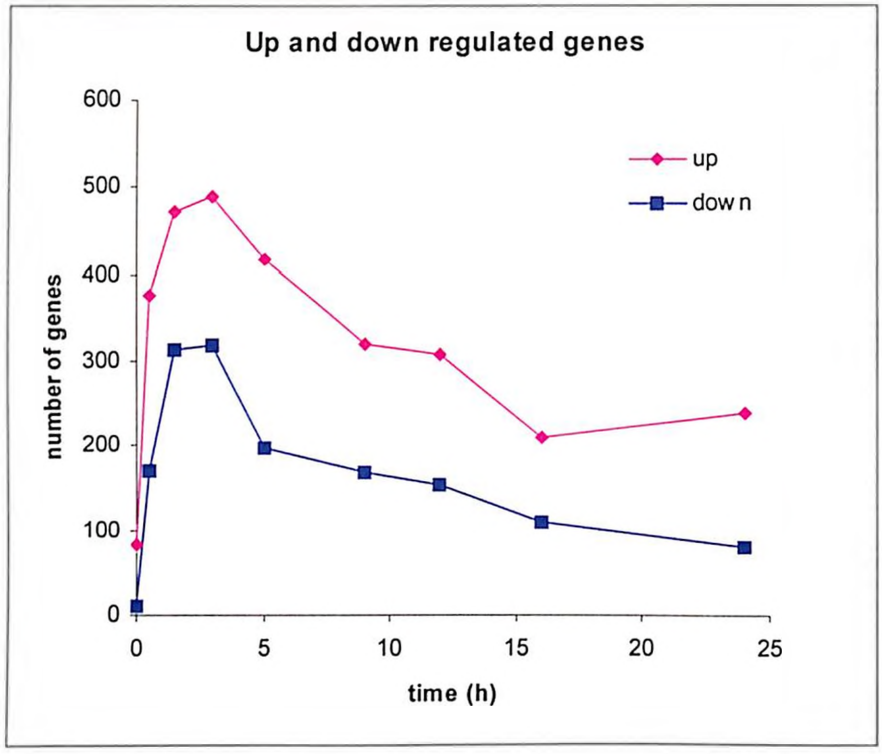

Figure 5.2B

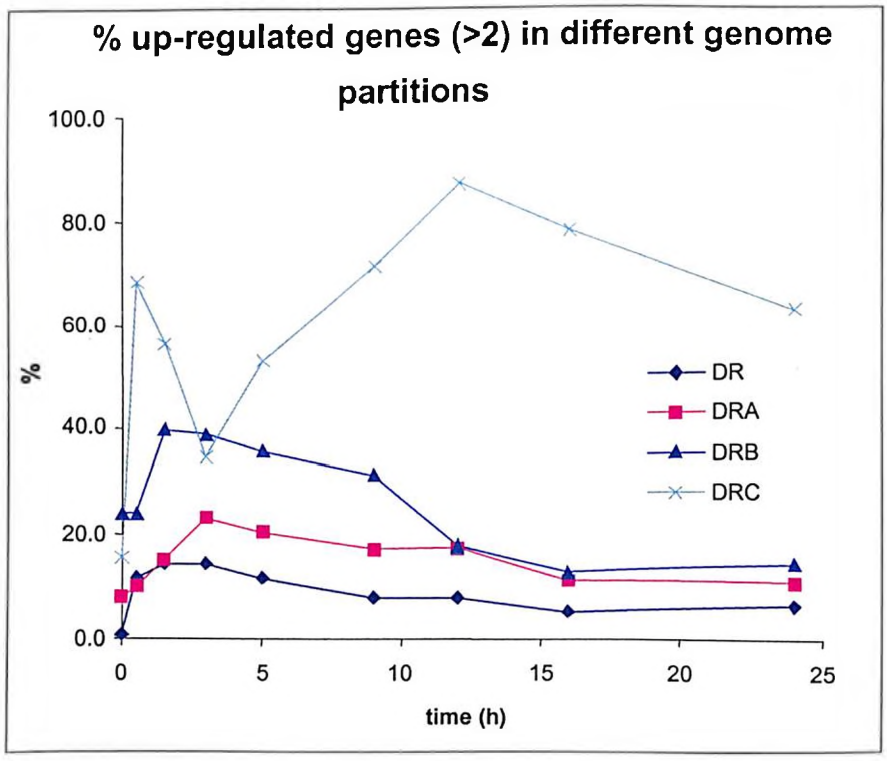

Figure 5.3. Activation and Repression of Different Functional Groups of *D. radiodurans* Genes. Designations of functional groups (from the COG database): J - Translation, ribosomal structure and biogenesis; K –Transcription; L - DNA replication, recombination and repair; D - Cell division and chromosome partitioning; O - Posttranslational modification, protein turnover, chaperones; M - Cell envelope biogenesis, outer membrane; N - Cell motility and secretion; P - Inorganic ion transport and metabolism; T - Signal transduction mechanisms; C - Energy production and conversion; G - Carbohydrate transport and metabolism; E - Amino acid transport and metabolism; F - Nucleotide transport and metabolism; H - Coenzyme metabolism; I - Lipid metabolism; Q - Secondary metabolites biosynthesis, transport and catabolism; R - General function prediction only; S - Function unknown. STRESS – genes involved in stress response, based on previous analyses of the *D. radiodurans* genome (Makarova *et al.*, 2001).

Figure 5.3A

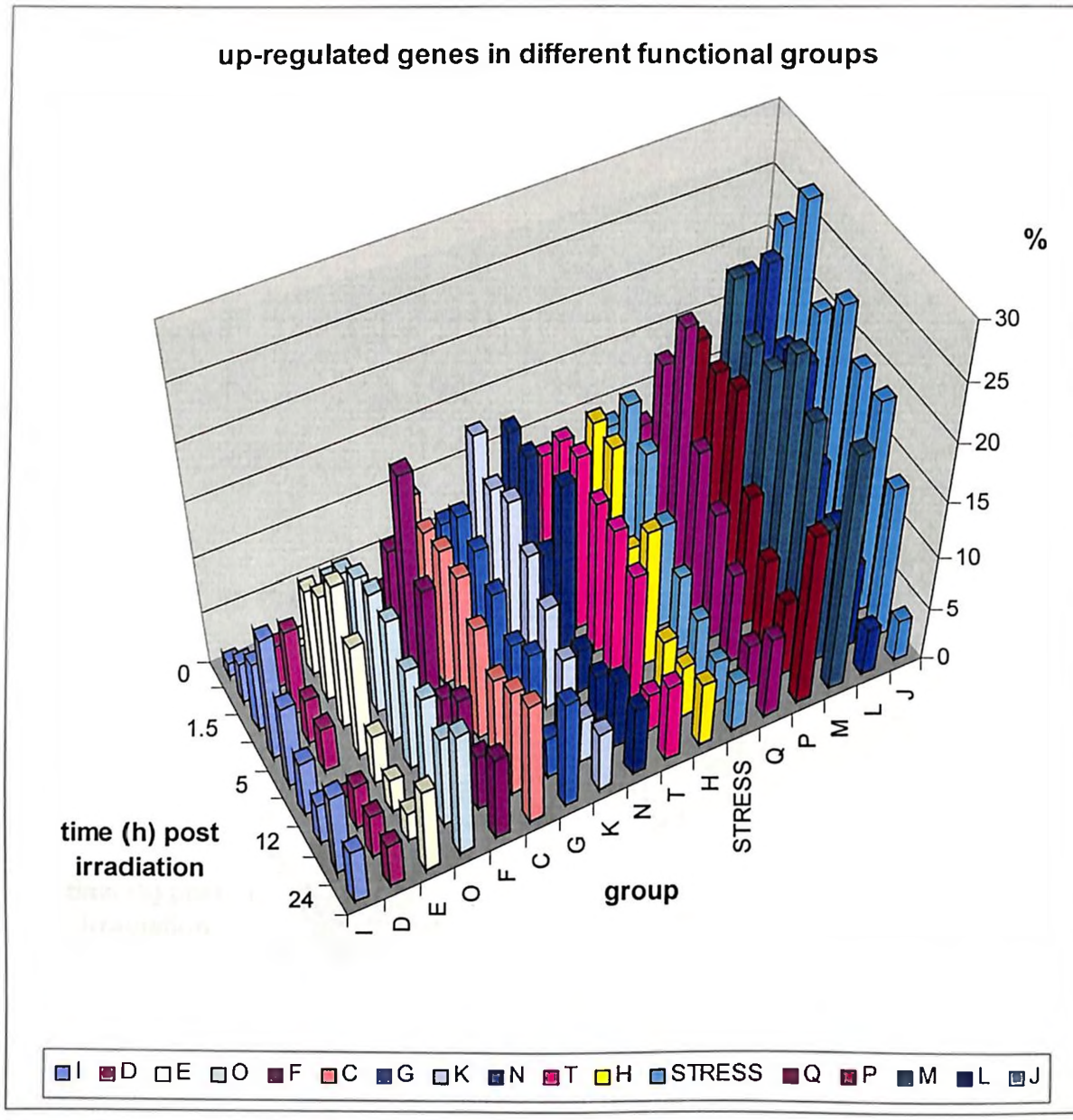
up-regulated genes in different functional groups
%
30
25
20
15
10
5
0
time (h) post irradiation
0
1.5
5
12
24
group
I
D
E
O
F
C
G
K
N
T
H
STRESS
Q
P
M
L
J

Figure 5.3B

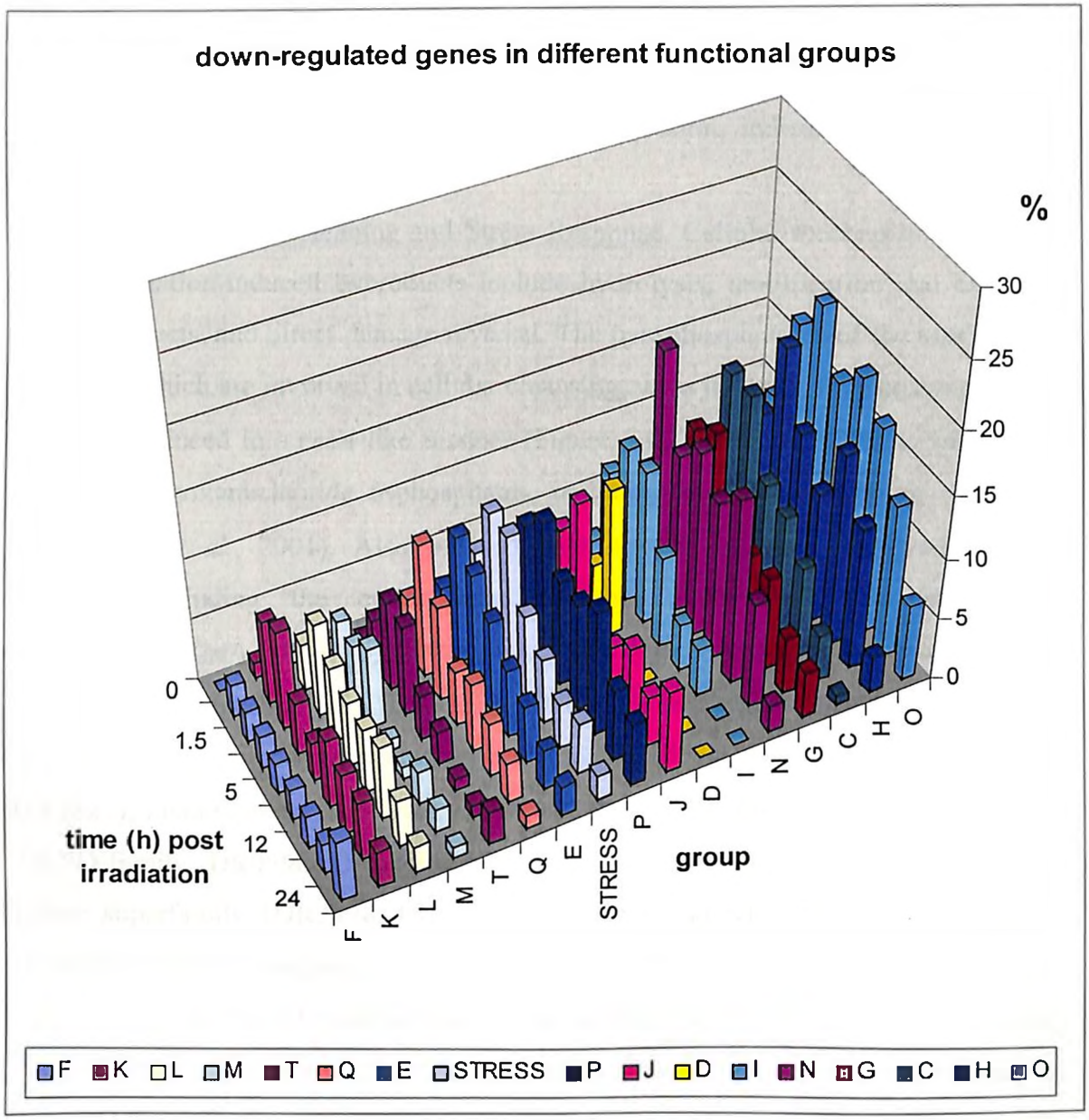
down-regulated genes in different functional groups
%
30
25
20
15
10
5
0
0
1.5
5
12
24
time (h) post irradiation
F
K
L
M
T
Q
E
STRESS
P
J
D
I
N
G
C
H
O
group
F K L M T Q E STRESS P J D I N G C H O

5.3.2.4 Coordinated Expression of DNA Repair Pathways, Metabolic Pathways and the Overall Stress Response of *D. radiodurans*

The recovery of *D. radiodurans* from an acute dose of radiation appears to be a complex process involving the coordination between numerous pathways. Immediately following exposure to acute radiation, as a general trend, induction/repression of most of the genes related to the cell's recovery was observed within the early- (0-3 hours) and mid- phases (3–9 hours). Most genes related to growth and cell division were either down-regulated or showed no changes in their expression, indicating a growth arrest (Figure 5.4).

Induction of Cell Cleaning and Stress Response. Cellular mechanisms known to deal with radiation-induced byproducts include hydrolysis, modification and export of damaged products, and direct damage reversal. The pyrophosphatases of the MutT/Nudix superfamily, which are involved in cellular cleansing, were induced. Five enzymes of this family were induced in a *recA*-like manner (Figure 5.4, Table 5.4). Others, with higher specificity to deoxynucleotide triphosphates, including the MutT ortholog, were also activated (Xu *et al.*, 2001). Also induced were several enzymes involved in DNA degradation including the extracellular nuclease (DRB0067) and intracellular exonuclease VII XseA (DR0186) (Table 5.3). Induction of proteases was also observed, including aminopeptidase P (DR0478), extracellular serine protease (DR0812, DRB0069), periplasmic carboxy-terminal protease (DR1491), alkaline serine exoprotease A (DR2322), metalloproteinase (DRA0249), and two membrane-associated proteases of the NLPD-family (DR0598, DR1549). Certain genes belonging to be a part of the α/β hydrolase superfamily {DR2478, DR2522, DRA0150, and DRB0097}, which degrade the damaged cell wall components, were induced (Table 5.5). Some export systems also appear to be activated in *D. radiodurans*. For example, protein-export membrane protein SecG (DR1825), MDR-type exporter (DR2098), ExbD/TolR biopolymer transport membrane protein (DR0457), as well as several transporters of a major facilitator family with undefined activities (DR0395, DR1307, DR2098, DRB0043, DRC0040), are all up-regulated (Table 5.5).

Figure 5.4. Hierarchical Clustering Analyses of Expression Profile Patterns. Gene expression patterns are displayed graphically. Three distinct patterns are sorted according to the hierarchical clustering analyses, *i.e.* (A) *recA*-like activation pattern, (B) growth-related activation pattern, and (C) repressed patterns. The top row represents the general pattern of the selected group where a Pearson correlation coefficient (r) is shown on the left side. All displayed graphs are organized in a row/column format. Each row of colored strips represents a single gene whose expression levels are color-recorded sequentially in every column of the same row that represents recovery time intervals. Red color denotes up-regulation, whereas green indicates down-regulation. Black indicates the control level. The variation in transcript abundance is positively correlated with the color darkness. **a**, Gene numbers are offered for tracking the primary information of the gene of interest. **b**, The maximum (for *recA*-like and growth-related activation pattern) or minimum (for the repressed pattern) expression level for each of the exhibited genes over the 24-h recovery period is presented as the dye intensity ratio of the irradiated sample to the non-irradiated control at **c**, the indicated time interval. Values in parentheses show the standard deviation for each mean expression ratio.

Figure 5.4

Gene#	Putative function[a]	Ratio (fold)[b]	Time (hr)[c]
A. *recA*-like activation pattern			
DR0911	DNA-directed rna polymerase beta subunit, *rpoC*	1.99 (±1.37)	0.5
DR2220	Tellurium resistance protein TerB	3.13 (±1.49)	5
DR2221	Tellurium resistance protein TerE	5.24 (±2.94)	3
DRB0069	Subtilisin serine protease	3.18 (±1.39)	3
DRB0067	Extracellular nuclease with Fibronectin III domains	4.37 (±1.21)	3
DR0261	8-oxo-dGTPase, *mutT*	3.36 (±1.68)	0.5
DRA0344	LEXA repressor, HTH+protease, *lexA*	1.80 (±1.08)	1.5
DR0099	SsDNA-binding protein, *ssb*	3.01 (±1.20)	0.5
DR2129	Ribosomal component L17 , *rplQ*	5.92 (±2.09)	1.5
DR2128	RNA polymerase alpha subunit, *rpoA*	4.03 (±2.80)	1.5
DR0324	Probable glutamate formiminotransferase	3.30 (±1.47)	0.5
DR2337	Uncharacterized protein	7.41 (±5.71)	1.5
DRA0346	PprA protein, involved in DNA damage resistance	3.52 (±1.94)	0.5
DR1825	Protein-export membrane protein	3.21 (±1.48)	1.5
DR1771	UVRA ABC family ATPase, *uvrA-1*	3.52 (±1.15)	1.5
DRA0345	Predicted esterase	10.05 (±4.39)	1.5
DR0422	Trans-aconitate methylase	18.85 (±7.46)	1.5
DR1143	Uncharacterized protein	8.85 (±4.26)	1.5
DR0003	Uncharacterized protein	14.03 (±5.53)	1.5
DR1776	Nudix family pyrophosphatase	4.70 (±2.83)	1.5
DR2340	RecA, *recA*	7.98 (±3.86)	1.5
DR2610	Periplasmic binding protein, *fliY*	4.13 (±1.67)	0.5
DR1645	Teichoic acid biosynthesis protein, *wecG*	5.88 (±2.79)	1.5
DR0696	V-type ATPase synthase, subunit K	7.19 (±2.16)	1.5
DR0421	Uncharacterized protein	4.94 (±2.30)	1.5
DR1775	Superfamily I helicase, *uvrD*	3.30 (±1.69)	1.5
DR1561	UDP-N-acetylglucosamine 2-epimerase, *wecB*	6.00 (±1.40)	1.5
DR2285	MutY, A/G-specific adenine glycosylase, *mutY*	2.36 (±0.40)	3
DR2356	Nudix family hydrolase	3.35 (±0.45)	3
DR2275	Excinuclease ABC subunit B, *uvrB*	4.93 (±1.81)	3
DR0206	Uncharacterized protein	5.45 (±2.65)	3
DR0204	Uncharacterized membrane protein	6.01 (±1.35)	3
DR1354	Excinuclease ABC subunit C, *uvrC*	3.78 (±0.42)	3
DR0203	Uncharacterized membrane protein	3.82 (±0.86)	1.5
DR0205	ABC transporter ATPase	4.10 (±2.45)	3
DR1357	ABC transporter, permease subunit	6.79 (±2.56)	1.5
DR2482	Predicted transcription regulator	5.75 (±2.92)	1.5
DR2483	McrA nuclease	5.43 (±1.22)	1.5
DRA0008	Conserved membrane protein	6.60 (±2.00)	3
DRA0234	Uncharacterized protein,	12.76 (±5.27)	1.5
DR1359	ABC transporter, periplasmic subunit	24.83 (±11.13)	1.5
DR2127	Ribosomal protein S4, *rpsD*	5.40 (±1.50)	3
DR1356	ABC transporter, ATP-binding protein	9.85 (±5.98)	3
DRB0136	Putative DEAH ATP-dependent helicase, *hepA*	5.22 (±0.46)	3
DR1548	Bacillus ykwD ortholog, PRP1 superfamily protein	5.62 (±2.35)	3
DR0207	ComEA related protein, secreted	15.47 (±8.31)	3
DRA0249	Metalloproteinase, leishmanolysin-like	6.47 (±4.43)	3
DR0665	Uncharacterized protein	11.66 (±5.74)	3
DR0596	Resolvasome RuvABC, subunit B, *ruvB*	3.22 (±1.31)	0.5
DR0912	DNA-directed rna polymerase beta subunit, *rpoB*	3.19 (±0.80)	0.5
B. Growth-related activation pattern			
DR1172	Lea76/LEa29-like desiccation resistance protein	2.66 (±0.60)	24
DR0461	Bacillus yacB ortholog	2.58 (±0.81)	24
DR1595	6-phosphogluconate dehydrogenase, *gnd*	2.30 (±0.52)	24
DRA0043	TDP-rhamnose synthetase	5.08 (±2.12)	12
DRA0042	Glucose-1-phosphate thymidylyltransferase, *rfbA*	3.70 (±1.19)	12
DRA0031	Glucose-1-phosphate thymidylyltransferase	2.48 (±1.64)	12
DRA0065	Chromosomal protein HU HupA, *hupA*	7.71 (±2.07)	24
DR2263	Bacterioferritin, Iron chelating protein	6.41 (±1.97)	16
DRA0275	Soluble cytochrome C	4.80 (±1.22)	24
DR1279	Superoxide dismutase (Mn)	3.91 (±1.43)	24
C. Repressed pattern			
DR1126	RecJ like DHH superfamily Phosphohydrolase	0.33 (±0.12)	12
DR1337	Transaldolase, *tal*	0.25 (±0.05)	3
DR0728	Fructokinase, *cscK*	0.37 (±0.13)	3
DR0977	Phosphoenolpyruvate carboxykinase, *pckA*	0.48 (±0.22)	1.5
DR1742	Glucose-6-phosphate isomerase, *pgi*	0.42 (±0.12)	1.5
DR1998	Catalase, CATX, *katA*	0.23 (±0.07)	3
DR1146	GSP26 general stress like protein	0.25 (±0.06)	1.5
DR0493	Formamidopyrimidine-DNA glycosidase, *mutM*	0.46 (±0.09)	1.5
DR0674	Argininosuccinate synthase, ASSY, *argG*	0.35 (±0.15)	3
DR2620	Cytochrome oxidase subunit I, COX1, *caaA*	0.45 (±0.25)	5

Induction of DNA Repair and Associated Systems. The cellular cleansing is accompanied by simultaneous activation of the major repair systems. Recovery from extreme conditions requires an increase in *de novo* biosynthesis of macromolecules, particularly proteins required for DNA repair; if protein biosynthesis is inhibited, irradiated cells die (Hansen, 1982). *De novo* transcription, therefore, must be a critical early component of the recovery process. Consistent with this requirement, genes coding for DNA-directed RNA polymerase subunits were substantially up-regulated during the early-mid- phases of repair. Approximately 35% of *D. radiodurans* genes implicated in DNA repair, recombination, and replication showed patterns of expression similar to that of *recA*; the products of these genes likely comprise the core of the DNA damage response regulon of *D. radiodurans* (Table 5.4). Only a few of these damage response genes stayed induced throughout all three phases of recovery. Like *recA*, some of the genes had a peak at 1.5-5 hours [*e.g.*, single-stranded DNA-binding protein, uracil DNA glycosylase, and 8-oxo-dGTPase (MutT); Table 5.3]. Among genes with a *recA*-like expression pattern, several are known to be activated by the SOS response of *E. coli* and *Bacillus subtilis*, including *recA*, *ssb*, *uvr*ABCD, and *ruv*B (Figure 5.4). Interestingly, unlike SOS response in other bacteria, both DNA gyrase subunits (DR0906 and DR1943) were induced with the *recA*-like expression pattern, suggesting that regulation of DNA supercoiling is important for DNA repair. Furthermore, in agreement with recent reports (Narumi *et al.*, 2001), the expression data show that none of the two paralogous *lexA* genes of *D. radiodurans* (Makarova *et al.*, 2001) responds to irradiation. Only a few of the pathways that are involved in direct damage reversal and base excision repair responded to irradiation. Specifically, we observed induction of the MutT ortholog (8-oxo-dGTPase), MutY (A-G mismatch DNA glycosylase) and uracil DNA glycosylase, but not many others (Table 5.3).

Specific Response of Metabolic Gene Systems. Among energy metabolism pathways, the V-type ATP synthase (DR0694-DR0702) genes were induced, which was expected given the increased demand for energy during recovery. Genes involved in cell wall biogenesis were also strongly induction, which was also expected given the need to restore membrane and associated ATP generation (Fig. 5.4 and Figure 5.3A). Genes encoding the TCA cycle were repressed in the early and mid phases, whereas genes

encoding the glyoxylate shunt were activated in this interval (Fig. 3A). In the late phase of recovery, glycolysis and the TCA cycle were progressively induced. It seems likely that the co-induction of genes for antioxidant proteins, in particular, superoxide dismutases (DR1546, DR1279) and catalase (DR1998), contributes to the removal of the toxic free radicals. Specific induction of nitrogen metabolism genes, including the nitrogen regulatory protein P-II (GlnB homolog, DR0692) (Table 5.5) and genes involved in the utilization of exogenous and intracellular carbohydrates, was detected before 9 hours had elapsed (Table 5.5). The operon coding for enzymes of sulfur metabolism, *i.e.*, sulfite reductase, APS kinase, PAPS reductase and sulfate adenylyltransferase (DRA0013-DRA0016), remained induced throughout recovery, with the peak of expression occurring at 3-5 hours (Table 5.4).

Genes encoding two ribonucleoside/ribonucleotide reductases (DRB0107-DRB0109, DR2374), the enzymes responsible for the final step of deoxyribonucleotide biosynthesis from ribonucleotide precursors, were induced in the early phase. The one encoded by DRB0107-BRB0109 remained extremely active throughout recovery, whereas DR2374 was repressed at the end of mid-phase. One of the genes that is strongly induced in the early-phase of post-irradiation recovery is the predicted trans-aconitate methylase (Cai and Clarke 1999), DR0422 (Table. 5.4). Trans-aconitate is not a normal metabolite in most bacteria and is an inhibitor of aconitase, a key enzyme of the TCA cycle (Lauble *et al.*, 1994). It seems likely that trans-aconitate is produced as a result of irradiation and the induction of DR0422 is required for its detoxification, setting the stage for activation of the TCA cycle at the late phase of recovery.

Figure 5.5

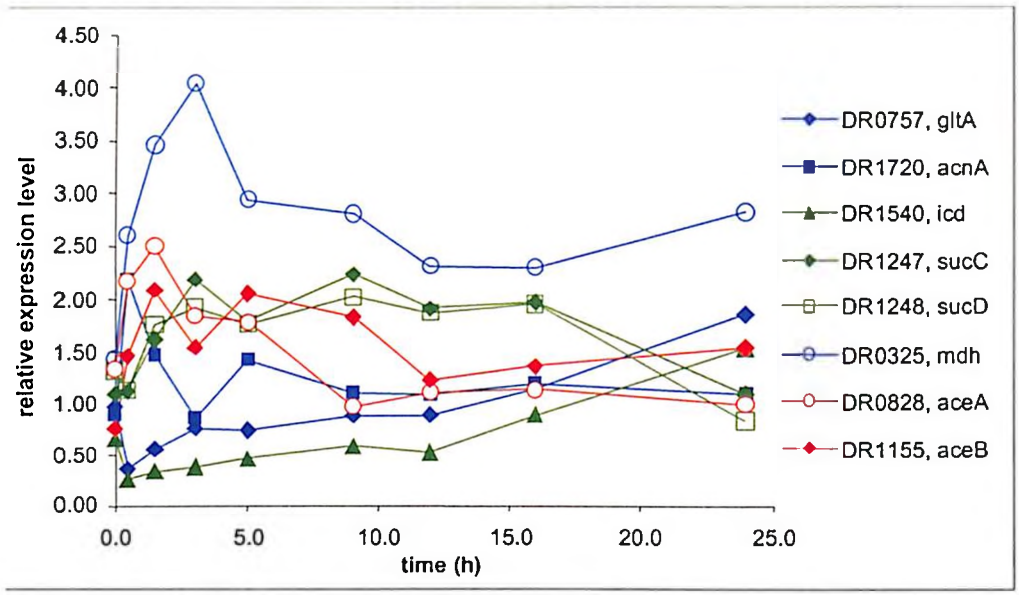

Figure 5.5. Expression Patterns of Selected Genes for TCA cycle and Glyoxylate Bypass Enzymes.

Eight representative genes are shown in this figure.

Expression patterns for the following genes are shown: *gltA*, citrate synthase II; *acnA*, aconitase; *icd*, isocitrate dehydrogenase; *sucC*, succinyl-CoA synthetase, beta chain; *sucD*, succinyl CoA synthetase, alpha chain; *mdh*, malate dehydrogenase; *aceA*, isocitrate lyase; *aceB*, malate synthase. Genes specific to the TCA cycle are shown in Green, Glyoxylate bypass genes in Red, and genes shared by both TCA cycle and Glyoxylate bypass, in Blue.

Genes not represented here include: Three subunits of 2-oxoglutarate dehydrogenese complex - *lpd*, lipoamide dehydrogenase (DR2526), *sucA*, 2-oxoglutarate dehydrogenase (DR0287), and *sucB*, dihydrolipoamide succinyltransferase (DR0083) are substantially down regulated like icd (DR1540). Malate synthase (DRA0277) of the Glyoxylate bypass is slightly down regulated. Four subunits of fumarate dehydrogenase complex - *sdhB*, fumarate/succinate dehydrogenase type iron sulfur protein (DR0951), *sdhA*, succinate dehydrogenase Rossman fold oxidoreductase (DR0952), *shhC* and *sdhD*, small succinate dehydrogenase associated proteins (DR0953, DR0954), and *fumC*, fumarase (DR2627) do not show significant changes in their expression levels during post irradiation recovery.

5.4 Discussion

Understanding biological systems and the roles of their constituents is facilitated by the ability to make quantitative, sensitive, and comprehensive measurements of how their proteome changes, *e.g.*, in response to environmental perturbations. To this end, some work of this thesis was dedicated to supporting high-throughput proteomic investigations for *D. radiodurans* (Lipton *et al.*, 2002). Specifically, peptides identified in *D. radiodurans* growing in rich and defined minimal medium (DMM) (Chapter 3, Table 3.1), and recovering from irradiation (Lipton *et al.*, 2002) contributed to the development of an accurate mass tag database for the organism (Lipton *et al.*, 2002). The high throughput proteomics approach was used to identify with high confidence >61% of the predicted proteome for *D. radiodurans*, which represents the broadest proteome coverage for any organism to date. The collaborative proteomics work (Lipton *et al.*, 2002) validated a majority of the predicted *D. radiodurans* ORFs (Makarova *et al.*, 2001) and justified the construction of a whole genome microarray for *D. radiodurans*.

Whole genome microarray work reported in this chapter examined the changes in genomic expression in *D. radiodurans* recovering from an acute exposure to 15 kGy, which is about its D_{37} (37% survival) under standard laboratory conditions (Daly *et al.*, 1994a, 1994b, Daly and Minton, 1995a, 1996). During the early- and mid-phases of recovery, no cell growth was observed, but within this interval many genes of diverse functional groups were induced (Table 5.3). In contrast, many genes for enzymes of general metabolism were not affected in this interval (Table 5.5, Figure 5.4), but were induced in the late-phase. Collectively, this supports the idea that most of the expression dynamics observed in the 9-hour lag-phase are a consequence of the effects of irradiation and not due to changes in nutrient or growth conditions resulting from transfer of irradiated *D. radiodurans* to fresh medium. Given the apparent complexity of *D. radiodurans*' irradiation response and the good correlation observed between its predicted and experimentally determined patterns of gene expression, the use of microarrays to identify *D. radiodurans* genes responsible for its radiation resistance holds promise as a useful approach.

Generally, the microarray expression data support the hypothesis that irradiated *D. radiodurans* suppresses oxidative stress levels, which could prevent additional loss of genome integrity elicited by metabolism-induced free radicals. *D. radiodurans* strongly represses the $O_2^{\bullet-}$ radical-generating steps of its TCA cycle (*e.g.*, *sdhB*) (Figure 5.5), and appears to minimize its biosynthetic and energy demands by inducing transporters of exogenous peptides and other secondary metabolites on which radiation resistance is highly dependent (Chapter 3), and correspondingly shows increased expression of extra- and intracellular proteases and nucleases (Table 5.3). In the mid-phase (3-9 hours), expression of most early-phase genes gradually subsided, followed by the induction, at ~12 hours, of genes known to support exponential cell division (Table 5.5). During the late-phase (12-24 hours), the TCA cycle was progressively de-repressed and genes involved in scavenging free radicals (*e.g.*, *sodA*, and *katA*) were correspondingly induced (Figure 5.4). This helps to explain the observation that *de novo* biosynthesis of amino acids, nucleotides, and coenzymes remains unchanged or even down-regulated, at least within the early and mid-phases. In contrast, the glyoxylate bypass appears to be strongly induced and could provide some biosynthetic intermediates needed for recovery without generating free radicals. Significantly, the response of the glyoxylate cycle following irradiation is similar to its response during growth in DMM (Chapter 4).

Genomic informatic (Makarova *et al.*, 2001) and proteomic analyses (Lipton *et al.*, 2002) (Table 5.1) for *D. radiodurans* supports that it has a functional TCA cycle. Remarkably unlike *E. coli* (Tao *et al.*, 1999), however, *D. radiodurans* represses TCA cycle activity in DMM where its biosynthetic and energy needs are increased (Figure 5.5) (Chapter 4, Section 4.3.4). This unusual TCA cycle response suggests that its normal mode of action may not be cyclic or highly dedicated to energy production. Evidence supporting the possible dominance of the glyoxylate bypass over the TCA cycle in *D. radiodurans* includes the observed increase in isocitrate lyase (*aceA*) in DMM (Figure 5.5) (Table 5.1) (Chapter 4, Section 4.3.4), and ability to utilize acetate as a sole carbon source, but not α-ketoglutarate, succinate, fumarate or malate (similar substrate utilization was observed for the other *Deinococci*) (Chapter 4, Table 4.1A). While the ability to generate ATP from a glyoxylate bypass is far less than a fully operational TCA cycle, it likely meets deinococcal energy and biosynthetic needs. Importantly, the

possible dominance of the glyoxylate bypass over the TCA cycle in DMM (Figure 5.5) would avoid high levels of free radicals generated by fumarate reductase (Imlay, 1995), and this may similarly apply during recovery from irradiation.

Further microarray evidence that metabolic systems are involved in recovery from irradiation includes the activation of nitrogen metabolism genes. For example, the nitrogen regulatory protein P-II (GlnB-like, DR0692) is activated. Generally, P-II senses nitrogen and is a key signal transduction regulator of glutamine/glutamate synthesis (Arcondeguy *et al.*, 2001). Glutamine/glutamate synthesis is a prerequisite for production of a wide variety of amino acids, where glutamine acts as a donor of NH_2 groups via transamination. Thus, P-II might help maintain high level of protein synthesis in *D. radiodurans* in the presence of ammonia (Arcondeguy *et al.*, 2001), (Reitzer and Magasanik, 1987). These findings underscore the importance of defining the global cellular processes within which protection and repair systems operate efficiently.

5.5 Conclusions

1. **The AMT based proteomic measurements provided a physical validation of >61% of predicted ORFs (Lipton *et al.*, 2002). Proteome expression analyses presented here support that the TCA cycle of *D. radiodurans* in DMM is suppressed compared to rich medium, but that its glyoxylate bypass is upregulated. The TCA cycle response in DMM is similar to that observed following irradiation using the whole genome microarray. Since intracellular free radical levels are increased in DMM and during radiation, the suppression of TCA cycle activity might be a cellular mechanism to minimize genomic damage under both conditions.**

2. **DNA microarrays covering ~94% of *D. radiodurans*' predicted genes were used to analyze the dynamic changes in global expression profiles of *D. radiodurans* recovering from acute irradiation (15 kGy). The expression data suggest that *D. radiodurans* efficiently coordinates its recovery by a complex**

network, within which both DNA repair and metabolic functions play a critical role.

3. Microarray expression patterns of seven randomly selected genes that were up-regulated immediately upon exposure to irradiation were independently evaluated by RT-PCR. Except for a single gene (DR0007), the expression patterns of the other genes were similar to those detected by microarray hybridization. These observations support that the expression array data presented in this study are of high quality.

4. The experimental data presented in this chapter reveals the hallmark features of recovery of *D. radiodurans* from acute high-dose irradiation. Across the genome, differences in the expression of functionally grouped genes that parallel the physiology of the early-, mid- and late-phases of post-irradiation recovery were observed. The metabolic repression pattern observed during the early-phase is consistent with the hypothesis that irradiated *D. radiodurans* cells suppress oxidative stress levels to prevent additional loss of genome integrity elicited by metabolism-induced free radicals.

Table 5.3 Radiation response patterns of genes involved in replication, repair and recombination functions in *D. radiodurans*

Gene Name[a]	Gene_ID	Protein description and comments	Pathway[b]	Relative basal level[c]	Response to radiation (folds)[d]	Time of response (hr)	STD	CV (%)
Ogt/Ybaz	DR0248	O-6-methylguanine DNA methyltransferase	DR	0.71	0.50	3	0.32	63.99
MutT	DR0261	8-oxo-dGTPase	DR	0.33	3.85	12	1.68	43.58
AlkA	DR2074 DR2584	3-methyladenine DNA glycosylase II	DR, BER	0.48 0.51	0.70 0.93	0.5-9 0.5-9		
MutY	DR2285	8-oxoguanine DNA glycosylase and AP-lyase, A-G mismatch DNA glycosylase	BER, MMY	0.19	2.36	3	0.40	16.83
Nth-2 Nth-1	DR2438 DR0289 DR0928	Endonuclease III and thymine glycol DNA glycosylase	BER	1.11 0.49 0.47	0.36 1.09 0.89	3 0.5-9 0.5-9	0.12	32.19
YhhF	DR0643	N6-adenine-specific methylase	BER	0.70	0.39	3	0.05	11.70
MutM/Fpg	DR0493	Formamidopyrimidine and 8-oxoguanine DNA glycosylase	BER	0.68	0.46	1.5	0.09	18.71
Nfi (Yjaf)	DR2162	Endonuclease V	BER	0.31	1.36	0.5-9		
PolA	DR1707	DNA polymerase I	BER	5.81	0.86	0.5-9		
Ung	DR0689 DR1663	Uracil DNA glycosylase	BER	0.68 2.71	2.03 2.52	12 24	1.41 0.76	69.35 30.20
Mug	DR0715	G/T mismatch-specific thymine DNA glycosylase	BER	0.85	0.17	3	0.01	7.80
	DR1751 DR0022	Uracil DNA glycosylase	BER	0.86 0.47	0.64 3.33	0.5-9 1.5	0.87	26.18
XthA	DR0354	Exodeoxyribonuclease III	BER	0.64	0.95	0.5-9		
RadA	DR1105	Predicted ATP-dependent protease	NER, BER	0.40	1.08	0.5-9		
Mfd	DR1532	Transcription-repair coupling factor; helicase	NER	1.25	0.69	0.5-9		
UvrA-1 UvrA-2	DR1771 DRA0188	ATPase, excinuclease subunit	NER	1.44 0.13	3.52 2.03	1.5 5	1.15 0.90	32.56 44.42
UvrB	DR2275	Helicase, excinuclease subunit	NER	0.80	4.93	3	1.81	36.76
UvrC	DR1354	Nuclease, excinuclease subunit	NER	1.02	3.78	3	0.42	11.04
UvrD	DR1775	Helicase II, excinuclease	NER,	1.19	3.30	1.5	1.69	51.25

		subunit; initiates unwinding from a nick	mMM, SOS					
MutL	DR1669	ATPase	mMM, VSP	0.42	0.99	0.5-9		
MutS	DR1976	ATPase	mMM, VSP	0.35	1.31	0.5-9		
XseA/ Nec7	DR0186	Exonuclease VII, large subunit	MM	1.07	2.19	1.5	0.83	37.89
SbcC	DR1922	ATPase, SbcCD exonuclease subunit	RER	1.36	1.39	0.5-9		
SbcD	DR1921	Exonuclease, SbcCD subunit	RER	0.55	1.82	3	0.27	15.06
RecA	DR2340	Recombinase; ssDNA-dependent ATPase; activator of LexA autoproteolysis	RER, SOS	1.46	7.98	1.5	3.86	48.40
RecD	DR1902	DNA-dependent ATPase or helicase; in other bacteria, regulatory subunit of the RecBCD recombinase (helicase-nuclease); RecB and RecC are missing in *D. radiodurans*.	RER	1.16	0.80	0.5-9		
RecF	DR1089	ATPase; required for daughter-strand gap repair	RER	0.10	0.59	1.5	0.32	54.76
RecG	DR1916	Holliday junction-specific DNA helicase; branch migration inducer	RER	1.03	2.66	0.5	0.87	32.62
RecJ	DR1126	Nuclease	RER	1.94	0.33	12	0.12	37.43
RecN	DR1477	ATPase	RER	1.28	0.93	0.5-9		
RecO	DR0819	Biochemical activity unknown; required for daughter-strand gap repair	RER	1.34	1.10	0.5-9		
RecQ	DR2444 DR1289	Helicase; suppressor of illegitimate recombination	RER	1.85 0.34	2.43 1.19	0.5 0.5-9	0.27	11.18
RecR	DR0198	Inactivated Toprim-domain protein; required for daughter-strand gap repair	RER	1.71	0.90	0.5-9		
RuvA	DR1274	Holliday-junction-binding subunit of the RuvABC resolvasome	RER	0.89	0.95	0.5-9		
RuvB	DR0596	Helicase subunit of the RuvABC resolvasome	RER	2.58	3.22	0.5	1.31	40.82

RuvB	DR0440	Endonuclease subunit of the RuvABC resolvasome	RER	3.99	0.20	24	0.09	45.47
DnaC	DR0507	Polymerase subunit of the DNA polymerase III holoenzyme	MP	0.81	0.43	12	0.15	35.32
DnaQ	DR0856	3'-5' exonuclease subunit of the DNA polymerase III holoenzyme	MP	0.31	1.97	0.5	1.04	52.62
DnlJ	DR2069	NAD-dependnet DNA ligase	MP	1.58	0.17	3	0.05	28.26
Ssb	DR0099	Single-strand binding protein; D. radiodurans R1 has three incomplete ORFs corresponding to different fragments of Ssb; it remains unclear whether D. radiodurans has a functional Ssb.	MP	3.92	3.01	0.5	1.20	39.80
LexA	DRA0344 DRA0074	Transcriptional regulator, repressor of the SOS regulon, autoprotease	SOS	0.51 4.74	1.80 0.80	1.5 0.5-9	1.08	59.92
YcjD	DR0221 DR2566	Predicted very short patch repair nuclease	VSP?	0.37 0.42	1.94 4.10	3 3	0.81 1.09	41.73 26.48
HAM1/ YggV	DR0179	Xantosine triphosphate pyrophosphatase, prevents 6-N-hydroxylaminopurin mutagenesis	DR	0.35	1.00	0.5-9		
Uve1/BS_Ywjd	DR1819	UV-endonuclease	NER	0.29	1.06	0.5-9		
Yejh/Rad25	DRA0131	Helicase of superfamily II, predicted nuclease; DRA0131 has an additional McrA nuclease domain	NER	0.07	0.51	3	0.32	62.57
	DR0690	Topoisomerase IB, probably of eukaryotic origin	?	0.41	1.10	0.5-9		
	DR1721	3'->5' nuclease	?	0.54	1.36	0.5-9		
Rsr	DR1262	RNA-binding protein Ro; ribonucleoproteins complexed with several small RNA molecules. Involved in UV-resistance	?	0.68	1.04	0.5-9		

		in Deinococcus						
Mrr Mrr-1 Mrr-2	DR1877 DR0508 DR0587	Nuclease	?	0.44 0.59 0.78	0.79 0.78 0.95	0.5-9 0.5-9 0.5-9		
XerC XerD XerC/D	DRA0155 DRB0104 DRC0018	Integrase/recombinase	RER	0.26 0.94 0.10	0.95 0.53 2.72	0.5-9 3 12	 0.11 0.77	 20.56 28.19
GyrA	DR1913	DNA gyrase, subunitA	general	4.12	3.29	0.5	1.56	47.51
GyrB	DR0906	DNA gyrase, subunitB	general	2.75	4.41	0.5	2.98	67.46
DnaE	DR0601	DNA primase	general	1.36	0.59	3	0.04	7.40
TopA	DR1374	DNA topoisomerase	general	2.58	0.45	9	0.10	23.03
DnaN	DR0001	DNA polymerase III, beta subunit	general	2.28	2.71	0.5	0.45	16.69
	DR2332	DNA polymerase III gamma and tau subunit, inactivated AAA superfamily ATPase	general	0.05	2.73	12	1.74	63.70
	DR2410	DNA polymerase III, gamma and tau subunit, AAA superfamily ATPase	general	4.15	0.29	9	0.14	47.65

Footnotes for Table 5.3

[a] The gene names are from *E. coli*, whenever an *E. coli* ortholog exists, or from *B. subtilis* (with the prefix BS_).

[b] Abbreviations of DNA repair pathways: DR- direct damage reversal; BER – base excision repair; NER- nucleotide excision repair; mMM – methylation-dependent mismatch repair; MMY – MutY - dependent mismatch repair; VSP – very short patch mismatch repair; RER – recombinational repair, SOS – SOS repair; MP – multiple pathways; potential new repair pathways are indicated by a question mark, general – genes that are also involved in replication, ? – unknown

[c] The ratio of the fluorescent intensity of a particular gene to the average intensity of all arrayed genes when non-irradiated sample is used as a labeled probe.

[d] The maximum, or minimum, or average ratio of the irradiated sample(s) harvested at the 'Time of response' to the non-irradiated control. There is no standard deviation (STD) and coefficient of variation (CV) for an average ratio of several time points.

Color coding: red – up regulated, blue – down regulated, brown – no changes.

Table 5.4 Selected genes and operons of *D. radiodurans* with a *recA*-like expression pattern

Gene_ID[a]	Function group[b]	Protein description and comments	Relative basal level	Maximum induction level (fold)	STD	CV	Maximum induction time (hr)
DR0003	-	Uncharacterized protein	1.32	14.03	5.53	39.39	1.5
DR0046	-	Leucine-rich repeat protein	0.18	2.14	0.35	16.21	3
DR0047	-	Uncharacterized protein	0.11	2.48	1.40	56.42	3
DR0048	S	Uncharacterized membrane protein, YcaP ortholog	0.33	3.90	0.55	14.01	3
DR0050	L	DinB/YfiT family protein	0.53	3.84	0.93	24.23	3
DR0051	S	Small cysteine-rich protein of the HesB family	0.70	5.93	3.32	55.97	3
DR0052	-	Uncharacterized conserved protein	0.34	6.50	2.15	33.14	1.5
DR0053	L	DinB/YfiT family protein	0.44	10.25	2.36	23.00	3
DR0070	ST?	Uncharacterized protein	0.08	3.89	1.72	44.18	9
DR0103	R	Predicted metal-binding protein	0.57	6.46	4.02	62.22	1.5
DR0140	-	Uncharacterized protein	0.97	6.44	2.87	44.60	1.5
DR0160	-	Conserved membrane protein	0.42	3.90	0.86	22.09	1.5
DR0161	S	AmsJ/WcaK related protein, possibly involved in exopolysaccharide biosynthesis	0.97	8.12	4.07	50.14	1.5
DR0203	R	Uncharacterized membrane protein	0.28	3.82	0.86	22.43	1.5
DR0204	-	Uncharacterized membrane protein	0.51	6.01	1.35	22.52	3
DR0205	Q	ABC transporter ATPase	0.49	4.10	2.45	59.75	3
DR0206	-	Uncharacterized protein	0.19	5.45	2.65	48.56	3
DR0207	L	ComEA related protein, secreted	0.26	15.47	10.31	66.66	3
DR0324	E	Predicted glutamate formiminotransferase	0.31	3.30	1.47	44.50	0.5
DR0363	E	ABC-type dipeptide transporter periplasmic binding protein, DppA	2.79	4.09	1.75	42.74	24
DR0365	E	ABC-type dipeptide transporter, permease ,DppC	2.11	1.48	0.84	56.88	5
DR0394	ST	Predicted kinase antibiotic/homoserine kinase homolog	0.29	7.51	2.76	36.69	1.5
DR0395	G	MDR-type permease	1.09	4.40	2.12	48.16	1.5

DR0396	-	Uncharacterized protein	1.15	5.57	2.39	42.78	1.5
DR0421	-	Uncharacterized protein	0.68	4.94	2.30	46.60	1.5
DR0422	Q	Trans-aconitate methylase	0.68	18.85	7.46	39.59	1.5
DR0477	E	Membrane permease, DhlC homolog	0.56	4.63	1.71	36.85	1.5
DR0478	E	Aminopeptidase P	0.77	2.86	0.55	19.36	0.5
DR0479	M	Penicillin-binding protein 1	0.77	7.07	2.42	34.21	1.5
DR0599	ST	Aminoglycoside N3'-acetyltransferase family	1.31	4.24	1.41	33.31	1.5
DR0609	R	Predicted kinase, adenylate kinase homolog	0.47	2.43	1.14	46.95	3
DR0610	-	Uncharacterized protein	0.25	6.10	4.51	73.93	3
DR0665	-	Uncharacterized protein	0.54	11.66	5.74	49.24	3
DR0694	C	Phage protein homolog	0.60	5.57	2.02	36.28	1.5
DR0812	O	Extracellular alkaline serine protease	0.59	3.32	1.24	37.52	3
DR0841	L	DinB/YfiT family protein	0.48	5.93	1.47	24.84	1.5
DR0842	ST	NimC-like (5-nitroimidazole antibiotics resistance) protein	2.62	1.89	0.69	36.67	24
DR0911	K	DNA-directed RNA polymerase beta' subunit	1.62	1.99	1.37	68.70	0.5
DR0912	K	DNA-directed RNA polymerase beta subunit	0.54	3.19	0.80	24.90	0.5
DR1143	-	Uncharacterized protein	0.49	8.85	4.26	48.13	1.5
DR1144	-	Uncharacterized conserved protein	1.10	2.69	1.31	48.82	1.5
DR1356	R	ABC transporter, ATPase subunit	0.40	9.85	5.98	60.68	3
DR1357	R	ABC transporter, permease subunit	0.31	6.79	2.56	37.67	1.5
DR1358	M	ABC transporter, periplasmic subunit	0.38	22.73	13.73	60.39	1.5
DR1359	M	ABC transporter, periplasmic subunit	0.50	24.83	11.13	44.82	1.5
DR1398	-	Uncharacterized protein	0.24	4.17	1.04	24.83	1.5
DR1548	T	Bacillus ykwD ortholog, Divergent member of the secreted PRP1, plant pathogenesis related protein superfamily	0.48	5.62	2.34	41.32	3
DR1556	-	Membrane-associated sensor histidine kinase	2.27	3.61	1.71	47.23	1.5
DR1557	T	Uncharacterized protein	1.37	5.06	1.57	31.04	1.5

DR1558	-	Receiver domain (flavodoxin, CheY family) of a two component system, contains a C- terminal helix-turn-helix (HTH) DNA-binding domain	1.12	5.64	1.49	26.43	1.5
DR1559	E	Uncharacterized protein	0.87	4.39	1.60	36.47	1.5
DR1639	L	Uncharacterized protein	1.15	4.41	1.84	41.73	1.5
DR1641	L	DinB/YfiT family protein	2.52	1.88	0.78	41.24	5
DR1642	-	DinB/YfiT family protein	0.27	3.71	1.30	35.02	1.5
DR1643	-	Uncharacterized protein	0.61	4.06	2.21	54.45	1.5
DR1644	Q	Uncharacterized protein	0.77	2.45	0.56	22.82	1.5
DR1672	-	SAM-dependent methyltransferase	0.41	1.24	0.73	59.15	12
DR1673	-	Predicted dehydrogenase	1.05	4.53	1.29	28.54	1.5
DR1744	L	Uncharacterized protein	1.47	5.02	1.64	32.69	1.5
DR1776	-	Nudix/MutT family pyrophosphatase	0.84	4.70	2.83	60.18	1.5
DR1850	L	Uncharacterized protein	0.62	4.36	1.13	26.00	1.5
DR1899	-	DinB/YfiT family protein	0.35	1.60	0.65	40.30	1.5
DR1900	-	Uncharacterized protein	0.51	3.14	1.04	33.14	1.5
DR1901	-	Uncharacterized protein	0.51	10.74	4.85	45.17	1.5
DR2097	E	Uncharacterized protein	0.14	6.95	2.08	29.93	1.5
DR2118	E	ABC-type branched amino acid transporter	0.26	3.04	1.38	45.32	5
DR2122	E	Branched amino acid periplasmic binding protein, LivBP	0.20	2.46	0.29	11.94	3
DR2128	ST	RNA polymerase alpha subunit	2.26	4.03	2.80	69.48	1.5
DR2220	ST	Tellurium resistance protein, TerB homolog	0.45	3.13	1.49	47.61	5
DR2221	ST	Tellurium resistance/cAMP-binding family protein	0.59	5.24	2.94	56.05	3
DR2223	ST	Tellurium resistance/cAMP-binding family protein	0.39	3.63	1.36	37.45	3
DR2225	-	Tellurium resistance/cAMP-binding family protein	0.58	2.14	0.41	19.30	3
DR2265	-	Large membrane protein	0.44	5.45	1.46	26.84	3
DR2337	T	Uncharacterized protein	0.11	7.41	5.71	77.05	1.5
DR2415	T	Receiver domain, CheY family and HTH	0.16	1.72	1.26	73.28	5
DR2416	-	Sensor histidine kinase	0.84	5.75	1.33	23.09	1.5
DR2481	K	Uncharacterized protein	0.39	4.66	1.27	27.17	1.5
DR2482	L	Predicted transcription regulator, HTH domain	0.36	5.75	2.92	50.84	1.5

		related to that of sigma factors					
DR2483	R	McrA family nuclease	0.80	5.43	1.22	22.49	1.5
DR2484	L	WD40 repeat protein	0.71	5.12	2.53	49.39	1.5
DR2566	-	Homolog of HpaII repair protein, small, conserved bacterial protein	0.42	4.10	1.09	26.48	3
DR2573	E	Uncharacterized protein	0.22	3.93	2.57	65.55	0.5
DR2610	R	Periplasmic binding protein, FliY	1.01	4.13	1.67	40.46	0.5
DRA0008	T	Conserved membrane protein (possible transporter)	0.26	6.60	2.00	30.26	3
DRA0009	T	Membrane-associated sensor histidine kinase	0.19	3.03	1.25	41.30	5
DRA0010	P	CheY -like sensor regulator and HTH domain	0.28	4.66	2.12	45.44	5
DRA0013	P	Sulfite reductase	0.65	8.27	1.84	22.31	24
DRA0014	E	PAPS synthase (APS kinase domain), CysC	0.37	4.33	1.66	38.36	24
DRA0015	P	PAPS reductase	0.54	11.42	5.73	50.18	24
DRA0016	T	Sulfate adenylyltransferase	0.42	12.12	5.83	48.07	24
DRA0049	T	Response regulator CheY family, flavodoxin	0.12	3.16	1.70	53.75	9
DRA0050	-	Phytochrome-like histidine kinase and GAF domain	0.30	2.18	1.21	55.52	3
DRA0234	E	Uncharacterized protein	0.17	12.76	5.27	41.29	1.5
DRA0249	K	Metalloprotease, leishmanolysin-like	1.61	6.47	4.43	68.42	3
DRA0344	ST	LexA repressor, HTH domain and protease	0.51	1.80	1.08	59.92	1.5
DRA0345	ST	Predicted esterase, homologs of *E. coli* erythromycin esterase type II (EreB)	0.68	10.05	4.39	43.72	1.5
DRA0346	R	PprA protein, possibly involved in DNA damage resistance mechanisms	0.65	3.52	1.94	55.14	0.5
DRB0067	O	Extracellular nuclease containing fibronectin III domains	0.29	4.37	1.21	27.58	3
DRB0069	R	Subtilisin family serine protease	0.92	3.18	1.39	43.62	3
DRB0070	-	ABC-class ATPase	0.64	4.00	1.91	47.74	1.5
DRB0071	H	Uncharacterized protein	0.11	2.60	0.53	20.51	3
DRB0072	E	Salicylate 1-monooxygenase	0.37	4.91	2.31	47.04	1.5
DRB0133	E	D-alanine permease	0.46	3.51	1.39	39.61	1.5

DRB0145	-	Uncharacterized protein	0.67	4.77	1.80	37.63	1.5

Footnotes for Table 5.4

[a] Note: Expression profile information in two last columns is shown only for one gene in an operon. All genes selected here are significantly induced (determined by statistical analyses)

[b] Designations of functional groups (from the COG database): see the legend for Table 5.3

Table 5.5

Master table for all normalized microarray raw data with standard deviation and t-test result. See the website:
http://www.esd.ornl.gov/facilities/genomics/TableA.pdf

Chapter 6: General Discussion

Ever since its discovery, ionization radiation has been known to have a lethal effect on microorganisms (Minck, 1896). Microorganisms, however, vary widely in their resistance to ionizing irradiation. The Gram-positive bacterium *D. radiodurans* (Anderson *et al.*, 1956) is historically best known for its extreme resistance to gamma radiation; it can grow continuously at 60 Gy/hour (Lange *et al.*, 1998; Brim *et al.*, 2000; Venkateswaran *et al.*, 2000) and can survive acute exposures that exceed 12 kGy without lethality or induced mutation (Daly and Minton, 1995a). *D. radiodurans* is also remarkably resistant to a wide range of other DNA damaging conditions including desiccation, ultraviolet radiation, and oxidizing agents (Minton 1994, 1995). These characteristics were the impetus for its genome sequencing (White *et al.*, 1999) and annotation (Makarova *et al.*, 2001), ongoing development for bioremediation (Lange *et al.*, 1998; Brim *et al.*, 2000; Brim *et al.*, 2003), broad proteome analysis (Lipton *et al.*, 2002), and whole genome expression analysis (Liu *et al.*, 2003).

Although it is believed that the multiple resistance phenotypes of *D. radiodurans* stem from efficient DNA repair processes (Daly *et al.*, 1994a; Daly and Minton 1995a; Daly and Minton 1996; Daly and Minton 1997; Daly *et al.*, 1994b), the mechanisms underlying its extraordinary repair capabilities remain poorly understood. Comparison of the predicted genes involved in repair and other forms of stress response in *D. radiodurans* to those of other bacteria revealed expansion of several relevant protein families in *D. radiodurans*, as well as conspicuous loss of some repair systems, *e.g.*, the RecBCD recombinase, but failed to identify an obvious genomic cognate of the resistance phenotypes (Makarova *et al.*, 2001). These findings suggest that the organism's extreme resistance phenotype may be attributable to functions not conventionally associated with DNA repair.

The principal aim of this dissertation was to understand the global interactions between the multiple cellular components that may facilitate the extreme radiation resistance phenotype of *D. radiodurans*. Comparative genomic and experimental analyses support the view that *D. radiodurans*' extreme radiation resistance phenotype is

complex, likely determined collectively by an assortment of cellular protection, metabolic, and DNA repair systems.

Evolution of the Extreme Radiation Resistance Phenotype

Previous reports suggest that the extreme radiation resistance phenotype of *D. radiodurans* may be the result of an evolutionary process that selected for organisms able to tolerate high levels of DNA damage (Mattimore and Battista, 1996; Makarova *et al.*, 2001). While naturally high radioactive environments are very rare on Earth, high levels of DNA damage can be inflicted on cells by certain environments that are not considered to be radioactive. For example, in cells exposed to desiccation or those exposed to background radiation for millions of years in permafrost. To examine the possible contribution of such non-radioactive environments to the evolution of the extreme resistance phenotype, radiation resistance profiles were constructed for aerobic bacteria isolated from diverse environments including ancient Siberian permafrost and arid surface soil samples (Chapter 2) and compared to bacteria isolated from radioactive soil sediments. Unlike permafrost conditions that are static, bacteria within arid soil environments are exposed to cycles of desiccation and rehydration (*e.g.*, rain) and therefore need to develop mechanisms against periodic exposure to the oxidative stress associated with rehydration (Mattimore and Battista, 1996). Since 80% of DNA damage caused by γ-radiation is believed to be due to production of reactive oxygen species (ROS), *e.g.*, hydroxyl radical ($^{\cdot}$OH) (Repine *et al.*, 1981), extreme conditions in arid soil are expected to select organisms that are resistant to radiation. As expected, many bacteria isolated from arid surface soils were found to be extremely radiation resistant (Figure 2.3-2.6), in contrast to bacteria isolated from Siberian permafrost and dry radioactive Hanford sediments that were typically radiation sensitive.

Based on their ability to resist chronic and acute irradiation, aerobic bacteria from permafrost, arid soils, and radioactive sediments could be categorized into 4 distinct groups: 1) bacteria that are resistant to both chronic irradiation and high doses of acute irradiation (D_{37} >4 kGy) (*e.g.*, *D. radiodurans*). This group of organisms may have efficient DNA protection and repair mechanisms; 2) bacteria that are resistant to chronic

irradiation, but sensitive to acute irradiation (D_{37} of < 0.5 kGy) (*e.g.*, MD846, Table 2.1). This group may have efficient DNA protection mechanisms, which may be based in metabolism, but less efficient DNA repair mechanisms; 3) bacteria that are sensitive to chronic irradiation but resistant to low doses of acute irradiation (D_{37} of 0.5-1 kGy) (*e.g.*, *E. coli*). These organisms may have inefficient DNA protection mechanisms, but moderately efficient DNA repair mechanisms; and 4) bacteria that are very sensitive to both chronic and acute irradiation (D_{37} < 0.5 kGy) (*e.g.*, *Shewanella* species). These organisms may have inefficient DNA protection and repair mechanisms. These observations together with a detailed computational analysis of *D. radiodurans*' whole genome sequence (Figure 2.10) suggest that an organism's ability to survive radiation may be attributable to a combination of metabolic-protection and DNA repair mechanisms. The nature of DNA protection systems are not well characterized, but likely are significantly affected by the metabolic repertoire of the cell (Black and Pritchard, 2003). Therefore, there is a need to systematically examine the role of metabolism in the radiation resistance phenotype.

As a part of this study, a 2-D genome-fingerprint method was developed and used successfully to confirm the identity of two novel *D. radiodurans* isolates (7B-1 and 7C-1) from radioactive sediments at Hanford (Chapter 2, Sections 2.25 and 2.3.1.4). The technique was expanded for expression analysis of *D. radiodurans* (Chapter 2). However, the utility of this approach was superseded by the construction of our whole genome microarray, but remains a useful tool in the study of gene expression in other bacteria with small genomes (~ 3Mbp) for which whole genome microarrays do not yet exist (Chapter 2).

Construction of Defined Minimal Medium (DMM) for *D. radiodurans*

To test the relationship between *D. radiodurans*' metabolic capabilities, ambient nutrient conditions, and radiation resistance predicted by genomic annotation (Makarova *et al.*, 2001), a DMM (Chapter 3, Table 3.1) was developed that was distinct from previously described defined synthetic media (Shapiro *et al.*, 1977; Raj *et al.*, 1960). Deinococcal DMM is much simpler than previously reported minimal medium, and

growth of *D. radiodurans* in such medium is completely dependent on a single carbon/energy source plus the sulfur containing amino acid methionine. A process of elimination was used to identify the minimal nutrients needed for luxurious growth of *D. radiodurans* at 32°C in absence of radiation (Table 3.1).

Under nutritionally restricted conditions, *D. radiodurans*' sensitivity to both chronic (60 Gy/hour) and acute doses (1 kGy - 20 kGy) of irradiation was tested. In contrast to cultures grown in rich (TGY) medium, the growth of *Deinococcus* was eliminated under chronic irradiation (Figure 3.2). Rapid DNA degradation and decreased cell viability was observed in *D. radiodurans* cultures grown over a period of 96 hours in DMM in a ^{137}Cs irradiator (Figure 3.3 A, B). The key nutrients required to restore deinococcal growth under chronic irradiation were identified (Table 3.1). However, both TGY and minimal medium grown *D. radiodurans* cells were resistant to acute doses of radiation up to a dose of 12 kGy. These results suggested that the *D. radiodurans* grown in defined minimal medium were not inherently sensitive to irradiation and that the DNA repair was found to be limited by metabolic capabilities of this organism. The analysis of *D. radiodurans*' complete genome sequence revealed several defects in its primary biosynthetic pathways (Table 3.2). The induction and functional integrity of the carbon and nitrogen metabolism integrating loci, *relA* and *spoT*, was tested by monitoring the production of their marker proteins, ppGpp and pppGpp during *D. radiodurans*' growth in DMM. Bacteria synthesize RelA in response to amino acid starvation leading to suppression of protein synthesis, DNA replication and transcription. *D. radiodurans relA* was found to be functional. As expected, RNA suppression was seen in cells grown in DMM (Figure 3.3 B) (Figure 3.4).

Metabolism, Oxidative Stress, and Radiation Resistance

During aerobic metabolism, microorganisms obtain energy from sugars or other organic molecules by allowing their carbon and hydrogen atoms to combine with oxygen (respiration) to produce CO_2 and water, respectively (Alberts *et al.*, 1998). Energy production by respiration typically occurs in four stages; 1) biopolymers are broken down into their corresponding monomers. For example, proteins, polysaccharides and fats are

broken down into amino acids, simple sugars, and fatty acids and glycerol, respectively; 2) monomers are then converted to acetyl CoA (*e.g.*, sugars are broken down by glycolysis); 3) acetyl CoA is then completely oxidized into CO_2 and H_2O by the TCA cycle, yielding large amounts of reducing equivalent and ATP; and 4) the electrons from reducing-equivalents are fed into the electron transport chain generating ATP by oxidative phosphorylation. However, energy production leads to the generation of ROS, which are toxic to biological macromolecules (*e.g.*, DNA and proteins). Some plants and microorganisms have an additional TCA cycle pathway called the 'glyoxylate bypass' that enables them to use acetate as the sole carbon source. While glyoxylate bypass is capable to generate precursors for essential components (e.g., purine, pyrimidine amino acids), it avoids production of high-levels of free radicals.

Since most of the DNA damage by ionizing radiation is caused by the generation of ROS, avoiding the production of oxidative stress during recovery likely is an important mechanism in radiation resistance. Therefore, the DMM developed for cultivation of *D. radiodurans* (Venkateswaran *et al.*, 2000) was used to compare the growth characteristics of all members of *Deinococcaceae* with emphasis on their metabolism and how it relates to their radiation resistance phenotype. While, all deinococcal members (except *D. geothermalis*) are unable to use common TCA cycle intermediates succinate, fumarate, malate, 2-oxoglutarate, citrate as carbon/energy sources (Chapter 3, Figure 3.1), they are able to use acetate as sole carbon/energy source, a diagnostic characteristic of an operational glyoxylate bypass. Since catabolism of most of the above mentioned TCA cycle intermediates generate ROS, the inability of the *Deinoccoceae* to use such intermediates might help minimize the production of metabolically induced free radicals. Consistently, RT-PCR analysis of selected TCA cycle genes of *D. radiodurans* during growth in DMM showed that its glyoxylate bypass was induced (Chapter 4, Table 4.3). Other circumstantial evidence supporting a restricted TCA cycle in *Deinococcus* is its dependence on an exogenous source of amino acids for growth and secretion of proteases (Figure 4.1). In contrast, *D. geothermalis* is able to grow on DMM without any exogenously provided amino acids or nicotinamide, and can utilize all TCA cycle intermediates for growth (Table 4.1 A and B). *D. geothermalis* is the most sensitive member of the family *Deinococcaceae* (Chapter 4, Figure 4.3).

Assuming that deinococci have customized their metabolic repertoire to avoid production of oxidative stress, it is possible that they are less dependent on ROS scavenging systems like SOD and catalase. Chapter 4 shows that SOD in *Deinococcus* is dispensable, even when growing on DMM where oxidative stress levels are expected to be much higher than in undefined rich medium. This is further supported by the observation that SOD deficient *D. radiodurans* shows only a marginal difference in growth under irradiation compared to wild-type (Chapter 4, Figure 4.2). Significantly, manganese levels in *D. radiodurans* are reported to be very high, and bacteria that accumulate high Mn levels typically have SOD systems that are dispensable (Jakubovics and Jenkinson. 2001). This collection of findings supports the important role of metabolism in the extreme radiation resistance phenotype.

Whole Transcriptome Analyses of *D. radiodurans* Recovering from Irradiation

The dynamic changes in *D. radiodurans*' global gene expression profiles following exposure to an acute dose (15 kGy) of irradiation were examined using microarrays covering ~94% of its total predicted open reading frames (ORFs). The observation that genes within diverse functional groups are differentially regulated in the early-mid-phase time intervals indicates that recovery from irradiation is a complex process that involves numerous cellular systems. Most enzymes of general metabolism are not affected in the first 9 hours following irradiation, supporting the notion that most of the expression dynamics observed in the 9-hour lag-phase is a consequence of the effects of irradiation and not due to changes in nutrient/growth conditions resulting from transfer of irradiated early stationary phase (ESP) *D. radiodurans* to fresh medium.

The expression data further support the hypothesis that irradiated *D. radiodurans* suppresses oxidative stress levels, which could prevent additional loss of genome integrity elicited by metabolism-induced free radicals. During the early- and mid-phases (0-9 h) of its recovery from acute irradiation, *D. radiodurans* appears to repress the $O_2^{\bullet-}$ radical generating steps of its TCA cycle which is reflected by repression of the key enzymes in these steps (*e.g.*, *sdhB*) (Chapter 5, Figure 5.5). Partial repression of the TCA cycle in *D. radiodurans* is accompanied by the simultaneous induction of its glyoxylate

bypass (induction of *aceA*, the key enzyme of the glyoxylate bypass). This unusual regulation of energy conversion pathways might provide key metabolic intermediates, while avoiding the high levels of free radicals produced by cyclic activity needed for generating reducing equivalents and energy. With energy limitations imposed on the cell by a repressed TCA cycle, it seems to make sense that *de novo* biosynthesis of amino acids, nucleotides and coenzymes remains unchanged or even down-regulated, at least within the first 9 hours of recovery. Instead, cells appear to rely heavily on exogenous sources of precursors, showing increased expression of many transporters, extracellular and intracellular proteases and nucleases (Chapter 5, Figure 5.4). Additionally, several enzymes involved in the utilization of exogenous and intracellular sugars are activated during the early-phase of recovery including transketolase (DR2256), phosphotransferase system enzyme II (DRB0073), 1-phosphofructokinase (DRB0074), pullulanase/amylase (DR1141), and maltase (DR1375).

The TCA cycle is repressed in the early- and mid- phases of recovery, but is activated in the third phase (9-24 hours) (growth restoration). Notably, activation of several genes involved in anti-oxidative stress response occurs simultaneously with the activation of the TCA cycle. It seems likely that the induced antioxidant proteins, in particular superoxide dismutases (DR1546, DR1279) and catalase (DR1998), are required to remove increased levels of free radical byproducts generated at the onset of growth when glycolysis and TCA cycle activity increases.

The importance of DNA repair mechanisms is manifested by the induction of its typical DNA repair pathways during its early and mid phase of recovery from irradiation (*e.g.*, NER, BER and RER) (Chapter 1, Section 1.2.5). Several uncharacterized genes that show a *recA* like expression pattern may also play a critical role in DNA protection, DNA repair, stress response and various regulatory pathways (Figure 5.4, Table 5.3, Table 5.4). Collectively, the microarray hybridization data reported here suggest that irradiated *D. radiodurans* avoids production of metabolically induced free radicals enabling its DNA repair systems to operate with little interference from the genotoxic effects of free radicals typically generated by aerobic metabolism.

Growth Analysis of *D. radiodurans* on Iron (Fe) and Manganese (Mn)

Recent work in our laboratory using the DMM developed by this thesis research showed that growth of *D. radiodurans* is independent of Fe, but highly dependent on Mn. This work has been submitted for publication (Vasilenko *et al.*, 2003). In contrast to *E. coli*, very high Mn and low Fe concentrations were detected in *D. radiodurans*, which could limit Fenton-type reactions that produce DNA-damaging hydroxyl radicals during irradiation. And, Mn is known to be a potent quenching agent against ROS (Posey and Gheradhini, 2000; Jakubovics and Jenkinson, 2001). To determine if the greater resistance of *D. radiodurans* compared to *E. coli* could be attributed to DNA protection, *D. radiodurans* and *E. coli* were cultured in TGY and irradiated on ice to doses extending to 50 kGy. Chromosomal DNA in *E. coli* was 15-fold more susceptible to *in vivo* irradiation damage than in *D. radiodurans*. These findings support that *D. radiodurans* avoids the production of $^{\bullet}OH$ radicals by limiting intracellular Fe^{2+}-dependent reduction of H_2O_2 produced by irradiation. The protective effects of high Mn and low Fe concentrations (Jakubovics and Jenkinson, 2001; Sonntag, C. von, 1987) could also help mitigate the lethal effects of desiccation/hydration-cycles (Mattimore and Battista, 1996) and exposure to H_2O_2 (Wang and Schellhorn, 1995) since DNA damage caused by these conditions is similar to that generated by ionizing radiation (Daly and Minton, 1995a; Repine *et al.*, 1981; Sonntag, C. von, 1987).

Genomic analyses indicate that the number of genes identified in *D. radiodurans* that are known to be involved in DNA repair is less than the number reported for *E.* coli (Makarova *et al.*, 2001). The number of DSBs/haploid genome estimated in *D. radiodurans* and *E. coli* at their respective D_{10} (10% survival) isosurvival doses was determined to be similar, and collectively, our laboratory now believes that the 15-fold difference in DNA protection observed between *D. radiodurans* and *E. coli* is sufficient to explain the 16-fold difference in dose determined to achieve the same 10% survival. The main difference between a surviving fraction of irradiated *E. coli* and *D. radiodurans* cells is the level of mutagenesis (Sweet and Moseley, 1976). For *E. coli*, substantial increases in mutagenesis occur as viability decreases following irradiation, but not for *D. radiodurans*, which shows no irradiation-induced mutations (Sweet and Moseley, 1976).

Efficient homologous recombination observed between the multiple identical genomes in *D.* radiodurans (Daly and Minton, 1995) is consistent with the ability of irradiated cells to prevent mutation.

We believe that previous emphasis on DNA repair as the dominant explanation Daly and Minton, 1995a; Mattimore and Battista, 1996; Moseley, 1984; Daly and Minton, 1996; Sweet and Moseley, 1976; Makarova *et al.*, 2001; Liu *et al.*, 2003; Battista *et al.*, 1999; Minton, 1996; Lin *et al.*, 1999) for the remarkable survival of *D. radiodurans* cultures at high irradiation doses has been overstated. Instead, we suggest that the extreme resistance of *D. radiodurans* is largely due to high levels of DNA protection in cells, which give rise to extraordinary CFU-based survival curves when grouped as tetracocci (Daly and Minton, 1995a; Murray *et al.*, 1983). The high Mn and low Fe levels of *D. radiodurans* likely are two of a synergistic set of intracellular conditions that contribute to cellular protection, including free radical scavenging systems such as the constitutive, highly expressed superoxide dismutase and catalase of *D. radiodurans* (McCord *et al.*, 1971), and metabolic pathway switching following irradiation (Liu *et al.*, 2003) (Chapter 5) that could prevent additional genome damage elicited by metabolism-induced free radicals during recovery.

List of References

Adak, S., A. M. Bilwes, K. Panda, D. Hosfield, K. S. Aulak, J. F. McDonald, J. A. Tainer, E. D. Getzoff, B. R. Crane, and D. J. Stuehr. 2002. Cloning, expression, and characterization of a nitric oxide synthase protein from *Deinococcus radiodurans*. Proc Natl Acad Sci U S A. Jan 8;**99**:107-12

Agostini, H. J., J. D. Carroll, and K. W. Minton. 1996. Identification and characterization of uvrA, a DNA repair gene of *Deinococcus radiodurans*. J Bacteriol **178**:6759-65.

Al-Bakri, G. H., M. W. Mackay, P. A. Whittaker, and B. E. Moseley. 1985. Cloning of the DNA repair genes mtcA, mtcB, uvsC, uvsD, uvsE and the leuB gene from *Deinococcus radiodurans*. Gene **33**:305-11.

Alberts, B., *et al.*, 1998. Essential Cell Biology. Garland publishing, Inc. New York and London.

Altschul, S. F., and E. V. Koonin. 1998. Iterated profile searches with PSI-BLAST--a tool for discovery in protein databases. Trends Biochem Sci **23**:444-7.

Altschul, S. F., T. L. Madden, A. A. Schaffer, J. Zhang, Z. Zhang, W. Miller, and D. J. Lipman. 1997. Gapped BLAST and PSI-BLAST: a new generation of protein database search programs. Nucleic Acids Res **25**:3389-402.

Anderson, A., H. Nordan, R. Cain, G. Parrish, and D. Duggan. 1956. Studies on a radoresistant micrococcus. I. Isolation, morphology, cultural charchteristoics, and resistance to gamma radiation. Food Thechnology **10**:575-578.

Anderson, R. 1983. Alkylamines: novel lipid constituents in *Deinococcus radiodurans*. Biochim.Biophys.Acta **753**:266-8.

Anderson, R., and K. Hansen. 1985. Structure of a novel phosphoglycolipid from Deinococcus radiodurans. J Biol Chem **260**:12219-23.

Andersson, A. M., N. Weiss, F. Rainey, and M. S. Salkinoja-Salonen. 1999. Dust-borne bacteria in animal sheds, schools and children's day care centres. J Appl Microbiol **86**:622-34.

Anton J., R. Rossello-Mora, F. Rodriguez-Valera, et al. 2000. Extremely halophilic bacteria in crystallizer ponds from solar salterns. Appl Environ Microbiol. **66**: 3052-3057.

Arcondeguy, T., R. Jack, and M. Merrick. 2001. P(II) signal transduction proteins, pivotal players in microbial nitrogen control. Microbiol Mol Biol Rev **65**: 80-105.

Arn, E.A. and J.N. Abelson. 1996. The 2'-5' RNA ligase of *Escherichia coli.* Purification, cloning, and genomic disruption. J Biol Chem **271:** 31145-31153.

Aust S. D., C. F. Chignell, T. M. Bray, B. Kalyanaraman, and R. P. Mason. 1993. Contemporary issues in toxicology. Free Radicals in Toxicology. Toxicology and applied pharmacology. **120**:168-178.

Azeddoug, H., and G. Reysset. 1994. Cloning and sequencing of a chromosomal fragment from Clostridium acetobutylicum strain ABKn8 conferring chemical-damaging agents and UV resistance to *E. coli* recA strains. Curr Microbiol **29:**229-35.

Battista, J. R., H. A. Howell, M. J. Park, A. Earl, and P. SN. 2002. The *Deinococcus radiodurans* microarray: changes in gene expression following exposure to ionizing radiation. In Genome. DOE Contractor-Grantee Workshop IX, pp. 88, Oakland, CA.

Battista, J. R., M. J. Park and A. E. McLemore. 2001.Inactivation of two homologues of proteins presumed to be involved in the desiccation tolerance of plants sensitizes *Deinococcus radiodurans* R1 to desiccation. Cryobiology Sep;**43**:133-9

Battista, J. R., A. M. Earl, and M. J. Park. 1999. Why is *Deinococcus radiodurans* so resistant to ionizing radiation?. Trends Microbiol **7:**362-5.

Battista, J. R. 1997. Against all odds: the survival strategies of *Deinococcus radiodurans*. Annu Rev Microbiol **51:**203-24.

Bhoo, S.H., S. J. Davis, J. Walker, B. Karniol, and R. D. Vierstra. 2001. Bacteriophytochromes are photochromic histidine kinases using a biliverdin chromophore. Nature. Dec 13;**414**:776-9

Bauer, C. E., S. Elsen, and T. H. Bird. 1999. Mechanisms for redox control of gene expression. Annu Rev Microbiol **53:**495-523.

Baumeister, W., O. Kubler, and H. P. Zingsheim. 1981. The structure of the cell envelope of *Micrococcus radiodurans* as revealed by metal shadowing and decoration. J Ultrastruct Res **75:**60-71.

Beard, W. A., and S. H. Wilson. 1995. Purification and domain-mapping of mammalian DNA polymerase beta. Methods Enzymol **262:**98-107.

Beauchamp, C., and I. Fridovich. 1971. Superoxide dismutase: improved assays and an assay applicable to acrylamide gels. Anal. Biochem. **44:**276-287.

Bessman, M. J., D. N. Frick, and S. F. O'Handley. 1996. The MutT proteins or "Nudix" hydrolases, a family of versatile, widely distributed, "housecleaning" enzymes. J Biol Chem **271**:25059-62.

Black, M., and H. W. Pritchard. 2002. Desiccation and Survival in Plants: Drying without Dying. CABI publishing. Wallingford, Oxon, UK.

Blaisdell, B. E., K. E. Rudd, A. Matin, and S. Karlin. 1993. Significant dispersed recurrent DNA sequences in the *Escherichia coli* genome. Several new groups. J Mol Biol **229**:833-48.

Bolling, M. E., and J. K. Setlow. 1966. The resistance of *Micrococcus radiodurans* to ultraviolet radiation. III. A repair mechanism. Biochim.Biophys.Acta **123**:26-33.

Bonacossa de Almeida C, Coste G, Sommer S, Bailone A. 2002. Quantification of RecA protein in *Deinococcus radiodurans* reveals involvement of RecA, but not LexA, in its regulation. Mol Genet Genomics 2002 Sep;**268**:28-41.

Brim, H., A. Venkateswaran, H. M. Kostandarithes, J. K. Fredrickson, and M. J. Daly. 2003. Engineering *Deinococcus geothermalis* for bioremediation of high-temperature radioactive waste environments. Appl Environ Microbiol. In Press.

Brim, H., S. C. McFarlan, J. K. Fredrickson, K. W. Minton, M. Zhai, L. P. Wackett, and M. J. Daly. 2000. Engineering *Deinococcus radiodurans* for metal remediation in radioactive mixed waste environments. Nat Biotechnol **18**:85-90.

Brooks, B. W., M. R.G.E., J. L. Johnson, S. E., C. R. Woese, and G. E. Fox. 1980. Red-pigmented micrococci: a basis for taxonomy. Int. J. Syst. Bacteriol. **30**:627-46.

Brown, P.O. and D. Botstein. 1999. Exploring the new world of the genome with DNA microarrays. Nat Genet **21:** 33-37.

Bueno, R., G. Pahel, and B. Magasanik. 1985. Role of glnB and glnD gene products in regulation of the glnALG operon of *Escherichia coli*. J Bacteriol **164**:816-22.

Cai, H., and S. Clarke. 1999. A novel methyltransferase catalyzes the methyl esterification of trans-aconitate in *Escherichia coli*. J Biol Chem. May 7;**274**:13470-9.

Capy, P., T. Langin, D. Higuet, P. Maurer, and C. Bazin. 1997. Do the integrases of LTR-retrotransposons and class II element transposases have a common ancestor? Genetica **100**:63-72.

Carbonneau, M. A., A. M. Melin, A. Perromat, and M. Clerc. 1989. The action of free radicals on *Deinococcus radiodurans* carotenoids. Arch Biochem Biophys **275**:244-51.

Carlioz, A., and D. Touati. 1986. Isolation of superoxide dismutase mutants in *Escherichia coli*: is superoxide dismutase necessary for aerobic life? EMBO Journal **5**:623-630.

Carpenter E. J., S. Lin, and D. E. Capone. 2000. Bacterial activity in South Pole snow. Appli. Environ. Microb. **66**: 4514-4517.

Carroll, J. D., M. J. Daly, and K. W. Minton. 1996. Expression of *recA* in *Deinococcus radiodurans*. J Bacteriol **178**:130-5.

Cashel, M., and K.E. Rudd. 1996. The stringent response of *Escherichia coli* and *Salmonella typhimurium*, p. 1410- 1438. In F. C. Neidhardt *et al.*, (ed.), Cellular and Molecular biology. American Society of Microbiology, Washington D.C.

Cashel, M. 1994. Detection on (p)ppGpp accumulation patterns in *Escherichia coli* mutants. Meth. Molec. Genet. **3**: 341-356: Acedemic Press.

Chevion, M. 1988. A site-specific mechanism for free radical induced biological damage: the essential role of redox-active transition metals. Free Radic. Biol. Med. **5**:27-37.

Chou, F. I., and S. T. Tan. 1990. Manganese(II) induces cell division and increases in superoxide dismutase and catalase activities in an aging deinococcal culture. J. Bacteriol. **172**: 2029-2035.

Christensen, E. A., and H. Kristensen. 1981. Radiation-resistance of micro-organisms from air in clean premises. Acta Pathol Microbiol Scand [B] **89**:293-301.

Chuang, S. E., and F. R. Blattner. 1993. Characterization of twenty-six new heat shock genes of *Escherichia coli*. J Bacteriol **175**:5242-52.

Cooper, G. M. 2000. The Cell - A Molecular Approach. 2nd ed. Sinauer Associates, Inc: Sunderland, Massachusetts.

Costantino, H. R., S. P. Schwendeman, R. Langer, A. M. Klibanov. 1998. Deterioration of lyophilized pharmaceutical proteins. Biochemistry (Mosc) Mar; **63**:357-63.

Counsell, T. J., and R. G. E. Murray. 1986. Polar lipid profiles of the genus *Deinococcus*. Int.J.Syst.Bacteriol **36**:202-206.

Cronan, J. E., and D. LaPorte. 1996 Tricarboxylic acid cycle and glyoxylate bypass, p. 206-216. *In* F. C Neidhardt, R. Curtiss III, J. L. Ingraham, E. C. C. Lin, K. B. Low, B. Magasanik, W. S. Reznikoff, M. Riley, M. Schaechter, and H. E.

Umbarger (ed.), *Escherichia coli* and *Salmonella*: cellular and molecular biology, 2nd ed. ASM Press, Washington, D.C.

Curnow, A. W., D. L. Tumbula, J. T. Pelaschier, B. Min, and D. Soll. 1998. Glutamyl-tRNA(Gln) amidotransferase in *Deinococcus radiodurans* may be confined to asparagine biosynthesis. Proc Natl Acad Sci U S A **95:**12838-43.

Curry, J., and M. K. Walker-Simmons. 1993. Unusual sequence of group 3 LEA (II) mRNA inducible by dehydration stress in wheat. Plant Mol Biol **21:**907-12.

Daly, M. J. 2000. Engineering radiation-resistant bacteria for environmental biotechnology [In Process Citation]. Curr Opin Biotechnol **11:**280-5.

Daly, M. J., and K. W. Minton. 1997. Recombination between a resident plasmid and the chromosome following irradiation of the radioresistant bacterium *Deinococcus radiodurans*. Gene **187:**225-9.

Daly, M. J., and K. W. Minton. 1996. An alternative pathway of recombination of chromosomal fragments precedes recA-dependent recombination in the radioresistant bacterium *Deinococcus radiodurans*. J Bacteriol **178:**4461-4471.

Daly, M. J., and K. W. Minton. 1995a. Interchromosomal recombination in the extremely radioresistant bacterium *Deinococcus radiodurans*. J Bacteriol **177:**5495-505.

Daly, M. J., and K. W. Minton. 1995b. Resistance to radiation. Science **270,** 1318.

Daly, M. J., O. Ling, and K. W. Minton. 1994a. Interplasmidic recombination following irradiation of the radioresistant bacterium *Deinococcus radiodurans*. J Bacteriol **176:**7506-15.

Daly, M. J., L. Ouyang, P. Fuchs, and K. W. Minton. 1994b. In vivo damage and *recA*-dependent repair of plasmid and chromosomal DNA in the radiation-resistant bacterium *Deinococcus radiodurans*. J Bacteriol **176:**3508-17.

Dardalhon-Samsonoff, M., and D. Averbeck. 1980. DNA-membrane complex restoration in *Micrococcus radiodurans* after X-irradiation: relation to repair, DNA synthesis and DNA degradation. Int. J. Radiat. Biol. **38:** 31-52.

Darzynkiewicz, Z. 1994. Simultaneous analysis of cellular RNA and DNA content. Meth. Cell Biol. **41:** 401-420.

Davis, N. S., G. J. Silverman, and E. B. Mausurosky. 1963. Radiation resistant, pigmented coccus isolated from haddock tissue. J.Bacteriol **86:**294-98.

Dean, C. J., J. G. Little, and R. W. Serianni. 1970. The control of post irradiation DNA breakdown in *Micrococcus radiodurans*. Biochem. Biophys. Res. Commun. **39**:126-34.

Dean, C. J., P. Feldschreiber, and J. T. Lett. 1966. Repair of x-ray damage to the deoxyribonucleic acid in *Micrococcus radiodurans*. Nature **209**:49-52.

Dose, K., A. Bieger-Dose, M. Labush, and M. Gill. 1992. Survival in extreme dryness and DNA-single strand breaks. Adv. Space Research. **12**:221-229.

Dure, L. D. 1993. A repeating 11-mer amino acid motif and plant desiccation. Plant J **3**(3):363-9.

Dewald, G. W. 1997. Gregor Johann Mendel and the beginning of genetics. Mayo Clin Proc. **52**:513-8.

Earl A. M., M. M. Mohundro, I. S. Mian, and J. R. Battista. 2002a. The IrrE protein of *Deinococcus radiodurans* R1 is a novel regulator of recA expression. J Bacteriol **184**:6216-24

Earl A. M., S. K. Rankin, K. P. Kim, O. N. Lamendola, and J. R. Battista. 2002b. Genetic evidence that the uvsE gene product of *Deinococcus radiodurans* R1 is a UV damage endonuclease. J. Bacteriol **184**:1003-9

Eisen, J. A., and P. C. Hanawalt. 1999. A phylogenomic study of DNA repair genes, proteins, and processes. Mutat Res **435**:171-213.

Embley, T. M., A. G. O'Donnell, R. Wait, and J. Rostron. 1987. Lipid and cell wall amino acid composition in the classification of members of the genus *Deinococcus*. System. Appl. Microbiol **10**:20-27.

Eshrov, E. D. 1990. Obshchaja geokriologija (generally geocryology). Nedra, Moscow, Russia.

Evans, T. C., Jr., D. Martin, R. Kolly, D. Panne, L. Sun, I. Ghosh, L. Chen, J. Benner, X. Q. Liu, and M. Q. Xu. 2000. Protein trans-splicing and cyclization by a naturally split intein from the dnaE gene of Synechocystis species PCC6803. J Biol Chem **275**:9091-4.

Evans, D. M., and B. E. Moseley. 1988. *Deinococcus radiodurans* UV endonuclease beta DNA incisions do not generate photoreversible thymine residues. Mutat Res **207**:117-9.

Evans, D. M., and B. E. Moseley. 1985. Identification and initial characterisation of a pyrimidine dimer UV endonuclease (UV endonuclease beta) from *Deinococcus*

radiodurans; a DNA- repair enzyme that requires manganese ions. Mutat Res **145**:119-28.

Evans, D. M., and B. E. Moseley. 1983. Roles of the *uvsC*, *uvsD*, *uvsE*, and *mtcA* genes in the two pyrimidine dimer excision repair pathways of *Deinococcus radiodurans*. J Bacteriol **156**:576-83.

Fabrega, C., M. A. Farrow, B. Mukhopadhyay, V. de Crecy-Lagard, A. R. Ortiz, and P. Schimmel. 2001. An aminoacyl tRNA synthetase whose sequence fits into neither of the two known classes. Nature **411**:110-4

Ferreira, A. C., M. F. Nobre, F. A. Rainey, M. T. Silva, R. Wait, J. Burghardt, A. P. Chung, and M. S. da Costa. 1997. *Deinococcus geothermalis* sp. nov. and *Deinococcus murrayi* sp. nov., two extremely radiation-resistant and slightly thermophilic species from hot springs. Int J Syst Bacteriol **47**:939-47.

Fishman-Lobell, J., N. Rudin, and J. E. Haber. 1992. Two alternative pathways of double-strand break repair that are kinetically separable and independently modulated. Mol Cell Biol. **3**:1292-303.

Fleischmann, R. D et al. 1995. Whole-genome random sequensing and assembly of *Haemophilus influenzae* Rd. Science. **269**: 469-512.

Fisher, D. I., S. T. Safrany, P. Strike, A. G. McLennan, and J. L. Cartwright. 2002. Nudix Hydrolases That Degrade Dinucleoside and Diphosphoinositol Polyphosphates Also Have 5-Phosphoribosyl 1-Pyrophosphate (PRPP) Pyrophosphatase Activity That Generates the Glycolytic Activator Ribose 1,5-Bisphosphate. J Biol Chem;**277**:47313-7

Franks, F., R. H. M. Hatley, and S. F. Mathias. 1991. Materials science and production of shelf stable biologicals. Bio-pharm **4**:38-42.

Fredrickson J. K, J.M. Zachara, F.J. Brockman, D.L.Blakwill, D. Kennedy, S.W. Li, H. M.. Kostandarithes, M.J. Daly, M.F. Romine and R.J. Serne. 2003. Geomicrobiology of High Level Nuclear Waste Contaminated Vadose Sediments at the Hanford Site, Washington. Submitted to *Appl. Environ. Microbiol.*

Frey, A. D., J. Farres, C. J. Bollinger, and P. T. Kallio. 2002. Bacterial hemoglobins and flavohemoglobins for alleviation of nitrosative stress in *Escherichia coli*. Appl Environ Microbiol **68**:4835-40.

Fridovich, I. 1999. Fundamental aspects of reactive oxygen species, or what's the matter with oxygen? Ann N Y Acad Sci. **893**:13-28.

Fridovich, I. 1995. Superoxide radical and superoxide dismutases. Annu. Rev. Biochem. **64**:97-112.

Friedberg, E. C. 1996. Relationships between DNA repair and transcription. Annu Rev Biochem **65:**15-42.

Friedmann E. I. 1993. Antarctic Microbiology. New York, Wiley-Liss.

Fujimori, A., Y. Matsuda, Y. Takemoto, Y. Hashimoto, E. Kubo, R. Araki, R. Fukumura, K. Mita, K. Tatsumi, and M. Muto. 1998. Cloning and mapping of Np95 gene which encodes a novel nuclear protein associated with cell proliferation. Mamm Genome **9:**1032-5.

Galas, D. J., and M. Chandler. 1989. Mobile DNA. American society of Microbiology, Washington, DC.

Galperin, M. Y., and E. V. Koonin. 1999. Functional genomics and enzyme evolution. Homologous and analogous enzymes encoded in microbial genomes. Genetica **106:**159-70.

Galperin, M. Y., D. A. Natale, L. Aravind, and E. V. Koonin. 1999. A specializes version of the HD hydrolase domain implicated in signal transduction. J.Mol.Microbiol.Biotechnol. **1:**303-305.

Georgiou, G. 2002. How to Flip the (Redox) Switch. Cell. **111**:607-10.

Gerard, E., E. Jolivet, D. Prieur, and P. Forterre. 2001.DNA protection mechanisms are not involved in the radioresistance of the hyperthermophilic archaea *Pyrococcus abyssi* and *P. furiosus*. Mol Genet Genomics **266**:72-8.

Gershon, D. 2002. Microarray technology: an array of opportunities. Nature. **416**:885-91.

Gilbert, D. L.1981. Oxygen and Free Living Processes: An inter-disciplinary Approach. Springer, New York.

Gottschalk, G. 1985. Bacterial Metabolism, 2nd ed. Springer-Verlag, New York, N. Y.

Gort A. S., D. M. Ferber, and J. A. Imlay. 1999. The regulation and role of the periplasmic copper, zinc superoxide dismutase of *Escherichia coli*. Mol. Microbiol. **32**:179-191.

Gupta, R. S. 1998. Protein phylogenies and signature sequences: A reappraisal of evolutionary relationships among archaebacteria, eubacteria, and eukaryotes. Microbiol Mol Biol Rev **62:**1435-91.

Guschin, D.Y., B.K. Mobarry, D. Proudnikov, D.A. Stahl, B.E. Rittmann, and A.D. Mirzabekov. 1997. Oligonucleotide microchips as genosensors for determinative and environmental studies in microbiology. Appl Environ Microbiol **63:** 2397-2402.

Gutman, P. D., J. D. Carroll, C. I. Masters, and K. W. Minton. 1994. Sequencing, targeted mutagenesis and expression of a recA gene required for the extreme radioresistance of *Deinococcus radiodurans*. Gene **141:**31-7.

Gutman, P. D., P. Fuchs, L. Ouyang, and K. W. Minton. 1993. Identification, sequencing, and targeted mutagenesis of a DNA polymerase gene required for the extreme radioresistance of *Deinococcus radiodurans*. J Bacteriol **175:**3581-90.

Gutman, P. D., H. L. Yao, and K. W. Minton. 1991. Partial complementation of the UV sensitivity of *Deinococcus radiodurans* excision repair mutants by the cloned denV gene of bacteriophage T4. Mutat Res **254:**207-15.

Gutteridge J. M. C. and Halliwell: Free Radicals and Antioxidants in the year 2000. A historical look to the future.

Guzder, S. N., P. Sung, V. Bailly, L. Prakash, and S. Prakash. 1994. RAD25 is a DNA helicase required for DNA repair and RNA polymerase II transcription [see comments]. Nature **369:**578-81.

Haber, J. E. 2000. Partners and pathways repairing a double-strand break. Trends Genet. **16**:259-264.

Halliwell, B. and J.M.C. Gutteridge. 1999. *In Free Radicals in Biology and Medicine*. Oxford University Press.

Hansen, M.T. 1982. Rescue of mitomycin C- or psoralen-inactivated *Micrococcus radiodurans* by additional exposure to radiation or alkylating agents. J Bacteriol **152:** 976-982.

Hansen, M. T. 1980. Four proteins synthesized in response to deoxyribonucleic acid damage in *Micrococcus radiodurans*. J Bacteriol **141:**81-6.

Hansen, M. T. 1978. Multiplicity of genome equivalents in the radiation-resistant bacterium *Micrococcus radiodurans*. J Bacteriol **134:**71-5.

Harsojo, S. Kitayama, and A. Matsuyama. 1981. Genome multiplicity and radiation resistance in *Micrococcus radiodurans*. J Biochem (Tokyo) **90:**877-80.

Hartzell, P., and D. Kaiser. 1991. Function of MglA, a 22-kilodalton protein essential for gliding in *Myxococcus xanthus*. J Bacteriol **173:**7615-24.

Harrington, C.A., C. Rosenow, and J. Retief. 2000. Monitoring gene expression using DNA microarrays. Curr Opin Microbiol **3:** 285-291.

Hebert R, A. 1992. A perspective on the biotechnological potential of extremophiles. Trends in Biotechnology. **10**: 395-402.

Huang Y, Anderson R. 2002. Enhanced immune protection by a liposome-encapsulated recombinant respiratory syncytial virus (RSV) vaccine using immunogenic lipids *from Deinococcus radiodurans*. Vaccine**20**:1586-92.

Hubbard, T. J., B. Ailey, S. E. Brenner, A. G. Murzin, and C. Chothia. 1999. SCOP: a Structural Classification of Proteins database. Nucleic Acids Res **27:**254-6.

Hutchinson, F. 1985. Chemical changes induced in DNA by ionizing radiation. *Prog* Nucleic Acid Res Mol Biol **32:**115-154.

Ibba, M., A. W. Curnow, and D. Soll. 1997. Aminoacyl-tRNA synthesis: divergent routes to a common goal. Trends Biochem Sci **22:**39-42.

Imlay, J. A. 1995. A metabolic enzyme that rapidly produces superoxide, fumarate reductase of *Escherichia coli*. J. Biol. Chem. **270**:19767-19777.

Imlay, J. A., and S. Linn. 1988. DNA damage and oxygen radical toxicity. Science. **240**:1302-1309.

Ito, H., Watanabe, H., Takeshia, M., and Iizuka, H. 1983. Isolation and identification of radiation resistant cocci belonging to the genus *Deinococcus* from sewage sludges and animal feeds. Agric. Biol. Chem. **47**: 1239-47.

Jakubovics, N.S., and H. F. Jenkinson. 2001. Out of iron age: new insights into the critical role of manganese homeostasis in bacteria. Microbiology **147**: 1709-1718.

Jilani, A., D. Ramotar, C. Slack, C. Ong, X. M. Yang, S. W. Scherer, and D. D. Lasko. 1999. Molecular cloning of the human gene, PNKP, encoding a polynucleotide kinase 3'-phosphatase and evidence for its role in repair of DNA strand breaks caused by oxidative damage. J Biol Chem **274:**24176-86.

Johnson, D. B. 1998. Biodiversity and ecology of acidophilic microorganisms. FEMS Microbiol. Ecol. **27**: 301-317.

Jordan A. and P. Reichard. 1998. Ribonucleotide reductases. Annu. Rev. Biochem. **67**:71-98.

Karlin S, and Mrazek J. 2001.Predicted highly expressed and putative alien genes of *Deinococcus radiodurans* and implications for resistance to ionizing radiation damage. Proc Natl Acad Sci U S A Apr 24;**98**:5240-5.

Kelly, S. G., and Post, F. G. 1991. In Microbiology Techniques (Star Publishing Company, Belmont, CA), pp. 175-182.

Keyser, K., A. S. Gort A., and J. A. Imlay. 1995. Superoxide and the production of oxidative DNA damage. J. Bacteriol. **177** :6782-6790.

Kim, J. I., A. K. Sharma, S. N. Abbott, E. A. Wood, D. W. Dwyer, A. Jambura, K. W. Minton, R. B. Inman, M. J. Daly, and M. M. Cox. 2002. RecA Protein from the extremely radioresistant bacterium *Deinococcus radiodurans*: expression, purification, and characterization. J Bacteriol **184**:1649-60.

Kim, J. I, and M. M. Cox. 2002.The RecA proteins of *Deinococcus radiodurans* and Escherichia coli promote DNA strand exchange via inverse pathways. Proc Natl Acad Sci U S A **99**:7917-21.

Kitayama, S., and A. Matsuyama. 1971. Mechanism for radiation lethality in M. radiodurans. Int J Radiat Biol Relat Stud Phys Chem Med **19**:13-9.

Kobatake, M., S. Tanabe, and S. Hasegawa. 1973. [New Micrococcus radioresistant red pigment, isolated from Lama glama feces, and its use as microbiological indicator of radiosterilization]. C R Seances Soc Biol Fil **167**:1506-10.

Kolari M, Schmidt U, Kuismanen E, Salkinoja-Salonen MS. 2002.Firm but slippery attachment of *Deinococcus geothermalis*. J Bacteriol May;**184**:2473-80.

Koonin, E. V., L. Aravind, and M. Y. Galperin. 2000. A comparative-genomic view of the microbial stress response, p. 417-444. *In* G. Storz and R. Hengge-Aronis (ed.), Bacterial stress responses. ASM Press, Washington, DC.

Koonin, E. V., and R. L. Tatusov. 1994. Computer analysis of bacterial haloacid dehalogenases defines a large superfamily of hydrolases with diverse specificity. Application of an iterative approach to database search. J Mol Biol **244**:125-32.

Krasin, F., and F. Hutchinson. 1977. Repair of DNA double-strand breaks in Escherichia coli, which requires recA function and the presence of a duplicate genome. J Mol Biol **116**:81-98.

Kreppel, L. K., and G. W. Hart. 1999. Regulation of a cytosolic and nuclear O-GlcNAc transferase. Role of the tetratricopeptide repeats. J Biol Chem **274**:32015-22.

Kristensen, H., and E. A. Christensen. 1981. Radiation-resistant micro-organisms isolated from textiles. Acta Pathol Microbiol Scand [B] **89**:303-9.

Krogh, B. O., and S. Shuman. 2002. A poxvirus-like type IB topoisomerase family in bacteria. Proc Natl Acad Sci U S A **99**:1853-8.

Kubler, O., and W. Baumeister. 1978. The structure of a periodic cell wall component (HPI) layer of *Micrococcus radiodurans*. Cytobiologie. **17**:1-9.

Kunst, F., N. Ogasawara, I. Moszer, *et al.* 1997. The complete genome sequence of the gram-positive bacterium *Bacillus subtilis*. Nature **390**:249-256.

Kurian K. M., C. J. Watson and A. H. Wyllie. 1999. DNA CHIP TECHNOLOGY. Journal of Pathology. **187**: 276-271.

Kuzminov, A. 1999. Recombinational repair of DNA damage in *Escherichia coli* and bacteriophage lambda. Microbiol Mol Biol Rev **63**:751-813, table of contents.

Lambert, L. H., T. Cox, K. Mitchell, R. A. Rossello-Mora, C. Del Cueto, D. E. Dodge, P. Orkand, R. J Cano. 1998. Staphylococcus succinus sp. nov., isolated from Dominican amber. Int J Syst Bacteriol. **48**:511-8.

Lancy, P., Jr., and R. G. Murray. 1978. The envelope of *Micrococcus radiodurans*: isolation, purification, and preliminary analysis of the wall layers. Can J Microbiol **24**:162-76.

Lander E. S., *et al.*, 2001. Initial sequencing and analysis of the human genome. Nature. 2001 409:860-921.

Lange, C. C., L. P. Wackett, K. W. Minton, and M. J. Daly. 1998. Engineering a recombinant *Deinococcus radiodurans* for organopollutant degradation in radioactive mixed waste environments [see comments]. Nat Biotechnol **16**:929-33.

Lauble, H., M.C. Kennedy, H. Beinert, and C.D. Stout. 1994. Crystal structures of aconitase with trans-aconitate and nitrocitrate bound. *J Mol Biol* **237**: 437-451.

Lee, M. L., F. C. Kuo, G. A. Whitmore, and Sklar, J. 2000. Proc Natl Acad Sci USA **97**, 9834-9839.

Lee, J.Y., C. Chang, H.K. Song, J. Moon, J.K. Yang, H.K. Kim, S.T. Kwon, and S.W. Suh. 2000. Crystal structure of NAD(+)-dependent DNA ligase: modular architecture and functional implications. Embo J **19**: 1119-1129.

Lehner, G., J. Delatorre, C. Lutz, and L. Cardemil. 2001. Field studies on the photosynthesis of two desert Chilean plants: Prosopis chilensis and Prosopis tamarugo. J Photochem Photobiol B. **64**:36-44.

Lemme, L., E. Peuchant, and M. Clerc. 1997. Deinoxanthin: A New Caratenoid Isolated from *Deinococcus radiodurans*. Tetraheroon **53**: 919-926.

Lennon, E., P. D. Gutman, H. L. Yao, and K. W. Minton. 1991. A highly conserved repeated chromosomal sequence in the radioresistant bacterium *Deinococcus radiodurans* SARK. J Bacteriol **173**:2137-40.

Leonard, C. J., L. Aravind, and E. V. Koonin. 1998. Novel families of putative protein kinases in bacteria and archaea: evolution of the "eukaryotic" protein kinase superfamily. Genome Res **8**:1038-47.

Lernee, L., E Peuchant, and M. Clerc. 1997. Deinoxanthin: A New Carotenoid Isolated from *Deinococcus radiodurans*. Tetrahedron. **53**: 919-926.

Lett, J. T., P. Feldschreiber, J. G. Little, K. Steele, and C. J. Dean. 1967. The repair of x-ray damage to the deoxyribonucleic acid in *Micrococcus radiodurans*: a study of the excision process. Proc R Soc Lond B Biol Sci. **167**:184-201.

Lewin, B. 2000. Genes VII. Oxford University press.

Lewis, N. F. 1971. Studies on a radio-resistant coccus isolated from Bombay duck (Harpodon nehereus). J Gen Microbiol **66:29**-35.

Liochev, S. I., and I. Fridovich. 1992. Fumarase C, the stable fumarase *of Escherichia coli*, is controlled by the *soxRS* regulon. Proc. Natl. Acad. Sci., USA. 89:5892-5896.

Lin, J., R. Qi, C. Aston, J. Jing, T. S. Anantharaman, B. Mishra, O. White, M. J. Daly, K. W. Minton, J. C. Venter, and D. C. Schwartz. 1999. Whole-genome shotgun optical mapping of *Deinococcus radiodurans*. Science **285**:1558-62.

Lipton, M. S., L. Pasa-Tolic', G. A. Anderson, D. J. Anderson, D. L. Auberry, J. R. Battista, M. J. Daly, J. Fredrickson, K. K. Hixson, H. Kostandarithes, C. Masselon, L. M. Markillie, R. J. Moore, M. F. Romine, Y. Shen, E. Stritmatter, N. Tolic', H. R. Udseth, A. Venkateswaran, K. K. Wong, R. Zhao, and R. D. Smith. 2002. Global analysis of the *Deinococcus radiodurans* proteome by using accurate mass tags. Proc Natl Acad Sci U S A **99**:11049-54.

Liu, Y., J. Zhou, M. Omelchenko, A. Beliaev, A. Venkateswaran, J. Stair, L. Wu, D. K. Thompson, D. Xu, I. B. Rogozin, E. K. Gaidamakova, M. Zhai, K. S. Makarova, E. V. Koonin, and M. J. Daly. 2003. Transcriptome dynamics of *Deinococcus radiodurans* recovering from ionizing radiation. Proc Natl Acad Sci U S A.**100**:4191-6.

Lodish, H., A. Berk, S. L. Zipursky, P. Matsudaira, D. Baltimore, and J. E. Darnell. 2000. Molecular Cell Biology. 4th Ed. W H Freeman & Co. New York.

Lowry, O., H., Rosebrough, N. J., Farr, A. L., and R. J. Randall. 1951. Protein measurement with the folin phenol reagent. J. Biol. Chem. **193**:265-275.

Macilwain, C. 1996. Science seeks weapons clean-up role. Nature **383**:375-379.

Makarova, K.S., L. Arvind, Yuri I. Wolf, R. l. Tautsov, Kenneth W. Minton, Eugene V. Koonin., and Michael J. Daly. 2001. Genome of extremely Radiation Resistant Bacterium *Deinococcus radiodurans* Viewed from the Perspective of Comparative Genomics. Micro. and Molecular Biol. Rev. **65**:44-79.

Makarova, K. S., L. Aravind, M. J. Daly, and E. Koonin. 2000. Specific expansion of protein families in the radioresistant bacterium *Deinococcus radiodurans*. Genetica. **108**:25-34.

Makarova, K. S., Y. I. Wolf, O. White, K. Minton, and M. J. Daly. 1999. Short repeats and IS elements in the extremely radiation-resistant bacterium *Deinococcus radiodurans* and comparison to other bacterial species [In Process Citation]. Res Microbiol **150:**711-24.

Mann M., R. C. Hendrickson, and A. Pandey. 2001. Analysis of proteins and proteomes by mass spectrometry. Annu Rev Biochem.**70**:437-73.

Marcotte, E. M., M. Pellegrini, H. L. Ng, D. W. Rice, T. O. Yeates, and D. Eisenberg. 1999. Detecting protein function and protein-protein interactions from genome sequences. Science **285:**751-3.

Markillie, L. M., S. M. Varnum, P. Hradecky, and K. K. Wong. 1999. Targeted mutagenesis by duplication insertion in the radioresistant bacterium *Deinococcus radiodurans*: radiation sensitivities of catalase (katA) and superoxide dismutase (sodA) mutants. J Bacteriol **181:**666-9.

Masters, C. I., and K. W. Minton. 1992. Promoter probe and shuttle plasmids for *Deinococcus radiodurans*. Plasmid **28:**258-61.

Masters, C. I., B. E. Moseley, and K. W. Minton. 1991a. AP endonuclease and uracil DNA glycosylase activities in *Deinococcus radiodurans*. Mutat Res **254:**263-72.

Masters, C. I., M. D. Smith, P. D. Gutman, and K. W. Minton. 1991b. Heterozygosity and instability of amplified chromosomal insertions in the radioresistant bacterium *Deinococcus radiodurans*. J Bacteriol **173:**6110-7.

Mathews, D. H., T. C. Andre, J. Kim, D. H. Turner, and M. Zuker. 1998. An updated recursive algorithm for RNA secondary structure prediction with improved free energy parameters. Am.Chem.Soc.Symp.Ser **682:**246-57.

Mattimore, V., and J. R. Battista. 1996. Radioresistance of *Deinococcus radiodurans*: functions necessary to survive ionizing radiation are also necessary to survive prolonged desiccation. J Bacteriol **178**:633-7.

Mattimore, V., K. S. Udupa, G. A. Berne, and J. R. Battista. 1995. Genetic characterization of forty ionizing radiation-sensitive strains of *Deinococcus radiodurans*: linkage information from transformation. J. Bacteriol. **177**: 5232-5237.

Maxcy, RB., and Rowley, DB. 1978. Radiation-resistant vegetative bacteria in a proposed system of radappertization of meats. In food preservation by irradiation. vienna: International Atomic Energy Agency.

Maxim A.M., and Gilbert W. 1977. A new method for sequencing DNA. Proc. Natl. Acad. Sci. **74**: 560-564.

Mechold, U., and H. Malke. 1997. Characterization of the stringent and relaxed responses of *Streptococcus equisimilis*. J. Bacteriol. **179**: 2658-2667.

Mechold, U., M. Cashel, K. Steiner, D. Gentry, and H. Malke. 1996. Functional analysis of *relA/spoT* gene homolog from *Streptococcus equisimilis*. J. Bacteriol. **178**: 1401-1411.

McCord, J. M., Keele, B. B. & Fridovich, I. 1971. An enzyme-based theory of obligate anaerobiosis: the physiological function of superoxide dismutase. *Proc. Natl. Acad. Sci. USA*, **68**:1024-1027.

McCullough, J., T. C. Hazen, S. M. Benson, F. Blaine-Metting, and A. C. Palmisano. 1999. Bioremediation of metals and radionuclides, US Dept. of Energy, Office of Biological and Environmental Research, Germantown, MD20874.

Messner, K. R., and J. A. Imlay. 1999. The identification of primary sites of superoxide and hydrogen peroxide formation in aerobic respiratory chain and sulfite reductase complex of *Escherichia coli*. J. Biol. Chem. **274**:10119-10128.

Messner, K. R., and J. A. Imlay. 2002. Mechanism of superoxide and hydrogen peroxide formation by fumarate reductase, succinate dehydrogenase, and aspartate oxidase. J. Biol. Chem. **277**:42563-42571.

Miller, J.H. and W.S.E. Reznikoff. 1978. *The Operon.* Cold Spring Harbor Laboratory, Cold Spring Harbor, NY.

Minck, F. 1896. Zur Frage der Wirkmamkeit der Rontgen-strahlung auf Bakterien, sowie die Moglichkeit ihrer eventuellen Awendung. Muenchn. Med. Wochensschr. **5**:101.

Minton, K. W. 1996. Repair of ionizing-radiation damage in the radiation resistant bacterium *Deinococcus radiodurans*. Mutat Res **363:**1-7.

Minton, K. W., and M. J. Daly. 1995. A model for repair of radiation-induced DNA double-strand breaks in the extreme radiophile *Deinococcus radiodurans*. Bioessays **17**(5):457-64.

Minton, K. W. 1994. DNA repair in the extremely radioresistant bacterium *Deinococcus radiodurans*. Mol Microbiol **13:**9-15.

Moseley, B. E. B. 1984. Radiation damage and its repair in non-sporulating bacteria. *Soc. Appl. Bacteriol. Symp. Ser.* **12**:147-174.

Moseley, B. E., and D. M. Evans. 1983. Isolation and properties of strains of *Micrococcus (Deinococcus) radiodurans* unable to excise ultraviolet light-induced pyrimidine dimers from DNA: evidence for two excision pathways. J Gen Microbiol **129:**2437-45.

Moseley, B. E. B., and H. R. J. Copland. 1978. Four mutants of Micrococcus radiodurans defective in the ability to repair DNA damaged by mitomycin-C, two of which have wild-type resistance to ultraviolet radiation. Mol. Gen. Genet. **160**:331-37.

Moseley, B. E., and J. K. Setlow. 1968. Transformation in *Micrococcus radiodurans* and the ultraviolet sensitivity of its transforming DNA. Proc Natl Acad Sci U S A **61:**176-83.

Mortia. R. Y. 1975. Psychrophilic bacteria. Bacteriology Review.

Mun, C., J. Del Rowe, M. Sandigursky, K. W. Minton, and W. A. Franklin. 1994. DNA deoxyribophosphodiesterase and an activity that cleaves DNA containing thymine glycol adducts in *Deinococcus radiodurans*. Radiat Res **138:**282-5.

Murray, R. G. E. 1992. The family *Deinococcaceae*, p. 3732-3744. *In* A. Ballows, H. G. Truper, M. Dworkin, W. Harder, and K. H. Schleifer (ed.), The Prokaryotes, vol. 4. Springer-Verlag, New York.

Murray, R. G. E. 1986. Family II. *Deinococcaceae*, p. 1035-43. *In* P. H. A. Sneath, N. S. Mair, M. E. Sharpe, and J. G. Holt (ed.), Bergey's manual of systematic bacteriology, vol. 2. The Williams & Wilkins Co., Baltimore, Md.

Murray, R. G. E., Hall, M. & Thompson, B. G. 1983. Cell division in *Deinococcus radiodurans* and a method for displaying septa. Can. J. Microbiol. **29**:1412-1423.

Murray, R. G. E., and C. F. Robinow. 1958. Presented at the The Seventh International Congress for Microbiology, Stockholm.

Narumi I, Satoh K, Kikuchi M, Funayama T, Yanagisawa T, Kobayashi Y, Watanabe H, Yamamoto K. 2001. The LexA protein from *Deinococcus radiodurans* is not involved in RecA induction following gamma irradiation. J Bacteriol **183**:6951-6

Narumi, I., K. Cherdchu, S. Kitayama, and H. Watanabe. 1997. The *Deinococcus radiodurans* uvr A gene: identification of mutation sites in two mitomycin-sensitive strains and the first discovery of insertion sequence element from deinobacteria. Gene **198**:115-26.

Narumi, I., K. Satoh, M. Kikuchi, T. Funayama, S. Kitayama, T. Yanagisawa, H. Watanabe, and K. Yamamoto. 1999. Molecular analysis of the *Deinococcus radiodurans recA* locus and identification of a mutation site in a DNA repair-deficient mutant, rec30. Mutat Res **435**:233-43.

Naudet, R. 1976. The Oklo nuclear reactors: 1800 Million years ago. Interdisciplinary Science Reviews **1**:74-84.

Nelson, K. E., R. A. Clayton, S. R. Gill, M. L. Gwinn, R. J. Dodson, D. H. Haft, E. K. Hickey, J. D. Peterson, W. C. Nelson, K. A. Ketchum, L. McDonald, T. R. Utterback, J. A. Malek, K. D. Linher, M. M. Garrett, A. M. Stewart, M. D. Cotton, M. S. Pratt, C. A. Phillips, D. Richardson, J. Heidelberg, G. G. Sutton, R. D. Fleischmann, J. A. Eisen, C. M. Fraser, and et al. 1999. Evidence for lateral gene transfer between Archaea and bacteria from genome sequence of Thermotoga maritima. Nature **399**:323-9.

Nelson K. E., I. T. Paulsen, J. F. Heidelberg, and C. M. Fraser. 2000. Status of genome projects for nonpathogenic bacteria and archaea. Nature Biotechnology. **18**: 1049-1054.

O'Halloran, T. V. 1993. Transition metals in control of gene expression [see comments]. Science **261**:715-25.

Olsen, G. J., and C. R. Woese. 1993. Ribosomal RNA: a key to phylogeny. Faseb J **7**(1):113-23.

Oyaizu, H. 1987. A radiation-resistant rod-shaped bacterium, *Deinobacter grandis* gen. nov., sp. nov., with peptidoglycan containing ornithine. Int. J. Syst. Bacteriol. **37**:62-67.

Pandey A., and Mann M. 2000. Proteomics to study genes and genomes. Nature. **405**: 837-846.

Park, S., and J. A. Imlay. 2003. High Levels of Intracellular Cysteine Promote Oxidative DNA damage by Driving the Fenton Reaction. Journal of Bac. **185**:1942-1950.

Perkel JM. 2001. Mass Spectrometry applications for applications for proteomics. The Scientist. August: 31-32.

Ponting, C. P., L. Aravind, J. Schultz, P. Bork, and E. V. Koonin. 1999. Eukaryotic signalling domain homologues in archaea and bacteria. Ancient ancestry and horizontal gene transfer. J Mol Biol **289**:729-45.

Posey, J. E. and Gheradhini, F. C. 2000. Lack of a role for iron in the Lyme disease pathogen. Science **288**:1651-1653.

Price P. B., O. V. Nagornov, R. Bay, D. Chirkin, Y. He, P, Miocinovic, A Richards, K Woschnagg, B. Koci, and V. Zagorodnov. 2002. Temperature profile for glacial ice at the South Pole: Implications for life in a nearby subglacial lake. PNAS. **99**:7844-7847.

Punita, S. J., M. A. Reddy, and H. K. Das. 1989. Multiple chromosomes of Azotobacter vinladdii. J.Bacteriol. **171**:3133-8.

Quintela, J. C., F. Garcia-del Portillo, E. Pittenauer, G. Allmaier, and M. A. de Pedro. 1999. Peptidoglycan fine structure of the radiotolerant *bacterium Deinococcus radiodurans* Sark. J Bacteriol **181**:334-7.

Quintela, J. C., E. Pittenauer, G. Allmaier, V. Aran, and M. A. de Pedro. 1995. Structure of peptidoglycan from *Thermus thermophilus* HB8. J Bacteriol **177**:4947-62.

Raj, H. D., F. L. Duryee, A. M. Deeney, C. H. Wang, A. W. Anderson, P. R. Elliker. 1960. Utilization of carbohydrates and amino acids by *Micrococcus radiodurans*. Can. J. Microbiol. **6**: 289-298.

Rainey, F. A., M. F. Nobre, P. Shumann, E. Stackebrandt, and M. S. Da Costa. 1997. Phylogenetic diversity of the deinococci as determined by 16S ribosomal DNA sequence comparison. Int. J. Syst. Bacteriol. **47**:510-514.

Rebeyrotte, N. 1983. Induction of mutation in *Micrococcus radiodurans* by N-methyl-N'-nitro-N- nitrosoguanidine. Mutat Res **108**:57-66.

Reitzer, L.J. and B. Magasanik. 1987. Ammonia assimilation and the biosynthesis of glutamine, glutamate, aspartate, asparagine, L-alanine, and D-alanine. In *Escherichia coli and Salmonella typhimurium: Cellular and Molecular Biology* (eds. F.C. Neidhardt J.L. Ingraham K.B. Low B. Magasanik M. Schaechter, and H.E. Umbarger). American Society for Microbiology, Washington, D.C.

Repine, J. E., O.W. Pfenninger, D.W. Talmage, E.M. Berger and D.E. Pettijohn. 1981. Dimethyl sulfoxide prevents DNA nicking mediated by ionizing radiation or/hydrogen peroxide-generated hydroxyl radical. Proc Natl Acad Sci U S A **78**:1001-3.

Reynolds, E. S. 1963. The use of lead citrate at high pH as an electron opaque stain in electron microscopy. J. Cell Biol. **17**:208-213.

Richmond, R. C., R. Sridhar, and M. J. Daly. 1999. Physicochemical survival pattern for the radiophile *Deinococcus radiodurans*: A polyextremophile model for life on Mars. SPIE 3755:210-222.

Richmond, C.S., J.D. Glasner, R. Mau, H. Jin, and F.R. Blattner. 1999. Genome-wide expression profiling in *Escherichia coli* K-12. Nucleic Acids Res **27:** 3821-3835.

Riley, R. G., J. M. Zachara, and F. J. Wobber. 1992. Chemical contaminants on DOE lands and selection of contaminant mixtures for subsurface science research. US Dept. of Energy, Office of Energy Research, Subsurface Science Program, Washington, DC 20585.

River Protection Project (RPP). Field Investigation Report for Waste Management Area S-SX. RPP-7885, Rev. Prepared for the Office of River Protection by CH2M Hill Hanford Group, Richland, Washington (2002).

Rivkina E. M., E. I. Friedmann, C. P. Mckay, and D. A. Gilichinsky. 2000. Metabolic activity of Permafrost bacteria below the freezing point. Appli. Environ. Microb. **66**:3230-3233.

Rohde W., J. W. Randles, P. Langridge, D. Hanold. 1990. Nucleotide sequence of a circular single-stranded DNA associated with coconut foliar decay virus. Virology. Jun;**176**:648-51.

Sadoff, H. L., B. Shimel, and S. Ellis. 1979. Characterization of Azotobacter vinelandii deoxyribonucleic acid and folded chromosomes. J Bacteriol **138:**871-7.

Sambrook, J., E. Fritsch, and T. Maniatis. 1989. Molecular Cloning: a laboratory manual, 2nd ed. Cold Spring Harbor Laboratory Press, Cold Spring Harbor, N. Y.

Sanders, S. W., and R. B. Maxcy. 1979. Isolation of radiation-resistant bacteria without exposure to irradiation. Appl. Environ. Microbiol. 1979 Sep; **38**:436-9.

Sandigursky, M., and W. A. Franklin. 1999. Thermostable uracil-DNA glycosylase from *Thermotoga maritima* a member of a novel class of DNA repair enzymes. Curr Biol **9**:531-4.

Sanger, F., Nickson s., and Coulson A. R. 1977a. DNA sequencing with chain terminating inhibitors. Proc. Natl. Acad. Sci. **74**:5463-5467.

Satoh K, Narumi I, Kikuchi M, Kitayama S, Yanagisawa T, Yamamoto K, Watanabe H. 2002. Characterization of RecA424 and RecA670 proteins from *Deinococcus radiodurans*. J Biochem (Tokyo) **131**:121-9

Schaffer, A. A., Y. I. Wolf, C. P. Ponting, E. V. Koonin, L. Aravind, and S. F. Altschul. 1999. IMPALA: matching a protein sequence against a collection of PSI-BLAST- constructed position-specific score matrices. Bioinformatics **15:**1000-11.

Schleifer, K. H., and O. Kandler. 1972. Peptidoglycan types of bacterial cell walls and their taxonomic implications. Bacteriol Rev **36:**407-77.

Schlenk, D. 1998. Occurrence of flavin-containing monooxygenases in non-mammalian eukaryotic organisms. Comp Biochem Physiol C Pharmacol Toxicol Endocrinol **121:**185-95.

Schulte-Frohlinde, D. 1986. Mechanism of radiation-induced strand break formation in DNA and polynucleotides. Adv. Space Res. **6**:89-96.

Schultz, J., R. R. Copley, T. Doerks, C. P. Ponting, and P. Bork. 2000. SMART: a web-based tool for the study of genetically mobile domains. Nucleic Acids Res **28:**231-234.

Schultz, J., F. Milpetz, P. Bork, and C. P. Ponting. 1998. SMART, a simple modular architecture research tool: identification of signaling domains. Proc Natl Acad Sci U S A **95:**5857-64.

Setlow, D. M., and D. E. Duggan. 1964. The resistance of *Micrococcus radiodurans* to ultraviolet radiation: Ultraviolet-induced lesions in the cell's DNA. Biochim. Biophys. Acta **87:**664-8.

Shanado, Y., J. Kato, and H. Ikeda. 1998. *Escherichia coli* HU protein suppresses DNA-gyrase-mediated illegitimate recombination and SOS induction. Genes Cells **3:**511-20.

Shapiro, A., D. DiLello, M. C. Loudis, D. E. Keller, S. H. Hutner. 1977. Minimal requirements in defined media for improved growth of some radioresistant pink tetracocci. Appl. Environ. Microbiol. **33**:1129-1133.

Shapiro, J. 2002. Radiation Protection. A guide for scientists, regulators and physicians. Fourth edition. Harvard University Press

Shen Y., and R. D. Smith. 2002. Proteomics based on high-efficiency capillary separations. Electrophoresis.**23**:3106-24.

Shi T., R. H. Reeves, D. A. Gilichinsky, and E. I. Friedmann. 1997. Characterization of viable bacteria from Siberian permafrost by 16s rDNA sequencing. Microb. Ecol. **33**:169-179.

Slater, T. F., K. H. Cheeseman, M. J. Davies, K. Proudfoot, and W. Xin. 1987. Free radical mechanisms in relation to tissue injury. Proc. Nutr. Soc. Feb;**46**:1-12

Sleytr, U. B., and A. M. Glauert. 1982. Bacterial cell walls and membranes, p. 41-76. *In* J. R. Harris (ed.), Electron microscopy of proteins, vol. **3**. Academic Press, London.

Sleytr, U. B., M. Kocur, A. M. Glauert, and M. J. Thornley. 1973. A study by freeze-etching of the fine structure of *Micrococcus radiodurans*. Arch Mikrobiol **94**:77-87.

Smith, K. C., and K. D. Martignoni. 1976. Protection of *Escherichia coli* cells against the lethal effects of ultraviolet and x irradiation by prior x irradiation: a genetic and physiological study. Photochem Photobiol **24**:515-23.

Smith RD, Anderson GA, Lipton MS, Masselon C, Pasa-Tolic L, Shen Y, Udseth HR. 2002a. The use of accurate mass tags for high-throughput microbial proteomics. OMICS **6**:61-9

Smith RD, Anderson GA, Lipton MS, Pasa-Tolic L, Shen Y, Conrads TP, Veenstra TD, Udseth HR. 2002b. An accurate mass tag strategy for quantitative and high-throughput proteome measurements. Proteomics **2**:513-23

Smith, M. D., C. I. Masters, E. Lennon, L. B. McNeil, and K. W. Minton. 1991. Gene expression in *Deinococcus radiodurans*. Gene **98**:45-52.

Smith, M. D., R. Abrahamson, and K. W. Minton. 1989. Shuttle plasmids constructed by the transformation of an *Escherichia coli* cloning vector into two Deinococcus radiodurans plasmids. Plasmid **22**:132-42.

Smith, M. D., E. Lennon, L. B. McNeil, and K. W. Minton. 1988. Duplication insertion of drug resistance determinants in the radioresistant bacterium *Deinococcus radiodurans*. J Bacteriol **170**:2126-35.

Snel, B., P. Bork, and M. Huynen. 2000. Genome evolution. Gene fusion versus gene fission. Trends Genet **16**:9-11.

Sobel, M. E., and K. Kruwlwich. 1973. Metabolism of D-fructose by *Arthrobacter pyridinolis*. J. Bacteriol. **113**: 907-913.

Sonntag, C. Von. 1987. The chemical basis of radiation biology. Taylor & Francis, London, ISBN 0-85066-375-X.

Sorenson, J. A. 1986. Perception of radiation hazards. Semin Nucl Med **16:**158-70.

Stan-Lotter H., T. J. McGenity, A. Legat *et al.* 1999. Very similar strains of Halococcus salifodinae are found in geographically seperated Permo-Triassic salt deposits. Microbiology. **145**: 3565-3574.

Sweet, D. M., and B. E. Moseley. 1976. The resistance of *Micrococcus radiodurans* to killing and mutation by agents which damage DNA. Mutat Res **34:**175-86.

Sweet, D. M., and B. E. Moseley. 1974. Accurate repair of ultraviolet-induced damage in *Micrococcus radiodurans*. Mutat Res **23:**311-8.

Tan, S. T., and R. B. Maxcy. 1986. Simple method to demonstrate radiation-inducible radiation resistance in microbial cells. Appl Environ Microbiol **51:**88-90.

Tanaka, A., H. Hirano, M. Kikuchi, S. Kitayama, and H. Watanabe. 1996. Changes in cellular proteins of *Deinococcus radiodurans* following gamma-irradiation. Radiat Environ Biophys **35:**95-9.

Tao, H., C. Bausch, C. Richmond, F. R. Blattner, and T. Conway. 1999. Functional genomics: expression analysis of *Escherichia coli* growing on minimal and rich medium. J. Bacteriol. **181**:6425-6440.

Tatusov, R. L., M. Y. Galperin, D. A. Natale, and E. V. Koonin. 2000. The COG database: a tool for genome-scale analysis of protein functions and evolution. Nucleic Acids Res **28:**33-36.

Tatusov, R. L., E. V. Koonin, and D. J. Lipman. 1997. A genomic perspective on protein families. Science **278:**631-7.

Taylor, B. L., and I. B. Zhulin. 1999. PAS domains: internal sensors of oxygen, redox potential, and light. Microbiol Mol Biol Rev **63:**479-506.

Tempest, P. R., and B. E. Moseley. 1982. Lack of ultraviolet mutagenesis in radiation-resistant bacteria. Mutat Res. **104**:275-80.

Thompson, B. G., R. Anderson, and R. G. E. Murray. 1980. Unusual polar lipids of *Micrococcus radiodurans* strain SARK. Can. J. Microbiol. **26:**1408-11.

Thompson, B. G., and R. G. E. Murray. 1982. The association of the surface array and the outer membrane of *Deinococcus radiodurans*. Can. J. Microbiol. **28:**1081-1088.

Thompson, B. G., and R. G. Murray. 1981. Isolation and characterization of the plasma membrane and the outer membrane of *Deinococcus radiodurans* strain Sark. Can J Microbiol **27**:729-34.

Thornley, M. J., R. W. Horne, and A. M. Glauert. 1965. The fine structure of *Micrococcus radiodurans*. Arch Mikrobiol **51**:267-89.

Thornley, M. J. 1963. Radiation resistance among bacteria. J.Appl.Bacteriol. **26**:539-47.

Tirgari, S., and B. E. B. Moseley. 1980. Transformation in *Micrococcus radiodurans*: measurement of various parameters and evidence of multiple independently segregatine genomes per cell. J. gen. Micro. **119**:287-296.

Toder, R. 2002. DNA arrays as diagnostic tools in human healthcare. Expert Rev Mol Diagn. **2**:422-8

Touati D. 2000. Iron and oxidative stress in Bacteria. Archives of Biochemistry and Biophysics. **373**: 1-6.

Touati, D., M. Jacques, B. Tardat, L. Bouchard, and S. Despied. 1995. Lethal oxidative damage and mutagenesis are generated by iron in delta *fur* mutants of *Escherichia coli*: protective role of superoxide dismutase. J. Bacteriol. **177**:2305-2314.

Taurova, T. P., E. S. Garnova, T. N. Zhilina. 1999. Phylogenetic diversity of alkaliphilic anaerobic saccharolytic bacteria isolated from a soda lake. Microbiology. **68**: 615-622.

Udupa, K. S., P. A. O'Cain, V. Mattimore, and J. R. Battista. 1994. Novel ionizing radiation-sensitive mutants of *Deinococcus radiodurans*. J Bacteriol **176**:7439-46.

Varghese, A. J. and R. S. Day. 1970. Excision of cytosine-thymine adduct from the DNA of ultraviolet-irradiated *Micrococcus radiodurans*. Photochem Photobiol. **11**:511-517.

Vasilenko, A., A. Venkateswaran, Y. Liu, M. Omelchenko, E. K. Gaidamakova, M. Zhai, H Brim, K. K. Wong, K. S. Makarova, D. Ghosal, J. Zhou, and M. J. Daly. 2003. Relationship between Metabolism, Oxidative Stress and Radiation Resistance in the Family *Deinococcaceae*. Submitted for publication.

Vasilenko, A, E. K. Gaidamakova, V. Matrosova, D. Ghosal, M. Zhai, A. Venkateswaran, H. Brim, M. Hess, M. Omelchenko, H. M. Kostandarithes, K. S.

Makarova, J. K. Fredrickson, and M. J. Daly. 2003. Role of DNA Protection in the Extraordinary Survival of *Deinococcus radiodurans*. Submitted to Science.

Van Gerwen, S.J., F. M. Rombouts, K. van't Riet, and M. H. Zwietering. A data analysis of the irradiation parameter D10 for bacteria and spores under various conditions. J Food Prot. 1999 62:1024-32.

Venkateswaran A., S. C. McFarlan, D. Ghosal, K. W. Minton, A. Vasilenko, K. Makarova, L. P. Wackett, and M. J. Daly. 2000. Physiologic determinants of radiation resistance in *Deinococcus radiodurans*. Appl Environ Microbiol. **66**:2620-6.

Venter, J. C. *et al.*, 2000. The sequence of Human Genome. Science. **291**: 1304-1351.

Vukovic-Nagy, B., B. W. Fox, and M. Fox. 1974. The release of a deoxyribonucleic acid fragment after x-irradiation of *Micrococcus radiodurans*. Int J Radiat Biol Relat Stud Phys Chem Med **25**:329-37.

Wang, R., K. Guegler, S.T. LaBrie, and N.M. Crawford. 2000. Genomic analysis of a nutrient response in Arabidopsis reveals diverse expression patterns and novel metabolic and potential regulatory genes induced by nitrate. *Plant Cell* **12**: 1491-1509.

Wang, P., and H. E. Schellhorn. 1995. Induction of resistance to hydrogen peroxide and radiation in *Deinococcus radiodurans*. Can J Microbiol **41**:170-6.

Watson, J. 2000. The double helix revisited. *Time Magazine*, **156**, July 3, (http://www.time.com/time/magazine/articles/0,3266,48104,00.html).

Wendrich, T. M., and M.A. Marahiel. 1977. Cloning and characterization of a relA/SpoT homologue from *Bacillus subtilis*. Mol. Microbiol. **26**: 65-79.

Werneburg, B. G., J. Ahn, X. Zhong, R. J. Hondal, V. S. Kraynov, and M. D. Tsai. 1996. DNA polymerase beta: pre-steady-state kinetic analysis and roles of arginine-283 in catalysis and fidelity. Biochemistry **35**:7041-50.

White, O., J. A. Eisen, J. F. Heidelberg, E. K. Hickey, J. D. Peterson, R. J. Dodson, D.H. Haft, M.L. Gwinn, W.C. Nelson, D.L. Richardson, K.S. Moffat, H. Qin, L. Jiang, W. Pamphile, M. Crosby, M. Shen, J.J. Vamathevan, P. Lam, L. McDonald, T. Utterback, C. Zalewski, K.S. Makarova, L. Aravind, M.J. Daly, K.W. Minton, R.D. Fleischmann, K.A. Ketchum, K.E. Nelson, S. Salzberg, H.O. Smith, J.C. Venter, and C.M. Fraser. 1999. Genome Sequence of the Radioresistant Bacterium *Deinococcus radiodurans* R1. *Science* **286**: 1571-1577.

Wickware. P. 2001. Proteomics technology: Character references. Nature. **413**: 869-875.

Wittwer, C. T., M. G. Herrmann, A. A. Moss, and R. P. Rasmussen. 1997. Continuous fluorescence monitoring of rapid cycle DNA amplification. BioTechniques **22**: 130-138.

Wolf, Y.I., I.B. Rogozin, A.S. Kondrashov, and E.V. Koonin. 2001. Genome alignment, evolution of prokaryotic genome organization, and prediction of gene function using genomic context. *Genome Res* **11:** 356-372.

Wolf, Y. I., S. E. Brenner, P. A. Bash, and E. V. Koonin. 1999. Distribution of protein folds in the three superkingdoms of life. Genome Res **9:**17-26.

Work, E., and H. Griffiths. 1968. Morphology and chemistry of cell walls of Micrococcus radiodurans. J Bacteriol **95:**641-57.

Xu, W., J. Shen, C.A. Dunn, S. Desai, and M. J. Bessman. 2001. The Nudix hydrolases of *Deinococcus radiodurans*. Mol Microbiol **39:** 286-290.

Xu D, Li G, Wu L, J. Zhou, Y. Xu. 2002. PRIMEGENS: robust and efficient design of gene-specific probes for microarray analysis. Bioinformatics **18**(11):1432-7

Yajima, H., M. Takao, S. Yasuhira, J. H. Zhao, C. Ishii, H. Inoue, and A. Yasui. 1995. A eukaryotic gene encoding an endonuclease that specifically repairs DNA damaged by ultraviolet light. Embo J **14:**2393-9.

Zaider, M., M. Bardas, and A. Fung. 1994. Molecular damage induced directly and indirectly by ionizing radiation in DNA. Int. J. Radiat. Biol. **66:**459-465.

http://www.netspace.org/MendelWeb/Mendel.html. Mendel's Paper in English: Experiments in Plant Hybridization (1865) by Gregor Mendel.

http://www.ncbi.nlm.nih.gov/PMGifs/Genomes/new_org.html. Prominent Organisms Taxonomy List, National Institutes of Health, Bethesda MD.

http://www.ncbi.nlm.nih.gov/PMGifs/Genomes/new_btax.html. Completed and Ongoing Eubacteria Geonome Projects.

List of Publications

APPLIED AND ENVIRONMENTAL MICROBIOLOGY, June 2000, p. 2620–2626 Vol. 66, No. 6
0099-2240/00/$04.00+0

Physiologic Determinants of Radiation Resistance in *Deinococcus radiodurans*

AMUDHAN VENKATESWARAN,[1] SARA C. MCFARLAN,[2] DEBABROTA GHOSAL,[1] KENNETH W. MINTON,[1] ALEXANDER VASILENKO,[1] KIRA MAKAROVA,[1,3]† LAWRENCE P. WACKETT,[2] AND MICHAEL J. DALY[1]*

Department of Pathology, Uniformed Services University of the Health Sciences, Bethesda, Maryland 20814[1]; Department of Biochemistry, Biological Process Technology Institute and Center for Biodegradation Research and Informatics, Gortner Laboratory, University of Minnesota, St. Paul, Minnesota 55108[2]; and National Center for Biotechnology Information, National Library of Medicine, National Institutes of Health, Bethesda, Maryland 20894[3]

Received 29 October 1999/Accepted 17 March 2000

Immense volumes of radioactive wastes, which were generated during nuclear weapons production, were disposed of directly in the ground during the Cold War, a period when national security priorities often surmounted concerns over the environment. The bacterium *Deinococcus radiodurans* is the most radiation-resistant organism known and is currently being engineered for remediation of the toxic metal and organic components of these environmental wastes. Understanding the biotic potential of *D. radiodurans* and its global physiological integrity in nutritionally restricted radioactive environments is important in development of this organism for in situ bioremediation. We have previously shown that *D. radiodurans* can grow on rich medium in the presence of continuous radiation (6,000 rads/h) without lethality. In this study we developed a chemically defined minimal medium that can be used to analyze growth of this organism in the presence and in the absence of continuous radiation; whereas cell growth was not affected in the absence of radiation, cells did not grow and were killed in the presence of continuous radiation. Under nutrient-limiting conditions, DNA repair was found to be limited by the metabolic capabilities of *D. radiodurans* and not by any nutritionally induced defect in genetic repair. The results of our growth studies and analysis of the complete *D. radiodurans* genomic sequence support the hypothesis that there are several defects in *D. radiodurans* global metabolic regulation that limit carbon, nitrogen, and DNA metabolism. We identified key nutritional constituents that restore growth of *D. radiodurans* in nutritionally limiting radioactive environments.

Most of the wastes generated during global nuclear weapons production between 1945 and 1986 were discharged into the ground and are now contaminating the subsurface at thousands of sites (16, 27; http://www.em.doe.gov/bemr96). In 1992, the United States Department of Energy (DOE) surveyed 91 of ~3,000 contaminated sites at 18 research facilities in the United States and reported that millions of cubic meters of such wastes contain mixtures of radionuclides (e.g., ^{235}U), heavy metals (e.g., Hg and Pb), and toxic organic compounds (e.g., toluene) (27). It is estimated that one-third of the DOE waste sites are radioactive, and radiation levels are as high as 10 mCi/liter (27).

Among the technologies currently being developed (19) for treatment of these environmental wastes are bioremediation strategies in which the extremely radiation-resistant organism *Deinococcus radiodurans* R1 is used (3). This bacterium has been the subject of whole-genome optical mapping (15) and sequencing (33) and has recently been engineered to express metal-remediating and organic compound-degrading genes (2, 14).

D. radiodurans R1 is a nonpathogenic, desiccation-resistant (22, 23), solvent-tolerant (14) soil bacterium that can survive acute (short) exposure to an ionizing irradiation dose of 1.5 Mrads, a dose that induces 150 to 200 DNA double-strand breaks per chromosome (7, 15). Also, it has been shown that this bacterium can grow in the presence of chronic (continuous) gamma irradiation (14); this is a process that requires simultaneous semiconservative DNA replication and homologous recombination (24). The molecular mechanisms that underlie the extreme radiation resistance phenotype have been the subject of several investigations (8–11, 17, 23). However, the role of the metabolic repertoire and physiological state of *D. radiodurans* at the time of irradiation has been characterized far less. Little is known about this relationship other than that (i) exponentially growing *D. radiodurans* cells are more sensitive to radiation than stationary-phase cells are (22, 31), (ii) increasing the concentration of Mn^{2+} in cells decreases genomic redundancy along with radiation resistance (6), and (iii) freezing or desiccating *D. radiodurans* substantially increases its radiation resistance (7, 18, 26).

In radioactive environments that do not kill an organism but rather limit or prevent metabolism, genetic damage accumulates, and survival depends on repairing and preventing the accumulation of irreversible (lethal) genetic damage (7–10). Genetic recovery of *D. radiodurans* after such DNA damage occurs is heavily dependent on energy metabolism and protein synthesis (22), and we have recently demonstrated the remarkable ability of *D. radiodurans* to grow in the presence of 6,000 rads/h under nutrient-rich conditions with no effect on its viability, growth rate, or ability to express cloned genes (14). By comparison, *Escherichia coli* is very quickly killed in such environments (14).

* Corresponding author. Mailing address: Department of Pathology, Rm. B3153, Uniformed Services University of the Health Sciences (USUHS), 4301 Jones Bridge Road, Bethesda, MD 20814-4799. Phone: (301) 295-3750. Fax: (301) 295-1640. E-mail: mdaly@usuhs.mil.

† Permanent address: Institute of Cytology and Genetics, Russian Academy of Sciences, Novosibirsk 630090, Russia.

TABLE 1. Minimal nutrient requirements for growth of *D. radiodurans* in the absence and in the presence of gamma irradiation (6,000 rads/h)[a]

Class	Component	Concn necessary for growth	
		(I) Without radiation	(II) With radiation
Buffer	Potassium phosphate buffer (pH 7.5 to 8.0)	20 mM	20 mM
Salts	Magnesium chloride tetrahydrate	0.2 mM	0.2 mM
	Calcium chloride dihydrate	0.1 mM	0.1 mM
	Manganese(II) acetate tetrahydrate	5.0 μM	5.0 μM
	Ammonium molybdate tetrahydrate	5.0 μM	5.0 μM
	Ferrous sulfate heptahydrate	5.0 μM	5.0 μM
Amino acids	L-Histidine	25 μg/ml	200 μg/ml
	L-Cysteine	30 μg/ml	30 μg/ml
	L-Glutamine		500 μg/ml
	L-Alanine		500 μg/ml
	L-Arginine		800 μg/ml
	L-Asparagine		800 μg/ml
	Glycine		300 μg/ml
	L-Leucine		500 μg/ml
	L-Lysine		300 μg/ml
	L-Methionine		100 μg/ml
	L-Proline		370 μg/ml
	L-Serine		300 μg/ml
	L-Threonine		200 μg/ml
	L-Tryptophan		200 μg/ml
	L-Tyrosine		200 μg/ml
	L-Valine		200 μg/ml
Vitamins[b]	Nicotinic acid	1.0 μg/ml	1.0 μg/ml
Carbon source		2 mg/ml	2 mg/ml

[a] Basal salt medium was autoclaved and then supplemented with sterile preparations of salts, amino acids, and nicotinic acid at the concentrations indicated. For solid medium, 1.5% (wt/vol) Noble agar was added before basal salt medium was autoclaved.

[b] Replacing nicotinic acid with Basal Medium Eagle Vitamin Solution (Gibco BRL) improved growth slightly. For growth in liquid minimal medium, the cells used for inoculation were pregrown on solid minimal medium.

The nutrient conditions at DOE radioactive waste sites are poor, and the effect of such nutrient conditions on the growth and survival of *D. radiodurans* was not known previously. Using a defined synthetic minimal medium, we examined the effect of nutrient conditions on the ability of *D. radiodurans* to survive acute or chronic exposure to radiation. We found that while the metabolic state of cells had little effect on cell survival following treatment with acute ionizing radiation, nutrient conditions had a profound effect on the survival and growth of *D. radiodurans* during chronic exposure to irradiation. Under nutrient-limiting conditions during chronic irradiation, DNA repair was found to be limited by the metabolic capabilities of the organism and not by any nutritionally induced defect in genetic repair. The results of our analyses support the hypothesis that global RNA synthesis is suppressed in *D. radiodurans* grown in nutrient-poor environments and the hypothesis that there are several defects in its metabolic pathways.

MATERIALS AND METHODS

Growth of cells. *D. radiodurans* R1 was grown on a nutrient-rich medium, TGY (1% Bacto Tryptone [Difco], 0.5% yeast extract, 0.1% glucose), or on minimal medium (Table 1) in the absence or in the presence of chronic irradiation at a rate of 6,000 rads/h (^{137}Cs Gammacell 40 irradiation unit; Atomic Energy of Canada Limited) at 22°C, as described previously (14). To facilitate growth, liquid minimal medium was inoculated with cells (10^4 to 10^5 cells/ml) that had been pregrown on solid minimal medium. All chemicals were obtained from Sigma Chemical Co.; Bacto Agar and Noble agar were obtained from Difco. In liquid cultures, cell density was determined at 600 nm by using a Beckman spectrophotometer. For acute high-level exposure to radiation, stationary-phase cultures were irradiated without a change of broth on ice at a rate of 1.33 Mrads/h (model 109 ^{60}Co Gammacell irradiation unit; J. L. Shepard and Associates). Following irradiation, cell viability was determined by performing a plate assay as described previously (7).

***rel* Gene function assay.** *rel* function was assayed by using the procedures described by Cashel (4). All eubacteria that have been tested so far are capable of forming guanine nucleotide analogs of GDP and GTP that have a pyrophosphate group esterified to the 3′-hydroxyl of the ribose moiety; these analogs are designated ppGpp and pppGpp, respectively. The RNA control locus *relA* encodes (p)ppGpp synthetase and sometimes forms a hybrid locus containing *spoT*, which encodes 3′-pyrophosphohydrolase (e.g., in *Bacillus subtilis* [32]). RelA is synthesized in bacteria in response to amino acid starvation and indirectly reduces protein synthesis by repressing stable RNA synthesis when the concentrations of amino acids cannot keep up with the demand during protein biosynthesis. RelA-induced RNA suppression has pleiotropic effects, including reductions in DNA replication, transcription, translation, and growth. Together with SpoT, RelA participates in integrating carbon metabolism and nitrogen metabolism (5). RelA activity in *D. radiodurans* cells was determined as follows. Cells were grown on solid TGY for 60 h or on solid minimal (fructose) medium (Table 1) for 170 h. Approximately 10^8 cells were suspended in phosphate-free labeling medium (PFLM) (0.1 M MOPS [morpholinepropanesulfonic acid], 0.2% dextrose, 100 μCi of carrier-free [^{32}P]orthophosphoric acid per ml) that contained or did not contain 1 mg of serine hydroxamate per ml (serine hydroxamate blocks translation and is used to induce *relA-spoT* activity). The authenticities of (p)ppGpp and pppGpp spots were established by using *Escherichia coli* wild-type strain CF1648 and a mutant *E. coli* strain (CF1652) lacking *relA* (20) as controls. A cell suspension (25 μl) was mixed with an equal volume of 13 M formic acid, placed on dry ice, and freeze-thawed twice. A 4-μl portion of the mixture was then spotted onto a cellulose-polyethyleneimine thin-layer chromatography (TLC) plate (Fisher Scientific), and the TLC plate was developed with 1.5 M KH_2PO_4 (pH 3.4). When the solvent front reached 15 cm, the plate was air dried and exposed overnight to X-ray film.

CSLM. Bacterial cells were harvested, washed with 0.1 M Tris-HCl–0.01 M EDTA buffer (pH 8.0), fixed in 77% ethanol (0°C), and stained with acridine orange. The stained preparations were visualized with a Bio-Rad model MRC-600 confocal scanning laser microscope (CSLM) interfaced with a Zeiss Axiovert microscope, as well as a Meridian model ULTIMA ACAS 570 CSLM; ×100 immersion objectives were used. Images were reproduced by using a New

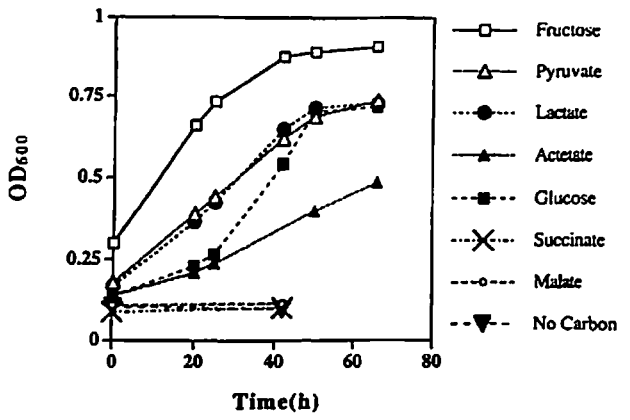

FIG. 1. Growth of *D. radiodurans* in liquid minimal media (Table 1, composition I) containing different carbon sources at a concentration of 2 mg/ml. An optical density at 600 nm (OD_{600}) of 1.0 was equivalent to $\sim 1 \times 10^8$ CFU/ml. Cells were pregrown on solid minimal (fructose) medium before they were inoculated into liquid minimal medium.

Codonics model NP1600 Postscript printer. Acridine orange-stained double-stranded nucleic acid forms a complex that has an absorption maximum at wavelengths between 450 and 490 nm; this complex fluoresces green and is used to localize DNA with a 520-nm barrier filter. An acridine orange-stained single-stranded nucleic acid complex has an absorption maximum at wavelengths between 510 and 560 nm; this complex fluoresces red and is used to localize RNA with a 590-nm barrier filter (12).

Nucleic acid manipulation. Total nucleic acid and DNA were prepared and electrophoresis was performed as described previously (7–10, 29).

RESULTS

Development of a minimal medium suitable for analysis of *D. radiodurans* growth. In the only previous description of a *D. radiodurans* minimal medium that was used to assess growth, Shapiro et al. described a synthetic medium that contained very high concentrations (30 to 600 μg/ml each) of 17 amino acids, which resulted in a medium containing more than 5 mg of amino acids per ml (28). In addition, this minimal medium included a large variety of minerals and vitamins that we have shown to be unnecessary for *D. radiodurans* growth. The excessive concentrations of nonessential nutrients made this medium neither minimal nor useful for our growth studies. In fact, *D. radiodurans* can grow in this medium in the absence of typical Embden-Meyerhof-Parnas (EMP) pathway substrates (e.g., fructose, glucose, and maltose). We, therefore, tried to develop a synthetic medium that is truly minimal, highly characterized, and suitable for testing the metabolic capabilities of *D. radiodurans*, as guided by our analysis of the genomic sequence.

To develop a synthetic minimal medium, we systematically tested many combinations of different amounts of carbohydrates, amino acids, salts, and vitamins in both liquid media and solid media (prepared with Noble agar). By a process of elimination, we identified minimal nutrient constituents and the concentrations of these nutrients necessary for luxuriant growth (Table 1). The synthetic medium which we developed for *D. radiodurans* is distinct from the media described by other workers (25, 28) in that it is much simpler and growth of *D. radiodurans* in the medium is completely dependent on a nonamino carbon source (e.g., fructose) (Fig. 1). In addition to a metabolizable carbon source, growth of *D. radiodurans* is dependent on exogenous amino acids and a vitamin; sulfur-rich amino acids together with nicotinic acid were particularly effective at supporting growth. However, we found that there was not a specific amino acid combination that was necessary since many different combinations of amino acids supported growth. A factor that strongly influenced the extent of growth was the total amino acid concentration in the growth medium (Fig. 2), not the composition of the amino acid pool. We found that carbon sources supported luxuriant to slow growth in the following order: fructose > pyruvate > lactate > glucose > oxaloacetate > acetate > glycerol (Fig. 1). There are numerous examples of free-living bacteria that exhibit absolute specificity for sugar metabolism (e.g., *Arthrobacter* strains can utilize fructose but not glucose [30]). Surprisingly, the tricarboxylic acid cycle intermediates fumarate, citrate, malate, and succinate did not support growth (Fig. 1).

Sensitivity of *D. radiodurans* grown in synthetic medium to chronic irradiation and acute irradiation. To investigate the effect of the nutritional state of *D. radiodurans* on the extreme radiation phenotype of this organism, cells were exposed to continuous gamma irradiation in a ^{137}Cs irradiator (6,000 rads/h) under different growth conditions. Control cultures were incubated in the absence of irradiation at the same temperature. When cells were grown on rich medium (TGY), growth was not affected by continuous exposure to 6,000 rads/h compared to growth on TGY in the absence of irradiation. By contrast, growth on the synthetic medium (Table 1, composition I) was eliminated by chronic exposure to 6,000 rads/h. To determine if chronic irradiation under minimal conditions was bactericidal or bacteriostatic, a series of inoculated minimal medium plates were exposed to 0.1, 0.2, 0.3, 0.4, or 0.5 Mrad in the irradiator. Following exposure, the plates were incubated in the absence of irradiation in order to monitor survival. We found that a dose of 0.3 Mrad was lethal to cells; this contrasts with the ability of *D. radiodurans* to survive 1.7 Mrads of acute irradiation without lethality if cells are allowed to grow and recover in rich medium (7–10). We also examined cell viability and the DNA repair capabilities of chronically irradiated *D. radiodurans* cells incubated in either liquid TGY or minimal medium (Fig. 3). Following incubation in the ^{137}Cs irradiator, cells were collected at intervals for up to 96 h. Some of the cells were plated to examine survival (Fig. 3A), and the remainder were frozen until total DNA was prepared and examined to determine whether degradation occurred (Fig. 3B). Rapid degradation of DNA occurred in cells incubated in minimal me-

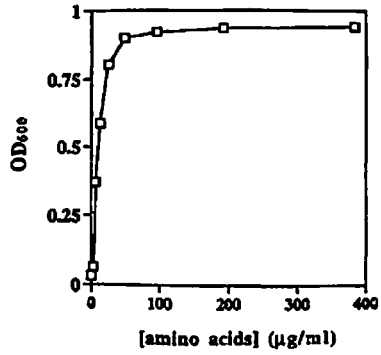

FIG. 2. Relationship between amino acid concentration and growth of *D. radiodurans* in liquid minimal medium. The nutrient conditions were the conditions described in Table 1 except for the amino acid composition. Fructose was the carbon source. The amino acid composition was as follows: glutamine, 25%; cysteine, 18%; and a mixture containing tyrosine, tryptophan, and phenylalanine and buffered with 5% glycine, 10%. Cultures were inoculated with 5×10^6 CFU/ml by using cells that were pregrown on solid minimal (fructose) medium (Table 1). Optical densities at 600 nm (OD_{600}) were determined 96 h after inoculation.

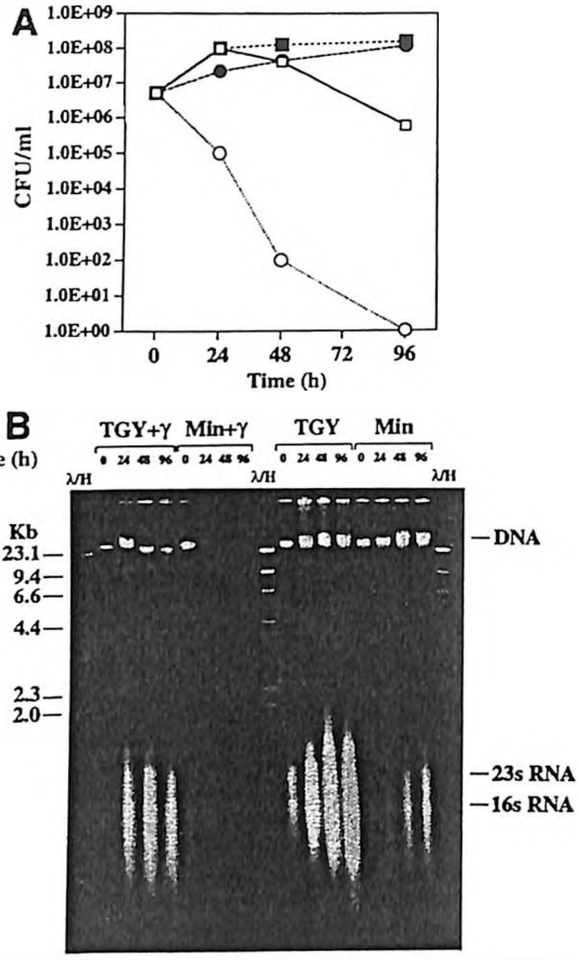

FIG. 3. Effect of nutrient conditions on the viability and DNA content of *D. radiodurans* exposed to chronic gamma irradiation in liquid culture. Cells were irradiated at a rate of 6,000 rads/h (144,000 rads/day) at 23°C. Both irradiated and control cultures were diluted to a concentration 5×10^6 CFU/ml at the start of the experiment. (A) Survival curves. Symbols: ■, control, TGY, no irradiation; □, TGY, gamma irradiation; ●, control, minimal (fructose) medium (Table 1, composition I), no irradiation; ○, minimal (fructose) medium (Table 1, composition I), gamma irradiation. (B) Total DNA was prepared from cells obtained at each of the time points shown in panel A. Each lane contained DNA from ~3×10^6 cells, as determined by hemocytometer counting (7). TGY+γ, cells that were grown in TGY and received gamma irradiation; Min+γ, cells that were grown in minimal (fructose) medium (Table 1, composition I) and received gamma irradiation; TGY and Min, controls incubated in the absence of irradiation. Lanes λ/H contained lambda phage DNA cut with *Hin*dIII. DNA sizes (in kilobases) are indicated on the left. The gel migration positions of DNA and rRNA are indicated on the right. Gel electrophoresis was performed with a 0.66% agarose gel for 17 h at 45 V.

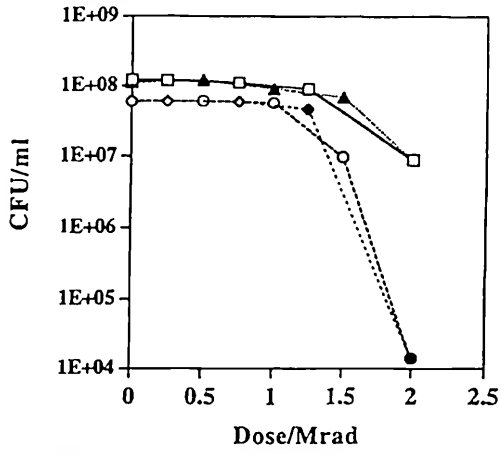

FIG. 4. Effect of growth substrate and recovery substrate on survival of *D. radiodurans* following acute gamma irradiation. Cells were grown to the early stationary phase and irradiated on ice at a rate of 1.33 Mrads/h. Symbols: □, cells pregrown in liquid TGY, irradiated, and plated onto solid TGY; ▲, cells pregrown in liquid TGY, irradiated, and plated onto solid minimal (fructose) medium (Table 1, composition I); ○, cells pregrown in liquid minimal (fructose) medium, irradiated, and plated onto solid TGY; ◆, cells pregrown in liquid minimal (fructose) medium, irradiated, and plated onto solid minimal (fructose) medium.

dium, whereas there was little evidence of DNA degradation in cells incubated in TGY. Some DNA degradation and a loss of viability in cells incubated in TGY were observed with the 48- and 96-h samples, and we believe that this was due to depletion of metabolizable nutrients and the inevitable accumulation of DNA damage in slowly replicating or nonreplicating cells. In contrast, the viability of cells that were incubated in minimal medium and irradiated decreased very substantially almost immediately. After 24 h of irradiation (144,000 rads) (Fig. 3B), the DNA was highly degraded, and all of the cells were dead by 96 h (576,000 rads) (Fig. 3).

To rule out the possibility that cells grown in minimal medium (Table 1, composition I) were inherently sensitive to irradiation and the possibility that certain nutrition-dependent repair factors were not present in our synthetic medium, TGY- and minimal medium-grown *D. radiodurans* cells were tested to determine their ability to survive during extremely high doses of acute gamma irradiation. Figure 4 shows that irrespective of the preirradiation growth medium or the postirradiation recovery substrate, the levels of resistance of *D. radiodurans* were very similar up to a dose of 1.2 Mrads; at doses greater than 1.2 Mrads, minimal medium-grown cells exhibited enhanced sensitivity.

The minimal nutrient conditions required to support growth at a dose of 6,000 rads/h were determined by increasing the concentrations of the nutrients shown in Table 1. When cells were exposed to continuous irradiation, growth was restored only when high concentrations of amino acids were provided together with an EMP or Entner-Doudoroff carbon substrate (Table 1 and Fig. 1). Increasing the concentration of the carbon source or the concentrations of the non-amino acid supplements to values greater than the values shown in Table 1 had no effect on resistance. Similarly, in the absence of a carbon source, high concentrations of amino acids alone did not support growth in the irradiator. Table 1 (composition II) shows the minimal medium nutrients and the concentrations of these nutrients that supported luxuriant *D. radiodurans* growth at a dose of 6,000 rads/h.

Physiologic genomic analysis of *D. radiodurans*. In the course of our annotation of the *D. radiodurans* genome (33), we found that most of the metabolic pathway genes that were key to our analysis were present. For example, the EMP and Entner-Doudoroff pathways were found to be intact, and *D. radiodurans* could grow on fructose, glucose, maltose, and mannose, as expected. However, we found three examples in which the primary biosynthetic pathways of amino acids were incomplete (Table 2). Furthermore, we found that *D. radiodurans* cannot utilize ammonia as a nitrogen source and that growth of this organism is entirely dependent on exogenous amino acids. We, therefore, carefully examined the genomic sequence for defects that could affect nitrogen assimilation.

TABLE 2. Effectiveness of carbon sources as precursors for *D. radiodurans* growth[a]

Carbon and energy source	Growth[b]	Biosynthetic pathway[c]	Genome data[d]	Defect
Pyruvate	+++	Alanine	Complete	
		Valine	Complete	
		Leucine	Complete	
Oxaloactate	++	Isoleucine	Complete	
		Threonine	Complete	
		Lysine	Incomplete	*dapABDF* absent
		Methionine	Complete	
		Aspartic acid	Complete	
Phosphoglycerate	+	Serine	Incomplete	*serCB* absent
		Glycine	Complete	
		Cysteine	Incomplete	*cysEJDN* absent

[a] Acetate and lactate are effective growth substrates, while the tricarboxylic acid cycle intermediates malate, succinate, fumarate, and citrate, are ineffective.
[b] +++, excellent growth; ++, good growth; +, poor growth.
[c] The pathways are the entry points for biosynthesis for the amino acids indicated from the carbon and energy sources listed.
[d] For genomic comparisons, we used metabolic pathways present in *E. coli*. All of the genes necessary for histidine biosynthesis were present.

Generally, the key step in assimilating inorganic nitrogen into amino acids is the synthesis of glutamine and glutamate from ammonia catalyzed by glutamine synthetase (*glnA*). In *D. radiodurans* R1 there are two copies of *glnA*; *glnA-1* (chromosomal position, 2049790) is disrupted by a frameshift mutation, while *glnA-2* (chromosomal position, 447280) appears to be intact. The glutamate synthase subunit genes (*gltB* and *gltD*) also appear to be functional (chromosomal position of operon, 181526); GltB/D integrates carbon metabolism and nitrogen metabolism by synthesizing glutamine from glutamate. Nevertheless, we found that strain R1 could not use 2-oxoglutarate as a growth substrate in minimal medium supplemented with a variety of inorganic nitrogen sources (e.g., ammonium sulfate), suggesting that there may be a defect in assimilation of ammonia in the glutamine synthetase-glutamate synthase cycle.

Correlation between amino acid-limited growth and *relA* activity. RelA and SpoT are responsible for integrating carbon metabolism and nitrogen metabolism (5), and when regulation of these gene products is defective, the genes can have pleiotropic effects on cells that can include dependence on exogenous amino acids for growth and suppression of cellular RNA levels (5). We, therefore, examined *rel* function in *D. radiodurans* at both a genomic informatic level and an experimental level.

We found that *D. radiodurans rel* encodes a predicted protein that is most similar (58% identity) (1) to the RelA/SpoT protein [(p)ppGpp synthetase/3′-pyrophosphohydrolase] of *Bacillus subtilis* (32). We tested the functional integrity of the putative *rel* locus in *D. radiodurans* by monitoring the synthesis of ppGpp and pppGpp under amino acid deprivation conditions (Fig. 5A). Cells were shifted from TGY or minimal medium to labeled phosphate medium (PFLM) containing a single carbon and energy source with or without serine hydroxamate (Fig. 5B and C). Under these conditions, ppGpp and pppGpp were rapidly synthesized and expressed at levels comparable to the levels observed in *E. coli* (Fig. 5). These data support the hypothesis that *rel* function is normal in *D. radiodurans* and is induced under amino-acid-limiting conditions.

Consistent with induction of *rel* functions, we found that cells grown in minimal medium (Table 1, composition I) contained substantially reduced levels of cellular RNA, as deter-

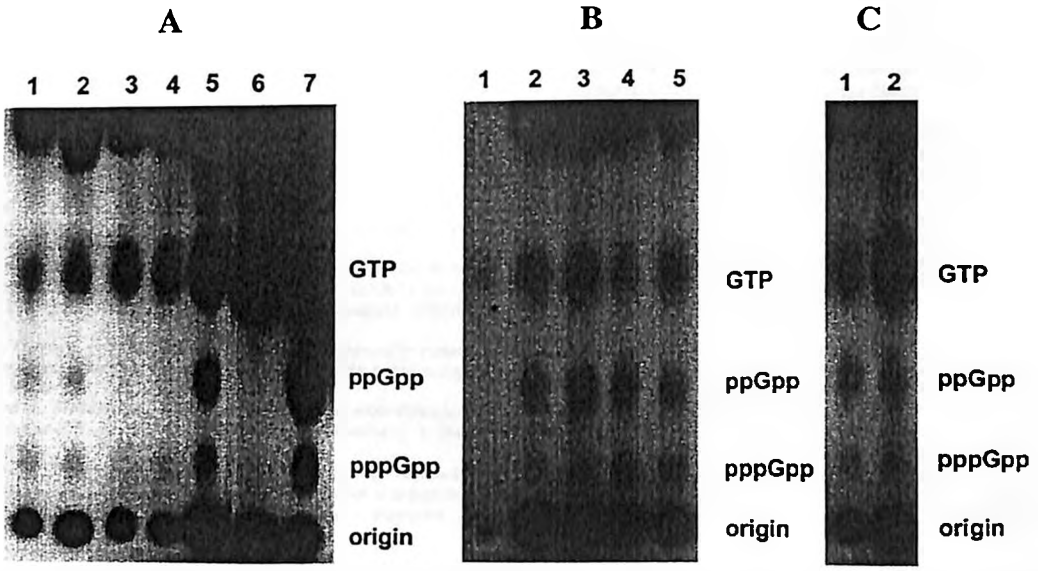

FIG. 5. (A) Production of pp(p)Gpp in *D. radiodurans* and *E. coli*. ^{32}P-labeled ppGpp and pppGpp were detected by polyethyleneimine-cellulose chromatography (see Materials and Methods). Stationary-phase cells grown in either TGY or minimal medium (Table 1) were suspended in PFLM (see Materials and Methods) with or without the amino acid analogue serine hydroxamate. Lanes 1 and 2, *D. radiodurans* cells obtained from minimal (fructose) medium (Table 1, composition I) and incubated in PFLM containing serine hydroxamate (equivalent to lanes 4 and 5 in panel B); lanes 3 and 4, *D. radiodurans* cells obtained from minimal (fructose) medium (Table 1) and incubated in PFLM containing the 16 amino acids listed in Table 1 (final amino acid concentration, 50 μg/ml); lane 5, *D. radiodurans* cells obtained from TGY and incubated in PFLM containing serine hydroxamate; lane 6, *E. coli* (*relA* deleted) incubated in PFLM containing serine hydroxamate (control); lane 7, *E. coli* wild type incubated in PFLM containing serine hydroxamate (control). (B) Formation of ppGpp and pppGpp in *D. radiodurans*. Cells were treated as described above in the presence of serine hydroxamate. Lane 1, control, no cells; lanes 2 and 3, cells grown in TGY; lanes 4 and 5, cells grown in minimal (fructose) medium (Table 1). (C) Formation of ppGpp and pppGpp in *D. radiodurans* grown in minimal medium. Cells were treated as described above. Lane 1, cells treated in the absence of serine hydroxamate; lane 2, cells treated in the presence of serine hydroxamate.

If this occurs, these cells are not able to generate the levels of precursors required for cell division, as well as DNA repair, and, consequently, the cells become overwhelmed by accumulated genetic damage. However, there is no direct evidence that correlates *relA* function and radiation sensitivity in *D. radiodurans* grown in minimal medium.

Our analysis of the minimal nutrient requirements for growth at a dose of 6,000 rads/h showed that in addition to a carbon source that is effectively metabolized by *D. radiodurans*, cells need to have a rich source of amino acids. In order to bioremediate radioactive DOE waste sites with genetically engineered *D. radiodurans* designed for growth on aromatic compounds (15), biostimulation with amino acids will probably be necessary. While further genetic engineering could correct defects in *D. radiodurans* amino acid-biosynthetic pathways, the concept of including a rich source of amino acids in bioremediating protocols is reasonable given the abundance of inexpensive, amino acid-rich by-products of the dairy industry.

ACKNOWLEDGMENTS

This research was funded largely by grant FG07-97ER20293 from the Environmental Science Management Program, Office of Biological and Environmental Research, DOE. Some of this work was also supported by grants FG02-97ER62492 and DE-FG02-98ER62583 from the DOE and by grant 5R01-GM39933-09 from the National Institutes of Health.

We thank Michael Cashel at the National Institutes of Health for his participation and for advice concerning the pp(p)Gpp synthesis analysis.

REFERENCES

1. **Altschul, S. F., T. L. Madden, A. A. Schaffer, J. Zhang, Z. Zhang, W. Miller, and D. J. Lipman.** 1997. Gapped BLAST and PSI-BLAST: a new generation of protein database search programs. Nucleic Acids Res. 25:3389–3402.
2. **Brim, H., S. C. McFarlan, J. K. Fredrickson, K. W. Minton, M. Zhai, L. P. Wackett, and M. J. Daly.** 2000. Engineering *Deinococcus radiodurans* for metal remediation in radioactive mixed waste environments. Nature Biotechnol. 18:85–90.
3. **Brooks, B. W., R. G. E. Murray, J. L. Johnson, E. Stackebrandt, C. R. Woese, and G. E. Fox.** 1980. Red-pigmented micro cocci: a basis for taxonomy. Int. J. Sys. Bacteriol. 30:627–646.
4. **Cashel, M.** 1994. Detection of (p)ppGpp accumulation patterns in *Escherichia coli* mutants. Methods Mol. Genet. 3:341–356.
5. **Cashel, M., and K. E. Rudd.** 1996. The stringent response in *Escherichia coli* and *Salmonella typhimurium*, p. 1410–1438. *In* F. C. Neidhardt et al. (ed.), Cellular and molecular biology. American Society for Microbiology, Washington, D.C.
6. **Chou, F. I., and S. T. Tan.** 1990. Manganese(II) induces cell division and increases in superoxide dismutase and catalase activities in an aging deinococcal culture. J. Bacteriol. 172:2029–2035.
7. **Daly, M. J., L. Ouyang, P. Fuchs, and K. W. Minton.** 1994. In vivo damage and *recA*-dependent repair of plasmid and chromosomal DNA in the radiation-resistant bacterium *Deinococcus radiodurans*. J. Bacteriol. 176:3508–3517.
8. **Daly, M. J., L. Ouyang, and K. W. Minton.** 1994. Interplasmidic recombination following irradiation of the radioresistant bacterium *Deinococcus radiodurans*. J. Bacteriol. 176:7506–7515.
9. **Daly, M. J., and K. W. Minton.** 1995. Interchromosomal recombination in the extremely radioresistant bacterium *Deinococcus radiodurans*. J. Bacteriol. 177:5495–5505.
10. **Daly, M. J., and K. W. Minton.** 1996. An alternative pathway of recombination of chromosomal fragments precedes *recA*-dependent recombination in the radioresistant bacterium *Deinococcus radiodurans*. J. Bacteriol. 178: 4461–4471.
11. **Dardalhon-Samsonoff, M., and D. Averbeck.** 1980. DNA-membrane complex restoration in *Micrococcus radiodurans* after X-irradiation: relation to repair, DNA synthesis and DNA degradation. Int. J. Radiat. Biol. 38:31–52.
12. **Darzynkiewicz, Z.** 1994. Simultaneous analysis of cellular RNA and DNA content. Methods Cell Biol. 41:401–420.
13. **Hansen, M. T.** 1978. Multiplicity of genome equivalents in the radiation-resistant bacterium *Micrococcus radiodurans*. J. Bacteriol. 134:71–75.
14. **Lange, C. C., L. P. Wackett, K. W. Minton, and M. J. Daly.** 1998. Engineering a recombinant *Deinococcus radiodurans* for organopollutant degradation in radioactive mixed waste environments. Nature Biotechnol. 16:929–933.
15. **Lin, J., R. Qi, C. Aston, J. Jing, T. S. Anantharaman, B. Mishra, O. White, M. J. Daly, K. W. Minton, J. C. Venter, and D. C. Schwartz.** 1999. Whole genome shotgun optical mapping of *Deinococcus radiodurans* using genomic DNA molecules. Science 285:1558–1561.
16. **Macilwain, C.** 1996. Science seeks weapons clean-up role. Nature 383:375–379.
17. **Mattimore, V., K. S. Udupa, G. A. Berne, and J. R. Battista.** 1995. Genetic characterization of forty ionizing radiation-sensitive strains of *Deinococcus radiodurans*: linkage information from transformation. J. Bacteriol. 177:5232–5237.
18. **Mattimore, V., and J. R. Battista.** 1996. Radioresistance of *Deinococcus radiodurans*: functions necessary to survive ionizing radiation are also necessary to survive prolonged desiccation. J. Bacteriol. 178:633–637.
19. **McCullough, J., T. C. Hazen, S. M. Benson, F. Blaine-Metting, and A. C. Palmisano.** 1999. Bioremediation of metals and radionuclides. U.S. Department of Energy Office of Biological and Environmental Research, Germantown, Md.
20. **Mechold, U., M. Cashel, K. Steiner, D. Gentry, and H. Malke.** 1996. Functional analysis of *relA/spoT* gene homolog from *Streptococcus equisimilis*. J. Bacteriol. 178:1401–1411.
21. **Mechold, U., and H. Malke.** 1997. Characterization of the stringent and relaxed responses of *Streptococcus equisimilis*. J. Bacteriol. 179:2658–2667.
22. **Minton, K. W.** 1994. DNA repair in the extremely radioresistant bacterium *Deinococcus radiodurans*. Mol. Microbiol. 13:9–15.
23. **Minton, K. W.** 1996. Repair of ionizing-radiation damage in the radiation resistant bacterium *Deinococcus radiodurans*. Mutat. Res. DNA Repair 363: 1–7.
24. **Minton, K. W., and M. J. Daly.** 1995. A model for repair of radiation-induced DNA DSB's in the extreme radiophile *Deinococcus radiodurans*. Bioessays 17:457–464.
25. **Raj, H. D., F. L. Duryee, A. M. Deeney, C. H. Wang, A. W. Anderson, and P. R. Elliker.** 1960. Utilization of carbohydrates and amino acids by *Micrococcus radiodurans*. Can. J. Microbiol. 6:289–298.
26. **Richmond, R. C., R. Sridhar, and M. J. Daly.** 1999. Physicochemical survival pattern for the radiophile *Deinococcus radiodurans*: a polyextremophile model for life on Mars. SPIE 3755:210–222.
27. **Riley, R. G., J. M. Zachara, and F. J. Wobber.** 1992. Chemical contaminants on DOE lands and selection of contaminant mixtures for subsurface science research. U.S. Department of Energy Office of Energy Research Subsurface Science Program, Washington, D.C.
28. **Shapiro, A., D. DiLello, M. C. Loudis, D. E. Keller, and S. H. Hutner.** 1977. Minimal requirements in defined media for improved growth of some radioresistant pink tetracocci. Appl. Environ. Microbiol. 33:1129–1133.
29. **Smith, M. D., E. Lennon, L. B. McNeil, and K. W. Minton.** 1988. Duplication insertion of drug resistance determinants in the radioresistant bacterium *Deinococcus radiodurans*. J. Bacteriol. 170:2126–2135.
30. **Sobel, M. E., and K. Kruwiwich.** 1973. Metabolism of D-fructose by *Arthrobacter pyridinolis*. J. Bacteriol. 113:907–913.
31. **Thornley, M. J.** 1963. Radiation resistance among bacteria. J. Appl. Bacterial. 26:334–345.
32. **Wendrich, T. M., and M. A. Marahiel.** 1977. Cloning and characterization of a relA/SpoT homologue from *Bacillus subtilis*. Mol. Microbiol. 26:65–79.
33. **White, O., J. A. Eisen, J. F. Heidelberg, E. K. Hickey, J. D. Peterson, R. J. Dodson, D. H. Haft, M. L. Gwinn, W. C. Nelson, D. L. Richardson, K. S. Moffet, H. Qin, L. Jiang, W. Pamphile, M. Crosby, M. Shen, J. J. Vamathevan, P. Lam, L. McDonald, T. Utterback, C. Zalewski, K. S. Makarova, L. Aravind, M. J. Daly, K. W. Minton, R. D. Fleishmann, K. A. Ketchum, K. E. Nelson, S. Salzberg, J. C. Venter, and C. M. Fraser.** 1999. Complete genome sequencing of the radioresistant bacterium *Deinococcus radiodurans* R1. Science 286:1571–1577.

Global analysis of the *Deinococcus radiodurans* proteome by using accurate mass tags

Mary S. Lipton*, Ljiljana Paša-Tolić*, Gordon A. Anderson*, David J. Anderson*, Deanna L. Auberry*, John R. Battista†, Michael J. Daly‡, Jim Fredrickson§, Kim K. Hixson*, Heather Kostandarithes¶, Christophe Masselon*, Lye Meng Markillie¶, Ronald J. Moore*, Margaret F. Romine§, Yufeng Shen*, Eric Stritmatter*, Nikola Tolić*, Harold R. Udseth*, Amudhan Venkateswaran‡, Kwong-Kwok Wong¶, Rui Zhao*, and Richard D. Smith*||

*Environmental Molecular Sciences Laboratory, §Biogeochemistry, ¶Molecular Biosciences, Pacific Northwest National Laboratory, P.O. Box 999, MSIN: K8-98, Richland, WA 99352; †Department of Biological Sciences, Louisiana State University, Baton Rouge, LA 70803; and ‡Department of Pathology, Uniformed Services University of the Health Sciences, Bethesda, MD 20814

Edited by Samuel Karlin, Stanford University, Stanford, CA, and approved June 26, 2002 (received for review March 22, 2002)

Understanding biological systems and the roles of their constituents is facilitated by the ability to make quantitative, sensitive, and comprehensive measurements of how their proteome changes, e.g., in response to environmental perturbations. To this end, we have developed a high-throughput methodology to characterize an organism's dynamic proteome based on the combination of global enzymatic digestion, high-resolution liquid chromatographic separations, and analysis by Fourier transform ion cyclotron resonance mass spectrometry. The peptides produced serve as accurate mass tags for the proteins and have been used to identify with high confidence >61% of the predicted proteome for the ionizing radiation-resistant bacterium *Deinococcus radiodurans*. This fraction represents the broadest proteome coverage for any organism to date and includes 715 proteins previously annotated as either hypothetical or conserved hypothetical.

The era of whole-genome DNA sequencing has yielded a nearly completed human genome (1) and many complete and initially annotated genomes for lower organisms, with several hundred more anticipated over the next few years. Effective exploitation of this information requires technologies that provide more comprehensive, higher-throughput, and quantitative analyses of proteomes (i.e., the array of proteins expressed by a cell, tissue, or organism at a given time).

To address this need, we have developed a method for identifying peptides based on accurate mass tags (AMTs) for each protein expressed by a given organism. This approach provides greater sensitivity and dynamic range than previously achievable, more comprehensive coverage of expressed proteins, a basis for precise quantitation, and greater throughput for measurements of proteomes, because protein identification using AMTs circumvents the need for routine tandem MS (MS/MS).

Our initial study has focused on the extremely radiation-resistant bacterium *Deinococcus radiodurans*, but the general approach can be used for any organism whose genome has been sequenced. Two independent annotations are available for the sequenced genome of *D. radiodurans* (2, 3). This organism has been the target of genetic manipulation for a decade, a candidate for bioremediation of radioactive waste sites, and a subject for the study of DNA repair pathways (3, 4). *D. radiodurans* has an extraordinary ability to tolerate both acute and chronic exposure to high levels of ionizing radiation. Exponentially growing cultures of the Gram-positive, nonmotile, red-pigmented, nonpathogenic bacterium are able to withstand 50–100 times more ionizing radiation than *Escherichia coli* (5, 6). *D. radiodurans* can survive 5,000–15,000 Gy of acute ionizing radiation with no loss of viability (depending on the culture conditions) (7), can grow continuously under 60 Gy/hr (8), and has the ability to reduce contaminant metals and radionuclides including Cr, Tc, and U to less soluble species (9). Its resistance to radiation and to other DNA-damaging conditions (e.g., UV light, hydrogen peroxide) and desiccation (10) is likely because of its efficient DNA damage repair (6, 11). It has been suggested that the multiple copies of the *D. radiodurans* genome (4–10 genome equivalents) (11) may be organized to facilitate recombinational repair processes (3, 12). However, the set of predicted genes for *D. radiodurans* appears conventional and does not reveal the basis for its extreme radiation resistance (3). The number of annotated DNA repair enzymes (2, 3) is less than reported for *E. coli*.

Most likely the DNA damage-resistance phenotype is determined collectively by a complex array of interacting proteins (3) as well as by many more subtle structural peculiarities of proteins and DNA. Neither of these resistance motifs is readily inferred from the *D. radiodurans* sequence, underscoring the potential importance of global studies to obtain a better understanding of the interactions involved, such as determining protein expression patterns under stressed and nonstressed conditions (i.e., proteome-wide analyses).

Experimental Protocol

Cell Culture. All cell cultures were inoculated with 10 ml of starter culture in either defined (13) or rich media incubated overnight to confluence. The specific culture conditions are as follows: Defined medium mid-logarithm (log) phase: cells were cultured at 32°C; OD_{600} 0.3–0.4. Defined medium late-log phase: cells were cultured at 32°C; OD_{600} 0.6. Defined medium stationary phase: cells were cultured at 32°C; OD_{600} 0.9. Tryptone/glucose/yeast (TGY) medium mid-log phase: cells were cultured at 32°C; OD_{600} 0.3–0.4. TGY medium late-log phase: cells were cultured at 32°C; OD_{600} 0.6. TGY medium stationary phase: cells were cultured at 32°C; OD_{600} 0.9. For specific stress conditions, all cells were grown to mid-log phase (OD_{600} 0.3–0.4) at 32°C in TGY media before stress unless otherwise noted. Heat shock: incubation temperature was raised to 42°C and further incubated for 1 hr before harvest. Cold shock: incubation temperature was lowered to 0°C and further incubated for 1 hr before harvest. Hydrogen peroxide: H_2O_2 was added to a final concentration of 60 μM and further incubated for 2 hr before harvest. One-week starvation: poststationary phase (OD_{600} 0.9) *D. radiodurans* culture was incubated at 32°C for 1 wk without the addition of fresh medium. Four-week starvation: poststationary phase (OD_{600} 0.9) *D. radiodurans* culture was incubated at 32°C for 4 wk without the addition of fresh medium. Chemical shock: 0.05% (vol/vol) trichloroethylene or xylene was added to the culture and incubated for 2 hr before harvest. Alkaline shock: the

This paper was submitted directly (Track II) to the PNAS office.

Abbreviations: LC, liquid chromatography; FTICR, Fourier transform ion cyclotron resonance; PMT, potential mass tag; AMT, accurate mass tag; MS/MS, tandem MS; TCA, trikarboxylic acid cycle; MMA, mass measurement accuracy; log, logarithm; SOD, superoxide dismutase.

See commentary on page 10943.

||To whom reprint requests should be addressed. E-mail: rds@pnl.gov.

pH of culture was raised from 6.5 to 8.5 with 1 N NaOH and incubated for 1 hr before harvest. For experiments with irradiated cells, *D. radiodurans* was cultured to stationary phase in rich media, diluted, and irradiated without change in broth on ice at 10 kGy/hr [^{60}Co Gammacell irradiation unit, J. L. Sheperd and Associates (San Fernando, CA) Shepard, Model JL 109]. After irradiation, cells were transferred to fresh media to recover before aliquots were taken at 10 time intervals: 0, 0.5, 1, 3, 5, 7, 9, 12, 24, and 36 hr. Cells were harvested by centrifugation at 10,000 × *g* at 4°C, washed three times with PBS, aliquoted, and quick frozen for storage at −80°C.

Cell Lysis and Tryptic Digestion. Cell lysis was achieved by bead beating using three 90-sec cycles at 4,500 rpm in a Biospec (Bartlesville, OK) Minibeadbeater, with a 5-min cool down on ice between cycles. Lysates were immediately placed on ice to inhibit proteolysis. Protein concentration was determined by the BCA assay kit (Pierce). Before liquid chromatography (LC) MS analysis, the protein samples were denatured and reduced by the addition of guanidine hydrochloride (Gdn·HCl) (6 M) and DTT (1 mM) and boiled for 5 min. On reducing the Gdn·HCl concentration to below 2 M with 100 mM NH_4HCO_3 and 5 mM EDTA (pH 8.4), protein samples were digested by using bovine pancreas sequencing grade modified trypsin (Promega) (trypsin/protein, 1:50, wt/wt) at 37°C for 16 hr. Protein lysates were ultracentrifuged for 30 min at 356,000 × *g*, and clear supernatant was dialyzed against 50 mM Tris·HCl at 4°C with 500 molecular weight cutoff cellulose ester membrane. Lysates were subsequently aliquoted and quick frozen in nitrogen and stored in −80°C freezer until analyzed.

Capillary LC Separations. The capillary LC system consisted of a pair of syringe pumps (100-ml ISCO model 100DM) and controller (series D ISCO) and an in-house manufactured mixer, capillary column selector, and sample loop for manual injections. Separations were achieved with 5,000 psi reversed-phase packed capillaries (150 μm i.d. × 360 μm o.d.; Polymicro Technologies, Phoenix) (14) by using two mobile-phase solvents consisting of 0.2% acetic acid and 0.05% trifluoroacetic acid (TFA) in water (A) and 0.1% TFA in 90% acetonitrile/10% water (B). The mobile-phase selection valve was switched from position A to B 10 min after injection, creating an exponential gradient as mobile phase B displaced A in the mixer. Flow through the capillary HPLC column was ≈1.8 μl/min when equilibrated to 100% mobile-phase A.

Initial Mass Tag Development. Eluant from the HPLC was infused into a conventional ion trap MS (LCQ, ThermoFinnigan, San Jose, CA) operating in a data-dependent MS/MS mode over a series of segmented m/z ranges and also with prior fractionation by using ion exchange chromatography. For each cycle, the three most abundant ions from MS analysis were selected for MS/MS analysis by using a collision energy setting of 35%. Dynamic exclusion was used to discriminate against previously analyzed ions. The collision induced dissociation spectra from the conventional ion trap mass spectrometer were analyzed using SEQUEST (15) and the genome sequence of *D. radiodurans*. Preliminary identifications were based on a minimum crosscorrelation score of 2, and these peptides were used as potential mass tags (PMTs) for validation by Fourier transform ion cyclotron resonance (FTICR) measurements. These analyses identified large numbers of polypeptide PMTs, of which ≈70% were then validated as AMTs based on the detection of a species having the predicted mass for the PMT to <1 ppm at the corresponding elution time in the LC-FTICR analysis. The methodology for PMT generation is described in detail elsewhere (16).

Validation of Mass Tags. The 11.4-tesla FTICR mass spectrometer developed at our laboratory uses an electrospray ionization (ESI) interface to an electrodynamic ion funnel assembly coupled to a radio frequency quadrupole for collisional ion focusing and highly efficient ion accumulation and transport to the cylindrical FTICR cell for analysis (17). Mass spectra were acquired with ≈10^5 resolution. To obtain the desired <1-ppm mass measurement accuracy (MMA), a program that uses the multiple charge states (e.g., 2+, 3+) produced by ESI for many protonated polypeptides (18) is applied, followed by the use of "lock masses" (i.e., confidently known species that serve as effective internal calibrants) for each spectrum derived from commonly occurring polypeptides that are identified with high confidence from one capillary LC MS/MS analysis (for each organism) obtained by using FTICR with accurate mass measurements (16). Our calculations show ≈50% of the peptides predicted from *in silico* tryptic digestion of *D. radiodurans* have unique masses at MMA ≤1 ppm, and these peptides can be used to identify 99.5% of the predicted proteins potentially expressed by the organism. The fraction of peptides useful as AMTs is actually greater than 50% due to our use of elution time data, which serves to distinguish previously identified peptides having otherwise indistinguishable masses.

Results

Strategy for AMT-Based Measurements. The approach utilizes instrumentation that combines high-pressure reversed-phase capillary LC with high magnetic field FTICR-MS (16, 19–21) and MS/MS. In our initial strategy, proteins extracted from cells grown under a variety of culture conditions are digested to yield a complex mixture of polypeptides that are analyzed to create a set of AMTs that serve as biomarkers for their parent proteins (16, 22). Our approach for defining AMTs provides high confidence for protein identification because of their initial identification by using MS/MS with standard database searching/identification (15) combined with validation by using high MMA and elution time (16). Although conventional capillary LC-MS/MS was used for most of the initial identifications, MS/MS with FTICR instrumentation was used in a limited number of cases to identify peptides present in concentrations too low to be analyzed effectively by conventional MS. The AMT-based protein identification allows subsequent high-throughput proteome measurements because only the distinctive masses and LC elution time are needed (16).

The *D. radiodurans* strain R1 genome consists of two chromosomes, one megaplasmid and one plasmid (3). Our analysis used the 3,116 protein-encoding ORFs predicted by the TIGR annotation (ftp://ftp.tigr.org/pub/data/d_radiodurans/GDR.pep) (2) (we exclude from this analysis 71 ORFs predicted to contain frame shifts). The proteomic measurements provide a physical validation that predicted ORFs actually encode a protein. A two-dimensional visualization of a portion of one analysis (Fig. 1) illustrates the ability to identify proteins from the peptides detected for *D. radiodurans* [grown in a defined minimal medium (13) and harvested at mid-log phase].

Overall Analysis Yields Identification of Over 60% of the Predicted Proteome. The 200 LC-MS/MS analyses of peptides from collective culture conditions yielded PMT identifications for 9,159 peptides having a SEQUEST score >2. Our measurements verified with high-confidence 6,997 AMTs, corresponding to 1,910 ORFs from *D. radiodurans*, representing 61% of the predicted ORFs (Table 1), the broadest proteome coverage for an organism achieved to date. Because the method uses two distinct MS measurements, matching accurate mass with MS/MS measurements, the use of the FTICR in these analyses lends higher confidence to those peptides identified compared to those detected (16). In a functional category breakdown (Table 2),

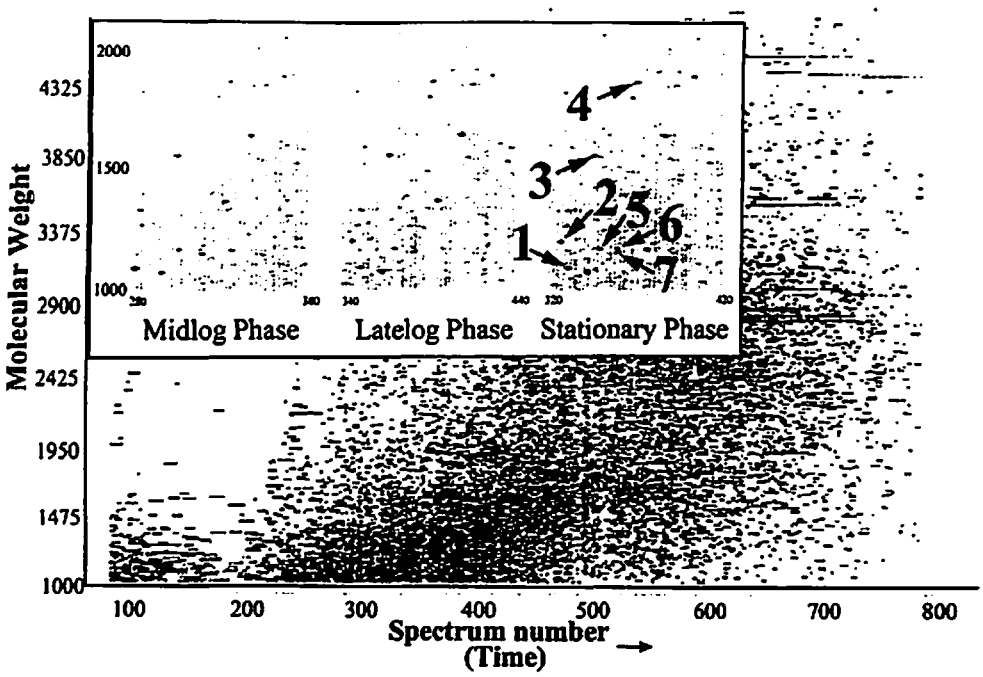

Fig. 1. Two-dimensional display of a capillary LC-FTICR analysis in which >50,000 putative polypeptides were detected from a tryptic digest of *D. radiodurans* proteins harvested in mid-log phase (OD_{600} 0.3–0.4; 30°C). *Inset* shows portions of displays for peptides from *D. radiodurans* harvested in mid-log (*Left*), late-log (*Center*), and poststationary (*Right*) phases (spot size reflects relative abundance). Each individual spot corresponds to a peptide that can be identified along with the parent protein using AMTs. Spot identifications: 1: DR1314 (hypothetical protein); 2: DR1790 (homolog of yellow/royal jelly protein of insects); 3: DR1314 (hypothetical protein); 4: DR0309 (elongation factor Tu); 5: DR2577 (S-layer protein); 6: DR0989 (membrane protein); and 7: DR1124 (S-layer protein).

coverages for categories associated with housekeeping functions were significantly higher than hypothetical proteins. In a single FTICR analysis, the masses for ≈1,500 AMTs are typically detected corresponding to ≈700 ORFs (depending on the culture condition) and 15–20% of the *D. radiodurans* proteome.

FTICR-Based Proteomics Can Provide Sensitive and Dynamic Range for Broad Proteome Coverage. One major challenge for proteomics is the large variation in the relative abundances of proteins (>5 orders of magnitude). A recognized disadvantage of conventional proteomic studies by using two-dimensional polyacrylamide gel electrophoresis separations coupled with protein identification by MS analysis is that, in general, only higher-abundance proteins are detected (23, 24). We have previously shown that ≈20 zmol (≈12,000 molecules) of protein can be detected during an FTICR analysis (25). In this work, capillary LC-FTICR measurements provided an overall dynamic range of 10^4-10^5 (16). The further expansion of the dynamic range of measurements by using a new DREAMS technology (26) offers the potential to detect proteins at less than one copy per cell given practical cell populations (10^8 cells per analysis). For more abundant proteins, broad coverage of peptide fragments was achieved; ribosomal proteins were identified with an average of 9 AMTs. Similarly, DNA polymerase I, considered to be the most abundant polymerase in prokaryotic cells (27), is predicted to be present in about 400 copies per cell in *E. coli* and was identified with six AMTs providing 20% coverage of the protein.

Another method for estimating protein abundance in a cell

Table 1. *D. radiodurans* proteome coverage

Category	Size	Predict ORFs	Obs ORFs	% coverage
Total	3.29 Mbp	3,116	1,910	61
Chromosome 1	2.65 Mbp	2,633	1,586	60
Chromosome 2	412 kbp	369	34	63
Mega plasmid	177 kbp	145	76	52
Small plasmid	46 kbp	40	4	35

Table 2. *D. radiodurans* proteome coverage by TIGR assigned functional category

Category	Total*	Seq cov†	St dev‡	Obs§	% Cat¶
Amino acid biosynthesis	80	21.5	15.1	70	88
Cofactor biosynthesis, etc.	61	16.1	9.7	41	67
Cell envelope	77	17.7	19	62	81
Cellular processes	89	21.9	21.5	64	72
Central metabolism	154	14.7	10.5	111	72
DNA metabolism	81	13.2	10.1	55	68
Energy metabolism	199	24.7	20	152	76
Fatty acid metabolism	53	23.8	16.2	40	75
Conserved hypothetical	499	16.6	13.1	276	55
Phage related/transposon	47	11.7	3.7	9	19
Protein fate	86	22.2	20.6	65	76
Protein synthesis	114	38.8	24.2	100	88
Nucleic acid synthesis	53	19.2	14.7	42	79
Regulatory functions	126	15.5	10.8	76	60
Transcription	28	18.5	11.8	22	79
Transport proteins	191	16.5	15.5	138	72
Unknown function	176	15.4	12.4	107	61
Hypothetical	1,002	18.7	14.2	479	48

*Number of ORFs assigned to each category by TIGR.
†Percentage of protein sequence represented by AMTs averaged over all proteins in a single category.
‡Standard deviation of sequence coverage for the entire category.
§Number of ORFs detected in each category.
¶Percentage of ORFs identified for each category.

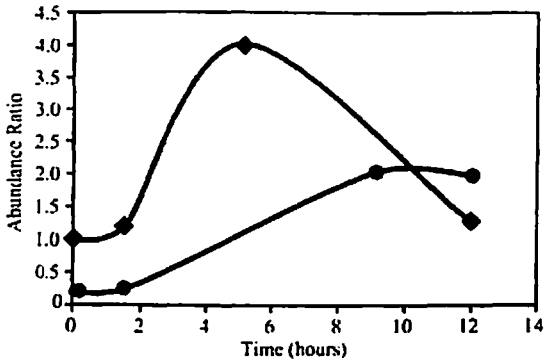

Fig. 3. Change in relative abundance of (●) RecA and (◆) DNA-directed RNA polymerase in cells after exposure to 17.5 kGy of ionizing radiation obtained be analysis of a mixture of cells grown on unlabeled media and the ^{15}N-labeled reference proteome (control, nonirradiated cells). Cells were prepared at 0, 3, 7, 9, and 12 hr after exposure.

dicted from DR0100 [putative single-stranded DNA-binding protein (SSB)] (2) that is reported to contain three frame shifts, supporting the existence of at least some functional SSB protein. AMTs were also identified for DR1624 (RNA helicase), DR2477 (3-hydroxyacyl-CoA dehydrogenase), and DRC0020 (putative modification methylase). AMTs were detected in all three reading frames of ORF DR2477, suggesting either that *D. radiodurans* is able to mediate the required two frame shifts or that there is a mistake in the genome sequence. Detected peptides corresponding to ORFs and frames in which they are coded are published as supporting information on the PNAS web site.

Stress Response, DNA Damage Repair, and Recognition Proteins and RecA. It is predicted that *D. radiodurans* encodes a spectrum of 148 stress response proteins (four are predicted to contain authentic frame shifts) (3). We identified 74 proteins predicted from the annotated genome with an average of six AMTs per protein corresponding to 24% overall sequence coverage. Two classes of annotated proteins shown to play roles in the detoxification processes are catalase (DR 1998 and DRA0259) and superoxide dismutase (SOD) (DR1279, DR1546, and DRA0202). We confirmed the presence of both predicted catalases with 48 (DR1998) and 37 (DRA0259) AMTs covering ≈80% and ≈50% of their sequences, respectively. Of the SOD proteins, we identified DR 1279 with 14 AMTs, corresponding to 87% coverage, whereas DR1546 and DRA0202 were identified with two and three AMTs, respectively. Of the predicted 75 proteins with potential DNA repair activities (23), we identified 39 with an average of three AMTs per protein corresponding to 12% coverage of the amino acid sequence. RecA is central to homologous recombinational repair of irradiation-induced double-strand breaks in *D. radiodurans* chromosomal and plasmid DNA (6, 7, 11, 31). Five different RecA AMTs (covering 34% of the sequence) were identified primarily in cells recovering from exposure to ionizing radiation.

Stable isotope labeling allows the quantitation of changes in protein expression levels. The protein expression pattern of *D. radiodurans* recovering from a dose of 17.5 kGy of ionizing radiation (growing on ^{14}N media) was compared with the protein expression pattern from control cells (growing on ^{15}N media) (Fig. 3). Initial studies indicate that the expression of RecA as well as DNA-directed RNA polymerase I is significantly induced during recovery from 17.5 kGy irradiation, consistent with previous observations (32).

Discussion

Comprehensive proteome analyses can be achieved with greater confidence by using AMTs for protein identifications because of the combined use of sequence-related information and accurate mass measurement. Although a catalog of proteins from a particular organism is useful for gene verification, the analysis of protein expression patterns under various culture conditions can be used to infer function, deduce metabolic pathways, identify regulatory networks, etc.

When *D. radiodurans* is exposed to ionizing radiation, a dose-dependent delay of cellular replication suggests the existence of a DNA damage checkpoint (33). During this delay, several phases of cellular detoxification are hypothesized (34), but details remain unclear. One detoxification process in *D. radiodurans* involves removal of the activated oxygen species by catalase and SOD. Although the biochemical function of these two enzymes is known (35), their role in radiation resistance is unclear. Basal levels of catalase in exponentially growing cultures of *D. radiodurans* have been shown to be over 100-fold greater than for *E. coli* (10, 35). Genetic inactivation of members of either protein group render *D. radiodurans* cells more sensitive to ionizing radiation at doses that exceed 16,000 Gy (36), whereas mutations in DR1279 result in a greater sensitivity to ionizing radiation compared with mutations in DR1998. We confirmed the presence of both catalases under most culture conditions, suggesting constitutive expression. Of the SOD proteins, we identified DR1279 under many culture conditions but detected DR1546 and DRA0202 proteins in only a few culture conditions and in relatively low abundance. Thus, DR1279 apparently dominates SOD function and also appears to be constitutively expressed.

Additional detoxification processes in *D. radiodurans* export substantial portions of its DNA as large or small oligonucleotides from the cell after irradiation (37), presumably to prevent reincorporation into the genome. Homologs of UvrA (including UvrA1) are believed to play a role in these processes because they have been linked to ABC transporter proteins (2), and UvrA serves as the site of attachment for nucleotide excision repair proteins to the cell membrane in *E. coli* (2, 38). The dramatic DNA damage resistance of *D. radiodurans* has been attributed to exceedingly efficient DNA repair mechanisms, although such mechanisms remain poorly understood (3, 34). We observed most of the predicted proteins associated with nucleotide excision repair (including the UvrA1, UvrB, UvrC, Mfd, and PolA) in both stressed and unstressed cultures, which may indicate that these processes are continuously removing damaged nucleotides from the cell. UV DNA damage endonuclease and DNA helicase II (UvrD) were not detected, suggesting that these proteins may be expressed only at low basal levels. The detoxification process originally ascribed to the activity of the MutT Nudix protein family has been refuted by Xu *et al.*, who found low levels of MutT activity for proteins putatively identified with MutT domains (39), consistent with the present observation of the MutT Nudix protein family predominantly in unstressed cells.

Although *D. radiodurans* can express a suite of stress response proteins, expression patterns have initially revealed few correlations between expression and stress response. One exception is for the hypothetical protein DR0070, which is observed only after alkaline treatment (Fig. 2). Closer examination of this ORF reveals a limited similarity to alkaline protease of *Bacillus subtilis* (39), surrounding the catalytic serine residue, and illustrates the use of such data to verify or suggest protein function.

One protein that has been closely linked with the DNA repair ability of *D. radiodurans* is RecA. RecA is detected predominantly in cells recovering from ionizing radiation and also at low levels in nonstressed cells, suggesting a low level of constitutive

expression, contrary to previously published work. Previous studies using conventional PAGE with a RecA immunoprobe were not sufficiently sensitive to detect these low levels of RecA in *D. radiodurans* grown under nonstress conditions (32). Besides RecA, few proteins typically associated with presynaptic or postsynaptic recombination events were detected.

Although this is the first study, to our knowledge, to demonstrate such comprehensive (>61%) proteome coverage, an additional significance of our approach lies in the breadth of proteomic studies now enabled. The present results provide a large set of AMT "protein biomarkers" for quantitative expression studies that can be conducted with greater sensitivity and higher throughput due to elimination of the need for MS/MS measurements. Such studies use cells grown on stable-isotope-labeled media whose proteins (and their peptide AMTs) serve as internal standards to establish relative expression levels (40, 41). Several studies have now demonstrated that precision of better than 10–20% is achievable (41–43), a significant improvement over conventional proteomics approaches or gene expression arrays. The observation that both RNA polymerase I and RecA were induced after exposure to ionizing radiation (Fig. 3), although not surprising, illustrates that the use of AMTs for quantitation also provides the rapid throughput that will be necessary to extract biological insights from global proteomic studies.

This research was supported by the U.S. Department of Energy, Office of Biological and Environmental Research. Pacific Northwest National Laboratory is operated by Battelle Memorial Institute for the U.S. Department of Energy through contract DE-AC06-76RLO 1830. A portion of this work was also supported by Grants DE-FG02-97ER62492 (from the Natural and Accelerated Bioremediation Research Program) and DE-F602-01ER63220 (from the Microbial Cell Program), Office of Biological and Environmental Research, U.S. Department of Energy (to M.J.D.).

1. Venter, J. C., Adams, M. D., Myers, E. W., Li, P. W., Mural, R. J., Sutton, G. G., Smith, H. O., Yandell, M., Evans, C. A., Holt, R. A., *et al.* (2001) *Science* **291**, 1304–1325.
2. White, O., Eisen, J. A., Heidelberg, J. F., Hickey, E. K., Peterson, J. D., Dodson, R. J., Haft, D. H., Gwinn, M. L., Nelson, W. C., Richardson, D. L., *et al.* (1999) *Science* **286**, 1571–1577.
3. Makarova, K. S., Aravind, L., Wolf, Y. I., Tatusov, R. L., Minton, K. W., Koonin, E. V. & Daly, M. J. (2001) *Microbiol. Mol. Biol. Rev.* **65**, 44–79.
4. Daly, M. J. (2000) *Biotechnology* **11**, 280–285.
5. Smith, K. C. & Martignoni, K. D. (1976) *Photochem. Photobiol.* **24**, 515–523.
6. Daly, M. J., Ouyang, L., Fuchs, P. & Minton, K. W. (1994) *J. Bacteriol.* **176**, 3508–3517.
7. Minton, K. W. (1994) *Mol. Microbiol.* **1**, 9–15.
8. Lange, C. C., Wackett, L. P., Minton, K. W. & Daly, M. J. (1998) *Nat. Biotechnol.* **16**, 929–933.
9. Fredrickson, J., Kostandarithes, H., Li, S., Plymale, A. & Daly, M. (2000) *Appl. Environ. Microbiol.* **66**, 2006–2011.
10. Mattimore, V. & Battista, J. R. (1996) *J. Bacteriol.* **178**, 633–637.
11. Kitayama, S. & Matsuyama, A. (1971) *Int. J. Radiat. Biol. Relat. Stud. Phys. Chem. Med.* **19**, 13–19.
12. Minton, K. W. & Daly, M. J. (1995) *Bioessays* **17**, 457–464.
13. Venkateswaran, A., McFarlan, S. C., Ghosal, D., Minton, K. W., Vasilenko, A., Makarova, K., Wackett, L. P. & Daly, M. J. (2000) *Appl. Environ. Microbiol.* **66**, 2620–2626.
14. Shen, Y., Tolić, N., Zhao, R., Paša-Tolić, L., Li, L., Berger, S. F., Harkewicz, R., Anderson, G. A., Belov, M. E. & Smith, R. D. (2001) *Anal. Chem.* **73**, 3011–3021.
15. Eng, J. K., McCormack, A. L. & Yates, J. R. (1994) *J. Am. Soc. Mass Spectrom.* **5**, 976–989.
16. Smith, R. D., Anderson, G. A., Lipton, M. S., Paša-Tolić, L., Shen, Y., Conrads, T. P., Veenstra, T. D. & Udseth, H. R. (2002) *Proteomics* **2**, 513–523.
17. Harkewicz, R., Belov, M., Anderson, D., Paša-Tolić, L., Masselon, C., Prior, D., Udseth, H. & Smith, R. (2001) *J. Am. Soc. Mass Spectrom.* **13**, 144–154.
18. Bruce, J. E., Anderson, G. A., Brands, M. D., Paša-Tolić, L. & Smith, R. D. (2000) *J. Am. Soc. Mass Spectrom.* **11**, 416–421.
19. Marshall, A. G., Hendrickson, C. L. & Jackson, G. S. (1998) *Mass Spectrom. Rev.* **17**, 1–35.
20. Shen, Y., Zhao, R., Belov, M. E., Conrads, T. P., Anderson, G. A., Tang, K., Paša-Tolić, L., Veenstra, T. D., Lipton, M. S., Udseth, H. R. & Smith, R. D. (2001) *Anal. Chem.* **73**, 1766–1775.
21. Li, L., Masselon, C., Anderson, G. A., Paša-Tolić, L., Lee, S.-W., Shen, Y., Zhao, R., Lipton, M. S., Conrads, T. P., Tolić, N. & Smith, R. D. (2001) *Anal. Chem.* **73**, 3312–3322.
22. Conrads, T. P., Anderson, G. A., Veenstra, T. D., Paša-Tolić, L. & Smith, R. D. (2000) *Anal. Chem.* **72**, 3349–3354.
23. Wilm, M., Shevchenko, A., Houthaeve, T., Breit, S., Schweigerer, L., Fotsis, T. & Mann, M. (1996) *Nature (London)* **379**, 466–469.
24. Shevchenko, A., Wilm, M., Vorm, O. & Mann, M. (1996) *Anal. Chem.* **68**, 850–858.
25. Belov, M., Gorshkov, M., Udseth, H. & Smith, R. (2001) *J. Am. Soc. Mass Spectrom.* **12**, 1312–1319.
26. Belov, M. E., Anderson, G. A., Angell, N. H., Shen, Y., Tolić, N., Udseth, H. R. & Smith, R. D. (2001) *Anal. Chem.* **73**, 5052–5060.
27. Patel, P. H., Suzuki, M., Adman, E., Shinkai, A. & Loeb, A. (2001) *J. Mol. Biol.* **308**, 823–827.
28. Sharp, P. M. & Li, W.-H. (1987) *Nucleic Acids Res.* **15**, 1281–1295.
29. Karlin, S. & Mrazek, J. (2000) *J. Bacteriol.* **182**, 5238–5250.
30. Curnow, A. W., Tumbula, D. L., Pelaschier, J. T., Min, B. & Soll, D. (1998) *Proc. Natl. Acad. Sci. USA* **95**, 12838–12843.
31. Moseley, B. E. & Evans, D. M. (1983) *J. Gen. Microbiol.* **129**, 2437–2445.
32. Carroll, J. D., Daly, M. J. & Minton, K. W. (1995) *J. Bacteriol.* **178**, 130–135.
33. Mattimore, V., Udupa, K. S., Berne, G. A. & Battista, J. R. (1995) *J. Bacteriol.* **177**, 5232–5237.
34. Battista, J. R. (1997) *Annu. Rev. Microbiol.* **51**, 203–224.
35. Chou, F. I. & Tan, S. T. (1990) *J. Bacteriol.* **172**, 2029–2035.
36. Markillie, L. M., V. S., Hradecky, P. & Wong, K. K. (1999) *J. Bacteriol.* **181**, 666–669.
37. Vukovic-Nagy, B., Fox, B. W. & Fox, M. (1974) *Int. J. Radiat. Biol. Relat. Stud. Phys. Chem. Med.* **25**, 329–337.
38. Bauche, C. & Laval, J. (1999) *J. Bacteriol.* **181**, 262–269.
39. Xu, W., Shen, J., Dunn, C. A., Desai, S. & Bessman, M. J. (2001) *Mol. Microbiol.* **39**, 286–290.
40. Gygi, S. P., Rist, B., Gerber, S. A., Turecek, F., Gelb, M. H. & Aebersold, R. (1999) *Nat. Biotechnol.* **17**, 994–999.
41. Paša-Tolić, L., Jensen, P. K., Anderson, G. A., Lipton, M. S., Peden, K. K., Martinovic, S., Tolić, N., Bruce, J. E. & Smith, R. D. (1999) *J. Am. Chem. Soc.* **121**, 7949–7950.
42. Gygi, S. P., Rist, B. & Aebersold, R. (2000) *Biotechnology* **11**, 396–401.
43. Jensen, P. K., Paša-Tolić, L., Anderson, G. A., Horner, J. A., Lipton, M. S., Bruce, J. E. & Smith, R. D. (1999) *Anal. Chem.* **71**, 2076–2084.

Transcriptome dynamics of *Deinococcus radiodurans* recovering from ionizing radiation

Yongqing Liu*†, Jizhong Zhou*†‡, Marina V. Omelchenko§, Alex S. Beliaev*¶, Amudhan Venkateswaran§, Julia Stair*, Liyou Wu*, Dorothea K. Thompson*‖, Dong Xu**, Igor B. Rogozin††, Elena K. Gaidamakova§, Min Zhai§, Kira S. Makarova††, Eugene V. Koonin††, and Michael J. Daly§‡‡

*Environmental Sciences and **Life Sciences Divisions, Oak Ridge National Laboratory, Oak Ridge, TN 37831; ‖Center for Microbial Ecology, Michigan State University, East Lansing, MI 48824; ††Center for Biotechnology Information, National Institutes of Health, Bethesda, MD 20894; and §Uniformed Services University of the Health Sciences, Bethesda, MD 20814

Communicated by Todd R. Klaenhammer, North Carolina State University, Raleigh, NC, January 22, 2003 (received for review October 14, 2002)

***Deinococcus radiodurans* R1 (DEIRA) is a bacterium best known for its extreme resistance to the lethal effects of ionizing radiation, but the molecular mechanisms underlying this phenotype remain poorly understood. To define the repertoire of DEIRA genes responding to acute irradiation (15 kGy), transcriptome dynamics were examined in cells representing early, middle, and late phases of recovery by using DNA microarrays covering ~94% of its predicted genes. At least at one time point during DEIRA recovery, 832 genes (28% of the genome) were induced and 451 genes (15%) were repressed 2-fold or more. The expression patterns of the majority of the induced genes resemble the previously characterized expression profile of *recA* after irradiation. DEIRA *recA*, which is central to genomic restoration after irradiation, is substantially up-regulated on DNA damage (early phase) and down-regulated before the onset of exponential growth (late phase). Many other genes were expressed later in recovery, displaying a growth-related pattern of induction. Genes induced in the early phase of recovery included those involved in DNA replication, repair, and recombination, cell wall metabolism, cellular transport, and many encoding uncharacterized proteins. Collectively, the microarray data suggest that DEIRA cells efficiently coordinate their recovery by a complex network, within which both DNA repair and metabolic functions play critical roles. Components of this network include a predicted distinct ATP-dependent DNA ligase and metabolic pathway switching that could prevent additional genomic damage elicited by metabolism-induced free radicals.**

The Gram-positive aerobic bacterium *Deinococcus radiodurans* R1 (DEIRA) has an extraordinary resistance to γ-radiation and a wide range of other DNA-damaging conditions, including desiccation and oxidizing agents (1, 2). Ionizing radiation induces DNA double-stranded breaks (DSBs) that are the most lethal form of DNA damage (3). After acute exposures to 10 kGy, early stationary phase (ESP) DEIRA can reassemble its 3.285-Mbp genome, which consists of four haploid genomic copies per cell (4), from hundreds of DNA DSB fragments without lethality or induced mutagenesis (5, 6). Also remarkable is DEIRA's ability to grow at 60 Gy/h without any discernable effect on its growth rate (7). Because most organisms, generally, can tolerate so few DSBs (8), radiation-induced DSBs and their repair have been difficult to study. In DEIRA, however, there are so many DSBs in fully viable irradiated cells after high-dose irradiation that the steps in DSB repair can be monitored directly in mass culture (5, 9–11). This characteristic has been exploited and used to examine the timing of DNA recombination (5, 10, 12) after high-dose irradiation and has revealed the sequential action of RecA-independent and -dependent pathways during repair (11).

Comparative genomic and experimental analyses support the view that DEIRA's extreme radiation resistance phenotype is complex, likely determined collectively by an assortment of protection and DNA repair systems. Remarkably, the number of genes identified in DEIRA that are known to be involved in DNA repair is less than the number reported for *Escherichia coli* (13), and most of the DNA repair genes identified in DEIRA have functional homologs in other prokaryotic species (13, 14). These findings suggest that the organism's extreme resistance phenotype may be attributable to still unknown genes and pathways. Despite these efforts, the molecular mechanisms underlying its resistance remain poorly understood. Thus, a systematic genome-wide examination of the genes and pathways involved in cell recovery would be useful for a further understanding of how DEIRA responds to and recovers from irradiation. Here we report the analysis of genomic expression within cells recovering from 15 kGy by using whole-genome DNA microarrays. We find that the hallmark components of DEIRA's recovery encompass differential regulation of systems involved in information storage and processing, metabolism, and many uncharacterized genes that respond to high-dose irradiation.

Materials and Methods

Cell Growth, Irradiation, and Mutant Construction. DEIRA strain R1 was grown at 32°C in liquid nutrient-rich medium TGY (1% tryptone/0.1% glucose/0.5% yeast extract) or on TGY solid medium (7). In liquid culture, cell density was determined at 600 nm by a Beckman Coulter spectrophotometer. For high-dose irradiation exposure, 150 ml of an early stationary phase (ESP) DEIRA culture [$OD_{600} = 1.0$, ~1×10^8 colony-forming units (cfu)/ml] was divided in half. Half of the culture (75 ml) was irradiated on ice to a total dose of 15 kGy (Model 109 ^{60}Cobalt gamma cell irradiation unit, J. L. Shepherd and Associates, San Fernando, CA). The nonirradiated control culture was incubated on ice for the same length of time (~98 min) as the culture being irradiated, followed by harvesting through brief (~1 min) centrifugation (~3,500 × *g*, ~2°C). Control cells were washed and then frozen in RNAlater solution (Ambion, Austin, TX) that had been maintained on ice and then stored at −80°C. After exposure to 15 kGy, the irradiated cell culture (75 ml) was diluted 20-fold by using fresh TGY medium (at a final volume of 1.5 liters) and incubated at 32°C in an orbital shaker. At the indicated recovery time points (0, 0.5, 1.5, 3, 5, 9, 12, 16, and 24 h), ~1×10^9 cells were harvested, washed, and frozen in RNAlater solution. Cell viability and cell numbers were determined by plate assay and hemocytometer count, respectively, as described (5). Three independent cell cultures and irradiation treatments of the same kind were performed and served as biological replicates for gene expression experiments, as well as for determining irradiation resistance profiles. To confirm the predicted involvement of one uncharacterized DEIRA gene implicated in postirradiation recovery (DR0070), a mutant was generated using previously developed DEIRA disruption protocols (15).

Abbreviations: DEIRA, *Deinococcus radiodurans* strain R1; DSB, double-strand break; SOS, error-prone DNA repair; TCA, tricarboxylic acid.

†Y.L. and J.Z. contributed equally to this work.

‡To whom correspondence should be addressed regarding microarray analysis and reprints. E-mail: zhouj@ornl.gov.

¶Present address: Biological Sciences Division, Pacific Northwest National Laboratory, Richland, WA 99352.

‡‡To whom correspondence should be addressed regarding *Deinococcus* biology and reprints. E-mail: mdaly@usuhs.mil.

Nucleic Acid Extraction, Microarray Fabrication, and Data Analysis. Protocols for DEIRA genomic DNA and total cellular RNA extraction and manipulation were as published (7, 11, 16, 18). Microarray construction was based on the genomic sequence data and annotation provided by the Institute for Genomic Research (Rockville, MD), where a total of 3,187 putative ORFs were assigned to the DEIRA genome (14). For PCR, gene-specific primers were selected using the PRIMEGENS software (ref. 17; http://compbio.ornl.gov/structure/primegens). Generally, a full or nearly full sequence of a gene was selected as a probe on microarrays if it was <75% similar to all other genes. For genes having higher than 75% similarity to another gene, a maximum internal region showing <75% was selected as a probe. For genes where no primers could be obtained under the cutoff value of 75% similarity, a cutoff value of 85% was used. In total, 3,046 pairs of gene-specific primers were designed and then synthesized by MWG Biotec (High Point, NC).

Each gene was amplified four times in a 96-well plate. The amplified PCR products (400 μl) were pooled together and purified as described (18). The purified PCR products were visualized by gel electrophoresis in the presence of ethidium bromide, and their respective sizes were verified by comparison to the expected product length, yielding a collection of 2,976 distinct ORFs. Microarray fabrication, hybridization, probe labeling, image acquisition, and processing were carried out as described (18, 19). Because nonirradiated ESP DEIRA cells inoculated into fresh medium yield a fully grown culture in the time taken by the 15 kGy-induced growth lag, our expression analyses compared total RNA derived from recovering DEIRA with total RNA from nonirradiated control cells. The ratios of the irradiated samples to the nonirradiated control were normalized using the Pooled-Common-Error model provided by the statistical analysis software ARRAYSTAT V.2.0 (Imaging Research, St. Catherine's, ON, Canada). The outliers, represented by the data points that were not consistently reproducible and had a disproportionately large effect on the statistical result, were removed. A standard t test was performed so that a two-tailed probability of a mean deviating from 1.0 could be calculated and used to determine the significance for each data point. Identification of groups of genes exhibiting similar expression patterns was performed using the pairwise average-linkage hierarchical clustering algorithm (20) provided in CLUSTER software (http://rana.stanford.edu/). The results of hierarchical clustering were visualized using TREEVIEW software (http://rana.stanford.edu/). The complete microarray data set for the recovery time course can be found in table A at www.esd.ornl.gov/facilities/genomics/TableA.pdf; *Supporting Text*, Figs. 5–9, and Tables 1–4 are published as supporting information on the PNAS web site, www.pnas.org (all of the supporting information can also be found at the Oak Ridge National Laboratory's Environmental Sciences Division web site, www.esd.ornl.gov/facilities/genomics/functional_genomics.html).

Results

Cell Growth, Inhibition, and Recovery. After a dose of 15 kGy, DEIRA recovery typically progresses through three phases (5, 9, 10, 21): (*i*) early phase (0–3 h), where cell growth is inhibited and *recA* is induced, but there is little evidence of DNA repair; (*ii*) mid phase (3–9 h), where growth inhibition and *recA* expression continue, but with progressive DNA repair; and (*iii*) late phase (9–24 h), where *recA* is repressed and cell growth is restored. Consistent with these reports (5, 6, 9–11), after the exposure of DEIRA to 15 kGy, ~150 DSBs per haploid genome were inflicted (data not shown). As expected, after the 9-h lag in growth, cells grew exponentially and reached stationary phase 15 h later (Fig. 5). To separate potentially damage-induced genes from cell-growth-related genes, we focused on the gene expression changes that occurred during the early and mid phases of recovery.

Quality of Microarray Hybridization Data. Because microarray hybridization exhibits inherent high variability, experimental replications are essential for obtaining reliable results (22). In this study, samples were taken at nine time intervals over a period of 24 h. At each time point, three replicated samples were obtained. Each microarray slide contained two duplicate sets of gene fragments, and the RNA obtained from each sample was hybridized with two microarrays by using fluorescent-dye reversal. Thus, 12 data points were available for each time point and enabled the use of statistical tests to determine significant changes in gene expression. Only those genes with statistically significant differences were further analyzed.

Three additional methods were used to test the robustness of the microarray hybridization data: (*i*) correlation of gene expression with predicted operon organization, (*ii*) real-time quantitative PCR, and (*iii*) confirmation of the involvement of an uncharacterized induced gene in postirradiation recovery.

Operons are the principal form of gene coregulation in prokaryotes, so the expression patterns of genes within an operon are expected to be strongly correlated. Consistently, our analysis of 435 genes within 141 predicted operons showed highly significant correlation of their expression patterns compared with genes in "random operons" (see *Supporting Text* and Fig. 6). An example of expression patterns for genes located in one predicted operon is shown in Fig. 6*A*. Further supporting coregulation of functionally linked genes in DEIRA, we found that dispersed genes encoding different subunits of several distinct enzymatic complexes are also similarly regulated (Fig. 6*B*).

Seven genes that were up-regulated immediately on exposure to irradiation were evaluated by real-time quantitative PCR. Except for a single gene, DR0007, the expression patterns of all other genes were similar (r = 0.729) to those detected by microarray hybridization (Tables 1 and 2).

The uncharacterized gene DR0070 encodes a hypothetical protein (199 aa in length) that is unique to DEIRA and that was highly expressed after radiation (Table 3). To confirm that this gene is involved in radiation resistance, DR0070 was disrupted. The radiation resistance of a mutant (MD891) with a confirmed homozygous disruption for DR0070 was compared with wild-type DEIRA (Fig. 7). Although MD891 shows no metabolic or growth deficiencies in the presence or absence of chronic γ-radiation (60 Gy/h), it is substantially more sensitive to acute irradiation than wild-type DEIRA (Fig. 7*A*).

General Patterns of Expression in Response to Irradiation. For genes with statistically significant expression ratios showing at least a 2-fold change, we found that 832 genes (28% of the genome) were induced and 451 genes (15%) were repressed at least at one time point during DEIRA recovery. Fig. 1*A* specifically shows differential regulation in the early and mid phases of recovery and illustrates that this time interval is an active period of coordinated gene expression, despite a highly fragmented genome. Within this large pool of significantly expressed genes, we operationally identified a subgroup that consists of genes with substantially greater expression levels and likely includes key players in the irradiation response. Table 3 lists genes and operons with *recA*-like expression patterns; DEIRA *recA* is critical to genomic restoration after irradiation (9–12), and its induction is considered a dominant marker for the onset of homologous recombination (ref. 21; Fig. 2). Table 4 lists the irradiation-response patterns of genes involved in replication, repair, and recombination functions in DEIRA.

A comparison of the percentage of responding genes for each of the four genomic partitions of DEIRA [DR_Main (2.65 Mbp), DRA (412 kbp), DRB (177 kbp), and DRC (46 kbp); ref. 14] unexpectedly showed that the majority of DRC genes were dramatically up-regulated during the mid and late phases of recovery, in marked contrast to the three other genomic partitions (Fig. 1*B*). Specifically, of the 41 DRC genes, 38 had

the predicted 2′–5′ RNA ligase (LigT) and the *recA* gene; both genes have similar expression profiles (Fig. 6). Furthermore, this gene organization is shared by *Thermotoga maritima*. Because RNA is also heavily damaged on irradiation, it is possible that the 2′–5′ RNA ligase is involved in the degradation of specific structures formed in damaged RNA (37). Alternatively, it could have an unrecognized function in DNA repair, perhaps in functional association with RecA, as suggested by colocalization of these genes within the same operon.

Generally, our expression data support the hypothesis that irradiated DEIRA strongly suppresses oxidative stress, perhaps as a mechanism to prevent additional loss of genome integrity. Notably, during the early and mid phases, when biosynthetic and energy demands are expected to be high, DEIRA represses its TCA cycle, particularly the O_2^- radical-generating step (i.e., sdhB; Fig. 3*A*; ref. 38). Furthermore, DEIRA appears to minimize its biosynthetic energy demands by inducing transporters of exogenous peptides and other secondary metabolites on which radiation resistance is highly dependent (7), and correspondingly shows increased expression of extra- and intracellular proteases and nucleases (Table 3). This helps explain the observation that *de novo* biosynthesis of amino acids, nucleotides, and coenzymes remains unchanged or is even down-regulated, at least within the early and mid phases (Figs. 2 and 8). In contrast, the glyoxylate bypass is strongly induced (Fig. 3*A*) and could provide some biosynthetic intermediates needed for recovery without generating free radicals. The gene for predicted transaconitate methylase (DR0422) is one of the most strongly induced in the early phase of recovery. Transaconitate is not a normal metabolite in most bacteria and is an attenuator of aconitase, a key enzyme of the TCA cycle (39). It seems possible that transaconitate is produced as a result of irradiation, and induction of DR0422 (Table 4) might be required for transaconitate detoxification. During the late phase, the TCA cycle was slowly induced, and genes involved in scavenging free radicals (e.g., *sodA* and *katA*) were correspondingly induced.

DEIRA has orthologs of 11 of 26 genes that comprise the SOS regulon in *E. coli* (40), and 7 of these genes respond to irradiation in DEIRA. However, it is notable that DEIRA does not have a homolog of the error-prone DNA polymerase *umuC*, a central gene of the SOS response in many bacteria (13). In agreement with recent reports (41), our expression data show that *lexA* (DRA0344) and the second *lexA* paralog (DRA0074) are not significantly induced after irradiation (Table 4). Taken together, these data suggest that a specific damage-response regulon is likely to exist in DEIRA, but that it is distinct from the classical *E. coli*-type SOS response in regard to the genes involved and the mode of regulation. The observed weak activation of the *lexA* paralogs (1.8-fold at 1.5–3 h) suggests that *lexA* might regulate other transcriptional regulators involved in the damage response or could selectively regulate a small subset of damage-response genes. Notwithstanding these possibilities, we searched for candidate transcriptional regulators that could play a major role in the response to DNA damage. Among >80 transcriptional regulators predicted to exist in DEIRA, we see significant induction of only a few corresponding genes (Fig. 9), with the largest induction ratio numbers observed for DRC0012, DR0171, DR2574, and DR2482. The induction of the DRC0012 regulator might be fortuitous, because it is encoded on the small plasmid DRC and belongs to the CsdG/RcsA family, whose members have not been identified as stress-response regulators. DR2482 contains a DNA-binding domain similar to those of *sigA*-like sigma factors (42) and, therefore, might function as a DNA-damage-specific sigma subunit of RNA polymerase. DR2574 belongs to the Xre family of transcriptional regulators, some of which were found to regulate stress response in bacteria (43, 44). Finally, DR0171 belongs to a specific DEIRA family of transcriptional regulators and has been shown to be involved directly in γ-radiation resistance (13, 45, 46). Therefore, we consider DR0171 and DR2574, which displayed *recA*-like expression patterns, to be two primary candidates for regulating the DNA irradiation response in DEIRA.

The present analysis of the transcriptome dynamics of DEIRA in response to acute irradiation revealed the complexity that could be expected of such a unique recovery process and, importantly, led to the identification of numerous previously unsuspected candidates for experimental analysis of genes and mechanisms that underlie the exceptional radiation resistance of this bacterium.

This research was funded by U.S. Department of Energy (Office of Biological and Environmental Research, Office of Science) Grants DE-FG02-01ER63220 from the Genomes to Life Program, DE-FG02-97ER62492 from the Natural and Accelerated Bioremediation Research Program, and ERKP385 from Microbial Genome Program, and by the Laboratory Directed and Research Development Program at Oak Ridge National Laboratory. Oak Ridge National Laboratory is managed by the University of Tennessee–Battelle LLC for the Department of Energy under Contract DOE-AC05-00OR22725.

1. Mattimore, V. & Battista, J. R. (1996) *J. Bacteriol.* 178, 633–637.
2. Minton, K. W. (1996) *Mutat. Res.* 363, 1–7.
3. Hutchinson, F. (1985) *Prog. Nucleic Acid Res. Mol. Biol.* 32, 115–154.
4. Hansen, M. T. (1978) *J. Bacteriol.* 134, 71–75.
5. Daly, M. J., Ling, O. & Minton, K. W. (1994) *J. Bacteriol.* 176, 7506–7515.
6. Lin, J., Qi, R., Aston, C., Jing, J., Anantharaman, T. S., Mishra, B., White, O., Daly, M. J., Minton, K. W., Venter, J. C. & Schwartz, D. C. (1999) *Science* 285, 1558–1562.
7. Venkateswaran, A., McFarlan, S. C., Ghosal, D., Minton, K. W., Vasilenko, A., Makarova, K. S., Wackett, L. P. & Daly, M. J. (2000) *Appl. Environ. Microbiol.* 66, 2620–2626.
8. Krasin, F. & Hutchinson, F. (1977) *J. Mol. Biol.* 116, 81–98.
9. Daly, M. J., Ouyang, L., Fuchs, P. & Minton, K. W. (1994) *J. Bacteriol.* 176, 3508–3517.
10. Daly, M. J. & Minton, K. W. (1995) *J. Bacteriol.* 177, 5495–5505.
11. Daly, M. J. & Minton, K. W. (1996) *J. Bacteriol.* 178, 4461–4471.
12. Daly, M. J. & Minton, K. W. (1997) *Gene* 187, 225–229.
13. Makarova, K. S., Aravind, L., Wolf, Y. I., Tatusov, R. L., Minton, K. W., Koonin, E. V. & Daly, M. J. (2001) *Microbiol. Mol. Biol. Rev.* 65, 44–79.
14. White, O., Eisen, J. A., Heidelberg, J. F., Hickey, E. K., Peterson, J. D., Dodson, R. J., Haft, D. H., Gwinn, M. L., Nelson, W. C., Richardson, D. L., *et al.* (1999) *Science* 286, 1571–1577.
15. Markillie, L. M., Varnum, S. M., Hradecky, P. & Wong, K. K. (1999) *J. Bacteriol.* 181, 666–669.
16. Zhou, J., Fries, M. R., Chee-Sanford, J. C. & Tiedje, J. M. (1995) *Int. J. Syst. Bacteriol.* 45, 500–506.
17. Xu, D., Li, G., Wu, L., Zhou, J. & Xu, Y. (2002) *Bioinformatics* 18, 1432–1436.
18. Thompson, D. K., Beliaev, A. S., Giometti, C. S., Tollaksen, S. L., Khare, T., Lies, D. P., Nealson, K. H., Lim, H., Yates, J., III, Brandt, C. C., *et al.* (2002) *Appl. Environ. Microbiol.* 68, 881–892.
19. Beliaev, A. S., Thompson, D. K., Khare, T., Lim, H., Brandt, C. C., Li, G., Murray, A. E., Heidelberg, J. F., Giometti, C. S., Yates, J., III, *et al.* (2002) *OMICS* 6, 39–60.
20. Eisen, M. B., Spellman, P. T., Brown, P. O. & Botstein, D. (1998) *Proc. Natl. Acad. Sci. USA* 95, 14863–14868.
21. Carroll, J. D., Daly, M. J. & Minton, K. W. (1996) *J. Bacteriol.* 178, 130–135.
22. Lee, M. L., Kuo, F. C., Whitmore, G. A. & Sklar, J. (2000) *Proc. Natl. Acad. Sci. USA* 97, 9834–9839.
23. Birrell, G. W., Brown, J. A., Wu, H. I., Giaever, G., Chu, A. M., Davis, R. W. & Brown, J. M. (2002) *Proc. Natl. Acad. Sci. USA* 99, 8778–8783.
24. Aravind, L., Makarova, K. S. & Koonin, E. V. (2000) *Nucleic Acids Res.* 28, 3417–3432.
25. Inamine, G. S. & Dubnau, D. (1995) *J. Bacteriol.* 177, 3045–3051.
26. Bessman, M. J., Frick, D. N. & O'Handley, S. F. (1996) *J. Biol. Chem.* 271, 25059–25062.
27. Xu, W., Shen, J., Dunn, C. A., Desai, S. & Bessman, M. J. (2001) *Mol. Microbiol.* 39, 286–290.
28. Battista, J. R., Park, M. J. & McLemore, A. E. (2001) *Cryobiology* 43, 133–139.
29. Battista, J. R., Howell, H. A., Park, M. J., Earl, A. & SN, P. (2002) in *Genome*. DOE Contractor-Grantee Workshop IX, Oakland, CA), pp. 88.
30. Aravind, L. (2000) *Genome Res.* 10, 1074–1077.
31. Jilani, A., Ramotar, D., Slack, C., Ong, C., Yang, X. M., Scherer, S. W. & Lasko, D. D. (1999) *J. Biol. Chem.* 274, 24176–24186.
32. Aravind, L. & Koonin, E. V. (1999) *J. Mol. Biol.* 287, 1023–1040.
33. Doherty, A. J. & Suh, S. W. (2000) *Nucleic Acids Res.* 28, 4051–4058.
34. Sanchez-Campillo, M., Dramsi, S., Gomez-Gomez, J. M., Michel, E., Dehoux, P., Cossart, P., Baquero, F. & Perez-Diaz, J. C. (1995) *Mol. Microbiol.* 18, 801–811.
35. Moseley, B. E. & Evans, D. M. (1983) *J. Gen. Microbiol.* 129, 2437–2445.
36. Eddy, S. R. (2001) *Nat. Rev. Genet.* 2, 919–929.
37. Arn, E. A. & Abelson, J. N. (1996) *J. Biol. Chem.* 271, 31145–31153.
38. Heale, E. S. & Linn, S. (1997) *J. Biol. Chem.* 272, 19095–19098.
39. Lauble, H., Kennedy, M. C., Beinert, H. & Stout, C. D. (1994) *J. Mol. Biol.* 237, 437–451.
40. Courcelle, J., Khodursky, A., Peter, B., Brown, P. O. & Hanawalt, P. C. (2001) *Genetics* 158, 41–64.
41. Narumi, I., Satoh, K., Kikuchi, M., Funayama, T., Yanagisawa, T., Kobayashi, Y., Watanabe, H. & Yamamoto, K. (2001) *J. Bacteriol.* 183, 6951–6956.
42. Campbell, E. A., Muzzin, O., Chlenov, M., Sun, J. L., Olson, C. A., Weinman, O., Trester-Zedlitz, M. L. & Darst, S. A. (2002) *Mol. Cell* 9, 527–539.
43. Gaur, N. K., Oppenheim, J. & Smith, I. (1991) *J. Bacteriol.* 173, 678–686.
44. Labie, C., Bouche, F. & Bouche, J. P. (1989) *J. Bacteriol.* 171, 4315–4319.
45. Battista, J. R. (1997) *Annu. Rev. Microbiol.* 51, 203–224.
46. Makarova, K. S., Aravind, L., Daly, M. J. & Koonin, E. V. (2000) *Genetica* 108, 25–34.
47. Altschul, S. F., Madden, T. L., Schaffer, A. A., Zhang, J., Zhang, Z., Miller, W. & Lipman, D. J. (1997) *Nucleic Acids Res.* 25, 3389–3402.
48. Lee, J. Y., Chang, C., Song, H. K., Moon, J., Yang, J. K., Kim, H. K., Kwon, S. T. & Suh, S. W. (2000) *EMBO J.* 19, 1119–1129.

APPLIED AND ENVIRONMENTAL MICROBIOLOGY, Aug. 2003, p. 000
0099-2240/03/$08.00+0 DOI: 10.1128/AEM.69.8.000–000.2003

Vol. 69, No. 8

Engineering *Deinococcus geothermalis* for Bioremediation of High-Temperature Radioactive Waste Environments

Hassan Brim,[1] Amudhan Venkateswaran,[1] Heather M. Kostandarithes,[2] James K. Fredrickson,[2] and Michael J. Daly[1]*

Department of Pathology, Uniformed Services University of the Health Sciences, Bethesda, Maryland 20814,[1] and Pacific Northwest National Laboratory, Richland, Washington 99352[2]

Received 5 May 2003/Accepted 4 June 2003

***Deinococcus geothermalis* is an extremely radiation-resistant thermophilic bacterium closely related to the mesophile *Deinococcus radiodurans*, which is being engineered for in situ bioremediation of radioactive wastes. We report that *D. geothermalis* is transformable with plasmids designed for *D. radiodurans* and have generated a Hg(II)-resistant *D. geothermalis* strain capable of reducing Hg(II) at elevated temperatures and in the presence of 50 Gy/h. Additionally, *D. geothermalis* is capable of reducing Fe(III)-nitrilotriacetic acid, U(VI), and Cr(VI). These characteristics support the prospective development of this thermophilic radiophile for bioremediation of radioactive mixed waste environments with temperatures as high as 55°C.**

Fn* The bacterium *Deinococcus geothermalis* (13) is remarkable not only for its extreme resistance to ionizing radiation but also for its ability to grow at temperatures as high as 55°C (13) and in the presence of chronic irradiation (8). The organism was isolated by Ferreira et al. (13) from hot springs together with *Deinococcus murrayi*. Both bacteria are moderately thermo- AQ: A philic and belong to the bacterial family *Deinococcaceae* (4, 7, 22), currently comprised of seven distinct nonpathogenic radiation-resistant species, of which *Deinococcus radiodurans* strain R1 is the best characterized (4). Advances in genetic engineering for *D. radiodurans* (9–12, 29) were a stimulus for its genome sequencing (17, 33), annotation (22), and proteomic (18) and transcriptome (19) analyses. The other deinococcal species have been reported as nontransformable or have not yet been tested for transformability by chromosomal or plasmid DNA and have been left unexplored by recombinant DNA technologies. Other genetic approaches including conjugation and protoplast fusion have not been successful in the *Deinococcaceae* (16).

A present genetic engineering goal for *D. radiodurans* is its development for bioremediation of U.S. Department of Energy (DOE) mixed radioactive environmental waste sites left over from nuclear weapons production during the Cold War (21, 25, 27, 28). These sites contain immense volumes of waste (3×10^6 m^3) that include radionuclides, heavy metals, and toxic organic compounds and have contaminated 40 million cubic meters of soil and 4 trillion liters of groundwater since 1946 (1, 21, 25, 27, 28). While there has been significant progress in engineering *D. radiodurans* for remediation of radioactive DOE waste environments (5, 8, 15), prospective treatment of contaminated sites with engineered *D. radiodurans* will be limited to temperatures below 37°C, its maximum growth temperature. However, there is a need to develop bioremediating bacteria that are resistant to both radiation and high temperatures because of the existence of thermally insulated contaminated environments where temperatures are elevated by the decay of long-lived radionuclides (e.g., ^{137}Cs and ^{90}Sr) (1). For example, soil columns beneath at least 67 radioactive leaking tanks at DOE's Hanford Site in south-central Washington State have been contaminated and have recorded temperatures as high as 70°C at depths of greater than 18 m (1). Since *D. geothermalis* and *D. murrayi* are both radiation resistant and thermophilic, they have become desirable targets for genetic development of bioremediating strains similar to those developed for *D. radiodurans* (5, 8, 15) but capable of survival and growth at higher temperatures. Given the need to develop bioremediating bacteria for treatment of radioactive high-temperature waste environments, *D. geothermalis* and *D. murrayi* were tested for their transformability with the autonomously replicating *Escherichia coli-D. radiodurans* shuttle AQ: B plasmid pMD66 (9), which expresses kanamycin (KAN) and tetracycline (TET) resistance in *D. radiodurans* and additionally expresses ampicillin resistance in *E. coli*.

pMD66 and its numerous derivatives (9–12) have been used successfully to functionally express cloned genes in *D. radiodurans* growing under chronic irradiation. Examples include the *mer* operon of *E. coli* (5), which encodes Hg(II) resistance and reduction, and the *Pseudomonas* operon *todC1C2BA* (15), which encodes partial degradation of toluene. The present work shows that *D. geothermalis* is capable of expressing Hg(II)-reducing functions cloned in pMD66 at elevated temperatures and under chronic radiation and, like *D. radiodurans* (14), is naturally capable of reducing a variety of other metal contaminants present in DOE waste sites.

MATERIALS AND METHODS

Bacterial strains, growth conditions, and transformation. *D. radiodurans* R1 (33), *D. geothermalis* DSM11300, and *D. murrayi* DSM11303 were grown in TGY broth (1% Bacto Tryptone, 0.1% glucose, 0.5% Bacto Yeast Extract) (Difco) or minimal medium (MM) (see Table 2) (32). Liquid cultures were inoculated at ~5×10^6 cells/ml. For solid medium, Bacto Agar (Difco) or Noble agar (Difco) was added to TGY or MM, respectively, to 1.5% (wt/vol). *D. radiodurans* was grown at 32°C, and *D. geothermalis* and *D. murrayi* were grown at 37°C or at higher temperatures as indicated. *E. coli* was grown in Luria-Bertani medium at

* Corresponding author. Mailing address: Uniformed Services University of the Health Sciences (USUHS), Rm. B3153, 4301 Jones Bridge Rd., Bethesda, MD 20814-4799. Phone: (301) 295-3750. Fax: (301) 295-1640. E-mail: mdaly@usuhs.mil.

37°C (9). pMD66 (9) (purified from *E. coli*) encodes ampicillin resistance (Ap^r), Km^r, and Tet^r in *E. coli* and Km^r and Tet^r in *D. radiodurans*. When pMD66 is prepared from *E. coli*, the plasmid transforms *D. radiodurans* with low efficiency (~50 transformants/μg) (9). However, when the same plasmid is purified from *D. radiodurans*, it transforms wild-type *D. radiodurans* with efficiencies as high as 10^6 transformants/μg (9). Plasmid transformation-restriction in *D. radiodurans* (9), therefore, distinguishes between the sources of plasmids. When purified from *E. coli*, the plasmid is called pMD66, and when purified from *D. radiodurans*, it is called pMD68 (9). The situation for a derivative (pMD300) of pMD66 encoding chloramphenicol resistance (Cm^r) is analogous (10). pMD300 purified from *E. coli* encodes Cm^r in *E. coli* and *D. radiodurans* and when purified from *D. radiodurans* is called pMD308 (10). Expression of heterologous genes and antibiotic resistance markers cloned into pMD66-type vectors is driven by two different deinococcal constitutive promoters (P1 and P2) (e.g., see Fig. 2A) that are active on autonomous plasmids in *D. radiodurans* or when integrated into *D. radiodurans* chromosomes (11, 12). pMD66-type plasmids contain a deinococcal origin of replication (dORI); an *E. coli* origin of replication (eORI); and resistance genes including *aphA* (encoding Km^r), *bla* (encoding Ap^r), and/or the *mer* operon (encoding mercury resistance) (3, 5).

The selective drug concentrations for deinococci were 8 μg of KAN per ml, 2.5 μg of TET per ml, and 3 μg of chloramphenicol per ml. For *E. coli*, antibiotics were added to Luria-Bertani medium as follows: KAN (50 μg/ml), TET (25 μg/ml), and chloramphenicol (30 μg/ml). Transformation of deinococci was by a $CaCl_2$-dependent technique described previously for *D. radiodurans* (16) but with the following modifications. Exponential cultures of deinococci were resuspended at 10^8 cells per ml in TGY broth–0.1 M $CaCl_2$–glycerol (20:8:3, vol/vol/vol). For transformation, 100 μl of the cell suspension and 5 μl of water containing various amounts of transforming DNA were added. The cell mixture was held on ice for 15 min and then incubated at 32°C for 30 min with gentle agitation. TGY (0.9 ml) was then added, and the mixture was incubated at 32°C (for *D. radiodurans*) or 37°C (for *D. geothermalis*) for 16 h with aeration before being plated on drug-selected agar.

Irradiation. Growth of cells in the presence of chronic irradiation, 50 Gy/h (^{137}Cs Gammacell 40 irradiation unit [Atomic Energy of Canada Limited]), was carried out as described previously (5, 8, 15). For high-level acute irradiation exposures, early-stationary-phase deinococcal cultures (optical density at 600 nm [OD_{600}] of 0.9 corresponds to ~10^8 CFU/ml) were irradiated without change of broth on ice at 10 kGy/h (^{60}Co Gammacell irradiation unit [J. L. Shepard and Associates; Model 109]). For the deinococcal species under investigation, three independent cell cultures and irradiation treatments of the same kind were performed. Following exposure to the indicated doses, cell suspensions were appropriately diluted and assayed for viability by plate assay on rich (TGY) medium (9). Viability data were used to construct survival curves with standard deviations according to conventional formats (9, 24). The effect of chronic exposure to gamma radiation and Hg(II) on the growth of engineered *D. geothermalis* was determined using TGY agar plates with and without 30 μM merbromin [Hg(II)] (5). Plates were spotted with ~10^5 cells and following plate inoculation were placed into the ^{137}Cs irradiator (50 Gy/h) for incubation at 50°C for 5 days.

AQ: C

DNA isolation and manipulation. Isolation of plasmid DNA and total DNA from *E. coli*, *D. radiodurans*, and *D. geothermalis*; use of enzymatic reagents; gel electrophoresis; plasmid rescue in *E. coli*; radiolabeling of DNA; hybridization; washing of blots; and autoradiography were performed as previously described (9–12). For Fig. 1B, *D. geothermalis* (wild-type) and *D. geothermalis*/pMD66 total DNA preparations were digested with *Eco*RI. The blot was double hybridized with a 1.5-kb *Xba*I genomic *recA* (*D. radiodurans*) probe and a 1.5-kb *Eco*RI-*Bpu*10I probe of pBR322 that is specific to pMD66.

F1

Mercury volatilization assay. Cells were pregrown to an OD_{600} of 0.5 in the presence of 20 μM merbromin [Hg(II)] as described previously (5). Cells of each strain were harvested, washed twice in fresh medium lacking Hg(II), and concentrated to an OD_{600} of 2.0 in fresh medium, followed by the inoculation of 10^7 cells of each into 200 μl of medium containing 30 μM merbromin contained in 300-μl wells of a microplate, respectively. The plates were covered with a sheet of X-ray film, held together with a weight, and incubated in the dark at 32 or 40°C. Following exposure for 14 h, the films were developed.

Metal reduction by *D. geothermalis*. The native metal reduction capabilities of *D. radiodurans* have been examined previously (14). The protocols for examining metal reduction by *D. geothermalis* are essentially identical to those used for *D. radiodurans* (6, 14, 30, 31) but at higher temperatures. The ability of *D. geothermalis* to reduce Fe(III) (as Fe-nitrilotriacetic acid [NTA]) was examined in cultures containing 10 mM lactate in basal medium at 45°C. For the experiment with Cr(VI) and U(VI), cultures were incubated in TGY at 40°C.

RESULTS

Transformation of *D. geothermalis* and *D. murrayi*. Plasmid transformation of *D. geothermalis* by using pMD66/68 was successful (Table 1), with stable introduction proven by hybridization with a pMD66 probe (Fig. 1A). *D. geothermalis* was also transformable with the Cm^r-encoding *D. radiodurans* plasmid pMD300/308 (data not shown). While the transformation efficiencies were much lower for *D. geothermalis* than for *D. radiodurans*, irrespective of the source of plasmid (Table 1), this was not a problem because the transforming DNA could be prepared and used in bulk. Electroporation as an alternative method of transformation was previously shown not to be effective for *D. radiodurans* (M. J. Daly, unpublished data), where the low electroporation efficiencies were attributed to the unusually thick cell wall structures of deinococci. Figure 1B shows the assessment of the copy number of pMD66 in *D. geothermalis* relative to the chromosomal content by comparing the hybridization of two similarly sized nonhomologous probes to total DNA prepared from *D. geothermalis*/pMD66. The *recA* probe (1.5 kb, derived from *D. radiodurans*) is a reporter of chromosome copy number, and the pMD66 probe (1.5 kb, derived from pBR322) is specific to the plasmid. The hybridization signal for the *recA* probe was determined by densitometry to be about one-third of the intensity arising from the pMD66 probe, suggesting that pMD66 exists in multiple copies in *D. geothermalis*.

T1

Stability of *D. geothermalis*/pMD66. Deinococcal sequences in pMD66/68 are derived exclusively from *D. radiodurans* strain SARK (9, 16), which has no detectable homology to *D. radiodurans* strain R1 or *D. geothermalis* (Fig. 1A). To test whether pMD66 is uniformly retained and repaired in *D. geothermalis* following acute irradiation, *D. geothermalis*/pMD66 was assessed for survival following various exposures to ionizing radiation and recovery on TGY, or on TGY supplemented with KAN as a marker for the presence of pMD66 (Fig. 1C). The survival of *D. geothermalis*/pMD66 plated on TGY-KAN was indistinguishable from that found for wild-type *D. geothermalis* on TGY. Plasmid rescue in *E. coli* from total DNA purified from a culture of *D. geothermalis*/pMD66 following recovery from 12 kGy showed that, of 1,000 Km^r *E. coli* colonies rescued, 100% were also Tet^r and Ap^r, supporting the idea

FIG. 1. Transformation of *D. geothermalis* with pMD66 and resistance of pMD66-transformed *D. geothermalis* to acute gamma radiation. (A) *D. geothermalis*/pMD66. Total DNA from the indicated strains was uncut or digested with *Pst*I before electrophoresis, blotting, and probing of the blot with a whole-plasmid radiolabeled pMD66 probe. Abbreviations: DEIRA, *D. radiodurans*; DEIGEO, *D. geothermalis*. (B) The copy number of pMD66 in *D. geothermalis*/pMD66 is about threefold higher than its chromosomal copy number. (C) Survival of *D. geothermalis*/pMD66 following acute gamma radiation. Symbols: open squares, *D. geothermalis* plated on TGY at 37°C; solid triangles, *D. geothermalis*/pMD66 plated on TGY-KAN at 37°C; solid diamonds, *D. radiodurans* plated on TGY at 32°C.

TABLE 1. Transformation of pMD66/68 into *D. geothermalis*, *D. radiodurans* and *E. coli*

	No. of transformants/μg of DNA for recipient[a]:		
	D. geothermalis	*D. radiodurans*	*E. coli*
Plasmid source[b]			
pMD66 (purified from *E. coli*)	$1 \times 10^1 \pm 2 \times 10^1$	$1 \times 10^2 \pm 8 \times 10^1$	$9 \times 10^4 \pm 3 \times 10^3$
pMD68 (purified from *D. radiodurans*)	$5 \times 10^1 \pm 2 \times 10^1$	$8 \times 10^5 \pm 1.5 \times 10^4$	$4 \times 10^5 \pm 2.1 \times 10^4$
AQ: F pMD66 (purified from *D. geothermalis*)	$5 \times 10^2 \pm 29 \times 10^1$	$4 \times 10^5 \pm 7 \times 10^3$	$4 \times 10^2 \pm 25 \times 10^1$

[a] Km^r transformants per microgram of plasmid purified from the indicated strains.
[b] pMD66, pMD68, and pMD66-*D. geothermalis* have identical restriction maps (Fig. 1A).

that irradiation-induced mutations and deletions are rare in *D. geothermalis*, as is the case in *D. radiodurans* (9, 11). These results show that pMD66 is retained in *D. geothermalis* without alteration following high-dose irradiation and recovery and is repaired with similar efficiency to its chromosomes.

Construction and characterization of Hg(II)-resistant *D. geothermalis*. The complete *E. coli* Hg(II) resistance (*mer*) operon (4.2 kb, encoding six proteins) (3, 5) has previously been functionally expressed in *D. radiodurans* by using a F2 pMD66 derivative, pMD727 (5) (Fig. 2A). In *D. radiodurans*, all six *mer* genes are necessary for reduction of Hg(II) to Hg(0). pMD727 was successfully transformed into *D. geothermalis* (Fig. 2B), yielding strain MD865. This construction placed the *mer* genes under the control of a constitutive *D. radiodurans* promoter (P2, Fig. 2A), and Southern analysis with a radiolabeled probe containing a 1.5-kb *Eco*RI-*Bgl*II fragment from the *mer* operon showed no significant homology with the *D. geothermalis* genome (Fig. 2B). Reduction of Hg(II) to volatile elemental Hg(0) by *D. geothermalis* strain MD865 was examined by testing for mercury volatilization, which causes film darkening (5, 26). Following 14 h of incubation with Hg(II) in a microplate at 32 or 40°C, covered by X-ray film, wild-type *D. geothermalis* showed modest Hg(0) volatilization. However, strain MD865 (*D. geothermalis*/*mer*$^+$) showed substantial Hg(0) volatilization based on film darkening compared to wild-type *D. geothermalis* at 32 or 40°C (Fig. 2C). MD865 also was resistant to 50 μM Hg(II) during growth at 50°C (Fig. 2D) and displayed luxuriant growth at 50°C in the presence of 50 Gy/h on solid medium containing 30 μM merbromin (data not shown). Wild-type *D. geothermalis* did not grow in medium containing 30 μM merbromin in the presence or absence of chronic radiation.

Reduction of metals. *D. geothermalis* reduced Fe(III)-NTA in the presence of lactate at 30°C (data not shown) and in the F3 presence of lactate or pyruvate at 45°C (Fig. 3A). At 40°C *D. geothermalis* rapidly reduced Cr(VI) in TGY cultures under both aerobic and anaerobic conditions (Fig. 3B). AQDS (anthraquinone-2,6-disulfonate) is a quinone-containing organic compound that can be utilized as an electron acceptor for respiration and growth by a variety of dissimilatory metal-reducing bacteria (20). As an electron acceptor, AQDS is reduced to the corresponding dihydroquinone (AH_2DS) (20). Reduction of U(VI) by *D. geothermalis* at 40°C occurred only in the presence of AQDS (Fig. 3C). These results are very similar to the reduction capabilities reported for *D. radiodurans* at lower temperatures (14).

Growth characteristics of *D. geothermalis*. *D. geothermalis* was tested for its amino acid utilization and growth on various Embden-Meyerhof-Parnas substrates. Table 2 shows that, in T2 the absence of irradiation, growth of *D. geothermalis* is independent of any amino acids and the bacterium can utilize ammonium sulfate and grow on tricarboxylic acid cycle intermediates. In the presence of chronic irradiation, growth of *D. geothermalis* is less dependent than that of *D. radiodurans* on Cys and His, or other exogenously provided amino acids (data not shown). Therefore, the metabolism of *D. geothermalis* appears substantially more robust than that in *D. radiodurans*. .

DISCUSSION

D. geothermalis is transformable with autonomous plasmids originally constructed for *D. radiodurans*. Thus, experimental advances in the genetic management of *D. radiodurans* over the last decade (5, 8, 24) could facilitate rapid development of *D. geothermalis* for fundamental and practical objectives. *D. geothermalis* is a thermophile (13) with substrate utilization-growth characteristics that are distinct from those of *D. radiodurans* (Table 2). Under nonirradiating conditions, *D. geothermalis* is not dependent on exogenous amino acids for growth and can utilize ammonium sulfate. These characteristics endow the species with the ability to grow in nutritionally restricted environments that do not support the growth of *D. radiodurans* (32). *D. geothermalis* is also able to grow over a broad temperature range extending to 55°C (13) and displays superior growth in the presence of chronic irradiation (50 Gy/h) in nutritionally restricted medium, compared to *D. radiodurans*. While these characteristics support the idea that *D. geothermalis* may be a more robust candidate than *D. radiodurans* for treatment of radioactive environmental waste environments

FIG. 2. Construction and characterization of Hg(II)-resistant-reducing *D. geothermalis*. (A) pMD727 (5) was transformed into *D. geothermalis*, AQ: E giving strain MD865. (B) Southern blot hybridization of *Eco*RI-digested total DNA from *D. geothermalis* (wild type, *mer* negative) and MD865 (*D. geothermalis*/*mer*$^+$) with a radiolabeled *mer* probe. pMD727 contains a unique *Eco*RI (E) site. Molecular size standards: λ/*Hin*dIII, as in Fig. 1A and B. Wild-type strain abbreviations are as in Fig. 1. (C) Hg(0) volatilization assays at 32 and 40°C for *D. geothermalis*, *D. radiodurans*, MD865 and MD735 (*D. radiodurans*/*mer*$^+$), and TGY (growth medium, no cells). (D) Growth curves for MD865 and MD735 in TGY plus 50 μM merbromin [Hg(II)] at 50°C.

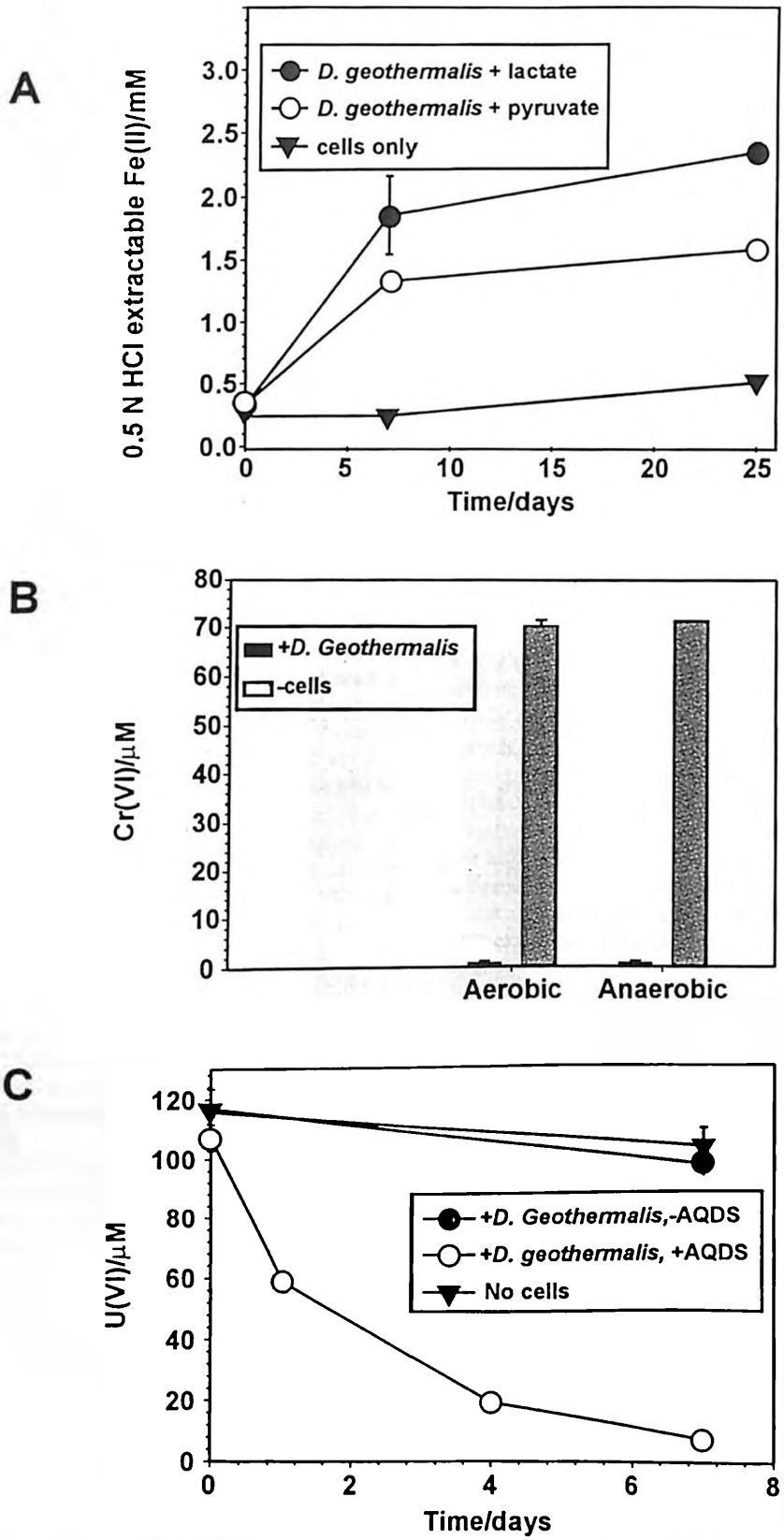

FIG. 3. Metalloreduction by wild-type *D. geothermalis*. (A) Fe(III)-NTA reduction coupled to oxidation of organic substrates at 45°C in the absence of oxygen. (B) Cr(VI) reduction in aerobic or anaerobic conditions as measured by loss of Cr(VI) from solution at 40°C. (C) Reduction of U(VI) in the presence or absence of AQDS as measured by loss of U(VI) at 40°C.

TABLE 2. Growth characteristics of *D. radiodurans* and *D. geothermalis* grown in mm[a]

Substrate[c]	Growth of strain[b]	
	D. radiodurans	*D. geothermalis*
Fructose + C,H,L,A,T,P	+++	+++
Fructose + Cys	+++	+++
Fructose −aa + $NH_4^+SO_4^{2-}$	−	+++
Fructose −NAD + Cys	−	+++
α-Ketoglutarate	−	++
Succinate	−	++
Fumarate	−	++
Oxaloacetate	−	++
Malate	−	+

[a] Deinococcal cells were grown in deinococcal MM (32) at 32°C. Deinococcal MM contained the indicated Embden-Meyerhof-Parnas substrate (2 mg/ml), NAD (1 μg/ml), cysteine (Cys) at 50 μg/ml, phosphate buffer (20 mM, pH 7.5), $CaCl_2$ (0.18 mM), and $MgSO_4$ (0.8 mM), and Mn^{2+} (5.4 μM $MnCl_2$) was added as the only transition metal cation.

[b] Growth on substrate: +++, good; ++, moderate; +, poor; −, absent.

[c] Abbreviations: Fructose + C,H,L,A,T,P, fructose plus Cys, His, Lys, Asp, Trp, and Pro, each at 50 μg/ml. + Cys, only cysteine added at 50 μg/ml. −aa, no amino acids added. + $NH_4^+SO_4^{2-}$, ammonium sulfate added to a final concentration of 15 mM. −NAD, no NAD added.

(32), until now there has been no genetic system available to exploit this species.

Our data show that plasmid-based transformation systems developed for *D. radiodurans* (Fig. 1 and 2) can be used to functionally express cloned genes in *D. geothermalis* at temperatures as high as 50°C (Fig. 2) and in the presence of chronic irradiation. Plasmids introduced into *D. geothermalis* are also efficiently expressed following exposure to high-level acute irradiation (Fig. 1C), without any apparent plasmid loss or mutagenesis. The differential hybridization results with a chromosome- and a plasmid-derived probe in MD865 (*D. geothermalis*/pMD66) (Fig. 1B) support the idea that pMD66 exists in multiple copies in *D. geothermalis*. The survival of *D. geothermalis*/pMD66 plated on TGY-KAN was indistinguishable from that found for wild-type *D. geothermalis* on TGY. As in *D. radiodurans*, this suggests that multiple identical plasmid copies serve as a substrate for efficient repair by homologous recombination (10). Therefore, these studies establish *D. geothermalis* and *D. radiodurans* as the only two extremely radiation-resistant vegetative bacteria that are currently amenable to genetic engineering.

The presence of pMD66 in *D. geothermalis* as a covalently closed circle was confirmed by plasmid rescue in *E. coli* (Table 1) (12), and restriction enzyme mapping and Southern analysis confirmed its predicted structure and stability in *D. geothermalis* (Fig. 1A). When total DNA containing pMD66 was purified from *D. geothermalis* and transformed back into wild-type *D. geothermalis*, there was only a small increase in the number of transformants over that with pMD66 purified from *E. coli*. In contrast, there was a large increase in transformation frequency observed in *D. radiodurans* with pMD66 purified from *D. radiodurans* or *D. geothermalis* over that with pMD66 purified from *E. coli* (Table 1). Therefore, the plasmid transformation capabilities of *D. geothermalis* appear to be significantly less for *D. radiodurans*. While the reasons for this difference are unclear, the fact that pMD66 purified from *D. geothermalis* could be used to transform *D. radiodurans* at high efficiency, but not *D. geothermalis*, suggests that transport of DNA into *D. geothermalis* is inefficient. Wild-type *D. murrayi* is naturally resistant to KAN and, therefore, was not tested for transformability with pMD66/68. However, *D. murrayi* is sensitive to chloramphenicol and could be a suitable host for plasmids encoding Cm^r, but we found it to be nontransformable with high concentrations of pMD300/308 (10) purified from *E. coli* or *D. radiodurans* and did not investigate this species further.

To demonstrate the utility of *D. geothermalis* for bioremediation purposes, we introduced the highly characterized Hg(II) resistance operon (*mer*) of *E. coli* (3) into *D. geothermalis* on an autonomously replicating *D. radiodurans* plasmid (Fig. 2A). Ionic Hg(II) is a prevalent contaminant of radioactive DOE waste sites, where the highest concentration level in contaminated areas has been reported as 10 μM (28). When present in *D. radiodurans*, the *mer* operon confers Hg(II) resistance and endows cells with the ability to reduce highly toxic Hg(II) to much less toxic elemental Hg(0) (5). Similarly, we show that strain MD865 (*D. geothermalis*/*mer*$^+$) is (i) resistant to the bactericidal effects of ionic Hg(II) at concentrations (50 μM; Fig. 2D) well above the highest concentration reported for Hg(II)-contaminated DOE waste sites, (ii) able to reduce toxic Hg(II) to much less toxic elemental and volatile Hg(0) (Fig. 2C), and (iii) able to functionally express the *mer* operon in highly irradiating environments (50 Gy/h) at temperatures as high as 50°C. It is notable that the mesophilic *E. coli* Mer proteins (3) were functional in *D. geothermalis* growing at 50°C. While mechanisms underlying thermophilicity appear to be complex and currently are not well characterized (23), there is some precedent for the interchangeability of genes from mesophiles and thermophiles. For example, the aspartate aminotransferase gene (*aspATSs*) of the hyperthermophile *Sulfolobus solfataricus* has been functionally expressed at mesophilic temperatures in *E. coli* (2). We believe that numerous other metal resistance functions from other bacteria, specific for other metals, could be cloned into *D. geothermalis* by this approach.

It was recently shown that under strict anaerobic conditions *D. radiodurans* can reduce Fe(III)-NTA coupled to the oxidation of lactate to CO_2 and acetate (14). *D. radiodurans* could also reduce U(VI) or Tc(VII) in the presence of AQDS and could directly reduce Cr(VI) in both anaerobic and aerobic conditions (14). The enzymatic reduction of multivalent metals and radionuclides can have a major impact on their solubility and, hence, mobility in the environment. Such changes in solubility make microbial metal reduction a suitable process for immobilizing metals and radionuclides within contaminated environments in situ (8, 25). Localized contaminated sediments and soils at DOE sites can have temperature levels that exceed those that can be tolerated by *D. radiodurans*. We show that the *D. geothermalis* suite of metal-reducing capabilities appears to be very similar to that reported in detail for *D. radiodurans* (14) but functional at higher temperatures (Fig. 3).

We are not aware of expression of any cloned genes in *D. geothermalis* previous to this report. Our demonstration that plasmids developed for *D. radiodurans* are functional in *D. geothermalis* strongly supports the idea that bioremediating gene constructs developed for *D. radiodurans* could be transferred to *D. geothermalis*. This could yield metabolically proficient, extremely radiation-resistant, and thermophilic bacteria suit-

able for the treatment of high-temperature mixed radioactive wastes.

ACKNOWLEDGMENTS

This research was funded by U.S. Department of Energy (Office of Biological and Environmental Research) grants DE-FG02-97ER62492 from the Natural and Accelerated Bioremediation Research Program and DE-FG02-01ER63220 from the Genomes to Life Program.

REFERENCES

1. **Agnew, S. F., and R. A. Corbin.** 1998. Analysis of SX farm leak histories: historical leak model. Los Alamos National Laboratory, Los Alamos, N.Mex.
2. **Arnone, M. I., L. Birolo, M. V. Cubellis, G. Nitti, G. Marino, and G. Sannia.** 1992. Expression of a hyperthermophilic aspartate aminotransferase in *Escherichia coli*. Biochim. Biophys. Acta 1160:206–212.
3. **Barrineau, P., P. Gilbert, W. J. Jackson, C. S. Jones, A. O. Summers, and S. Wisdom.** 1985. The structure of the *mer* operon. Basic Life Sci. 30:707–718.
4. **Battista, J. R.** 1997. Against all odds: the survival strategies of *Deinococcus radiodurans*. Annu. Rev. Microbiol. 51:203–224.
5. **Brim, H., S. C. McFarlan, J. K. Fredrickson, K. W. Minton, M. Zhai, L. P. Wackett, and M. J. Daly.** 2000. Engineering *Deinococcus radiodurans* for metal remediation in radioactive mixed waste environments. Nat. Biotechnol. 18:85–90.
6. **Brina, R., and A. G. Miller.** 1992. Direct detection of trace levels of uranium by laser-induced kinetic phosphometry. Anal. Chem. 64:1413–1418.
7. **Brooks, B. W., R. G. E. Murray, J. L. Johnson, E. Stackebrandt, C. R. Woese, and G. E. Fox.** 1980. Red-pigmented micrococci: a basis for taxonomy. Int. J. Syst. Bacteriol. 30:627–646.
8. **Daly, M. J.** 2000. Engineering radiation-resistant bacteria for environmental biotechnology. Curr. Opin. Biotechnol. 11:280–285.
9. **Daly, M. J., L. Ouyang, P. Fuchs, and K. W. Minton.** 1994. In vivo damage and *recA*-dependent repair of plasmid and chromosomal DNA in the radiation-resistant bacterium *Deinococcus radiodurans*. J. Bacteriol. 176:3508–3517.
10. **Daly, M. J., L. Ouyang, and K. W. Minton.** 1994. Interplasmidic recombination following irradiation of the radioresistant bacterium *Deinococcus radiodurans*. J. Bacteriol. 176:7506–7515.
11. **Daly, M. J., and K. W. Minton.** 1995. Interchromosomal recombination in the extremely radioresistant bacterium *Deinococcus radiodurans*. J. Bacteriol. 177:5495–5505.
12. **Daly, M. J., and K. W. Minton.** 1996. An alternative pathway of recombination of chromosomal fragments precedes *recA*-dependent recombination in the radioresistant bacterium *Deinococcus radiodurans*. J. Bacteriol. 178:4461–4471.
13. **Ferreira, A. C., M. F. Nobre, F. A. Rainey, M. T. Silva, R. Wait, J. Burghardt, A. P. Chung, and M. S. da Costa.** 1997. *Deinococcus geothermalis* sp. nov. and *Deinococcus murrayi* sp. nov., two extremely radiation-resistant and slightly thermophilic species from hot springs. Int. J. Syst. Bacteriol. 47:939–947.
14. **Fredrickson, J. K., H. M. Kostandarithes, S. W. Li, A. E. Plymale, and M. J. Daly.** 2000. Reduction of Fe(III), Cr(VI), U(VI) and Tc(VII) by *Deinococcus radiodurans* R1. Appl. Environ. Microbiol. 66:2006–2011.
15. **Lange, C. C., L. P. Wackett, K. W. Minton, and M. J. Daly.** 1998. Engineering a recombinant *Deinococcus radiodurans* for organopollutant degradation in radioactive mixed waste environments. Nat. Biotechnol. 16:929–933.
16. **Lennon, E., and K. W. Minton.** 1990. Gene fusions with *lacZ* by duplication insertion in the radioresistant bacterium *Deinococcus radiodurans*. J. Bacteriol. 172:2955–2961.
17. **Lin, J., R. Qi, C. Aston, J. Jing, T. S. Anantharaman, B. Mishra, O. White, M. J. Daly, K. W. Minton, J. C. Venter, and D. C. Schwartz.** 1999. Whole genome shotgun optical mapping of *Deinococcus radiodurans* using genomic DNA molecules. Science 285:1558–1561.
18. **Lipton, M. S., L. Pasa-Tolić, G. A. Anderson, D. J. Anderson, D. L. Auberry, J. R. Battista, M. J. Daly, J. K. Fredrickson, K. K. Hixson, H. Kostandarithes, C. Masselon, L. M. Markillie, R. J. Moore, M. F. Romine, Y. Shen, E. Stritmatter, N. Tolić, H. R. Udseth, A. Venkateswaran, K. K. Wong, R. Zhao, and R. D. Smith.** 2002. Global analysis of the *Deinococcus radiodurans* proteome using accurate mass tags. Proc. Natl. Acad. Sci. USA 99:11049–11054.
19. **Liu, Y., J. Zhou, M. V. Omelchenko, A. S. Beliaev, A. Venkateswaran, J. Stair, L. Wu, D. K. Thompson, D. Xu, I. B. Rogozin, E. K. Gaidamakova, M. Zhai, K. S. Makarova, E. V. Koonin, and M. J. Daly.** 2003. Transcriptome dynamics of *Deinococcus radiodurans* recovering from ionizing radiation. Proc. Natl. Acad. Sci. USA 100:4191–4196.
20. **Lovley, D. R., E. L. Coates, J. D. Blunt-Harris, E. J. P. Phillips, and J. C. Woodward.** 1996. Humic substances as electron acceptors for microbial respiration. Nature 382:445–448.
21. **Macilwain, C.** 1996. Science seeks weapons clean-up role. Nature 383:375–379.
22. **Makarova, K. S., L. Aravind, Y. I. Wolf, R. L. Tatusov, K. W. Minton, E. V. Koonin, and M. J. Daly.** 2001. Genome of the extremely radiation-resistant bacterium *Deinococcus radiodurans* viewed from the perspective of comparative genomics. Microbiol. Mol. Biol. Rev. 65:44–79.
23. **Makarova, K. S., Y. I. Wolf, and E. V. Koonin.** 2003. Potential genomic determinants of hyperthermophily. Trends Genet. 19:172–176.
24. **Mattimore, V., and J. R. Battista.** 1996. Radioresistance of *Deinococcus radiodurans*: functions necessary to survive ionizing radiation are also necessary to survive prolonged desiccation. J. Bacteriol. 178:633–637.
25. **McCullough, J., T. C. Hazen, S. M. Benson, F. Blaine-Metting, and A. C. Palmisano.** 1999. Bioremediation of metals and radionuclides. Office of Biological and Environmental Research, U.S. Department of Energy, Germantown, Md.
26. **Nakamura, K., and H. Nakahara.** 1988. Simplified X-ray film method for detection of bacterial volatilization of Hg chloride by *Escherichia coli*. Appl. Environ. Microbiol. 54:2871–2873.
27. **Office of Environmental Management, U.S. Department of Energy.** 1996. 1996 baseline environmental management report. Office of Environmental Management, U.S. Department of Energy, Washington, D.C. [Online.] http://www.em.doe.gov/bemr96.
28. **Riley, R. G., J. M. Zachara, and F. J. Wobber.** 1992. Chemical contaminants on DOE lands and selection of contaminant mixtures for subsurface science research. Subsurface Science Program, Office of Energy Research, U.S. Department of Energy, Washington, D.C.
29. **Smith, M. D., E. Lennon, L. B. McNeil, and K. W. Minton.** 1988. Duplication insertion of drug resistance determinants in the radioresistant bacterium *Deinococcus radiodurans*. J. Bacteriol. 170:2126–2135.
30. **Stookey, L. L.** 1970. Ferrozine—a new spectrophotometric reagent for iron. Anal. Chem. 42:779–781.
31. **Urone, P. F.** 1955. Stability of colorimetric reagent for chromium, s-diphenylcarbazide, in various solvents. Anal. Chem. 27:1354–1355.
32. **Venkateswaran, A., S. C. McFarlan, D. Ghosal, K. W. Minton, A. Vasilenko, K. S. Makarova, L. P. Wackett, and M. J. Daly.** 2000. Physiologic determinants of radiation resistance in *Deinococcus radiodurans*. Appl. Environ. Microbiol. 66:2620–2626.
33. **White, O., J. A. Eisen, J. F. Heidelberg, E. K. Hickey, J. D. Peterson, R. J. Dodson, D. H. Haft, M. L. Gwinn, W. C. Nelson, D. L. Richardson, K. S. Moffet, H. Qin, L. Jiang, W. Pamphile, M. Crosby, M. Shen, J. J. Vamathevan, P. Lam, L. McDonald, T. Utterback, C. Zalewski, K. S. Makarova, L. Aravind, M. J. Daly, K. W. Minton, R. D. Fleishmann, K. A. Ketchum, K. E. Nelson, S. Salzberg, J. C. Venter, and C. M. Fraser.** 1999. Complete genome sequencing of the radioresistant bacterium *Deinococcus radiodurans* R1. Science 286:1571–1577.

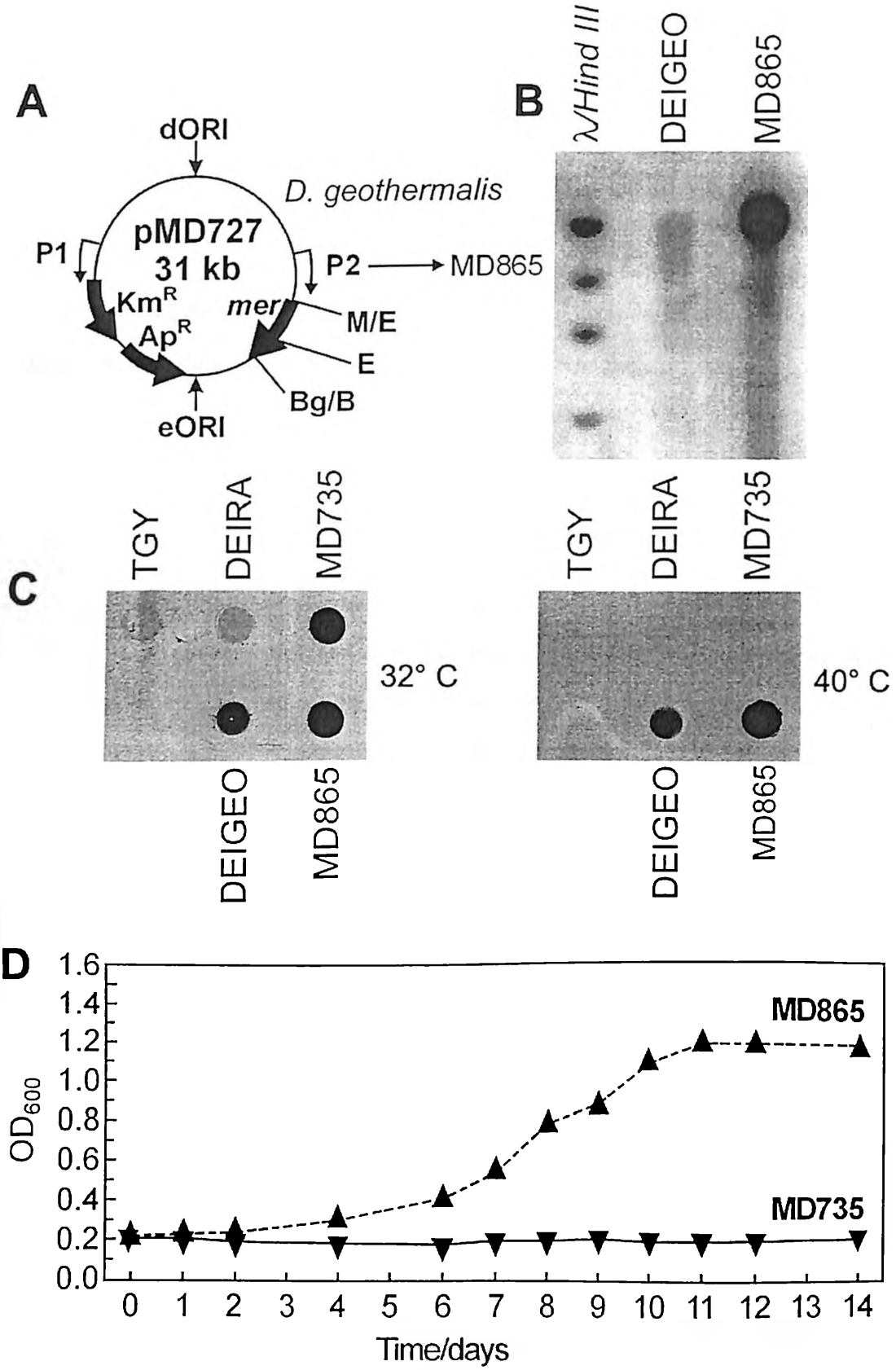

DNA Protection in the Extraordinary Survival of *Deinococcus radiodurans* Exposed to Ionizing Radiation

A. Vasilenko,[1] E. K. Gaidamakova,[1] V. Y. Matrosova,[1] D. Ghosal,[1] M. Zhai,[1] A. Venkateswaran,[1] H. Brim,[1] M. Hess,[1] M. V. Omelchenko,[1,2] H. M., Kostandarithes,[3] K. S. Makarova,[2] J. K. Fredrickson,[3] M. J. Daly[1]*

[1]Department of Pathology, Uniformed Services University of the Health Sciences, Bethesda, MD 20814, USA. [2]National Center for Biotechnology Information, National Institutes of Health, Bethesda, MD 20894, USA. [3]Pacific Northwest National Laboratory, Richland, WA 99352, USA.

*To whom correspondence should be addressed. E-mail: mdaly@usuhs.mil.

The bacterium *Deinococcus radiodurans* is extremely resistant to ionizing radiation. We propose that the extreme resistance phenotype of *D. radiodurans* is based mostly on DNA protection rather than efficient repair of double-stranded breaks (DSBs). The DNA protection is facilitated by very high intracellular manganese and low iron concentrations, which could quench radiation-induced oxidative stress and prevent Fenton-type reactions that generate DNA-damaging hydroxyl radicals produced during irradiation. We report that in the absence of repair, a given dose of ionizing radiation induces substantially fewer DSBs in *D. radiodurans* than in the more radiation-sensitive species *Escherichia coli* and *Shewanella oneidensis*, which contain relatively low Mn but high cellular Fe concentrations. We find that among the most radiation resistant bacterial groups reported that do not form resistant endospores, deinococci, enterococci, and lactobacilli share metabolic and physiologic traits including Mn accumulation, Fe-independence, resistance to Fe chelators, and luxuriant growth under chronic γ-radiation.

Deinococcus radiodurans is a non-pathogenic, free-living, obligate aerobic bacterium that typically grows in rich medium as clusters of two cells (diplococci) in the early stages of growth, and as four cells (tetracocci) in the late stages (1). In addition to being radiation resistant, the organism can withstand exposures to desiccation (2) and hydrogen peroxide (H_2O_2) (3). The irradiation dose yielding 37% survival (D_{37}) of logarithmically growing *D. radiodurans* is about 55-fold greater than *E. coli* (4). Irradiation-induced DSBs will lead to cell death if they are not repaired, and to deletions and other genetic rearrangements if rejoined by non-homologous repair processes. *D. radiodurans* maintains 4-8 haploid copies of its genome per cell (5), and the repair of chromosomal DSBs is known to be mediated by *recA*-independent (single-stranded annealing) (6) and *recA*-dependent (7) homologous recombination (8), but no error-prone SOS response is observed in *D. radiodurans* (9). Yet, the identity of the genetic systems underlying those repair processes in *D. radiodurans* remains unknown in spite of detailed global cellular analyses including whole genome sequencing and annotation, and transcriptome profiling of cells recovering from high-dose irradiation (9). The lack of a clearly identifiable unique DNA repair system in *D. radiodurans* has given rise to three competing views of the mechanisms responsible for its extraordinary survival; (i) there are novel repair functions encoded among hypothetical genes predicted by genomic annotation (9, 10); or (ii) *D. radiodurans* uses conventional DNA repair pathways, but with much greater efficiency than other bacteria (9, 10); or (iii) DNA repair in *D. radiodurans* is facilitated by its ringlike chromosomal structures (11). These hypotheses emphasize DNA repair, with little consideration given to the possibility that highly robust mechanisms of DNA protection may be key to the extreme resistance phenotype.

One repair model for *D. radiodurans* (11) attributes the extreme resistance phenotype to a mechanism that involves the fusion of ringlike nucleoids, in adjacent cell compartments of tetracocci or diplococci, that have undergone error-free end-joining of

irradiation-induced DSBs. We have developed a defined minimal medium (DMM) (12) for *D. radiodurans* and have reported morphological differences between cells grown in DMM versus cells grown in undefined rich medium (TGY) (12). In DMM, *D. radiodurans* grows predominantly as diplococci, even in the late stages of growth (12). To better resolve the morphology and ultrastructure of wild-type *D. radiodurans* grown in DMM or TGY, we examined cells by transmission electron microscopy (TEM) to determine the prevalence of ringlike nucleoids (Fig. 1), and also tested cells for their resistance to gamma-radiation (Fig. 2). The radiation resistance of late-log phase (LLP) *D. radiodurans* cultures grown in TGY (Fig. 2), that contained cells that lacked ringlike nucleoids (Fig. 1A), was slightly greater than the resistance of early-stationary phase (ESP) *D. radiodurans* cultures grown in DMM (Fig. 2), that contained cells with ringlike nucleoids (Fig. 1C, E). The occurrence of ringlike nucleoids in *D. radiodurans* cultures was dependent on growth phase. ESP *D. radiodurans* cultures contained ringlike nucleoids (Fig. 1B, C, D, E), but LLP cultures did not (Fig. 1A). The slightly greater resistance of cells grown in TGY compared to DMM at doses > 10 kGy has been reported previously (12) and is believed to be the result of cell grouping. Whereas four cells of a tetracoccus need to be killed to eliminate a colony-forming unit (CFU), only two cells of a diplococcus need to be killed. The rod-shaped *Deinococcus grandis* grows as single cells (13) and displays very similar resistance to irradiation in either TGY or DMM medium (Fig. 2), and ESP cells rarely displayed nuclear structures that could be described as ringlike (Fig. 1F,G). So far, neither comparative genomic (9) or experimental analyses (6-9, 11) unequivocally support any molecular model that explains the extreme radioresistance of *Deinococcaceae*.

While studying the relationship between growth conditions and nucleoid structure, we determined that the optimal growth of *D. radiodurans* in DMM was absolutely dependent on the addition of Mn(II) (Fig. 3A). We further examined the dependence of *D. radiodurans* growth on Fe, Co, Mo, and Cd (Fig. 3B), and found that its growth in

DMM is not dependent on any of these transition metals. Growth of obligate aerobic bacteria in Fe-deficient medium is unusual, and to further examine the extent of Fe-independence of *D. radiodurans* we tested its growth in DMM (prepared with Mn, but without Fe) that contained the Fe chelators 2,2'-dipyridyl (Dp, Fe(II)-chelator) and deferoxamine mesylate (Ds, Fe(III)-chelator). *D. radiodurans* growth was similar in Fe-deficient DMM in the absence or presence of 100 μM Dp plus 100 μM Ds (Fig. 3C). Survival of *D. radiodurans* following irradiation of cells pre-grown in the presence of iron chelators was the same as cells pre-grown without iron chelators (Fig. 2). However, recovery of *D. radiodurans* irradiated to 9 kGy was accelerated in liquid DMM that contained these two Fe chelators (100 μM, each) (Fig. 3C). Other bacteria with high Mn and low Fe requirements include *Lactobacillus plantarum* and *Borrelia burgdorferi* (14, 15). *Lactobacilli* are facultative anaerobes and frequently isolated as surviving contaminants from irradiated (5 kGy) meat (16), and the spirochete *B. burgdorferi* is an extracellular pathogen adapted to host iron limitation (14). Bacteria that can grow in Fe-deficient media appear to have an absolute requirement for Mn (15), and *D. radiodurans* fits this paradigm.

^{59}Fe and ^{54}Mn were used to assay intracellular Fe and Mn accumulation in *D. radiodurans* relative to the dissimilatory metal-reducing bacterium *S. oneidensis* MR-1, an organism that contains an abundance of heme-containing *c*-type cytochromes (17) (Fig. 3D). *S. oneidensis* accumulated less than 5×10^2 atoms/cell of ^{54}Mn while *D. radiodurans* accumulated 1.08×10^5 atoms/cell (~2.74 mM, assuming an average cell volume of $6.5 \times 10^{-2} \mu m^3$ (Fig. 1E, 3D)); high Mn(II) concentrations in *D. radiodurans* have also been reported using neutron activation analysis (18). In contrast, *D. radiodurans* accumulated only 2.7×10^3 atoms/cell of ^{59}Fe while the value was 10-fold more for *S. oneidensis* (Fig. 3D); 7×10^5 Fe and 3.8×10^4 Mn atoms per cell have been reported in *E. coli* using this assay (14). The intracellular Mn/Fe accumulation ratio for *D. radiodurans* is 40; for *E. coli* is 0.05 (14); and for *S. oneidensis* is 0.02. Compared to

D. radiodurans, *L. plantarum* and *B. burgdorferi* are reported to accumulate similar concentrations of ^{54}Mn atoms (~10^5-10^6) on a per cell basis and ^{59}Fe accumulation was also much lower in comparison (14, 15). The specific activity of the ^{59}Fe used in our experiments allowed detection of about 10^2-10^3 atoms of ^{59}Fe per cell. Since ^{59}Fe accumulated to only just above background levels in *D. radiodurans* and its growth and recovery from irradiation in the presence of high concentrations of Fe-chelators (Fig. 3C) was not detrimental, we conclude that this bacterium's Fe requirement is very low. Intracellular concentrations of Mn were also determined using an inductively coupled plasma-mass spectrometry method (ICP-MS) (14) and found to be 1.25 (±0.04) nmol Mn/mg protein for *D. radiodurans* and <0.01 for *S. oneidensis*. The value of 1.25 for *D. radiodurans* is similar to the value of 1.9 nmol Mn/mg protein previously reported for *B. burgdorferi* (14). Currently, little is known about transport of trace metals and other essential ions in *D. radiodurans*. We investigated whether ^{54}Mn transport in *D. radiodurans* is energy-dependent by measuring ^{54}Mn accumulation in cells in the presence of carbonyl cyanide *m*-chlorophenylhydrazone (CCCP), an uncoupler of energy dependent ion transport (14). CCCP inhibited ^{54}Mn accumulation by >75% in *D. radiodurans* and ^{59}Fe accumulation in *S. oneidensis* by > 97% (Fig. 3D). Similarly, CCCP blocked ^{54}Mn accumulation in *B. burgdorferi* (14). Inhibition of Mn transport by CCCP is consistent with the important role of Mn in *D. radiodurans* and *B. burgdorferi.*

Upon exposure to ionizing radiation, most DNA damage (~80%) is reported to be caused by the action of hydroxyl (·OH) radicals, the remaining damage (~20%) is due to other mechanisms including direct physical interaction between γ-photons and DNA (19, 20). However, while the chemistry of oxidative DNA damage is largely understood, the impact of different physiological environments on the 80:20 ratio of irradiation-induced DNA damage is unknown. In the presence of water and O_2, ionizing radiation is known to generate H_2O_2 by free radical chemistry arising from the radiolysis of water (19, 20). Within cells, unbound Fe(II) ions are very dangerous because they catalyse

Fenton-type reactions of H_2O_2 that form ·OH radicals, which cause DNA strand breaks and protein damage (20). Since H_2O_2 is relatively stable compared to the short-lived, reactive ·OH radical (20), irradiation-produced H_2O_2 is able to diffuse within cells, where Fe(II) released from proteins during irradiation can become the focus of additional ·OH formation. In contrast to Fe(II), Mn(II) does not participate in Fenton chemistry and confers a highly protective effect against free radicals (15).

In assessing the radiation resistance of bacterial cultures, failure to correct for cell-grouping can lead to exaggerated resistance values based on CFU counts. Because *D. radiodurans* does not grow as a monococcus (1), the D_{37} for a single-celled population cannot be determined experimentally. In TGY, actively growing cultures of *D. radiodurans* consist mostly of diplococci (1) (Fig. 1A). The ratio of diplococci and tetracocci in an actively growing TGY culture (OD_{600} 0.9) is about 75%:25% (Fig. 1A). For a TGY culture of *D. radiodurans* (OD_{600} 0.9), the D_{37} value is ~12 kGy (Fig. 2). The survival of individual cells within such a culture is statistically calculated to be ~10% (D_{10}) (21). In TGY, the experimentally determined D_{10} values for wild-type *E. coli* (K12) (1 cell/CFU) and *S. oneidensis* (MR-1) (1 cell/CFU) are ~0.75 kGy and ~0.1 kGy (Fig. 2), respectively. Therefore, under the described growth conditions (Fig. 2), *D. radiodurans* is about 16-fold more radiation resistant than *E. coli*, and 120-fold more resistant than *S. oneidensis*.

To determine if the greater resistance of *D. radiodurans* could be attributed to DNA protection, the strains were cultured in TGY to OD_{600} 0.9 and irradiated on ice to doses extending to 50 kGy (Fig. 4A). The survival curves and cell-grouping for the cultures used in DNA preparation (Fig. 4A) were essentially the same as reported in Fig. 2. We found that chromosomal DNA in *E. coli* and *S. oneidensis* was substantially more susceptible to *in vivo* irradiation damage than in *D. radiodurans* (Fig. 4A). Following acute irradiation, DNA repair in *D. radiodurans* occurs only at growth temperatures and

in the presence of fresh medium (22). Therefore, the relatively high molecular size of DNA in *D. radiodurans* cells irradiated on ice for 6 hours and without the addition of nutrients (Fig. 4A) is inferred to be the result of chemical protection of DNA. The number of genomic DSBs inflicted per Gy for *D. radiodurans* (3.3 Mbp) was 0.015 DSB/Gy (3.3 Mbp/4.4 kbp/50 kGy (Fig. 4A)); for *E. coli* (4.6 Mbp) was 0.22 DSB/Gy (at 32 and 50 kGy); and for *S. oneidensis* (5.1 Mbp) was 0.24 DSB/Gy (at 32 and 50 kGy) (Fig. 4A). Since the number of DSBs suffered by a genome is a measure of irradiation-induced oxidative stress (20), DNA in *D. radiodurans* is about 15-fold more resistant to irradiation-induced damage than DNA in *E. coli* or *S. oneidensis*.

For *D. radiodurans*, the value of 0.015 DSB/Gy (Fig. 4A) is equivalent to the 220 DSBs/haploid genome observed by TEM of DNA prepared from agarose-embedded *D. radiodurans* cells exposed to 17.5 kGy (*i.e.*, 0.013 DSB/Gy) (23). Assuming a linear relationship between DSB damage and dose over the range 0-50 kGy, the estimated number of DSBs inflicted in *D. radiodurans* at 12 kGy (approximate D_{10} value adjusted for a monococcus in an OD_{600} 0.9 culture) (21) is 180 DSBs/haploid genome, *i.e.*, 0.015 DSB/Gy. At the D_{10} dose for *E. coli* (~0.75 kGy, Fig. 2), a similar number of DSBs/chromosome (*i.e.*, 164) are estimated compared to *D. radiodurans*, but the number of DSBs estimated in *S. oneidensis* at 0.1 kGy (D_{10}) is about 7-fold less (24 DSBs/chromosome; *i.e.*, 0.24 DSB/Gy). Since our estimates of DSB damage at D_{10} doses did not factor for any protection against free radicals conferred by enzymatic scavenging systems, the number of DSBs inflicted at D_{10} doses may be lower. For example, the presence of Mn(II)-dependent superoxide dismutase (SOD) in cells at the time of irradiation could provide protection at low temperatures (24). However, enzymatic protection systems likely become overwhelmed by progressive oxidative inactivation as levels of H_2O_2 and reactive oxygen species (ROS) increase during the course of irradiation (0-50 kGy). *S.* oneidensis (17) encodes Fe-dependent SOD, but not Mn-SOD, and thus may be predisposed to SOD-inactivation by ·OH radicals at

relatively low irradiation doses, and have increased susceptibility to metabolism-induced ROS during recovery. In contrast, *D. radiodurans* and *E. coli* both encode Mn-SOD (9, 24).

As part of a global strategy to avoid cellular damage, *D. radiodurans* may avoid the production of ·OH radicals by limiting intracellular Fe(II)-dependent reduction of H_2O_2 produced by irradiation or metabolism. The high intracellular Mn(II) concentration in *D. radiodurans* may also serve as a potent quenching agent against ROS, as proposed for other Mn(II)-accumulating organisms (15). The protective effects of high Mn and low Fe concentrations (15, 20) could also help mitigate the lethal effects of desiccation/hydration-cycles (2) and exposure to H_2O_2 (3) since DNA damage caused by these conditions is similar to that generated by ionizing radiation (7, 19, 20). We believe it is significant that among the most radiation resistant non-spore forming bacterial groups reported, the phylogenetically distinct deinococci (9), and enterococci (25) and lactobacilli (16) share metabolic and physiologic traits including growth in environments deficient in Fe (14, 15, 26) (Fig. 3) and/or containing Dp and Ds (Fig. 4B), Mn(II) acquisition (14, 15, 27), desiccation resistance (2, 28), and luxuriant growth under chronic ionizing radiation (0.05 kGy/hour) in the presence or absence of Dp plus Ds (Fig. 4B).

Genomic analyses show that the number of genes identified in *D. radiodurans* that are known to be involved in DNA repair is less than the number reported for *E. coli* (9), and polyploidy in itself is insufficient for radioresistance (9). The number of DSBs/haploid genome estimated in *D. radiodurans* [180] and *E. coli* [164] at their respective D_{10} isosurvival doses is similar (Table 1), and we suggest that the difference in DNA protection observed between these species is sufficient to explain most of the difference in dose to achieve the same 10% survival (Table 1). Efficient homologous recombination observed between the 4-8 identical genomes/cell in *D. radiodurans* (5, 7)

is consistent with the ability of irradiated cells to prevent mutation (7, 8), and aggregation of multiple identical genomes into condensed nuclei (Fig. 1) (1, 11) may facilitate such repair by simplifying the search for repair templates. However, we believe that previous emphasis on DNA repair as the dominant explanation (2, 4, 6-10, 22, 23) for the remarkable survival of *D. radiodurans* cultures at high irradiation doses has been overstated. Instead, we suggest that the extreme resistance of *D. radiodurans* is largely due to high levels of DNA protection in cells (Fig. 4A, Table 1), which give rise to extraordinary CFU-based survival curves, especially when grouped as tetracocci (1,7) (Fig.2). The high Mn and low Fe levels of *D. radiodurans* (Fig. 3D) likely are the foundation of a synergistic set of intracellular protection systems including free radical scavengers such as the highly expressed Mn-SOD and catalase of *D. radiodurans* (9, 24), a homolog of the DPS protein in *E. coli* (9), carotenoid pigments (24), and metabolic pathway switching following irradiation (9) that could help prevent additional genome damage elicited by free radicals induced by metabolism during recovery.

References

1. M. J. Thornley, R. W. Horne, A. M. Glauert, *Arch. Mikrobiol.* **51**, 267 (1965); R. G. E. Murray, M. Hall, B. G. Thompson, *Can. J. Microbiol.* **29**, 1412 (1983).
2. V. Mattimore, J. R. Battista, *J. Bacteriol.* **178**, 633 (1996).
3. P. Wan, H. E. Schellhorn, *Can. J. Microbiol.* **41**, 170 (1995).
4. B. E. B. Moseley, *Soc. Appl. Bacteriol. Symp. Ser.* **12**, 147 (1984).
5. M. T. Hanson, *J. Bacteriol.* **134**, 71 (1978).
6. M. J. Daly, K. W. Minton, *J. Bacteriol.* **178**, 4461 (1996).
7. M. J. Daly, K. W. Minton, *J. Bacteriol.* **177**, 5495 (1995).
8. D. M. Sweet, B. E. B. Moseley, *Mutat. Res.* **34**, 175 (1976).

9. K. S. Makarova, *et al.*, *Microbiol. Mol. Biol. Rev.* **65**, 44 (2001); O. White, *et al.*, *Science* **286**, 1571 (1999); Y. Liu, *et al.*, *Proc. Natl. Acad. Sci. USA* **100**, 4191 (2003).

10. J. R. Battista, A. M. Earl, M.-J. Park, *Trends Microbiol.* 7, 362 (1999).

11. S. Levin-Zaidman, *et al.*, *Science* **299**, 254 (2003).

12. A. Venkateswaran, *et al.*, *Appl. Environ. Microbiol.* **66**, 2620 (2000); H. Brim, *et al.*, *Appl. Environ. Microbiol.* **69**, (2003), in press.

13. H. Oyaizu, *et al.*, *Int. J. Syst. Bacteriol.* **37**, 62 (1987).

14. J. E. Posey, F. C. Gheradhini, *Science* **288**, 1651 (2000).

15. N. S. Jakubovics, H. F. Jenkinson, *Microbiology* **147**, 1709 (2001).

16. J. W. Hastings, W. H. Holzapfel, *J. Appl. Bacteriol.* **62**, 209 (1987).

17. J. F. Heidelberg, *et al.*, *Nature Biotechnol.* **20**, 1118 (2002); R. E. Wildung, *et al.*, *Appl. Environ. Microbiol.* **66**, 2451 (2000).

18. P. J. Leibovitz, L. S. Schwartzberg, A. K. Bruce, *Photochem. Photobiol.* **23**, 45 (1976).

19. J. E. Repine, *et al.*, *Proc. Natl. Acad. Sci. U S A* **78**, 1001 (1981).

20. C. von Sonntag, Taylor & Francis, London, ISBN 0-85066-375-X (1987); A. U. Khan, M. Kasha, *Proc. Natl. Acad. Sci. U S A* **91**, 12365 (1994).

21. For the survival curve of *D. radiodurans* (TGY, open triangle) presented in Fig. 2, the cell-grouping was ~75% diplococci and ~25% tetracocci (Fig. 1A). Under the assumptions that the survival of cells, constituting the CFU, is independent from each other, that survival of a single cell is enough to unsure the survival of a CFU, and that the relative frequency of a k-cell CFU is known to be f_k ($\Sigma f_k = 1$), the relationship between the individual cell survival and the CFU

survival follows the equation: $p(x) = \Sigma f_k p_k(x) = \Sigma f_k(1 - [1 - p_1(x)]^k)$ where, for a radiation dose x, $p(x)$ is the survival probability for an arbitrary CFU in the mixture, $p_k(x)$ is the survival probability for a k-cell CFU and $p_1(x)$ is the survival probability for an individual cell. For a culture consisting of diplococci and tetracocci (75%:25%), survival of 10% of individual cells (D_{10}) translates to 37% of CFU survival (D_{37}); *i.e.*, for the TGY culture (Fig. 2, open triangle), the D_{10} of individual cells is 12 kGy (±1). For the DMM culture (Fig. 2, solid triangle), the D_{10} for individual cells is 10 (±1).

22. K. W. Minton, *Mol. Microbiol.* **1**, 9 (1994).

23. J. Lin, *et al.*, *Science* **285**, 1558 (1999).

24. M. E. McAdam, F. Levelle, R. A. Fox, E. M. Fielden, *Biochem. J.* **165**, 81 (1977); J. M. McCord, B. B. Keele, I. Fridovich, *Proc. Natl. Acad. Sci. USA* **68**, 1024 (1971); M. A. Carbonneau, A. M. Melin, A. Perromat, M. Clerc. *Arch. Biochem. Biophys.* **275**, 244 (1989).

25. S. J. van Gerwen, F. M., Rombouts, K. van't Riet, M. H. A. Zwietering, *J Food Prot.* Sep. **62**, 1024 (1999).

26. C. J. Efthymiou, S. Saadi, S. L. Young, E. A. Helfand, *Ann. Clin. Lab. Sci.* **17**, 226 (1987).

27. Y. L. Low, *et al.*, *J. Med. Microbiol.* **52**,113 (2003).

28. M. J. Bale, P. M. Bennett, J. E. Beringer, M. Hinton, *J. Appl. Bacteriol.* **75**, 519 (1993); G. E. Gardiner, *et al.*, *Appl. Environ. Microbiol.* 66, 2605 (2000).

29. H. Brim, *et al.*, *Nat. Biotechnol.* 18, 85 (2000).

30. This research was funded by the U. S. Department of Energy (DOE) (Office of Biological and Environmental Research) grants from the Genomes to Life program (DE-FG02-01ER63220) and from the Natural and Accelerated

Bioremediation Research program (DE-FG02-97ER62492). Pacific Northwest National Laboratory is operated for the DOE by Battelle Memorial Institute under Contract DE-AC06-76RLO 1830. We are grateful to Dr. Yuri Wolf of the National Center for Biotechnology Information, National Institutes of Health (NIH), Bethesda, MD, USA for statistical analysis of CFU survival, and Dr. M. Cashel (NIH) for providing *E. coli* strain K12 (MG1655).

Table 1. Summary of data.

Strains	Genome size/Mbp	Mn/Fe accumulation ratio	Cell grouping/CFU at OD_{600} 0.9	DSBs/haploid genome at 50 kGy (Fig. 4A)	D_{10} (adjusted for cell grouping) (Fig. 2)	DSBs /Gy	Estimated number of DSBs at D_{10}
D. radiodurans	3.3	40	Tetracoccus (25%): diplococcus (75%) (Fig. 1A)	750	12 kGy (21)	0.015	180
E. coli	4.6	0.05	1	10,952	0.75 kGy	0.22	164
S. oneidensis	5.1	0.02	1	12,143	0.1 kGy	0.24	24

Fig. 1. Transmission electron microscopy (TEM). **A**, *D. radiodurans* (ATCC BAA-816) grown in TGY (1% bactotryptone, 0.5% yeast extract, and 0.1% glucose), late-log phase (LLP). **B**, *D. radiodurans* grown in TGY, early-stationary phase (ESP). **C**, *D. radiodurans* grown in DMM (ESP). **D**, *D. radiodurans*, diplococcus, TGY, ESP. **E**, *D. radiodurans*, diplococcus, DMM, ESP. **F & G**, *D. grandis* (DSM 3963) grown in TGY (ESP). Abbreviations: TGY, rich medium; DMM, defined minimal medium; tet, tetracoccus; dip, diplococcus. Scale bars 0.5 μm. LLP for *Deinococcus* in TGY corresponds to ~OD_{600} 0.9 after incubation for ~12 h at 32°C; ESP for *Deinococcus* in TGY corresponds to OD_{600} 1.2 after incubation for ~24 h at 32°C; in DMM, ESP for *Deinococcus* corresponds to ~ OD_{600} 0.9 after ~48 h. Additional images can be found at http://131.158.180.98/~vasilenko/. TEM, bacterial suspensions were rinsed in 0.1 M cacodylate buffer (pH 7.4), fixed in 2.5% gluteraldehyde in the same buffer, and post-fixed in 1% osmium tetraoxide. Fixed samples were embedded in Epon-Araldite resin, and 50-70 nm sections were stained with uranyl acetate followed by lead citrate. Samples were examined with a Philips CM 100 electron microscope.

Fig. 2. Survival of strains exposed to acute doses of γ-radiation. The indicated strains were inoculated into TGY or DMM (12) medium at 10^6 CFU/ml and grown to OD_{600} 0.9 in the presence or absence of Dp + Ds (50 μM each). Cells were then irradiated without change of broth on ice with ^{60}Co at 8.3 kGy/hour (^{60}Co Gammacell irradiation unit [J. L. Shepard and Associates, Model 109]). At the indicated doses, CFU counts were determined by plating appropriate culture dilutions on solid TGY. Values are from three independent trials, with standard deviations shown. CFU, colony-forming units. Open triangle, *D. radiodurans* (ATCC BAA-816), TGY (LLP, Fig. 1A); Solid triangle, *D. radiodurans*, DMM (ESP, Fig. 1C, E); Solid circle, *D. radiodurans*, DMM +Dp + Ds (ESP); Open circle, *D. grandis* (DSM 3963), TGY (LLP); Solid diamond, *D. grandis*, DMM (ESP, Fig. 1F, G); Open diamond, *E. coli* (K12, strain MG1655), TGY; Solid square, *S. oneidensis* (MR-1), TGY.

Fig. 3. Role of transition metals in wild-type *D. radiodurans*. **A**, Growth dependence on Mn(II) in DMM. **B**, Dependence on transition metals. *D. radiodurans* was inoculated at 10^6 CFU/ml into DMM (12) containing 2.5 μM Mn(II) (manganous chloride), Fe(II) (ferrous sulfate), Co(II) (cobalt chloride), Mo(II) (ammonium molybdate), or [Cd(II) (cadmium sulphate) (2.5 μM) + Mn(II) (2.5 μM)]. For each trial, three independent incubations were at 32°C for 67 h prior to measuring cell density at OD_{600}, with standard deviations shown. Note, Cd(II) is a competitive inhibitor of Mn(II). Trace, 0.2 μM each of Mo, Cu, Cr, Bo, Zn, & I. **C**, Comparison of growth of cells following irradiation (^{60}Co, 9 kGy). Irradiated and control cells were inoculated (1/20 dilution) into DMM (2.5 μM Mn(II)) + /- 100 μM Dp and 100 μM Ds, at 32°C. Pre-irradiation growth conditions were as in Fig. 2. Growth was monitored at OD_{600}. Values are from three independent trials, with standard deviations shown. **D**, *D. radiodurans* accumulated ^{54}Mn, but not ^{59}Fe, in an energy-dependent manner. When a column-value is low, see inset circle for designation and correspondence to key. Standard deviations are shown. ^{59}Fe and ^{54}Mn accumulation was as described by Posey and Gheradhini (2000) (14). Radiolabeled metal was added to cell suspensions of 6.3×10^7 and 1×10^9 CFU/mL for *D. radiodurans* and *S. oneidensis*, respectively, at a final concentration of 0.018 and 0.0057 μCi/ml, respectively, for ^{59}Fe or ^{54}Mn (Isotope Products Laboratories; ^{59}Fe 100 Ci/g; ^{54}Mn 10 Ci/g). CCCP (100 μM) was added and cells were incubated at 30°C for 1 h before adding either ^{59}Fe or ^{54}Mn. Cell density was determined by direct microscopic counting after staining with acridine orange to allow resolution of individual cells, whether they occurred singly, in pairs, or in tetrads.

Fig. 4. A, *In vivo* susceptibility of genomic DNA to irradiation induced DSBs. Cells were grown in TGY to OD_{600} 0.9 and irradiated (^{60}Co) on ice to the indicated doses (kGy). Total DNA was purified and analysed by agarose (0.8%) gel electrophoresis[6]. Molecular size standards are shown (kbp). The number of genomic DSBs per Gy was determined using agarose gels containing diluted DNA samples, and densitometry

(Fluorimager 595, ImageQuant software). The integrated average molecular size of DNA fragments distributed within the indicated samples is shown. CFU survival frequencies for the cultures used for DNA preparation are given at the bottom of each lane. D_{10} values are shown in bold. **B**, Growth of bacteria on TGY plates under genotoxic conditions. I, TGY control; II, TGY + 0.05 kGy/hour (^{137}Cs); III, TGY + Dp + Ds (each, 250 μM); IV, TGY + 0.05 kGy/hour + Dp + Ds (each, 250 μM). Growth under chronic irradiation was tested in a ^{137}Cs Gammacell 40 irradiation unit [Atomic Energy of Canada Limited]) for 3 days at 22°C (29). Abbreviations: DR, *D. radiodurans* (ATCC BAA-816); DG, *D. grandis* (DSM 3963); SO, *S. oneidensis* (MR-1); EF, *Enterococcus faecium* (ATCC 19434); LP, *L. plantarum* (ATCC 14917); EC, *E. coli* (K-12).

Fig. 1

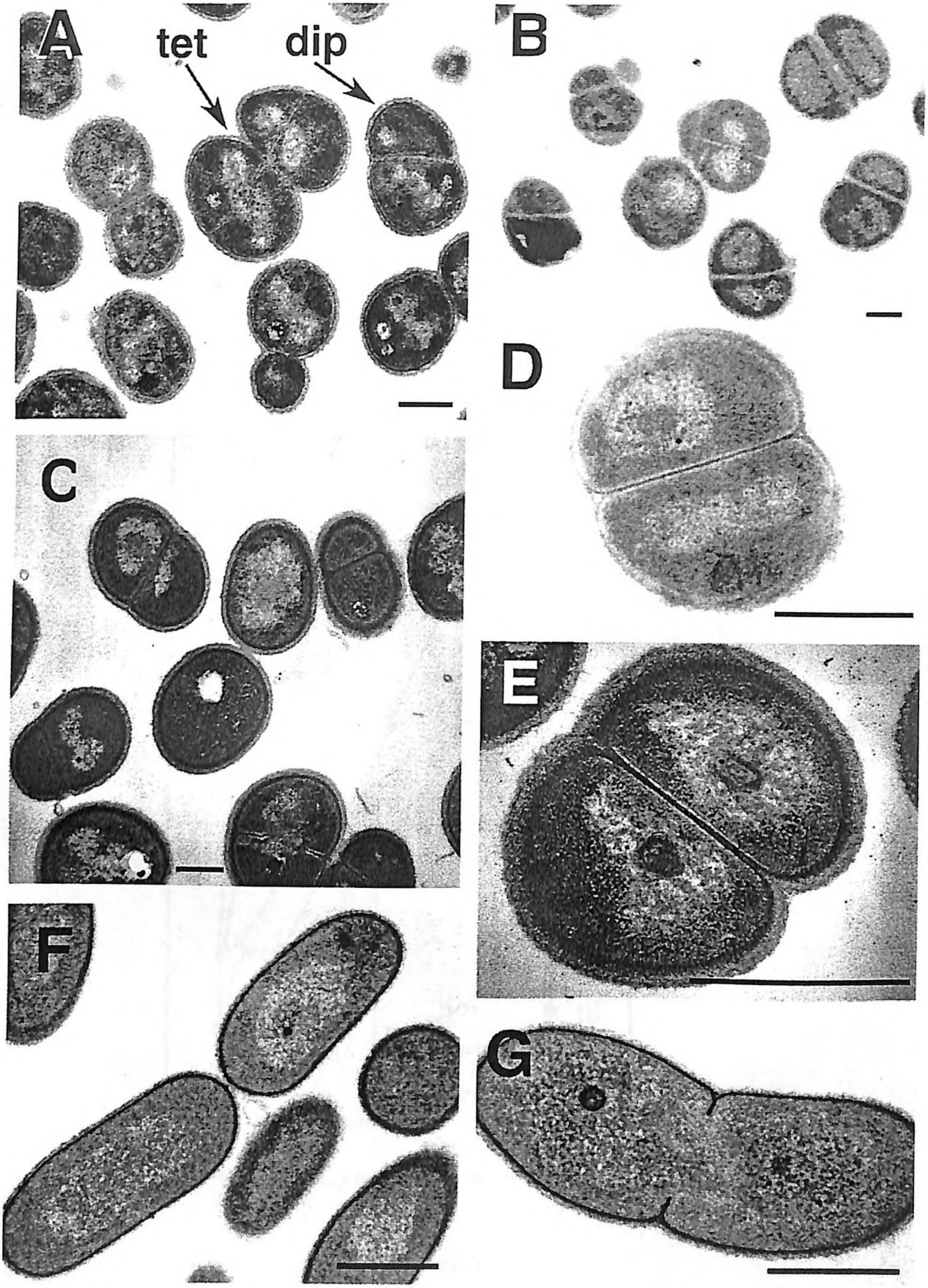

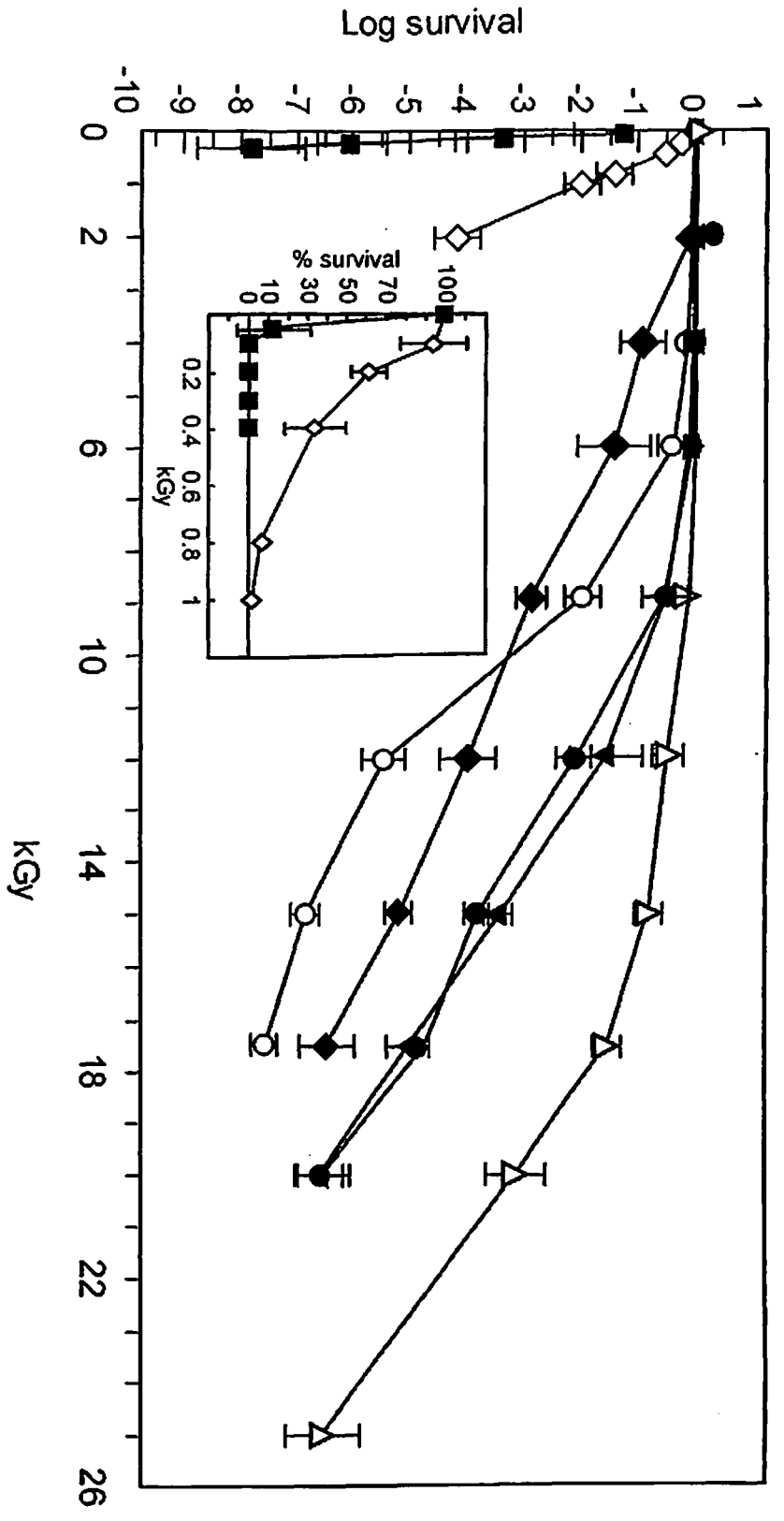
Log survival
-10
-9
-8
-7
-6
-5
-4
-3
-2
-1
0
1
0
2
6
10
14
18
22
26
kGy
% survival
0
10
30
50
70
100
0.2
0.4
0.6
0.8
1
kGy

Fig. 2

Fig. 3

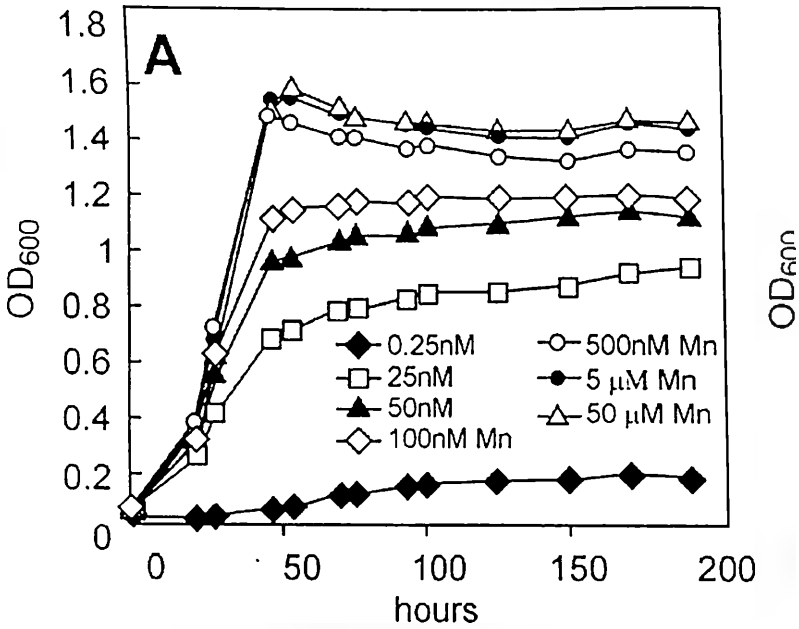
A
1.8
1.6
1.4
1.2
1
0.8
0.6
0.4
0.2
0
OD600
0
50
100
150
200
hours
0.25nM
25nM
50nM
100nM Mn
500nM Mn
5 μM Mn
50 μM Mn
C
1.6

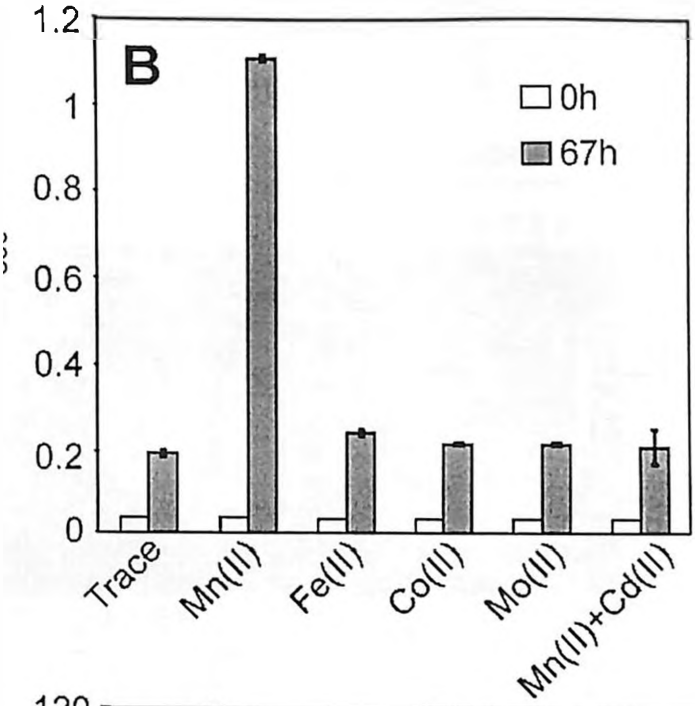
B
0h
67h
1.2
1
0.8
0.6
0.4
0.2
0
Trace
Mn(II)
Fe(II)
Co(II)
Mo(II)
Mn(II)+Cd(II)

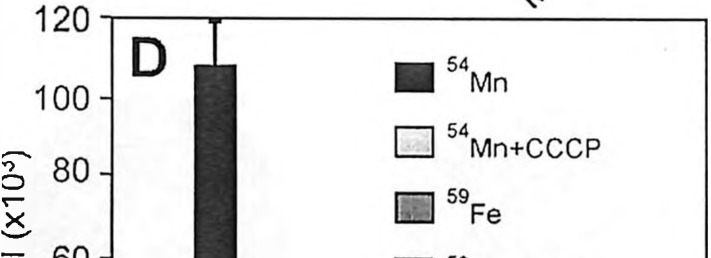
D
54Mn
54Mn+CCCP
59Fe
120
100
80
60

Fig. 4

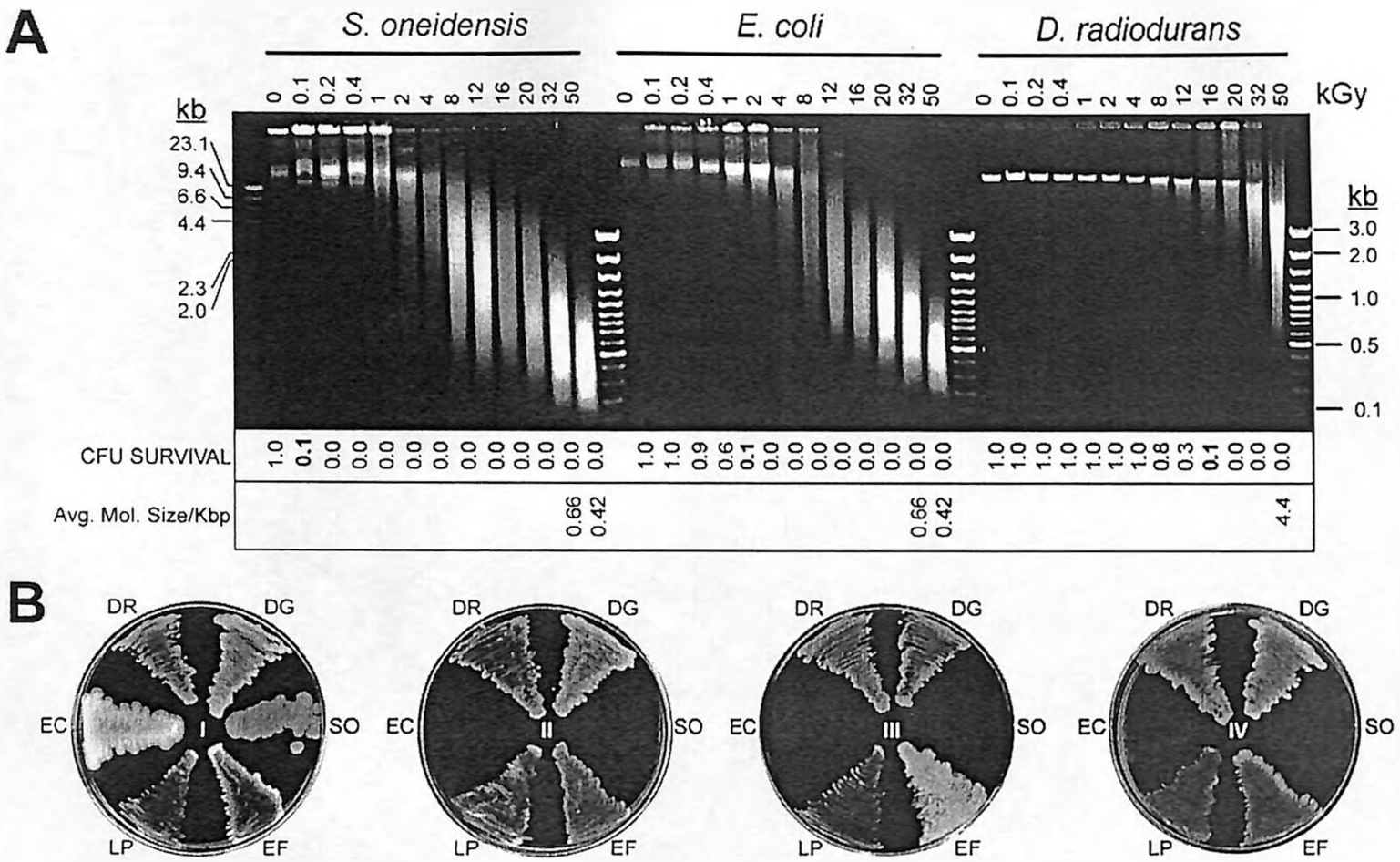
A
S. oneidensis
E. coli
D. radiodurans
kGy
kb
23.1
9.4
6.6
4.4
2.3
2.0
3.0
2.0
1.0
0.5
0.1
CFU SURVIVAL
Avg. Mol. Size/Kbp
0.66
0.42
4.4
B
DR
DG
EC
SO
LP
EF
I
II
III
IV